



710
2017

Berichte

zur Polar- und Meeresforschung

Reports on Polar and Marine Research

**The Expedition PS103
of the Research Vessel POLARSTERN
to the Weddell Sea in 2016/2017**

Edited by

Olaf Boebel

with contributions of the participants

Die Berichte zur Polar- und Meeresforschung werden vom Alfred-Wegener-Institut, Helmholtz-Zentrum für Polar- und Meeresforschung (AWI) in Bremerhaven, Deutschland, in Fortsetzung der vormaligen Berichte zur Polarforschung herausgegeben. Sie erscheinen in unregelmäßiger Abfolge.

Die Berichte zur Polar- und Meeresforschung enthalten Darstellungen und Ergebnisse der vom AWI selbst oder mit seiner Unterstützung durchgeführten Forschungsarbeiten in den Polargebieten und in den Meeren.

Die Publikationen umfassen Expeditionsberichte der vom AWI betriebenen Schiffe, Flugzeuge und Stationen, Forschungsergebnisse (inkl. Dissertationen) des Instituts und des Archivs für deutsche Polarforschung, sowie Abstracts und Proceedings von nationalen und internationalen Tagungen und Workshops des AWI.

Die Beiträge geben nicht notwendigerweise die Auffassung des AWI wider.

Herausgeber

Dr. Horst Bornemann

Redaktionelle Bearbeitung und Layout

Birgit Reimann

Alfred-Wegener-Institut
Helmholtz-Zentrum für Polar- und Meeresforschung
Am Handeshafen 12
27570 Bremerhaven
Germany

www.awi.de
www.reports.awi.de

Der Erstautor bzw. herausgebende Autor eines Bandes der Berichte zur Polar- und Meeresforschung versichert, dass er über alle Rechte am Werk verfügt und überträgt sämtliche Rechte auch im Namen seiner Koautoren an das AWI. Ein einfaches Nutzungsrecht verbleibt, wenn nicht anders angegeben, beim Autor (bei den Autoren). Das AWI beansprucht die Publikation der eingereichten Manuskripte über sein Repository ePIC (electronic Publication Information Center, s. Innenseite am Rückdeckel) mit optionalem print-on-demand.

The Reports on Polar and Marine Research are issued by the Alfred Wegener Institute, Helmholtz Centre for Polar and Marine Research (AWI) in Bremerhaven, Germany, succeeding the former Reports on Polar Research. They are published at irregular intervals.

The Reports on Polar and Marine Research contain presentations and results of research activities in polar regions and in the seas either carried out by the AWI or with its support.

Publications comprise expedition reports of the ships, aircrafts, and stations operated by the AWI, research results (incl. dissertations) of the Institute and the Archiv für deutsche Polarforschung, as well as abstracts and proceedings of national and international conferences and workshops of the AWI.

The papers contained in the Reports do not necessarily reflect the opinion of the AWI.

Editor

Dr. Horst Bornemann

Editorial editing and layout

Birgit Reimann

Alfred-Wegener-Institut
Helmholtz-Zentrum für Polar- und Meeresforschung
Am Handeshafen 12
27570 Bremerhaven
Germany

www.awi.de
www.reports.awi.de

The first or editing author of an issue of Reports on Polar and Marine Research ensures that he possesses all rights of the opus, and transfers all rights to the AWI, including those associated with the co-authors. The non-exclusive right of use (einfaches Nutzungsrecht) remains with the author unless stated otherwise. The AWI reserves the right to publish the submitted articles in its repository ePIC (electronic Publication Information Center, see inside page of verso) with the option to "print-on-demand".

Titel: vLBV (vectorized Little Benthic Vehicle) FIONA wird zu Wasser gelassen um eine Tiefseeverankerung zu finden und eine Bergeleine daran anzubringen (Foto: Frieder Hamm, BLE).

Cover: vLBV (vectorized Little Benthic Vehicle) FIONA is being launched to find a deep-sea mooring and attach a recovery rope (Photo: Frieder Hamm, BLE).

The Expedition PS103 of the Research Vessel POLARSTERN to the Weddell Sea in 2016/2017

Edited by

Olaf Boebel

with contributions of the participants

Please cite or link this publication using the identifiers

hdl:10013/epic.51699 or <http://hdl.handle.net/10013/epic.51699> and

https://doi.org/10.2312/BzPM_0710_2017

ISSN 1866-3192

PS103

16 December 2016 - 3 February 2017

Cape Town - Punta Arenas



Chief scientist
Olaf Boebel

Coordinator
Rainer Knust

Contents

1.	Zusammenfassung und Fahrtverlauf	2
2.	Weather Conditions	9
3.	Scientific Programmes	11
3.1	HAFOS: Maintaining the AWI's Long Term Ocean Observatory in the Weddell Sea	11
3.1.1.	Physical oceanography	11
3.1.2	Ocean acoustics	55
3.1.3	Transport variations of the Antarctic Circumpolar Current	79
3.2	EK80 Acoustic Signal Emission Measurements	87
3.3	Sea Ice Physics	89
3.3.1	Deployments of autonomous ice tethered platforms (buoys)	89
3.3.2	Along track observations of sea ice conditions	93
3.4	INTERPELAGIC: Interactions between Key Players of the Southern Ocean Zooplankton: Amphipods, Copepods, Krill and Salps	95
3.5	Algenom: Molecular Ecology and Microevolutionary Genomics of Primary Producers	112
3.6	MicroPath: Effects of Environmental Changes on Microbial Pathways Relevant for the Production of Climate-Active Gases	121
3.7	ISOTAM: Stable N - isotopes of Ammonium and Ammonia in and over the Atlantic Ocean	130
3.8	Phytooptics	136
	APPENDIX	141
A.1	Teilnehmende Institute / Participating Institutions	142
A.2	Fahrtteilnehmer / Cruise Participants	143
A.3	Schiffsbesatzung / Ship's Crew	145
A.4	Stationsliste / Station List PS103	147

1. ZUSAMMENFASSUNG UND FAHRTVERLAUF

Olaf Boebel

AWI

Die Antarktisexpedition PS103 führte von Kapstadt, Südafrika, über die *Neumayer-Station III*, Antarktis, in das Weddellmeer und weiter nach Punta Arenas, Chile (Abb. 1.1). Die Expedition beinhaltete logistische und wissenschaftliche Vorhaben. Die logistischen Aufgaben (Versorgung *Neumayer III* mit Treibstoff und Vorräten) wurden vollständig umgesetzt. Nahezu alle Ziele der wissenschaftlichen Vorhaben wurden in bewährter Zusammenarbeit zwischen Schiff und Wissenschaft erreicht. Insbesondere konnten die durch den Abbruch der Expedition PS89 ausgefallenen Verankerungsaufnahmen der 2010er und 2012er Verankerungen erfolgreich nachgeholt werden.

Die wissenschaftlichen Arbeiten lassen sich in stationsgebundene, meereisbasierte, vom fahrenden Schiff aus durchgeführte, sowie helikoptergestützte Arbeiten unterteilen. Folgende stationsgebundene Aufgaben wurden durchgeführt:

- Fahren von 53 CTD Stationen mit Rosette und I-ADCP;
- 41 Netzfänge mit dem Handnetz;
- 3 Netzfänge mit dem Multinetz (S3);
- 50 Netzfänge mit dem Bongo Netz;
- Aufnahme von 1 Tiefseepegel (PIES) entlang des GoodHope Schnittes;
- Aufnahme von 17 Verankerungen sowie Auslage 18 Verankerungen;
- 14 RAFOS Schallquellen Kalibrierungen;
- 6 ROV Einsätze (3 Erprobungen, 3 Einsätze);
- Auslegung von 12 Argo Floats;
- 1 Test akustischer Auslöser.

Folgende Arbeiten wurden vom fahrenden Schiff aus durchgeführt:

- Kontinuierliche Erfassung von Temperatur, Salzgehalt und Strömungsprofilen;
- 7 Beprobungen der Luft auf gasförmiges Ammoniak und partikuläres Ammonium;
- Beprobung oberflächennaher Durchflussproben auf gelöstes NH₄;
- Probennahme (und in großen Teilen phytooptische Analyse) von 294 oberflächennahen Durchflussproben und von 142 Proben aus der CTD;
- Analyse von 40 Wasserproben auf Salzgehalt von 15 Stationen;
- 190 Laborexperimente an den gewonnenen biologischen Proben.

Weitere Arbeiten erfolgten vom Meereis aus:

- Installation von 2 Eisstationen.

Letztendlich dienten die Helikopter als Transportmittel um vom Schiff abgesetzte Arbeiten durchzuführen. Insgesamt ergaben sich 19 Flüge mit 9:14 h kumulativer Dauer:

- 2 Flüge zur Eiserkundung (0:48 h);
- 10 wissenschaftliche Flüge (04:03) zum Ausbringen der Eisstationen und der Wartung des PALAOA Observatoriums;
- 2 Personentransporte bei *Neumayer III* (1:24);
- 5 Trainingsflüge (02:59).

Tabelle 1.1 stellt die Verteilung der Forschungszeiten nach Gerät dar.

Die Reise begann am 16. Dezember 2016, 18:00 LT in Kapstadt, Südafrika. Enroute Standard Messungen sowie phytooptische und chemische Analysen der oberflächennahen Seewasserproben sowie der atmosphärischen Grenzschicht begannen mit Passieren der südafrikanischen 12-Meilen Zone. Bei 45° S begannen die Beprobung der gesamten Wassersäule mittels Kranzwasserschöpfer, Bongo-, Multi-, und Handnetz sowie die Erfassung hydrographischer Tiefenprofile mittels der CTD. Beides, enroute und stationsgebundene Beprobungen, konnte wie geplant während des gesamten Reiseverlaufs bis in die Drake Straße ohne Einschränkungen fortgeführt werden. Insbesondere wurde an den Verankerungspositionen, sowie südlich von 65° S in Abständen von 30 nm, und am Schelfhang der Antarktischen Halbinsel in Abständen von ca. 15 nm, CTDs gefahren.

Bei 49° S begannen die im Rahmen des Hauptantrages vorgesehenen umfangreichen Erneuerungen der Tiefseeverankerungen des HAFOS Observatoriums, zunächst mit der Aufnahme eines PIES Tiefseepegels. Diese verlief trotz der Auslagedauer von 6 Jahren problemlos. Begünstigt durch die ungewöhnlich geringe Meereisbedeckung war der Reisefortschritt entlang des 0° Schnittes zügig. Auch am südlichsten Ende dieses Schnittes herrschte offenes Wasser, wodurch es möglich wurde, eine in 2010 ausgelegte Verankerung, deren Aufnahme bereits in 2012 und 2014 nicht gelungen war, mittels „Tucking“ zu bergen. Der 0°-Schnitt war zum 31. Dezember abgearbeitet, das Anlaufen der Atka-Bucht wurde jedoch wegen schlechter Wetterbedingung verschoben und zunächst noch 2 Verankerungen nördlich von Neumayer gewartet. Am 4. Januar 2017 lag *Polarstern* mit dem frühen Morgen am Nordost-Anleger des Atka Eishafens zur Entladung bereit. Die Löscharbeiten erfolgten in bewährter Zusammenarbeit mit dem Neumayer Team zügig und ohne Probleme. Mit Beendigung der Löscharbeiten bei Neumayer am 6. Januar 2017 18:00 war das Schiff jedoch durch ehemalige Festeisschollen derart massiv eingeschlossen, dass ein Freikommen erst zum 9. Januar 12:00 gelang, wodurch effektiv 2,5 Forschungstage verloren gingen. Im Zentralen Weddellmeer mussten die decksgebundenen Forschungsarbeiten für weitere 3 Tage ausgesetzt werden, um die Ursache geringer Mengen von Öl, die aus dem Schiff austraten, zu finden. Nachdem das Leck gefunden und beseitigt worden war (eine kleine Leckage in einem durch einen Treibstofftank geführten Überlaufrohr eines Ballastwassertanks) wurde am 18. Januar 13:00 der Forschungsbetrieb wieder aufgenommen.

Im zentralen Weddellmeer wurden eisbeständige Argo Floats ausgelegt die eine ganzjährige Messung von Salz- und Temperaturprofilen in den oberen 2.000 m ermöglichen. Um deren Positionierung unter dem Meereis sicherzustellen wurden weitere Verankerungen entlang

eines Zick-Zack-Kurses zur Halbinsel erneuert. Hierbei kam auch erstmals das neue MicroROV Seabotix vLBV300 zum Einsatz, um ältere Verankerungen (mit 4 – 6 Jahren Auslegezeit), die hydroakustisch nicht mehr ausgelöst werden konnten, aufzunehmen. Hierzu wurde mit Hilfe des ROVs eine Bergeleine an die Verankerungsleine verbracht und dort eingeklinkt. Dies gelang in kurzer Zeit bei allen 3 angesteuerten Verankerungen. Die Steuerung des ROVs basierte dabei zunächst auf den Angaben von POSIDONIA und GAPS, im Nahbereich dann auf dem Sonar- und Kamerabild des ROVs. Anzumerken ist hierzu der während der gesamten Reise uneingeschränkt und durchweg zuverlässige Betrieb von POSIDONIA (schiffsintegriert) und GAPS (Brunnenkorb), welcher eine Grundvoraussetzung für einen erfolgreichen Einsatz der ROVs, aber auch einer effizienten Verankerungsaufnahme ist.

Nach Querung des Weddellmeeres schloss die Expedition mit der Auslage einer Verankerung bei Elephant Island sowie der abschließenden Beprobung der Wassersäule in der Drake Passage. Eine GPS-Station auf Gibbs Island, die aufgenommen werden sollte, konnte wegen schlechten Wetters nicht angefliegen werden. Die Reise endete am 2. Februar 2017 11:00 LT in Punta Arenas (Chile).

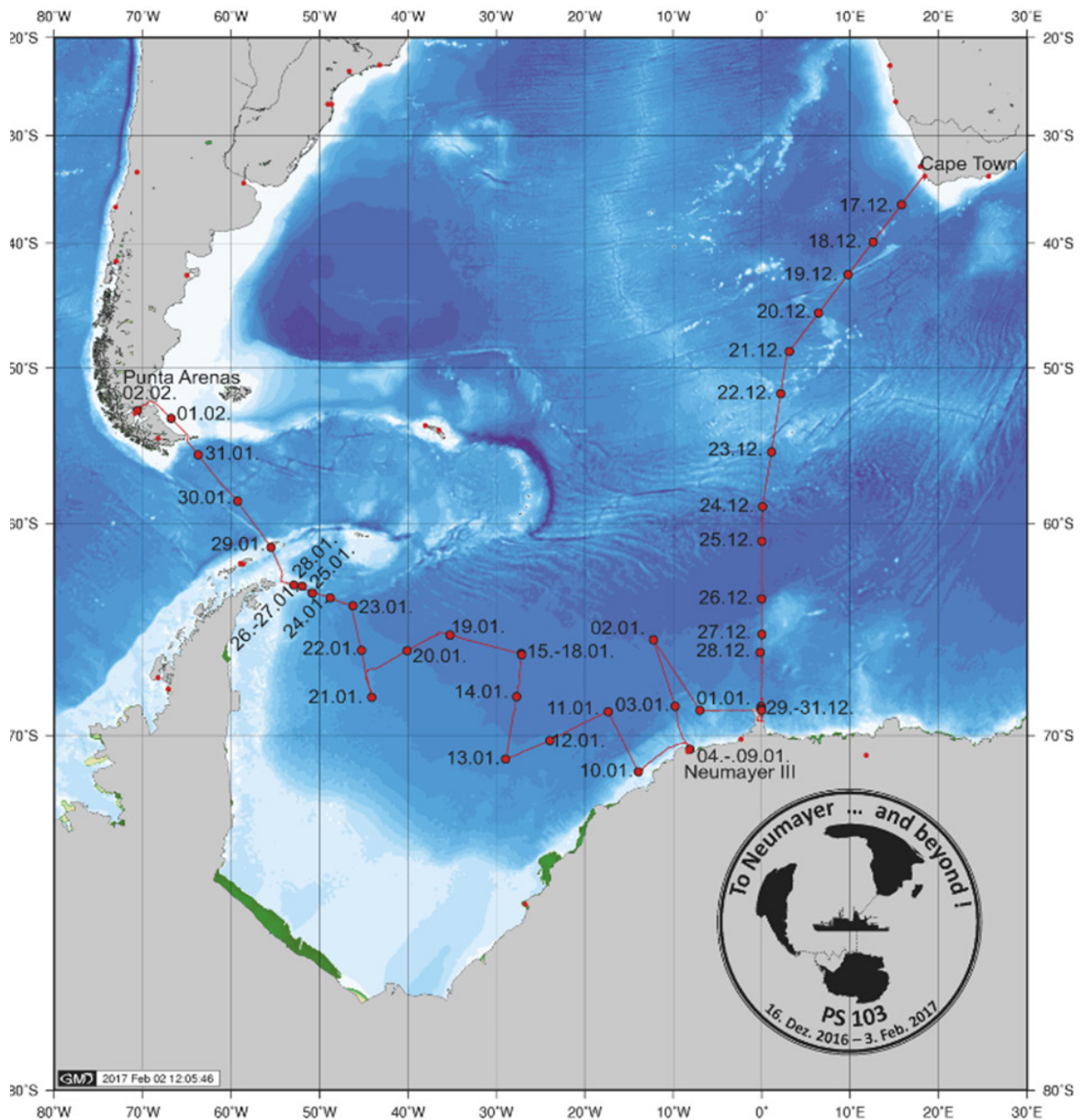


Abb. 1.1: Fahrtverlauf der Antarktis Expedition PS103. Beginn der Reise war am 16 Dezember 2016 in Kapstadt, Südafrika, Ende am 2 Februar 2017 in Punta Arenas, Chile. Siehe <https://doi.pangaea.de/10.1594/PANGAEA.875075> für eine Darstellung des master tracks in Verbindung mit der Stationsliste.

Fig. 1.1: Track of expedition PS103 to the Antarctic, starting Cape Town on 16 December 2016, ending in Punta Arenas, Chile, on 2 February 2017. See <https://doi.pangaea.de/10.1594/PANGAEA.875075> to display the master track in conjunction with the list of stations

SUMMARY AND ITINERARY

The expedition PS103 to the Antarctic took *Polarstern* from Cape Town, South Africa, via the German *Neumayer Station III*, Antarctica, to the Weddell Sea and on to Punta Arenas, Chile (Fig. 1.1). The expedition comprised logistic and scientific undertakings. Thereof, the logistic tasks (provision of *Neumayer III* with fuel and supplies) were fully achieved. Nearly all scientific tasks were completed, based on the well-proven collaboration between the crew and the scientific party. In particular, we successfully retrieved several deep-sea moorings deployed in 2010 and 2012, which had to be left untouched in 2014 due to the early cessation of the *Polarstern* PS89 expedition.

The scientific work may be divided into station bound, sea ice-based, underway and helicopter-borne studies. The following activities were conducted on station:

- Casting 53 CTD stations with rosette sampler and I-ADCP;
- 41 net hauls using the hand net;
- 3 net hauls using the mulit-net (S3);
- 50 net hauls using the bongo net;
- Recovery of 1 Pressure sensor equipped Inverted Echosounder (PIES);
- Recovery (17) and deployment (18) of oceanographic deep-sea moorings;
- 13 calibrations of RAFOS sound sources;
- 6 ROV deployments (3 tests, 3 missions);
- Deployment of 12 Argo floats;
- 1 test of acoustic releases.

The following tasks were executed while underway:

- Continuous measurements of temperature, salinity and upper ocean velocities;
- 7 air samplings for gaseous ammonia and particulate ammonium;
- Flow-through sampling of near-surface waters for NH₄;
- Sampling (and to a large part phytooptic analysis) of 294 near-surface flow-through samples and 142 samples from the CTD;
- Analysis of 40 water samples from 15 stations for salinity;
- 190 lab experiments on biological samples.

Additional studies were sea-ice borne:

- Installation of 2 ice observatories.

Finally, the helicopters served as means of transport for studies set apart from the ship. In total, 19 flights of 9:14 h cumulative duration were flown:

- 2 flights for sea ice surveillance;
- 10 scientific flights (4:03 h) to deploy the sea ice observatories and to maintain the PALAOA observatory;
- 2 transports of personnel at *Neumayer III* (1:24);
- 5 training flights (2:59).

Table 1.1 shows the distribution of research times by instrument.

The *Polarstern* expedition PS103 started on 16 December 2016, 18:00 LT in Cape Town, South Africa. Underway standard measurements as well as phytooptical and chemical analyses of near surface water samples as well as of the atmospheric boundary layer commenced when passing the South African 12-mile zone. At 45°S we started measuring CTD profiles and sampling of the entire water column, employing a rosette sampler, bongo-, multi-, and hand-nets. Both, underway and station-bound sampling, was continued without constraints throughout the remainder of the expedition until reaching Drake Passage. In particular, CTDs were cast at all mooring positions, south of 65°S along the Greenwich meridian at 30 nm intervals, and up the continental slope to the tip of the Antarctic Peninsula with station spacing of 15 nm.

At 49°S we took up this expedition proposal's primary tasks, a comprehensive turn-around of the deep-sea moorings of the oceanographic HAFOS observatory. The first candidate was a PIES deep-sea pressure gauge, which, in spite of its deployment period of 6 years, was retrieved without problems. This year's extraordinarily low ice cover facilitated our fast progress along the 0°-section towards the South. Even at the southernmost extreme of this section, open waters prevailed, which allowed recovering a mooring, which had failed to surface during previous recovery efforts in 2012 and 2014, by "tucking". The 0°-section was completed on 31 December 2016, our arrival at Atka Bay however was postponed due to bad weather conditions there, allowing to first retrieve 2 more mooring north of Neumayer Station. On 4 January 2017 early in the morning, *Polarstern* had docked the Atka Bay's north-eastern berth, ready to resupply Neumayer Station. The loading operations progressed quickly, building on a well-proven collaboration between the ship's crew and the Neumayer team. Loading was completed by 6 January 2017 18:00, however, the ship was trapped by old, thick fast-ice floes, preventing its departure until 9 January, noon, consuming 2.5 research days. In the central Weddell Sea, deck-bound research had to be interrupted for another 3 days, when small amounts of oil leaked, the source of which had to be investigated. After the leakage was identified and attended to (a small fracture in an overflow pipe from a ballast water tank to the outside, which however, crossed a fuel tank), the research programme was resumed on 18 January 2017, 13:00.

Throughout the Weddell Sea, ice-resilient Argo floats were deployed to provide year-round profiles of salinity and temperature covering the upper 2,000 m. To position these whilst under the seasonal sea ice cover, additional moorings were deployed along a zigzag course towards the Antarctic Peninsula. When several moorings (of 4-6 years deployment period) failed to

respond to the release commands, our new MicroROV Seabotix vLBV300 was set to mission for the very first time. The ROV was used to attach a recovery rope to the mooring rope. This was executed successfully on all three attempts within short time. Piloting of the ROV thereby is based on data from POSIDONIA and GAPS, as well as sonar and video images provided by the ROV. It should be noted, that throughout the entire expedition, the unrestricted and reliable use of the hull-mounted POSIDONIA and GAPS (in the ship's well) provided the basis for the successful deployment of the ROV but also for expedient mooring recoveries in general.

After crossing of the Weddell Sea, the expedition came to a close with a mooring deployment near Elephant Island, as well as some final sampling of the water column in Drake Passage. A GPS station, to be recovered on Gibbs Island, had to be left in place due to bad weather. The expedition ended on 2. February 2017 11:00 LT in Punta Arenas (Chile).

Tab. 1.1: Verteilung der Forschungszeiten nach Gerät

Tab. 1.1: Distribution of reasearch times by instrument

Instrument	Anzahl	Gesamtzeit [dd hh:mm]
CTDs	53	4 05:36
Handnetze	41	0 02:35
Multinetz (S5)	3	0 01:52
Bongo Netze	50	0 18:21
PIES Aufnahmen.	1	0 02:11
Verankerungen (Aufnahme & Auslage)	38	4 08:44
Kalibration von Schallquellen	14	0 17:26
ROV	6	0 05:29
Ice stations	2	0 01:04
Float deployments	12	0 00:00
Test of releases	1	0 02:37
SUMME	221	10 18:55

2. WHEATHER CONDITIONS

Max Miller, Hartmut Sonnabend

DWD

On Friday evening, December 16 2016, 18:00 pm, *Polarstern* left Cape Town for the campaign PS103. Light and variable winds, 22° C and sunny skies were observed.

The subtropical high built a ridge towards the ocean south of Africa. Right after leaving the harbour we met the Cape-Doctor – a local wind system. For 4 hours winds peaked around Bft 7 and evened out at Bft 4 afterwards.

On Saturday (Dec. 17) a low formed southwest of Gough Island. It deepened rapidly to a storm and moved east. During the night to Monday (Dec. 19) *Polarstern* reached its northwest side. Westerly winds freshened and peaked at Bft 9 on Monday morning causing a sea state of 7 m. In the afternoon the storm moved away and winds clearly abated.

On our way more south, lows crossed the track of *Polarstern*. However, winds increased only for short times up to Bft 7 to 8 combined with as nearing 4 m. South of 60°S winds veered more and more towards East.

On Wednesday morning (Jan. 04) we reached *Neumayer Station III* at abating easterly winds. During the second half of the week cargo work was conducted under light and variable winds. But on Sunday (Jan. 08) and Monday the strengthening Antarctic High and a storm west of Bouvet Island caused an increase of the easterly winds along the ice edge up to Bft 6.

On Tuesday (Jan. 10) and Wednesday we observed only light and variable winds while a following ridge crossed our area.

A new low had arrived at the northern end of Antarctic Peninsula and slowly moved towards Weddell Sea. on Thursday (Jan. 12). *Polarstern* operated at its southeast side with freshening winds up to Bft 7. On Saturday (Jan. 14) we reached its centre area and winds calmed down.

Another low moved from Drake Passage towards the South Orkney Islands. On Tuesday (Jan. 17) it headed slowly further southeast while weakening. Winds from Northeast to East did not exceed Bft 6 and starting on Friday (Jan. 20) it continued to abate. Therefore the sea state rose up to 3 m only for short times. During the upcoming weekend, weak pressure gradient was present over Weddell Sea.

On Monday (Jan. 23) a low formed near Cape Horn, moved east and intensified. On Wednesday (Jan. 25) we were located at its edge for short and south to south-westerly winds peaked at Bft 6. During the night to Thursday the following ridge caused mostly calm conditions.

A new storm west of Drake Passage moved towards Bellingshausen Sea. From Thursday (Jan. 26) on we operated at its east side. During the weekend winds veered west and freshened often up to Bft 7. Starting on Sunday (Jan. 29) evening *Polarstern* crossed the Drake Passage at westerly winds Bft 7 to 8. The sea state did not exceed 4 m. Winds veered northwest and abated but remained gusty as we arrived at the eastern entrance of the Strait of Magellan.

On Thursday morning, February 02, 2017, *Polarstern* reached Punta Arenas at temporarily gusty (around Bft 7) winds from northwest.

Weather statistics of this expedition are provided in Fig. 2.1 - Fig. 2.4.

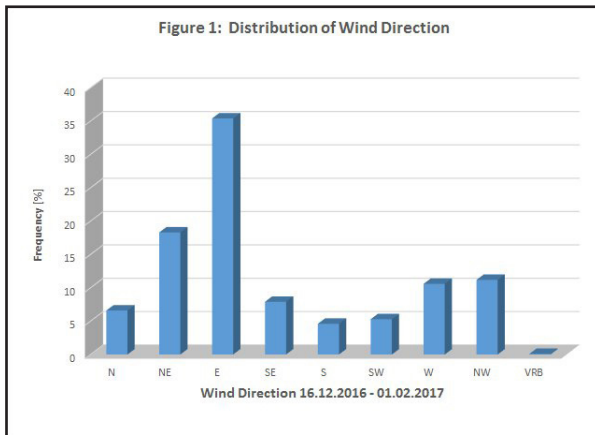


Fig. 2.1: Distribution of wind directions during PS103

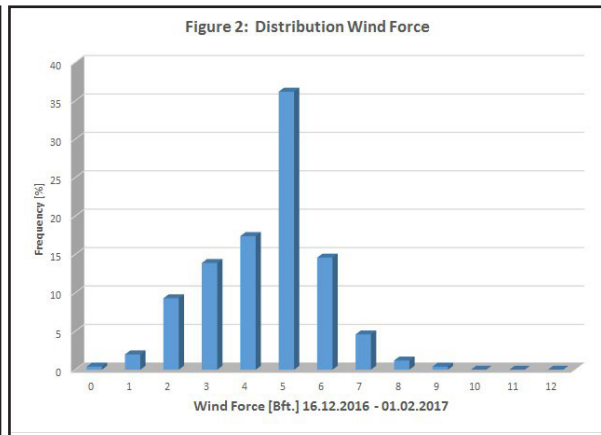


Fig. 2.2: Distribution of wind force during PS103

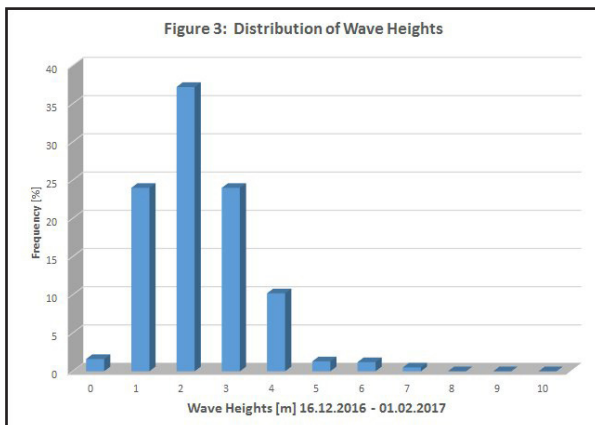


Fig. 2.3: Distribution of wave heights during PS103

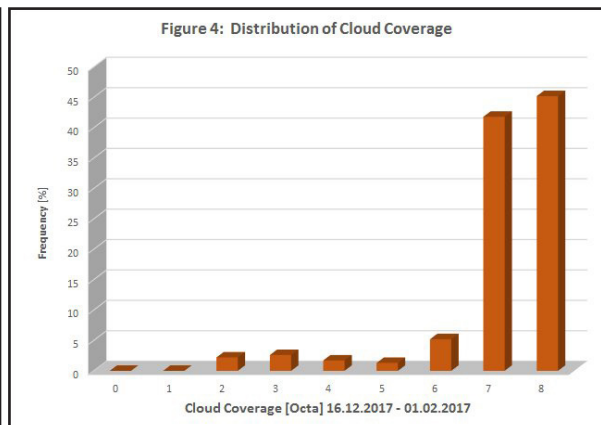


Fig. 2.4: Distribution of cloud coverage during PS103

3. SCIENTIFIC PROGRAMMES

3.1 HAFOS: Maintaining the AWI's Long Term Ocean Observatory in the Weddell Sea

3.1.1. Physical oceanography

Olaf Boebel¹, Jakob Allersholt^{1,2}, Maria Falla¹,
Rainer Graupner¹, Frieder Hamm^{1,3}, Hendrik
Hampe^{1,2}, Ioana Ivanciu^{1,4}, Katrin Latarius¹,
Matthias Monsees¹, Nicolas le Paih¹, Gerd
Rohardt¹, Mathias Rucker van Caspel¹, Stefanie
Spiesecke¹, Sandra Tippenhauer¹, Sarah
Zwicker¹

¹AWI
²HS B'hvn
³BLE
⁴CAU / GEOMAR
⁵Uni Bremen

Grant No: AWI_PS103_01

Outline and objectives

Due to its ability to internally store and transport vast amounts of heat and CO₂, the ocean is a key element of the global climate system. Its response to changes in the forcing is expressed and controlled by its stratification, which is governed by the vertical distribution of temperature and salinity. Until the turn of the century, shipborne observations had been the only means of obtaining sufficiently accurate vertical profiles of water mass properties, but progress in sensor technology now allows using automated systems. The current backbone of the Global Ocean Observing System (GOOS) is the Argo system, which consists of an array of more than 3,000 profiling floats, distributed throughout the world oceans. Provided by an international group of oceanographic institution, it aims at establishing a real-time data stream of mid- and upper (< 2,000m) ocean temperature and salinity profiles augmented by a mid-depth oceanic circulation pattern due to the floats' intrinsic drift between profiles.

However, Argo in its current form is restricted to oceanic regions that are ice free year-round, as the floats need to surface to be localized and to transmit their profile data via satellite link. HAFOS (Hybrid Antarctic Float Observing System) constitutes an extension of this system into seasonally ice-covered waters of the Weddell Gyre, overcoming these limitations through a combination of well tested technologies to close the observational gaps in the Antarctic Ocean. To this end, AWI pushed technological developments to extend the operational range of Argo floats into seasonally ice-covered regions by initiating the development of the NEMO float (Navigating European Marine Observer) which features an ice sensing algorithm (ISA, [Klatt et al., 2007]), triggering the abort of a floats' ascent to the sea surface when the presence of sea ice is likely as determined from the existence of a layer of near surface winter water. To be able to (retrospectively) track the floats that continued their mission under sea ice, RAFOS [Rossby et al., 1986] (Ranging And Fixing Of Sound) technology is used based on an array of currently 14 moored RAFOS sound sources (with 11 redeployed during this expedition).

To determine trends and fluctuations in the characteristics of the main Antarctic water masses (Warm Deep Water, WDW and Antarctic Bottom Water, ABW), a set of more than a dozen hydrographic moorings has been maintained and expanded throughout the past 30 years by

3.1.1 Physical oceanography

AWI. HAFOS builds on this backbone by having added RAFOS sound sources for under-ice tracking of Argo floats since 2002. Near bottom recorders continue truly climatological time series as sentinels for climate change in the formation areas of bottom waters whereas the profiling floats record the water mass properties in the upper ocean layers. Passive acoustic monitoring allows linking marine mammal distribution in the open ocean to ongoing ecosystem changes, thereby complementing the physical measurements with biosphere observations at its highest trophic level. The effort focuses on a region where year-round marine mammal observations are notoriously sparse and difficult to obtain.

HAFOS complements international efforts to establish an ocean observing systems in the Antarctic as a legacy of the International Polar Year 2007/2008 (IPY) and as a contribution to the Southern Ocean Observing System (SOOS), which is under development under the auspices of the Scientific Committee of Antarctic Research (SCAR) and the Scientific Committee on Oceanic Research (SCOR).

Work at sea

Most oceanographic instruments are, by and large, designed for deployment periods of maximal 3 years before they need to be recovered for maintenance and battery replacement. Hence, one major goal of *Polarstern* expedition PS 103 was to recover and redeploy moorings deployed during ANT-XXVII/2 (2010/11), ANT-XXIX/2 (2012/13) and ANT-XXX/2 (PS89, 2014/15) to be able to continue these observations for another 2-3 years. In addition, during transits between mooring locations, 12 NEMO floats were deployed, as previous deployments in this area date back to 2012/2013, with those floats having reached or soon will reach their end-of-life.

Hydrographic moorings

The oceanographic studies during *Polarstern* cruise PS103 concentrate on two major areas, the Greenwich Meridian and the Weddell Sea, continuing more than 30 years of *in-situ* observations in the Atlantic sector of the Southern Ocean. Moorings were exchanged to obtain time series of water mass properties throughout the deep and the surface layers. For this purpose, the moorings host current meters, temperature and salinity sensors, sound sources and passive acoustic recorders. While, during the previous expeditions ANT-XXIX/2 and ANT-XXX/2 (PS89), the recovery of moorings in ice-covered areas was significantly facilitated by using the ultra-short line positioning system (POSIDONIA), it still had not been possible to retrieve 3 moorings due to extreme ice conditions. For this reason, special equipment (an ice drill, a ROV (remotely operated vehicle) and an ATV (all-terrain vehicle) had been acquired to recover moorings directly from the sea ice and independent of the ship; see section "Mooring recovery with a ROV".

To enhance the vertical resolution and to calibrate moored sensors, CTD stations have been occupied at the mooring locations. The CTD/water sampler consists of a SBE911plus CTD system in combination with a carousel water sampler SBE32 with 24 12-l bottles. To determine the distance to the bottom, an altimeter from Benthos was mounted. A transmissometer CSTAR and a fluorometer EcoFLR from Wetlabs, and a SBE43 oxygen sensor from Seabird Electronics were incorporated in the sensor package. Additionally, a lowered ADCP system was attached to the rosette sampler to measure the current velocity profile, see Chapter Current velocity profiles measured during CTD casts with an LADCP.

To spread out CTD observations horizontally, Argo compatible NEMO floats were deployed enroute. The drift of these NEMO floats will distribute them to sampling sites across the Weddell Gyre. Moorings contain sound sources, providing RAFOS signals for retrospective under-ice positioning of NEMO floats and passive acoustic recorders to record ambient (biotic and abiotic) sounds.

3.1 HAFOS: Maintaining the AWI's long term ocean observatory in the Weddell Sea

The following three tables list the unsuccessful mooring recovery attempts in Tab. 3.1.1.1, the successful mooring recoveries in Tab. 3.1.1.2 and the moorings deployed in Tab. 3.1.1.3 during cruise PS103. A map of the mooring's locations is presented in Fig. 3.1.1.1.

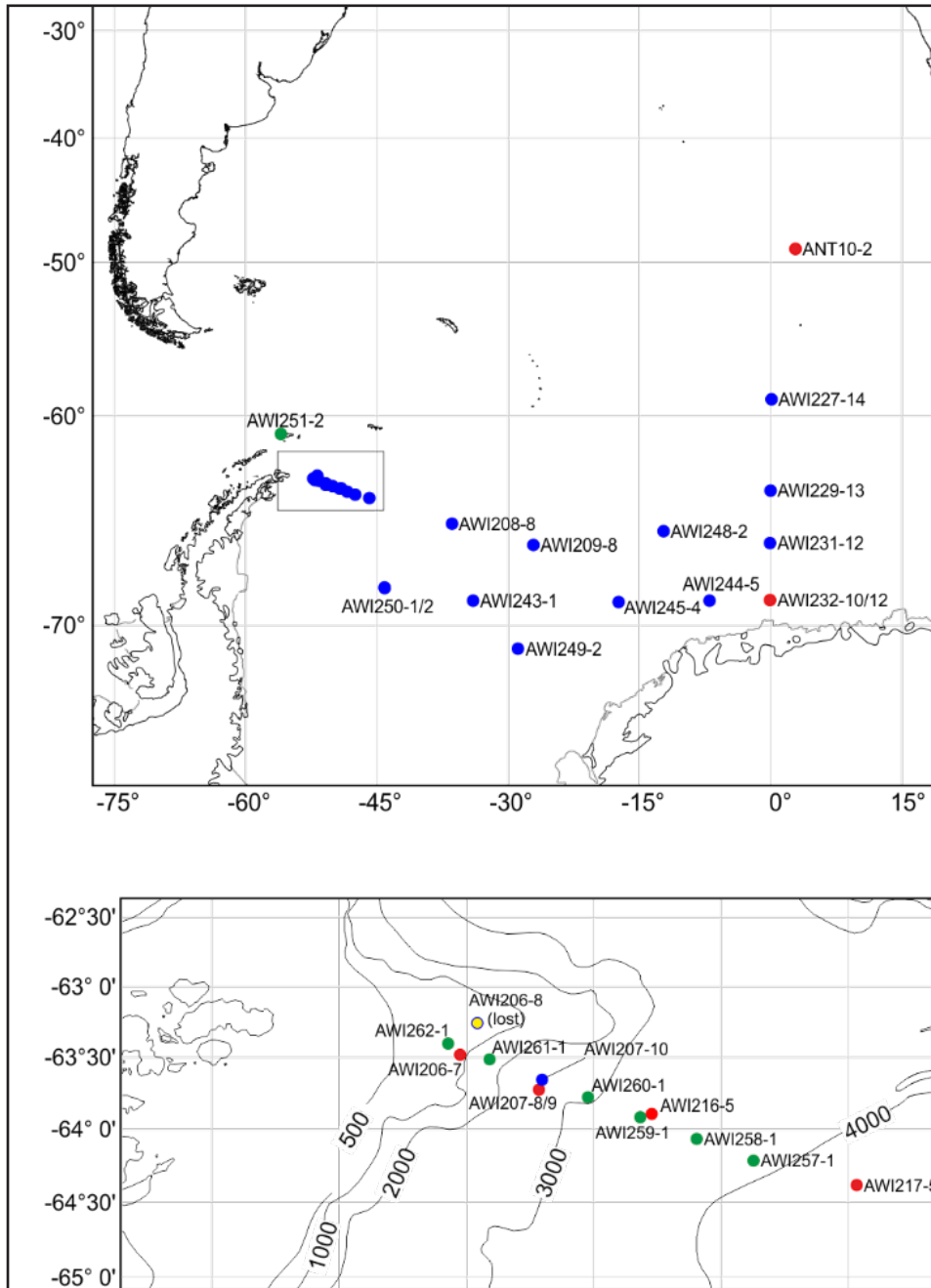


Fig. 3.1.1.1: Map of mooring locations occupied since 2014/15 or earlier. ANT10-2 is the location of the recovered PIES. The lower panel is an enlarged map, see box indicated in the top panel. Red dots indicate moorings recovered and blue dots moorings exchanged during this expedition (PS103). Newly deployed moorings are indicated as green dots while the yellow dot shows the lost mooring AWI-206-8.

Tab. 3.1.1.1: Unsuccessful mooring recoveries

3.1.1 Physical oceanography

Mooring	Latitude	Longitude	depth [m]	Deployment		Remark
AWI250-1	68° 28.95' S	44° 06.67' W	4100	05.01.2013	14:53	pending
AWI206-8	63° 15.51' S	51° 49.59' W	917	14.01.2013	06:00	lost

Tab. 3.1.1.2: Mooring recoveries during PS103

* indicates the PIES, + mooring deployed during ANT-XXIX/2, ++ mooring deployed during ANT-XXVII/2; all other moorings deployed during ANT-XXX/2 (PS89)

Mooring	Latitude	Longitude	Depth [m]	Deployment		Recovery	
ANT10-4*	49° 00.77' S	02° 50.05' E	4056	21.12.2016	13:56	06.12.2010	05:08
AWI227-13	59° 02.67' S	00° 05.37' E	4600	13.12.2014	16:37	24.12.2016	07:14
AWI229-12	63° 54.94 S	00° 00.17' W	5209	20.01.2015	11:38	26.12.2016	06:54
AWI229-11	64° 00.31' S	00° 00.22' W	5165	17.12.2014	11:43	26.12.2016	10:03
AWI231-11	66° 30.41' S	00° 00.66' W	4472	19.12.2014	18:00	28.12.2016	09:28
AWI232-12	68° 59.89' S	00° 05.00' W	3360	23.12.2014	10:00	30.12.2016	12:53
AWI232-10**	69° 00.00' S	00° 00.11' W	3344	19.12.2010	10:20	31.12.2016	11:58
AWI244-4	69° 00.34' S	06° 58.95' W	2900	16.01.2015	14:20	01.01.2017	08:55
AWI248-1+	65° 58.09' S	12° 15.12' W	5011	27.12.2012	10:00	02.01.2017	10:00
AWI245-3+	69° 03.47' S	17° 23.32' W	4746	28.12.2012	22:00	11.01.2017	08:00
AWI249-1+	70° 53.55' S	28° 53.47' W	4364	30.12.2012	14:00	13.01.2017	06:00
AWI209-7+	66° 36.45' S	27° 07.26' W	4830	01.01.2013	16:00	15.01.2017	06:00
AWI208-7+	65° 37.23' S	36° 25.32' W	4732	03.01.2013	14:00	19.01.2017	14:00
AWI217-5+	64° 22.94' S	45° 52.12' W	4410	09.01.2013	16:00	23.01.2017	08:00
AWI216-5+	63° 53.61' S	49° 05.17' W	3513	12.01.2013	02:00	24.01.2017	12:00
AWI207-8**	63° 43.20' S	50° 49.54' W	2500	06.01.2011	14:00	26.01.2017	12:00
AWI207-9+	63° 43.57' S	50° 51.64' W	2500	12.01.2013	10:00	25.01.2017	12:00
AWI206-7**	63° 28.93' S	52° 05.87' W	950	06.01.2011	22:00	27.01.2017	14:00

Tab. 3.3: Mooring deployments during PS103

Mooring	Latitude	Longitude	Depth [m]	Deployment	
AWI227-14	59° 03.03' S	00° 06.43' E	4641	24.12.2016	16:15
AWI229-13	64° 00.49' S	00° 00.84' W	5197	26.12.2016	19:25
AWI231-12	66° 31.03' S	00° 04.49' W	4577	28.12.2016	15:24
AWI244-5	69° 00.32' S	06° 59.56' W	2946	01.01.2017	16:09
AWI248-2	65° 58.12' S	12° 13.87' W	5047	01.01.2017	16:56
AWI245-4	69° 03.64' S	17° 23.45' W	4736	11.01.2017	18:20
AWI249-2	70° 53.54' S	28° 53.47' W	4401	13.01.2017	16:32
AWI209-8	66° 36.45' S	27° 07.29' W	4872	18.01.2017	15:24
AWI208-8	65° 41.79' S	36° 41.01' W	4766	19.01.2017	22:15
AWI250-2	68° 27.84' S	44° 08.71' W	4137	21.01.2017	19:09
AWI257-1	64° 12.94' S	47° 29.42' W	4293	23.01.2017	17:23
AWI258-1	64° 03.99' S	48° 22.83' W	3933	24.01.2017	08:36
AWI259-1	63° 55.02' S	49° 16.09 W	3449	24.01.2017	15:35

3.1 HAFOS: Maintaining the AWI's long term ocean observatory in the Weddell Sea

Mooring	Latitude	Longitude	Depth [m]	Deployment	
AWI260-1	63° 46.70' S	50° 05.38' W	2819	25.01.2017	08:39
AWI207-10	63° 39.36' S	50° 48.68' W	2555	26.01.2017	10:27
AWI261-1	63° 30.87' S	51° 38.14' W	1700	26.01.2017	18:55
AWI262-1	63° 24.20' S	52° 17.22' W	672	28.01.2017	09:44
AWI251-2	61° 01.26' S	55° 58.84' W	331	29.01.2017	15:36

Details regarding the instrumentation of the deployed moorings are listed in Tab. 3.1.1.4.

Tab. 3.1.1.4: Instrumentation of deployed moorings

Mooring	Latitude Longitude	Water Depth [m]	Date Time	Instrument Type	Instrument Serial Number	Instrument Depth [m]
AWI227-14	59° 03.03' S	4641	24.12.2016	PAM	1004	1070
	00° 06.43' E		16:15	SBE37	218	4597
AWI229-13	64° 00.49' S	5197	26.12.2016	RCM11	296	202
	00° 00.84' W		19:25	SBE37	1228	300
				SBE37	2089	400
				SBE37	2388	500
				SBE37	2389	600
				SBE37	8127	650
				SBE37	8128	700
				RCM11	461	709
				PAM	1053	993
				SBE37	233	5152
AWI231-12	66° 31.03' S	4577	28.12.2016	PAM	1021	223
	00° 04.49' W		15:24	PAM	1022	570
				PAM	1023	859
				PAM	1024	1064
				PAM	1026	2074
				SBE37	235	4535
AWI244-5	69° 00.32' S	2946	01.01.2017	SOSO	D0049	842
	06° 59.56' W		16:09	PAM	1057	1044
				SBE37	1232	2903
AWI248-2	65° 58.12' S	5047	01.01.2017	SOSO	D0024	833
	12° 13.87' W		16:56	PAM	1058	1035
				SBE37	1233	5003
AWI245-4	69° 03.64' S	4736	11.01.2017	SOSO	D0048	802
	17° 23.45' W		18:20	PAM	1005	1004
				SBE37	8130	4693
AWI249-2	70° 53.54' S	4401	13.01.2017	SOSO	D0028	837
	28° 53.47' W		16:32	PAM	1061	1041
				SBE37	8131	4357
AWI209-8	66° 36.45' S	4872	18.01.2017	SOSO	D0047	854
	27° 07.29' W		15:24	PAM	1008	1053
				SBE37	9487	4864
AWI208-8	65° 41.79' S	4766	19.01.2017	SOSO	D0030	830
	36° 41.01' W		22:15	PAM	1009	1032
				SBE37	9488	4758

3.1.1 Physical oceanography

Mooring	Latitude Longitude	Water Depth [m]	Date Time	Instrument Type	Instrument Serial Number	Instrument Depth [m]
AWI250-2	68° 27.84' S	4137	21.01.2017	SOSO	D0045	834
	44° 08.71' W		19:09	PAM	1003	1036
				SBE37	10931	4094
AWI257-1	64° 12.94' S	4293	23.01.2017	SOSO	D0026	803
	47° 29.42' W		17:23	SBE37	2234	200mab
				AVT	9768	150mab
				SBE39	7862	130mab
				SBE37	10948	100mab
				SBE39	7861	70mab
				AVT	9390	50mab
				SBE39	7860	40mab
				SBE37	10928	10mab
				AVT	9782	8mab
AWI258-1	64° 03.99' S	3933	24.01.2017	SBE37	9491	200mab
	48° 22.83' W		08:36	AVT	9187	150mab
				SBE39	7865	130mab
				SBE37	10939	100mab
				SBE39	7864	70mab
				AVT	9770	50mab
				SBE39	7863	40mab
				SBE37	10946	10mab
				AVT	9998	8mab
AWI259-1	63° 55.02' S	3449	24.01.2017	RCM11	506	350mab
	49° 16.09' W		15:35	SBE37	2090	300mab
				SBE39	7868	250mab
				SBE39	7867	200mab
				SBE39	7866	150mab
				RCM11	568	100mab
				SBE37	10929	99mab
				RCM11	500	40
				SBE37	2093	8mab
AWI260-1	63° 46.70' S	2819	25.01.2017	RCM11	462	350mab
	50° 05.38' W		08:39	SBE37	9832	300mab
				SBE39	7871	250mab
				SBE39	7870	200mab
				SBE39	7869	150mab
				RCM11	486	100mab
				SBE37	2092	99mab
				RCM11	504	40
				SBE37	2101	8mab
AWI207-10	63° 39.36' S	2555	26.01.2017	AVT	11613	305
	50° 48.68' W		10:27	SBE37	10930	318
				RCM11	569	808
				SOSO	D0048	959
				PAM	1029	1061
				RCM11	619	356mab
				SBE37	10947	355mab
				SBE39	7877	300mab

3.1 HAFOS: Maintaining the AWI's long term ocean observatory in the Weddell Sea

Mooring	Latitude Longitude	Water Depth [m]	Date Time	Instrument Type	Instrument Serial Number	Instrument Depth [m]
				SBE39	7876	250mab
				SBE39	7872	200mab
				AVT	10503	150mab
				SBE37	2395	149mab
				AVT	8037	40mab
				SBE37	10941	10mab
AWI261-1	63° 30.87' S	1700	26.01.2017	PAM	1011	842
	51° 38.14' W		18:55	AVT	9783	352mab
				SBE37	1234	350mab
				SBE56	6988	300mab
				SBE56	6987	250mab
				SBE56	6986	200mab
				AVT	9786	150mab
				SBE37	9490	149mab
				AVT	9997	40mab
				SBE37	10938	8mab
AWI262-1	63° 24.20' S	672	28.01.2017	AVT	8048	350mab
	52° 17.22' W		09:44	SBE37	10933	300mab
				SBE56	6991	250mab
				SBE56	6990	175mab
				AVT	8402	150mab
				SBE56	6989	100mab
				SBE37	10935	50mab
				AVT	8403	40mab
				SBE37	10936	8mab
AWI251-2	61° 01.26' S	331	29.01.2017	PAM	1031	215
	55° 58.84' W		15:36	PAM	AU0231	220
				SBE37	3814	319

Abbreviations

mab	Depth of instruments given in meters above bottom
AZFP	Acoustic Zooplankton and Fish Profiler
AVT	Aanderaa Current Meter with Temperature Sensor
DCS	Aanderaa Doppler Current Sensor
PAM	Passive Acoustic Monitor (Type: AURAL or SONOVAULT)
PIES	Pressure Inverted Echo Sounder
RCM11	Aanderaa Doppler Current Meter
SBE16	SeaBird Electronics Self Recording CTD to measure Temp., Cond. and Pressure
SBE37	SeaBird Electronics, Type: MicroCat, to measure Temperature and Conductivity
SBE39	SeaBird Electronics, to measure Temperature and Pressure
SBE56	SeaBird Electronics, to measure Temperature
SOSO	Sound Source for SOFAR-Drifter

Sound source array

A major goal of this expedition was to refurbish the sound sources used for tracking the NEMO

3.1.1 Physical oceanography

floats under the ice. Due to the early termination of the last expedition (PS89), many sound sources had been operating for 4 years and were believed to require urgent refurbishment. Surprisingly, 7 of the 11 recovered sound sources were still operational. The observed time drift of the Develogic sound sources is remarkably small (max. 10 s over 4 years). The Rossby sound sources have a programmed scheduling adjustment set (Tab. 3.1.1.5). A total of 9 new sound sources were deployed. AWI 250-01 could not be recovered. It is not known if the Webb RAFOS sound source hosted by this mooring is still operating, which is why a second sound source, hosted by mooring AWI250-02 deployed nearby, was set to a sweep time different from the Webb source. A summary of sound source activities is given in Tab. 3.1.1.5, Tab. 3.1.1.6 as well as Fig. 3.1.1.2.

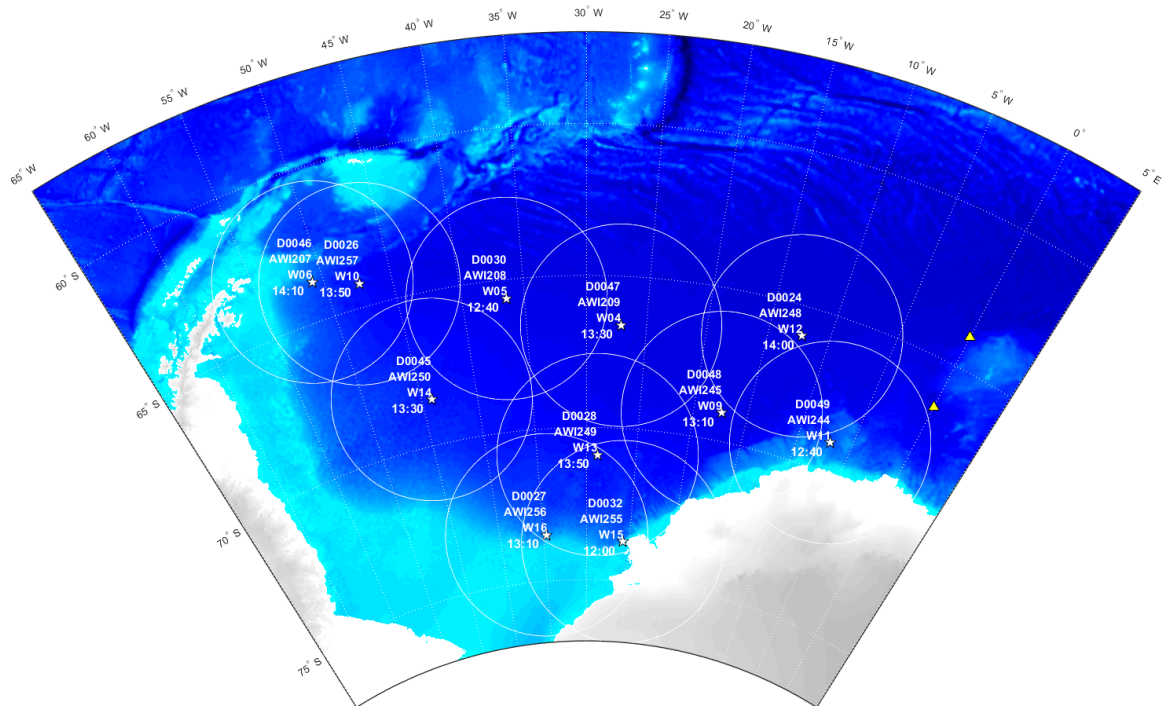


Fig. 3.1.1.2: HAFOS sound source array. White stars with concentric circles: sources (re) deployed on PS103 with 200 nm range. Left to the marked position: Serial number of sound source, mooring number, sound source position number and sweep time (GPS); Yellow triangles: Sources which were only recovered on PS103.

3.1 HAFOS: Maintaining the AWI's long term ocean observatory in the Weddell Sea

Tab. 3.1.1.5: Recovery of sound sources during PS103

Mooring /SoSo site	SN	Mooring Position Latitude Longitude	Date deploy	Date recover	Water depth [m]		Pong time [GPS]	Mission duration [days / years]	Time after recovery [GPS]	Time after recovery [Instrument]	Drift [s]	Scheduled adjustment [s] over deployment period	resulting drift in s/ day	Comments
					Deploy depth [m]	Depth [m]								
229-12 W1	D0048 E0064	63° 54.94' S 000° 00.17' W	2014-12-20	2016-12-26	5209	798	12:30	706 1.9	--	--	--	--	--	Mechanical condition good; Electronics: batteries burned out, time drift could not be checked
231-11 W2	D0026 E0066	66° 30.41' S 000° 00.66' W	2014-12-19	2016-12-28	4472	851	13:00	739 2.0	--	--	--	--	--	Mechanical condition good; Electronics: no communication established; Additional battery pack: batteries burned out
244-4 W11	D0047 E0047	69° 00.34' S 006° 58.95' W	2015-01-17	2017-01-01	2900	806	12:40	715 1.9	--	--	--	--	--	Mechanical condition good; Electronics: no communication established
248-1 W12	D0028 E0031	65° 58.09' S 012° 15.12' W	2012-12-27	2017-01-02	5011	839	14:00	1467 4.0	03.01.2017 09:19:18	03.01.2017 09:19:19	1	--	0.001	Mechanical condition good; Electronics: running, sweeps active (Checked with dummy load)
249-1 W13	D0030 E0039	70° 53.55' S 028° 53.47' W	2012-12-30	2017-01-13	4364	843	13:50	1475 4.0	13.01.2017 13:59:03	13.01.2017 13:59:13	10	--	0.007	Mechanical condition good; Electronics: running, sweeps active (Checked with dummy load)
245-3 W9	R0030 E0023	69° 03.48' S 017° 23.32' W	2012-12-28	2017-01-11	4746	822	13:10	1475 4.0	11.01.2017 10:52:18	11.01.2017 10:45:32	-406	-448.18	-0.275	Mechanical condition good; Electronics: running
209-7 W4	D0025 E0037	66° 36.45' S 027° 07.29' W	2013-01-01	2017-01-15	4830	805	13:30	1475 4.0	15.01.2017 13:22:33	15.01.2017 13:22:35	2	--	0.001	Mechanical condition good; Silicon oil leaking; Electronics: running, sweeps active (Checked with dummy load)
208-7 W5	D0029 E0036	65° 37.23' S 036° 25.32' W	2013-01-03	2017-01-19	4732	856	12:40	1477 4.0	19.01.2017 13:08:58	19.01.2017 13:08:50	-8	--	-0.005	Mechanical condition good; Silicon oil leaking; Electronics: running, sweeps active (Checked with dummy load)

3.1.1 Physical oceanography

Mooring /SoSo site	SN	Mooring Position		Date deploy	Date recover	Water depth		Pong time [GPS]	Mission duration [days / years]	Time after recovery [GPS]	Time after recovery [Instrument]	Drift [s]	Scheduled adjustment [s] over deployment period	resulting drift in s/ day	Comments
		Latitude	Longitude			Deploy depth [m]	[m]								
207-8 W6	R0032	63° 43.20' S	050° 49.54' W	2011-01-06	2017-01-26	2500	807	01:10	2212	--	--	--	--	--	Mechanical condition good; Electronics: no communication established
207-9 W6	R0027 E0028	63° 43.57' S	050° 51.64' W	2013-01-21	2017-01-25	2500	807	14:10	1475 4.0	information missing	information missing	--	341.34	--	Mechanical condition good; Electronics: running
217-5 W10	R0034 E0029	64° 22.94' S	045° 52.12' W	2013-01-09	2017-01-23	4410	807	13:50	1475 4.0	23.01.2017 12:21:18	23.01.2017 12:31:17	599	554.20	0.406	Mechanical condition good; Electronics: running

*) During deployment: GPS=UTC+16s. At recovery: GPS=UTC+18s. Sign of offsets according to "true time = instrument time + offset", hence: positive (+): unit is late, negative (-): unit is early.

¹⁾ Applies to Rossby sound sources only (Information from source internal logfile)

²⁾ Rossby schedule adjustment not included

Tab. 3.1.1.6: Deployment of sound sources during PS103. *) UTC was used for setting time: GPS= UTC +18s

Mooring / SoSo site	SN	Corr. water depth /m	LAT	LON	Deployment date	Sound source depth /m	Schedule GPS*) time	Comments
245-04 W9	D0048 EI0045	4736	69°03.64' S	017°23.45' W	2017-01-11	802	13:10	1st sweep 2017-01-12
248-02 W12	D0024 EI0049	5047	65°58.12' S	012°13.87' W	2017-01-02	833	14:00	1st sweep 2017-01-02
244-05 W11	D0049 EI0046	2946	'69°00.32' S	006°59.56' W	2017-01-01	842	12:40	1st sweep 2017-01-02
249-02 W13	D0028 EI0031	4401	'70°53.54' S	028°53.47' W	2017-01-13	837	13:50	1st sweep 2017-01-14
209-08 W04	D0047 EI0067	4872	'66°36.45' S	027°07.29' W	2017-01-18	854	13:30	1st sweep 2017-01-20
208-08 W05	D0030 EI0039	4766	65°41.79' S	036°41.79' W	2017-01-19	830	12:40	1st sweep 2017-01-20
250-02 W14	D0045 EI0060	4137	'68°27.84' S	044°08.71' W	2017-01-21	834	13:30	1st sweep 2017-01-22
257-01 W10	D0026 EI.0055	4170	'64°12.94' S	047°29.42' W	2017-01-23	923	13:50	1st sweep 2017-01-25
207-09 W06	D0046 EI0044	2490	'63°39.36' S	050°48.68' W	2017-01-26	808	14:10	1st sweep 2017-01-27

RAFOS source calibration

A detailed description of the objectives and approach of tuning the RAFOS sources *in-situ* is given in the expedition report of ANT-XXIX/2 (Boebel, 2015). During PS103, sources intended for the refurbishment of the sound source array were tuned directly at sea under hydrographic conditions similar to the deployment site. In total, 7 sound sources were subjected to tuning during 14 calibration sessions, comprising 3 previously tuned systems (D0045, D0047 and D0049) and 3 Develogic NTSS sound source systems with anodized aluminium resonator tubes (D0018, D0044 and D0046). Two of these sound sources remain in an unfinished state.

Tuning (i.e. shortening the length of a resonator tube until it resonates at the RAFOS centre frequency 265 Hz) of the new resonator tubes was performed in 3 steps as follows:

1. Determination of the frequency response of the resonator “off works” by using consecutive 5-Hz wide, 80s sweeps covering 235 Hz to 265 Hz.
2. First cutting of resonator tube by about 80 % of length reduction as estimated to reach target frequency.
3. Determination of frequency response after first cut by using five 5-Hz wide, 80s sweeps from 245 Hz to 265 Hz plus two additional RAFOS sweeps (259.38 Hz – 260.9 Hz, duration 80s).
4. Second cutting to reach target frequency.
5. Determination of frequency response of final tube length by using the same sweeps as in the step 3.

3.1.1 Physical oceanography

Sound sources were calibrated in waters of at least 2,000 m depth lowering the horizontally mounted sound sources to 800m with the CTD winch.

The first tuning session was conducted on December 30, 2016. Sound Source D0049 was lowered to 800 m with an icListen acoustic recorder (by OceanSonics, Canada) attached to the (CTD winch's) wire 45 m above the sound source. To track uncertainties in sound pressure level measurements, the sound pressure level of this previously (2014/15) tuned system was determined again (Tab. 3.1.1.8).

For the second tuning session on January 12, 2017, one acoustic recorder (icListen, by OceanSonics, Canada) was strapped onto the end of a 40 m long mooring rope below the sound source. Sampling rate was set to 3,200 Hz (no gain). To avoid entangling with the winch's wire (when the ship rolls), extra weights of 30 kg and 9 kg were added to the rope beneath the recorder. A second acoustic recorder (icListen, by OceanSonics, Canada) was attached to the wire 45 m above the sound source. A sound velocity profiler (by Valeport, UK) was attached below the weights for sound velocity and temperature measurements. Unfortunately, this session turned out to be unproductive. The first sound source (D0043) failed to produce a sweep. When switching to the second source, the upper icListen (SN1413) was removed to commence data analyses, and the remaining three sources (D0044, D0045, D0046) were tuned with only one icListen (SN1415) in the water, which failed to record throughout the entire session.

For the January 14, 2017 session, a different acoustic recorder type (SonoVault SN1009, by Develogic, Germany) was attached to the mooring line 45m below the sound source. Sampling rate was set to 6857 Hz with gain set to 29.8 dB. An additional weight of 10 kg was attached below the sound source alongside with the sound velocity profiler. The sound velocity profiler was detached after the measurement of the first sound source to save battery life and start downloading profile data. To ensure redundancy of the acoustic recordings, 3 icListen were attached 45 m above the sound source directly to the winch cable. The icListens with serial numbers 1415 and 1413 turned out to be defect and data could not be used for analysis. Therefore, only the data from icListen 1414 and SonoVault SV1009 were used for analysis.

For the tuning on the 24 and 25 of January 2017, SV1013 and SV1011 were employed, respectively, using the same recording parameters as for SV1009 before. The icListen 1414, used parallel to SV SV1011 on 25 January failed recording.

After completion of the tuning procedures, recordings from the acoustic recorder(s) were saved from their internal storage to hard disk. Using Adobe Audition, sweeps corresponding to a given sound source were manually extracted using spectrogram displays and saved as single files. Thereafter these single sweeps were merged and saved as a single file containing the complete sweep from 225 Hz to 260 Hz.

A custom MATLAB™ script was used to determine the (current) resonance frequency of the highest root-mean-square amplitude. A second MATLAB™ script used the current resonance frequency, current tube length and environmental parameters (e.g. sound velocity at tuning depth, water density) to derive the target resonance tube length and the excess length to be cut from the current tube. For tuning results see Tab. 3.1.1.8. Sound pressure levels varied between 173.3 and 176.3 dB re 1μPa @ 1m, less than the factory value of 180 dB, and with the highest value attained be the only anodized source fully tuned so far.

Tab. 3.1.1.7: Information on measurements of SPL

Sound Source serial number	State	Date	Comment	Recorder	Position Rec. relative to SoSo [m]	Recording
D0049	RFS	2016-12-30	OK	icL1414	-40	ok
D0043	T3	2017-01-12	Amplifier disable error, leaking silicon oil	icL1413	+40	ok
				icL1415	-40	failed
D0044	T1	2017-01-12	Recorder failed	icL1415	-40	failed
	T1	2017-01-14	New Resonator	SV1009	-45	ok
				icL1413	+45	fail
icL1414	+45	ok				
	T2	2017-01-24	OK	SV1013	-45	ok
				icL1414	+45	ok
	T3 + RFS	2017-01-25	Electronics failed	SV1011	-45	ok
				icL1414	+45	failed
D0045	RFS	2017-01-12	Recorder failed	icL1415	-40	failed
	RFS	2017-01-14	Deployed in AWI250-02	SV1009	-45	ok
				icL1413	+45	failed
				icL1415	+45	failed
D0046	T1	2017-01-12	Recorder failed	icL1415	-40	failed
	T1	2017-01-14	New Resonator	SV1009	-45	ok
				icL1413	+45	failed
				icL1414	+45	ok
				icL1415	+45	failed
	T2	2017-01-24	OK	SV1013	-45	ok
	T3 + RFS	2017-01-25	Deployed in AWI207-09	SV1011	-45	ok
				icL1414	+45	failed
D0047	RFS	2017-01-14	Deployed in AWI209-08	SV1009;	-45m	ok
				icL1413;	+45m	fail
				icL1414;	+45m	ok;
D0018	T1	2017-01-14	New Resonator	SV1009	-45	ok
				icL1413	+45	failed
				icL1414	+45	ok

Legend: RFS: RAFOS sweep; T1,2,3: First, second or third tuning session. Recorder position relative to Sound Source: negative = below sound source on rope; positive = above sound source on wire.

3.1.1 Physical oceanography

Tab. 3.1.1.8: Tuning results and status information for PS103. Sound pressure levels in parenthesis indicate results from 2014 (ANT XXIX/2, PS89) prior to drilling the mounting holes into the resonator.

SN		Tuning 1	Tuning 2	Tuning 3	Resonance frequency in Hz	Sound pressure level [dB _{rms}]
D0049 painted	Tuning Date			30.12.2016	260.40	175.9 (175.2)
	Time 1st Sweep			18:20		
	Recorder			icListen		
	Recorder Gain /dB			--		
D0045 painted	Tuning Date	PS89	PS89	14.01.2017	260.20	173.3 (171.9)
	Time 1st Sweep			11:18:03		
	Recorder			SV1009/icL		
	Recorder Gain /dB			29.8/--		
D0044 anodized	Tuning Date	14.01.2017	24.01.2017	-		
	Time 1st Sweep	12:32:38	16:58			
	Recorder	SV1008/icL	SV1013			
	Recorder Gain /dB	29.8/--	41.44			
D0047 painted	Tuning Date	PS89	PS89	14.01.2017	260.60	174.8 (174.7)
	Time 1st Sweep			14:02:43		
	Recorder			SV1009/icL		
	Recorder Gain /dB			29.8/--		
D0018 anodized	Tuning Date	14.01.2017	-	-		
	Time 1st Sweep	15:11:55				
	Recorder	SV1009/icL				
	Recorder Gain /dB	29.8/--				
D0046 anodized	Tuning Date	14.01.2017	24.01.2017	25.01.2017	261.00	176.3
	Time 1st Sweep	09:40:00	18:20	15:26:49		
	Recorder	SV1009/icL	SV1013	SV1011		
	Recorder Gain /dB	29.8/--	41.44	41.5		

CTD observations

CTD casts were conducted pursuing three independent objectives:

- To revisit the spatially highly resolved repeat CTD section along the Greenwich meridian, mainly the southern inflow branch, after two years;
- To collect temperature and salinity data at PIES and mooring positions for the estimation of the drifts of the moored sensors;
- To revisit the spatially highly resolved repeat CTD section at the tip of the Antarctic Peninsula, after four years.

Time constraints did not allow repeating the complete Greenwich section's from 55°S southwards. As soon as it became obvious that favourable sea ice conditions will prevail almost along the entire cruise route, deep CTDs were carried out along the southern inflow branch by approximately 30 nm distance.

The rosette assembly comprised a SBE 911plus CTD system, combined with a carousel type SBE32 with 24 Niskin water samplers of 12 litre volume. Additionally, the assembly was equipped with an oxygen sensor SBE43, a Wetlabs C-Star transmissometer (wave length 650 nm; path length 25 cm), a Wetlabs Eco-FLR fluorometer, and a Benthos/DataSonics altimeter type PSA 916D.

CTD data was logged with Seabird's SeaSaveV7 data acquisition software to a local PC in raw format. ManageCTD, a Matlab™ based script developed at AWI, was employed to execute Seabird's SBEDataProcessing software, producing CTD profiles adjusted to 1-dbar intervals. ManageCTD additionally embedded metadata (header) information extracted from the DShip-ActionLog before conducting a preliminary de-spiking and data validation of the profile data.

Pre-processed data were saved in OceanDataView compatible format, to provide near real-time visualization of e.g. potential temperature and salinity, particularly to provide enroute (i.e. during the expedition) visualization of the unfolding hydrographic section.

The CTD was equipped with double sensors (Tab. 3.1.1.8) for temperature (SBE3plus) and conductivity (SBE4C). These sensors were calibrated prior to the expedition. Enroute comparison of the calibrated sensors nevertheless revealed differences of about of 2 mK in temperature and 1 $\mu\text{S}\cdot\text{cm}^{-1}$ in conductivity for *in-situ* measurements between the sensors.

Tab. 3.1.1.9: CTD-Sensor configuration

	#1 (primary); calibrated	#2 (secondary); calibrated
Temperature (SBE3plus)	2678; 13-Aug-2016	5027; 12-Aug-2016
Conductivity (SBE4c)	2618; 26-Jul-2016	2325; -Jul-2016

During this expedition, data from 43 full ocean depth CTD profiles were collected (Tab. 3.1.1.10). In addition, 10 shallow CTDs were cast to take water samples by other groups. A map of location of the CTD stations is presented in Fig. 3.1.1.3.

3.1.1 Physical oceanography

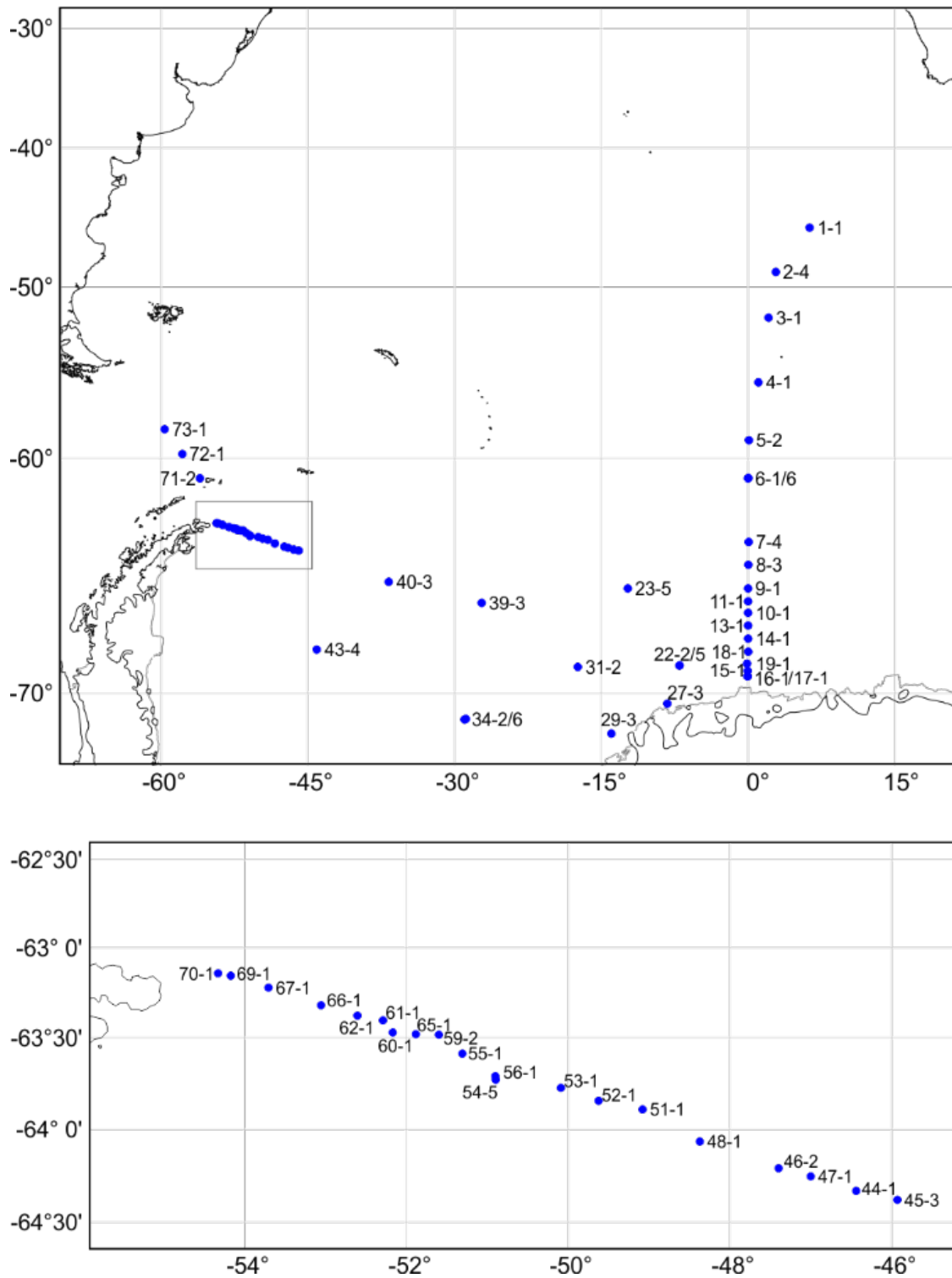


Fig. 3.1.1.3: Top: Map of locations of CTD stations. Labels indicate station and cast numbers as given in the station list. Bottom: Enlarged map of the CTD section at the tip of the Antarctic Peninsula; see box in map on top.

3.1 HAFOS: Maintaining the AWI's long term ocean observatory in the Weddell Sea

Tab. 3.1.1.10: List of CTD profiles taken during PS103. Mooring labels (last column) printed in plain font indicate mooring recoveries, bold print indicates mooring deployments

Station	Date/Time	Latitude	Longitude	Depth [m]	Alti- meter [m]	Max. Pres. (dbar)	Mooring
1-1	20-Dec-2016 13:22	45 57.294 S	6 17.238 E			305	
2-4	21-Dec-2016 18:17	49 0.834 S	2 50.226 E	4058	10	4104	
3-1	22-Dec-2016 13:30	51 59.610 S	2 6.012 E	2833		303	
4-1	23-Dec-2016 13:18	55 52.650 S	1 3.336 E	4088		304	
5-2	24-Dec-2016 11:25	59 2.958 S	0 4.668 E	4652	10	4704	AWI227-13/14
6-1	25-Dec-2016 10:02	61 0.018 S	0 0.018 W	5392	8	5477	
6-6	25-Dec-2016 13:42	60 58.296 S	0 1.302 E	5395		101	
7-4	26-Dec-2016 20:46	63 59.772 S	0 3.882 E	5197	44	5276	AWI229-11/12/13
8-3	27-Dec-2016 06:32	65 0.108 S	0 1.908 E	3710	22	3727	
9-1	27-Dec-2016 15:10	66 0.126 S	0 0.276 E	3425	7	3430	
10-1	28-Dec-2016 00:07	67 0.024 S	0 0.210 E	4709	10	4760	
11-1	28-Dec-2016 07:33	66 32.214 S	0 0.570 E	4593	10	4638	AWI231-11/12
13-1	28-Dec-2016 23:43	67 30.000 S	0 0.042 W	4634	7	4683	
14-1	29-Dec-2016 05:37	68 0.528 S	0 0.024 E	4511	10	4551	
15-1	29-Dec-2016 16:14	69 12.276 S	0 1.710 W	2818	10	2816	
16-1	29-Dec-2016 19:33	69 24.204 S	0 2.598 W	1974	7	1960	
17-1	29-Dec-2016 21:11	69 24.264 S	0 3.246 W	1961		1013	
18-1	30-Dec-2016 05:31	68 29.952 S	0 1.950 E	4267	6	4300	
19-1	30-Dec-2016 11:04	68 56.730 S	0 5.790 W	3519	9	3523	AWI232-10/12
22-2	01-Jan-2017 12:30	69 0.720 S	7 1.122 W	2948	8	2937	AWI244-4/5
22-5	01-Jan-2017 16:31	69 0.582 S	6 58.698 W	2929		141	
23-5	02-Jan-2017 20:04	66 0.114 S	12 17.148 W	5043	9	5110	AWI248-1/2
27-2	09-Jan-2017 15:25	70 21.918 S	8 16.104 W	660	10	640	
29-3	10-Jan-2017 17:07	71 21.870 S	13 58.650 W	389	6	379	
31-2	11-Jan-2017 13:13	69 3.744 S	17 23.526 W	4771	2	4833	AWI245-3/4
34-2	13-Jan-2017 11:57	70 54.012 S	28 59.142 W	4408	5	4448	AWI249-1/2
39-3	18-Jan-2017 17:36	66 35.934 S	27 12.984 W	4871	8	4928	AWI209-7/8
40-3	20-Jan-2017 00:30	65 43.542 S	36 43.812 W	4762	6	4816	AWI208-7/8
43-4	21-Jan-2017 21:15	68 25.440 S	44 5.874 W	4143	9	4167	AWI250-2
44-1	23-Jan-2017 00:30	64 19.938 S	46 26.388 W	4425	5	4463	
45-3	23-Jan-2017 06:10	64 22.800 S	45 55.782 W	4453	8	4488	AWI217-5
46-2	23-Jan-2017 19:23	64 12.624 S	47 23.796 W	4224	7	4251	AWI257-1
47-1	23-Jan-2017 23:35	64 15.276 S	47 0.006 W	4322	6	4354	
48-1	24-Jan-2017 05:45	64 4.038 S	48 22.362 W	3937	8	3952	AWI258-1
51-1	24-Jan-2017 20:31	63 53.550 S	49 4.806 W	3510	3	3517	AWI216-5
52-1	25-Jan-2017 00:54	63 50.748 S	49 37.266 W	3228	7	3219	AWI259-1
53-1	25-Jan-2017 04:47	63 46.512 S	50 5.298 W	2818	7	2801	AWI260-1
54-5	25-Jan-2017 18:19	63 43.818 S	50 53.670 W	2519		328	

3.1.1 Physical oceanography

Station	Date/Time	Latitude	Longitude	Depth [m]	Alti- meter [m]	Max. Pres. (dbar)	Mooring
55-1	25-Jan-2017 20:52	63 35.262 S	51 18.378 W	2224	7	2198	
56-1	26-Jan-2017 00:09	63 42.648 S	50 53.946 W	2519	6	2498	AWI207-8/9/10
59-2	26-Jan-2017 20:17	63 28.992 S	51 35.784 W	1956	8	1931	AWI261-1
60-1	27-Jan-2017 00:12	63 28.254 S	52 10.044 W	884	7	859	
61-1	27-Jan-2017 01:47	63 24.246 S	52 17.364 W	677	9	655	AWI262-1
62-1	27-Jan-2017 04:14	63 22.686 S	52 36.204 W	498	6	480	
65-1	27-Jan-2017 18:02	63 28.818 S	51 52.854 W	1186	6	1161	AWI206-7
66-1	27-Jan-2017 23:29	63 19.224 S	53 3.198 W	458	8	438	
67-1	28-Jan-2017 03:00	63 13.338 S	53 42.168 W	315	6	301	
69-1	28-Jan-2017 16:37	63 9.390 S	54 10.140 W	250	7	239	
70-1	28-Jan-2017 17:47	63 8.550 S	54 19.602 W	285	5	271	
71-2	29-Jan-2017 16:33	60 59.952 S	56 2.094 W	772	13	738	AWI251-2
72-1	30-Jan-2017 03:20	59 46.476 S	57 49.182 W	3732		304	
73-1	30-Jan-2017 14:15	58 28.392 S	59 38.688 W	3772		310	

Salinometer measurements

To monitor the accuracy and precision of the CTD's conductivity sensors, water samples were taken on 15 deep CTD casts for salinity/conductivity measurements. Each time, double samples were drawn from the water sampler. To investigate the influence of pressure on conductivity, samples were taken at 2,000 m and >4,000 m depth. The sample location has to be within a homogeneous water layer, which are revealed by little scattering of temperature and conductivity differences between sensor pairs. Salinities of the water samples were determined on board using an Optimare Precision Salinometer (OPS). All samples were measured in five sessions. Every session started with standardization using Standard Sea Water batch no. P158; K15 = 0.99970, with expiry date 2018-03-25.

Enroute comparisons between *in-situ* CTD data and salinometer based salinity measurements of water samples indicated that the conductivity sensor (SBE4c #2618) used in the primary sensor pair featured better accuracies (Fig. 3.1.1.4, red dots). For this sensor pair, the salinity correction is constant -0.0017 for the entire cruise.

During CTD casts, temperature and conductivity differences between sensors pairs were plotted versus pressure. It was observed that the temperature difference increased with depth; see Tab. 3.1.1.11, column T0-T1. Conductivity differences between the two sensor pairs could be resolved by applying a pressure correction to the secondary temperature sensor (Fig. 3.1.1.4). The pressure correction was assumed linear and its parameters were determined empirically by minimizing differences in temperature between the two sensors. A definitive determination of the sensors' behaviour however requires post-expedition lab calibrations, for which the sensors will be returned to Seabird Electronics after PS105. Hence all results reported hereinafter are preliminary.

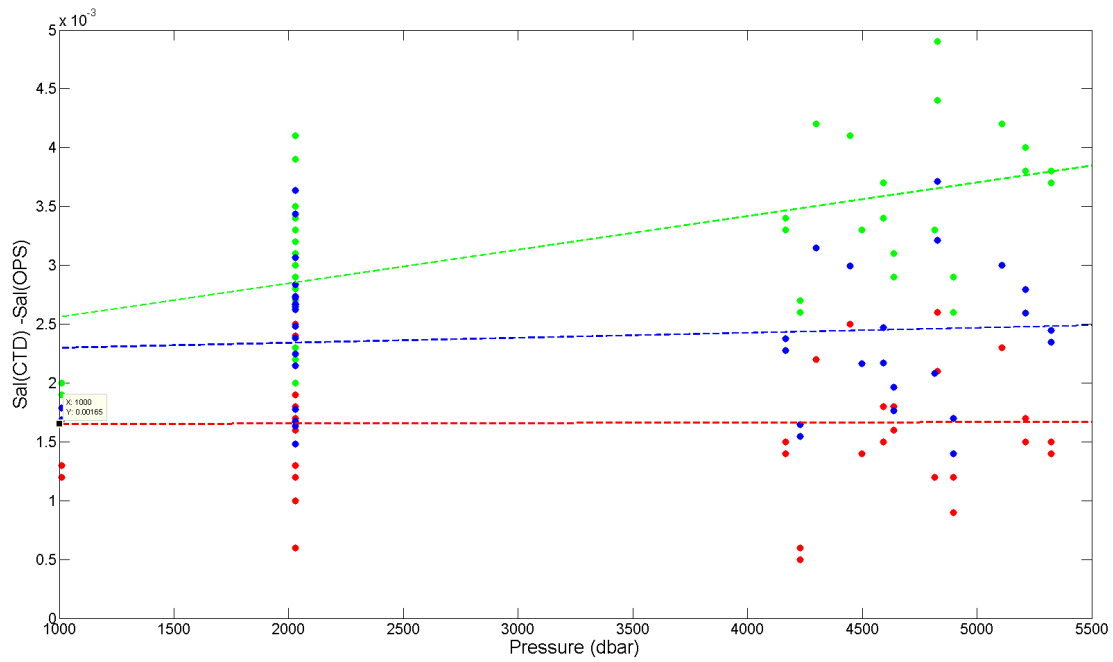


Fig. 3.1.1.4: Deviation in salinity between OPS measurements and in-situ CTD measurements for samples from 1000, 2000 and below 4000 m depth. Red dots showing the deviation calculated from the salinity sensor of the primary sensor pair, green dots from the salinity sensor of the secondary sensor pair. The blue dots show the salinity deviation after correction of the pressure effect on the secondary temperature sensor. The dashed lines displayed the corresponding regressions.

Tab. 3.1.1.11: Salinity samples from the water sampler and measured with the OPS

Stat.	Date/Time	Press	S0	S1	SAL _{OPS}	S0-OPS	S1-OPS	T0-T1	C0-C1
2_4	21.12.2016	4061	34,6876	34,6886	34,6878	-0,0002	0,0008	0,0016	0,0006
					34,6874	0,0002	0,0012		
					34,6875	0,0001	0,0011		
5_2	24.12.2016	4591	34,6482	34,6501	34,6467	0,0015	0,0034	0,0024	0,0007
					34,6464	0,0018	0,0037		
6_1	25.12.2016	5325	34,6466	34,6489	34,6452	0,0014	0,0037	0,0029	0,0007
					34,6451	0,0015	0,0038		
7_4	26.12.2016	5210	34,647	34,6493	34,6453	0,0017	0,004	0,0031	0,0007
					34,6455	0,0015	0,0038		
		2030	34,6704	34,6718	34,6687	0,0017	0,0031	0,0021	0,0007
					34,6686	0,0018	0,0032		
11_1	28.12.2016	4638	34,6538	34,6551	34,6522	0,0016	0,0029	0,0018	0,0005
					34,652	0,0018	0,0031		
		1012	34,6896	34,6903	34,6884	0,0012	0,0019	0,0017	0,0009
					34,6883	0,0013	0,002		
14_1	29.12.2016	4498	34,6538	34,6557	34,6524	0,0014	0,0033	0,0016	-0,0001

3.1.1 Physical oceanography

Stat.	Date/Time	Press	S0	S1	SAL _{OPS}	S0-OPS	S1-OPS	T0-T1	C0-C1
					34,6524	0,0014	0,0033		
		2030	34,6707	34,6723	34,6691	0,0016	0,0032	0,0020	0,0005
					34,6691	0,0016	0,0032		
18_1	30.12.2016	4298	34,6541	34,6561	34,6519	0,0022	0,0042	0,0024	0,0004
					34,6519	0,0022	0,0042		
		2029	34,6702	34,6718	34,6685	0,0017	0,0033	0,0015	0,0001
					34,6684	0,0018	0,0034		
22_2	01.01.2017	2030	34,6667	34,6679	34,6648	0,0019	0,0031	0,0021	0,0008
					34,6644	0,0023	0,0035		
23_5	02.01.2017	5109	34,6471	34,649	34,6448	0,0023	0,0042	0,0023	0,0004
					34,6448	0,0023	0,0042		
		2030	34,6675	34,6681	34,6651	0,0024	0,003	0,0008	0,0003
					34,6652	0,0023	0,0029		
31_2	11.01.2017	4828	34,6484	34,6507	34,6463	0,0021	0,0044	0,0027	0,0005
					34,6458	0,0026	0,0049		
		2030	34,6699	34,6716	34,6677	0,0022	0,0039	0,0023	0,0006
					34,6675	0,0024	0,0041		
34_2	13.01.2017	4447	34,6518	34,6534	34,6493	0,0025	0,0041	0,0034	0,0016
					34,6493	0,0025	0,0041		
		2030	34,6712	34,6719	34,6687	0,0025	0,0032	0,0020	0,0012
					34,6687	0,0025	0,0032		
39_3	18.01.2017	4895	34,6423	34,644	34,6414	0,0009	0,0026	0,0024	0,0007
					34,6411	0,0012	0,0029		
		2030	34,6659	34,667	34,6643	0,0016	0,0027	0,0027	0,0015
					34,6642	0,0017	0,0028		
40_3	19.01.2017	4815	34,6439	34,646	34,6427	0,0012	0,0033	0,0030	0,0010
					34,6427	0,0012	0,0033		
		2030	34,6659	34,6669	34,6647	0,0012	0,0022	0,0026	0,0014
					34,6646	0,0013	0,0023		
43_4	21.01.2017	4167	34,648	34,6499	34,6466	0,0014	0,0033	0,0026	0,0007
					34,6465	0,0015	0,0034		
		2030	34,6694	34,6706	34,6684	0,001	0,0022	0,0019	0,0008
					34,6684	0,001	0,0022		
46_2	23.01.2017	4229	34,6448	34,6469	34,6443	0,0005	0,0026	0,0020	0,0001
					34,6442	0,0006	0,0027		
		2030	34,6676	34,669	34,667	0,0006	0,002	0,0012	0,0000
					34,667	0,0006	0,002		

Current velocity profiles measured during CTD casts with an LADCP

The lowered ADCP system (LADCP) consist of two RDI Workhorse Monitor ADCP 300 kHz including the external battery housing where attached to the CTD/Water Sampler in a master and slave configuration. The master – SN 23293 – was the downward looking and the slave – SN 23292 – was the upward looking ADCP. The external battery was placed at a distance off the ADCPs, sufficient to avoid any influence on the compasses inside the ADCPs. All 24 bottle sites were available for water sampling due to a new ADCP mounting which does not occupy the space of a water sampler bottle.

The ADCPs where operated using the LADCP tool V1.7 from GEOMAR. The used settings and commands are given in Tab. 3.1.1.12 below.

Tab. 3.1.1.12: Settings and commands for the LADCP

```
flow_control=11101
pings_per_ensemble=1
time_between_pings=0
time_per_ensemble=1.2
master_slave=1
wait_ensembles_before_sync=0
master_slave_when_to_sync=011
wait_time_before_sync=5500
power_output=255
[Slave-Commands]
mode_15=1
ambiguity_velocity=250
bin_number=20
bin_length=1000
blank_after_transmit=0
broadband=1
sensor_source=0111101
coordinate_transformation=00111
flow_control=11101
pings_per_ensemble=1
time_between_pings=0
time_per_ensemble=1.2
master_slave=2
master_slave_when_to_sync=011
wait_time_before_start_without_sync=200
power_output=255
```

3.1.1 Physical oceanography

The software “Net Time Server” was used for time synchronisation of the LADCP with the ship’s UTC time server from station 1 to 22. The programme’s trial version expired on 1.01.2017. From that time on until the end of the cruise, the LADCP computer time was synchronized with the ships NTP server directly (server 192.168.20.3).

Processing of the LADCP data was conducted using the GEOMAR LADCP processing version 10.21 from April 2016. This routine requires input from the CTD, which was provided using a data conversion programme called prladcp running on the LADCP computer. The routine prladcp executes the Seabird® software SBEdataprocessing and initiates the steps datcnv, celltm, binavg, and trans. The resulting data file is a 1-second time series of the CTD down-and up cast. In addition, the corresponding CTD profile data is required at a resolution of 1 dbar. This file is provided by the programme ManageCTD running on the CTD-computer.

The NMEA navigational data string needs to be recorded throughout the CTD cast. For this purpose, the respective option must be selected in Seabird® software SeasaveV7, which was used for CTD data acquisition. This selection had not been made for the first 6 profiles, requiring manual entering of the start and stop positions and maximum depth to process LADCP profiles. Current profiles from the vessel mounted ADCP were merged into data processing too; see section Vessel mounted ADCP”.

During station numbers 22 to 40 a wing was attached at the frame of the water sampler to reduce the rotation during the up- and down cast. However, this did not seem to improve the data quality and the wing was removed again. Rather, we identified the small amount of scatterers in the water column as the most likely source of the poor data quality. The range was often less than 150 m due to weak backscatter, while 200 m is the limit for a good quality. The small amount of particles was confirmed by the C-STAR transmissometer readings.

Attempts were undertaken to improve the data quality by reducing the lowering speed of the CTD water sampler from usually 1.0 m/s to 0.8 m/s during stations 52, 59, 60, 61, 62 at the tip of the Antarctic Peninsula. The data quality here was significantly improved over those taken in the deep Weddell Basin. However, as the C-STAR readings also indicated significant increase of scatterers in the water column, it is impossible to decide whether the reduced lowering speed is responsible because along the section.

Tab. 3.1.1.13: Allocation between CTD Station and LADCP profile number.

Station	LADCP profile number	Comment
1-1	1	
2-4	2	
3-1	3	
4-1	4	
5-2	5	
6-1	6	
6-6	-	no ladcp because only to 40m
7-4	7	
8-3	8	
9-1	9	
10-1	10	
11-1	11	
13-1	12	
14-1	13	

3.1 HAFOS: Maintaining the AWI's long term ocean observatory in the Weddell Sea

Station	LADCP profile number	Comment
15-1	15	
16-1	16	
17-4	-	no ladcp
18-1	17	
19-1	18	
22-2	19	
22-5	22	
23-5	23	
27-2	27	
29-3	28	
31-2	31	
34-2	34	
34-3	-	no ladcp because only to 40m
39-3	39	several files exist due to the delay of station 39 caused by the leakage
40-3	40	
43-4	43	
44-1	44	
45-3	45	
46-2	46	
47-1	47	
48-1	48	
51-1	51	
52-1	52	
53-1	53	
54-5	54	
55-1	55	
56-1	56	
59-2	59	
60-1	60	
61-1	61	
62-1	62	
65-1	65	
66-1	66	
67-1	67	
69-1	69	
70-1	70	
71-2	71	
72-1	72	
73-1	73	

3.1.1 Physical oceanography

Vessel mounted ADCP

The vessel mounted ADCP (VM-ADCP) is installed in the ship's hull and protected by an acoustic window. The ADCP measures vertical profiles of upper ocean velocities throughout the expedition. Measurements commenced when leaving the EEZ of South Africa and ended prior to entering the EEZ of Argentina/Chile. The VM-ADCP operated with the configuration given in Tab. 3.1.1.14. On board data processing was conducted using the GEOMAR software sadcp to guarantee compatibility with the LADCP processing. The software was modified slightly to properly handle the turn of the year, which had not been accounted for in the original software version.

Tab. 3.1.1.14: Configuration file for the VM-ADCP during PS103

```
; Disable single-ping bottom track (BP),
; Set maximum bottom search depth to 1200 meters (BX)
BP000
;BX12000
; output velocity, correlation, echo intensity, percent good
ND111100000
; Ping as fast as possible
TP000000
; Since VmDas uses manual pinging, TE is ignored by the ADCP
; and should not be set.
;TE0000000; Set to calculate speed-of-sound, no depth sensor, external synchro heading
; sensor, pitch or roll being used, no salinity sensor, use internal transducer
; temperature sensor
EZ1011101
; Output beam data (rotations are done in software)
EX00000
; Set transducer misalignment (hundredths of degrees).
; Ignored here but set in VmDAS options.
;EA00000
; Set transducer depth (decimeters)
ED00110
; Set Salinity (ppt)
ES35
;set external triggering and output trigger; no trigger
CX0,0
; save this setup to non-volatile memory in the ADCP
CK
ADCP Command File for use with VmDas software.
;
```

```
; ADCP type: 150 Khz Ocean Surveyor
; Setup name: for Polarstern in 6/2014
; Setup type: Low resolution, long range profile (Narrowband)
;
; NOTE: Any line beginning with a semicolon in the first
; column is treated as a comment and is ignored by
; the VmDas software.
;
; NOTE: This file is best viewed with a fixed-point font (e.g. courier).
; Modified Last: 12Jun2014
;-----/
; Restore factory default settings in the ADCP
cr1
; set the data collection baud rate to 115200 bps,
; no parity, one stop bit, 8 data bits
; NOTE: VmDas sends baud rate change command after all other commands in
; this file, so that it is not made permanent by a CK command.
cb611
; Set for narrowband single-ping profile mode (NP), 100 (NN) 4 meter bins (NS),
; 2 meter blanking distance (NF), 390 cm/s ambiguity vel (WV)
WP000
NP001
NN080
NS0400
NF0400
;WV390
```

Argo float deployments

During PS103 a total of 12 NEMO floats (Navigating European Marine Observer), produced by Optimare Sensorsysteme, Germany, were deployed. All floats had been appropriated by AWI and are equipped with identical sensor suits. They feature an adjustable Ice Sensing Algorithm (ISA-2), set to -1.65°C between 40 and 10 dbar, with a surfacing response retarded by 1 profile. Interim data storage (iStore) internally saves all profiles that could not be transmitted in real-time due to ISA-triggered aborts of surfacing attempts and transmits these profiles during ice-free conditions. RAFOS technology is used for under ice tracking. For data transmission Iridium SBD is used. The floats were ballasted to drift at a depth of 800 m and acquire profiles from 2000m depth upwards every 10 days, for the first 4 profiles every 3 days. The first profile is taken directly after deployment after having sagged to 2,000 m. One additional Nemo float (S/N 275) was not deployed as the iridium antenna was broken. The deployment positions are plotted in Fig. 3.1.1.5 (with float serial numbers given as 3-digit bold numbers). Float identification information is given in Table 3.1.1.15, sorted by time of deployment.

3.1.1 Physical oceanography

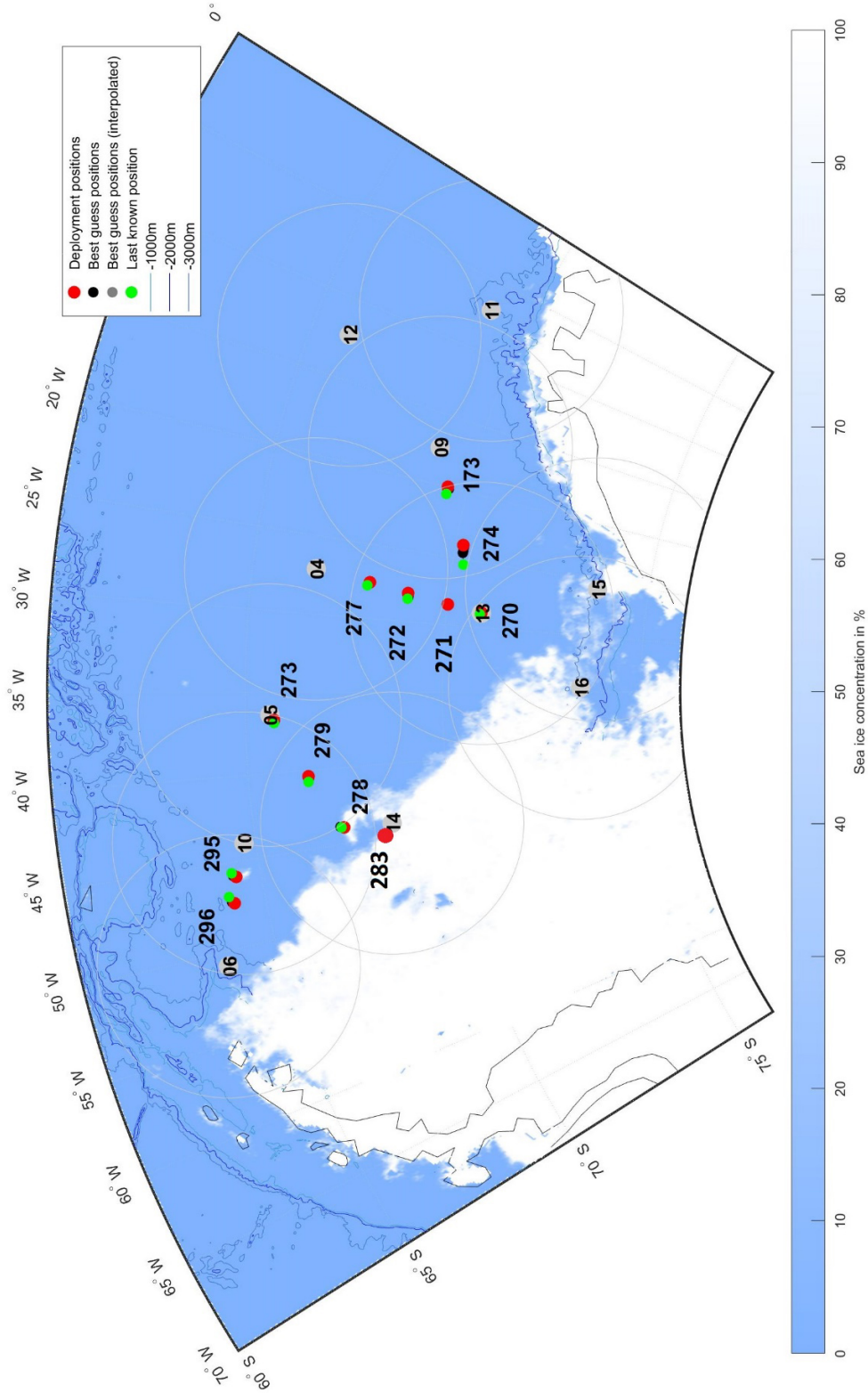


Fig. 3.1.1.5: Positions of NEMO float deployments. Three digit numbers indicate each NEMO's S/N. Position and range of sound sources are indicated by grey dots (with two digit numbers) and circles. Sea ice concentration from the University of Bremen (http://www.iup.uni-bremen.de:8084/amr2/Antarctic_AMSR2.hdf).

Tab. 3.1.1.15: NEMO float deployments

S/N	IMEI	WMO ID	Test ok	Magnet sweep @	Deployed @	Lat	Lon	temp water [°C]	Sea ice [%]	Ship Speed/dir [kn]/[°]	Wind Speed/dir [m/s]/[°]	Station No	Water Depth [m]	Station No of CTD
173	300 034 0136 45150	6900887	1	2017 01 11, 21:12	2017 01 12, 00:41	69°30.021'S -69.5003	19°59.161'W -19.9860	1.60	0	4.3/279	10.8/41	32_1	4688	
274	300 234 0110 86990	7900468	1	2017 01 12, 08:52	2017 01 12, 17:38	70°12.093'S -70.2016	23°55.288'W -23.9215	1.06	0	4.0/94	16.7/57	33_6	4468	
270	300 234 0111 83690	7900464	1	2017 01 13, 09:37	2017 01 13, 17:18	70°53.015'S -70.8836	28°50.034'W -28.8339	-0.86	20	4.3/83	9.5/67	34_7	4409	34_2
271	300 234 0109 85880	7900465	1	2017 01 13, 18:55	2017 01 13, 22:40	70°00.863'S -70.0144	28°29.916'W -28.4986	0.01	0	3.4/17	8.7/87	35_1	4597	
272	300 234 0110 82340	7900466	1	2017 01 13, 23:55	2017 01 14, 05:08	68°59.547'S -68.9925	27°58.338'W -27.9723	-0.82	*	3.3/356	8.2/57	36_1	4695	
277	300 234 0110 84990	7900471	1	2017 01 14, 16:22	2017 01 14, 19:56	68°00.104'S -68.0017	27°32.210'W -27.5368	-0.81	*	3.5/13	4.6/5	38_1	4730	
273	300 234 0110 86170	7900467	1	2017 01 19, 21:52	2017 01 20, 02:20	65°43.754'S -65.7292	36°43.336'W -36.7223	-0.12	0	2.4/130	8.8/61	40_5	4762	40_3
279	300 234 0110 88980	7900473	1	2017 01 20, 08:09	2017 01 20, 12:43	66°31.089'S -66.5182	40°23.258'W -40.3876	-0.30	0	4.9/243	6.8/59	41_1	4577	
278	300 234 0109 89870	7900472	1	2017 01 20, 16:22	2017 01 20, 21:43	67°16.117'S -67.2686	43°55.839'W -43.9306	-1.12	1	4.4/291	4.9/97	42_1	4037	
283	300 234 0613 16900	7900477	1	2017 01 21, 16:30	2017 01 21, 22:59	68°25.331'S -68.4220	44°05.387'W -44.0898	-1.54	50	3.2/14	3.3/105	43_7	4144	43_4
295	300 234 0613 19910	7900488	1	2017 01 23, 06:15	2017 01 23, 11:11	64°22.168'S -64.3695	45°52.764'W -45.8794	-0.61	0	2.8/181	4.1/107	45_6	4460	45_3
296	300 234 0613 17900	7900489	1	2017 01 23, 15:52	2017 01 23, 20:54	64°12.627'S -64.2105	47°23.431'W -47.3905	0.12	0	2.7/87	5.7/102	46_3	4226	46_2

3.1.1 Physical oceanography

Operational results

Hydrographic moorings

Details of the recovered moorings, their instrumentation and the length of each retrieved data record are listed in Tab. 3.1.1.16. In general, the instruments performed well, providing, with few exceptions, data for the full deployment period. Some instruments had recorded data for prolonged deployment periods of up to 6 years.

Tab. 3.1.1.16: Moorings and PIES recovered during PS103. A * indicates the PIES, + the moorings deployed during cruise ANT-XXIX/2 and ++ the moorings deployed during cruise ANT-XXVII/2. The date and time of the recovery is the date and time of the first release command.

Mooring PIES	Latitude Longitude	Water Depth [m]	Date Time a. deployed b. recovered	Instrument Type	Serial Number	Instrument Depth [m]	Record Length in days [Remarks]
ANT10-4*	49° 00.77' S	4056	21.12.2016	PIES	250	4056	[1a]
	02° 50.05' E		13:56 06.12.2010 05:08	DCS	31	4007	[1a]
AWI227-13	59° 02.67' S	4600	13.12.2014	PAM	1056	1020	[1b]
	00° 05.37' E		16:37 24.12.2016 07:14	SBE37	8125	4557	741
AWI229-12	63° 54.94 S	5209	20.01.2015	SOSO	D0048	798	[2]
	00° 00.17' W		11:38	PAM	1055	1001	[1b]
			26.12.2016 06:54	SBE37	228	5167	705
AWI229-11	64° 00.31' S	5165	17.12.2014	AVT	8395	202	739
	00° 00.22' W		11:43	SBE37	8129	203	739
			26.12.2016	SBE37	9831	300	739
			10:03	SBE37	10943	400	739
				SBE37	10944	500	739
				SBE37	11419	600	739
				SBE37	10420	700	739
				RCM 11	501	709	654
				PAM	1057	970	[1b]
				SBE37	227	5121	739
AWI231-11	66° 30.41' S	4472	19.12.2014	SOSO	D0026	851	[2]
	00° 00.66' W		18:00	PAM	1058	973	[1b]
			28.12.2016 09:28	SBE37	11421	4429	739
AWI232-12	68° 59.89' S	3360	23.12.2014	AVT	8367	290	738
	00° 05.00' W		10:00	AVT	9211	798	738
			30.12.2016	PAM	1059	999	[1b]
			12:53	RCM 11	472	1806	541
				SBE37	11422	3306	738
				RCM 11	25	3307	718
AWI232-10**	69° 00.00' S	3344	19.12.2010	ULS	69	182	[1c]
	00° 00.11' W		10:20	AVT	8400	280	1305
			31.12.2016	AVT	9219	787	1578
			11:58	PAM	1003	1288	[1b]

3.1 HAFOS: Maintaining the AWI's long term ocean observatory in the Weddell Sea

Mooring PIES	Latitude Longitude	Water Depth [m]	Date Time a. deployed b. recovered	Instrument Type	Serial Number	Instrument Depth [m]	Record Length in days [Remarks]
				RCM 11	212	1845	650
				PAM	846-I/403	2046	[3]
				SBE37	441	3290	2203 ¹
				RCM 11	216	3291	442
AWI244-4	69° 00.34' S	2900	16.01.2015	SOSO	0047	806	[2]
	06° 58.95' W		14:20	PAM	1061	998	[1b]
			01.01.2017	SBE37	12470	2857	715
			08:55				
AWI248-1+	65° 58.09' S	5011	27.12.2012	SOSO	0028	839	[2]
	12° 15.12' W		10:00	PAM	1013	1081	[1b]
			02.01.2017	SBE37	9841	4968	1467
			10:00				
AWI245-3+	69° 03.47' S	4746	28.12.2012	SOSO	23	822	[2]
	17° 23.32' W		22:00	PAM	1012	1065	[1b]
			11.01.2017	SBE37	9839	4703	1475
			08:00				
AWI249-1+	70° 53.55' S	4364	30.12.2012	SOSO	39	843	[2]
	28° 53.47' W		14:00	PAM	1014	1085	[1b]
			13.01.2017	SBE37	9847	4321	1475
			06:00				
AWI209-7+	66° 36.45' S	4830	01.01.2013	SBE16	2420	225	1475
	27° 07.26' W		16:00	PAM	1027	226	[1b]
			15.01.2017	SOSO	0025	805	[2]
			06:00	PAM	1028	1007	[1b]
				PAM	1029	2516	[1b]
				SBE37	7728	4773	<u>855</u>
				SBE37	7729	4822	<u>964</u>
AWI208-7+	65° 37.23' S	4732	03.01.2013	SBE16	1167	300	<u>1189</u>
	36° 25.32' W		14:00	SOSO	0029	856	[2]
			19.01.2017	PAM	1030	958	[1b]
			14:00	SBE37	7730	4674	<u>889</u>
				SBE37	7731	4724	<u>725</u>
AWI250-1	68° 28.95' S	4100	05.01.2013	SOSO	23	798	[4]
	44° 06.67' W		16:00	PAM	1031	1041	[4]
	tried to	recover	21.01.2017	SBE37	9848	4057	[4]
AWI217-5+	64° 22.94' S	4410	09.01.2013	SOSO	29/34	807	[2]
	45° 52.12' W		16:00	PAM	1020	960	[1b]
			23.01.2017	SBE37	9496	4316	1475
			08:00	SBE37	9497	4366	1475
				RCM11	135	4367	1227
AWI216-5+	63° 53.61' S	3513	12.01.2013	SBE37	9493	3356	1474
	49° 05.17' W		02:00	SEB37	9494	3406	1474
			24.01.2017	SBE37	9495	3456	1474
			12:00	RCM11	215	3457	835
AWI207-8++	63° 43.20' S	2500	06.01.2011	RCM11	294	255	<u>1076</u>
	50° 49.54' W		14:00	SEB37	1235	256	2211
			26.01.2017	AVT	8405	750	<u>1198</u>

3.1.1 Physical oceanography

Mooring PIES	Latitude Longitude	Water Depth [m]	Date Time a. deployed b. recovered	Instrument Type	Serial Number	Instrument Depth [m]	Record Length in days [Remarks]
			12:00	SBE37	2235	2101	<u>1810</u>
				SBE37	1605	2300	<u>612</u>
				RCM11	297	2306	<u>1971</u>
				SBE37	1607	2491	2211
				RCM11	311	2492	<u>518</u>
AWI207-9 ⁺	63° 43.57' S	2500	12.01.2013	AVT	11888	225	956
	50° 51.64' W		10:00	SEB16	2413	252	1474
			25.01.2017	RCM11	474	756	<u>566</u>
			12:00	SOSO	27	807	[1]
				PAM	1033	1012	[1]
				SBE37	7732	2102	<u>834</u>
				SBE37	7733	2300	<u>740</u>
				AVT	10530	2308	<u>1385</u>
				SBE37	9492	2489	1474
				AVT	10498	2492	<u>1422</u>
AWI206-7 ⁺⁺	63° 28.93' S	950	06.01.2011	ULS	65	143	[1]
	52° 05.87' W		22:00	AVT	8417	254	<u>1113</u>
			27.01.2017	SEB37	2723	501	[6]
			14:00	RCM11	312	502	<u>591</u>
				SBE16	2418	708	[6]
				PAM	844	709	[1]
				SBE37	2097	909	2021
				PAM	1006	912	[1]
				RCM11	313	913	<u>941</u>
AWI206-8 ⁺	63° 15.51' S	917	14.01.2013	AVT	11889	276	[5]
	51° 49.59' W		06:00	PAM	232LE	277	[5]
	try to	recover	27.01.2017	SBE16	1975	499	[5]
				RCM11	508	500	[5]
				SBE16	1976	706	[5]
				PAM	0002	907	[5]
				SBE16	1977	908	[5]
				RCM11	100	909	[5]

Remarks:

Underlined numbers of days of record length indicated shorter records due to battery or memory failures.

- [1a] see section on PIES recovery
- [1b] see section on Ocean Acoustics
- [1c] to be processed
- [2] non recording instrument
- [3] instrument lost
- [4] recovery failed
- [5] mooring lost
- [6] no data recorded

Abbreviations:

mab	Depth of instruments given in meters above bottom
AZFP	Acoustic Zooplankton and Fish Profiler
AVT	Aanderaa Current Meter with Temperature Sensor
DCS	Aanderaa Doppler Current Sensor
PAM	Passive Acoustic Monitor (Type: AURAL or SONOVAULT)
PIES	Pressure Inverted Echo Sounder
RCM11	Aanderaa Doppler Current Meter
SBE16	SeaBird Electronics Self Recording CTD to measure Temp., Cond. and Pressure
SBE37	SeaBird Electronics, Type: MicroCat, to measure Temperature and Conductivity
SBE39	SeaBird Electronics, to measure Temperature and Pressure
SBE56	SeaBird Electronics, to measure Temperature
SOSO	Sound Source for SOFAR-Drifter

The Posidonia positioning system

A detailed description of mooring recoveries under heavy sea-ice conditions is given in Boebel (2013). Essential to such recoveries is a robust and timely localization of the mooring's transponders by the Posidonia hydroacoustic positioning system. Posidonia can be operated with two different antennas. The mobile antenna, which requires installation while on station in the ship's moon pool, can be used on stations only. The installation is undertaken by 4 to 6 crew members and lasts 30 to 45 minutes. By contrast, the hull-mounted antenna is permanently installed inside the box keel and protected by a movable window. The window can be opened remotely from the ship's bridge, rendering Posidonia operational within in less than 3 minutes. During PS103 all Posidonia operations used the hull-mounted antenna. On occasion, the Posidonia electronic hung up, particularly after switching from tracking to release mode. This required the USBL-Box to be switched off and on for a reset. While on previous expeditions this required a manual shut-off at the USBL Box on the E-Deck, this now can be executed remotely from the bridge (B-Deck) on the Posidonia computer, courtesy of an app developed at sea by W. Markert.

In-situ calibration of moored instruments

All Seabird® instruments (SBE37, SBE39plus, and SBE56) were compared *in-situ* with the 911plus CTD system prior to mooring deployment or after recovery. Eight SBE37 units can be attached at a time to the frame of the water sampler. For the *in-situ* calibration the sampling interval was set to 10 seconds and programmed to begin sampling prior to the CTD reaching its maximum depth. The CTD/RO was stopped at the maximum depth for 5 minutes to obtain approximately 30 records for comparison with the CTD reading. If the temperature- and conductivity differences in SeasaveV7 display indicated an inhomogeneous water layer, the CTD/RO was lifted by 50 or 100 m prior to beginning the *in-situ* calibration. The *in-situ* comparison of the SBE56s were not processed during the expedition.

3.1.1 Physical oceanography

Tab. 3.1.1.17: Comparison for Seabird sensors SBE37 moored during PS103. Columns CTD and PRES indicate the corresponding station number and the CTD pressure during the 5 minute stop.
 $TEMP_{corr} = TEMP_{reading} + \text{deltaTemp}$; $COND_{corr} = COND_{reading} + \text{deltaCond}$

SN	deltaTemp	deltaCond	MOORING	CTD	PRES
218	-0.0012	0.0180	AWI227-14	2-4	4061
233	-0.0030	0.0168	AWI229-13		
1228	0.0003	0.0070	AWI229-13		
2089	0.0002	0.0092	AWI229-13		
2388	0.0007	0.0210	AWI229-13		
2389	0.0015	0.0227	AWI229-13		
8127	-0.0006	0.0034	AWI229-13		
8128	-0.0005	0.0053	AWI229-13		
1234	0.0026	0.0100	AWI261-1	31-2	4828
9832	0.0020	0.0036	AWI260-1		
10933	0.0024	0.0024	AWI262-1		
10935	0.0022	0.0045	AWI262-1		
10936	0.0029	0.0033	AWI262-1		
10938	0.0018	0.0027	AWI261-1		
2090	0.0036	0.0088	AWI259-1	34-2	4320
2092	0.0037	0.0133	AWI260-1		
2093	0.0036	0.0105	AWI259-1		
2101	0.0034	0.0094	AWI260-1		
2395	0.0029	0.0091	AWI207-10		
6928	0.0031	0.0206	not deployed		
7690	0.0044	0.0046	not deployed		
9491	0.0018	0.0036	AWI258-1	39-3	4896
10928	0.0019	0.0075	AWI257-1		
10929	0.0019	0.0063	AWI259-1		
10939	0.0018	0.0093	AWI258-1		
10941	0.0023	0.0066	AWI207-10		
10946	0.0022	0.0046	AWI258-1		
10947	0.0013	0.0044	AWI207-10		
2234	0.0034	0.0135	AWI257-1	40-3	4687
3814	0.0036	0.0081	not deployed		
10930	0.0021	0.0061	AWI207-10		
10931	0.0030	0.0123	AWI250-2		
10948	0.0028	0.0047	AWI257-1		
235	-0.0035	0.0215	AWI231-12	6-1	5325
1232	0.0027	0.0124	AWI244-5		
1233	0.0016	0.0117	AWI248-2		
8131	0.0015	-0.0010	AWI249-2		
9487	0.0018	0.0053	AWI209-8		
8130	0.0023	0.0062	AWI245-4		
9488	0.0020	0.0057	AWI208-8		

3.1 HAFOS: Maintaining the AWI's long term ocean observatory in the Weddell Sea

Tab. 3.1.1.18: Offsets for Seabird sensors SBE39plus moored during PS103. Columns CTD and PRES indicate the corresponding station number and the CTD pressure during the 5 minute stop. $TEMP_{corr} = TEMP_{reading} + deltaTemp$.

SN	deltaTemp	deltaCond	MOORING	CTD	PRES
7867	0.0021		AWI259-1		
7869	0.0023		AWI260-1		
7870	0.0023		AWI260-1		
7872	0.0023		AWI207-10		
7860	0.0000		AWI257-1		
7861	0.0003		AWI257-1		
7862	0.0001		AWI257-1		
7863	-0.0003		AWI258-1		
7864	-0.0005		AWI258-1		
7865	-0.0000		AWI258-1		
7866	-0.0003		AWI259-1		
7868	-0.0000		AWI259-1		
7871	0.0003		AWI260-1		
7876	-0.0004		AWI207-10		
7877	-0.0002		AWI207-10		

Tab. 3.1.1.19: Offsets for Seabird sensors SBE37 and SBE16 recovered during PS103. Columns CTD and PRES indicate the corresponding station number and the CTD pressure during the 5 minute stop. For moorings marked by an *, *in-situ* comparisons were conducted upon deployment during PS89 and during recovery on PS103. Their data was adjusted based on a linear interpolation between prior and post recovery offsets. For all other instruments, only the post recovery offset was applied as a constant offset.

$$TEMP_{corr} = TEMP_{reading} + deltaTemp; \quad COND_{corr} = COND_{reading} + deltaCond$$

MOORING	SN	Deploy deltaTemp	Deploy deltaCond	Recover deltaTemp	Recover deltaCond
227-13*	8125	0,0006	0,0031	0,0019	0,0012
229-11*	8129	0,0006	0,0022	0,0018	0,0025
229-11*	9831	-0,0003	0,0018	0,0009	0,0058
229-11*	10943	0,0002	0,0009	0,0020	0,0027
229-11*	10944	0,0013	0,0029	0,0028	0,0034
229-11*	11419	0,0004	0,0005	0,0017	0,0006
229-11*	11420	-0,0005	0,0019	0,0015	0,0006
231-11*	11421	-0,0006	0,0010	0,0013	-0,0009
229-11*	227	-0,0008	0,0229	0,0004	0,0168
232-12*	11422	-0,0003	0,0009	0,0010	-0,0012
229-12*	228	-0,0028	0,0125	-0,0027	0,0129
232-10	441			-0,0133	0,0176
244-4*	12470	0,0009	-0.0010	0,0009	-0,0010
248-1	9841			0,0025	0,0070

3.1.1 Physical oceanography

MOORING	SN	Deploy deltaTemp	Deploy deltaCond	Recover deltaTemp	Recover deltaCond
245-3	9839			0,0033	0,0026
249-1	9847			0,0010	0,0010
209-7	2420			0,0017	0,0057
209-7	7728			0,0029	0,0017
209-7	7729			0,0030	0,0018
208-7	1167			0,9473	3,2657
208-7	7730			0,0007	0,0001
208-7	7731			0,0009	-0,0002
217-5	9496			0,0016	-0,0049
217-5	9497			0,0050	-0,0025
216-5	9493			0,0011	-0,0059
216-5	9494			0,0026	-0,0045
216-5	9495			0,0021	-0,0049
207-9	2413			-0,0053	0,0131
207-9	7732			0,0020	0,0003
207-9	7733			0,0025	-0,0010
207-9	9492			0,0018	0,0035
207-8	1235			0,0009	-0,0033
207-8	2235			0,0021	-0,0006
207-8	1605			0,0024	0,0013
207-8	1607			0,0014	0,0129
206-7	2097			0,0011	0,0021

Argo float deployments

For Argo floats, an onboard profile data processing was set up during the expedition. Data were received from all but float S/N 283, which probably remained under the sea ice directly after deployment, and float S/N 271, which likely was damaged during deployment. A comparison of the first float profile (taken within approximately 8 hours after launch) with the CTD taken at the same location match for temperature and salinity, except for S/N 270, which depicts a salinity offset increasing with depth (Fig. 3.1.1.6). One float (S/N 274), for unknown reasons, only delivers profiles less than 200 m deep.

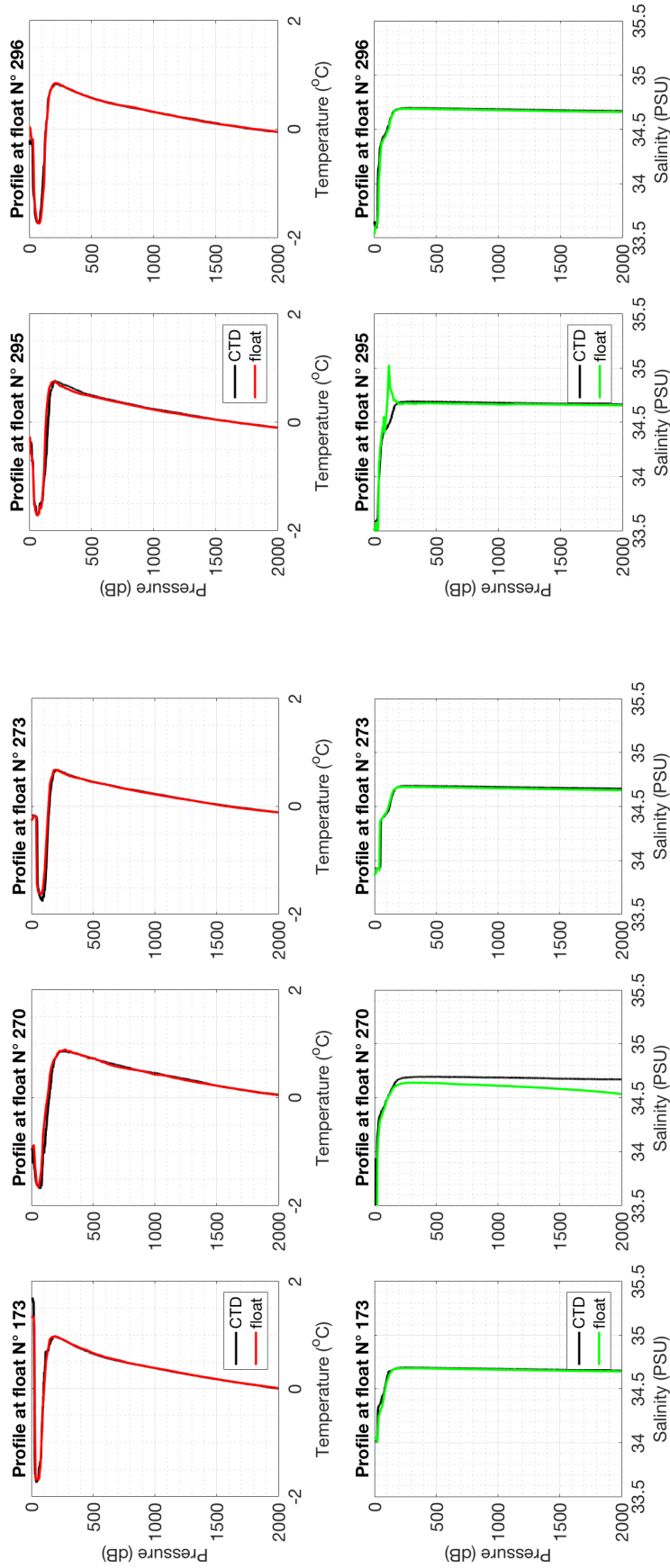


Fig. 3.1.1.6: First transmitted profiles of floats with S/N 173 270, 273, 295 and 296 together with CTD profile near to the deployment position (see Table 3.10); top: temperature: float – red, CTD – black, bottom: salinity: float – green, CTD – black

3.1.1 Physical oceanography

Deployments of MiniROV vLBV300 (Fiona) for mooring recovery

The Seabotix MiniROV vLBV300 (baptized Fiona) was acquired by AWI in 2016 for the purpose of recovering moorings under heavy sea ice condition. Fiona is equipped with a Gemini 720i multibeam sonar, an Aqua Vision DIVECAM-650C colour camera (650 TV lines of resolution and 0,1 lux @ f2.0 sensitivity), an Outland Technology UWC-300 b/w camera (600 horizontal lines and 0,001 lux sensitivity), a GAPS compatible 1310A transponder from AppliedAcoustics and a three-jawed grabber. The ROV was delivered directly from the factory to Cape Town aboard *Polarstern*, with the designated pilots having undergone prior training at the manufacturer's site in San Diego.

The anticipated scenario was that of a mooring having released, with its elements being assembled under the sea ice and the mooring rope hanging in long loops down. Fiona was thought to then be deployed under the ice through a natural or man-made hole to attach a recovery rope to a nearby loop of the mooring rope. After retrieving the mooring rope through the access hole, the mooring would have been retrieved by the mooring rope. This approach requires a thin recovery rope, as no major load would develop when hauling in part of the mooring rope. Hence the rope was selected as thin as possible, to minimize the drag on the ROV in case long lengths would be needed to capture the mooring rope.

However, as heavy sea-ice conditions have not been encountered during this expedition, this scenario did not come to bear. Rather, we were faced with a number of older moorings whose acoustic releases failed to let go of the anchor weight. With these moorings top floatations being within the depth rating of Fiona (300 m), the idea developed to attempt retrieving these moorings by attaching the recovery rope directly to the mooring line while still at depth.

On 21 Jan. 2017 we attempted to recover mooring AWI-250-1. Both mooring and ship occupied a lead in otherwise ice covered waters, with the ship being positioned about 40 m to the side off the mooring position, a setup that proved favorable and was used for the other two recoveries as well. The attachment of the recovery rope was successful, however when attempting to heave the mooring, the recovery rope broke within a knot used to extend the 200 m long piece by another piece. With the breaking load of the 3 mm Dyneema recovery rope being 1.5 tons, and the knot reducing this to about one half, the setup had been considered "on the edge" but not impossible beforehand (The anchor has a weight of about 1 to with approximately 300 kg floatation in the mooring). The breakage resulted in the mooring remaining at depth, which provides another chance for its recovery in two years' time.

For the second ROV based recovery attempt, we replaced the original recovery rope with the ship's 8 mm Dyneema rope, which also was terminated by a rope thimble and splice which could be threaded directly into the recovery carabiner. With this setup we managed to retrieve both mooring AWI-206-7 and AWI-207-8. When tightening the recovery rope on AWI-207-8, one of its releases' clutch opened and the mooring surfaced on its own. For AWI-206-7 however, both releases' clutches remained closed and the entire mooring was hauled up, first by the recovery rope, then by the mooring rope. Wind and wave conditions during these latter two deployments started at about 5 Bft, abating during the station. Table 3.1.1.20 lists the deployments of MiniROV vLBV300 (Fiona).

Tab. 3.1.1.20: Deployments of MiniROV vLBV300 (Fiona) during PS103

Date	Station	Mooring	Dive's duration	Depth	Remarks
07.01.17	24-1	Instrument test	47 min	120	Test recovered after pressure sensor failure and loss of communication.
08.01.17	25-1	Instrument test	2 min	0	Immediate abort due to failure of pressure sensor and loss of communication.
10.01.17	29-2	Instrument test	32 min	15	Test of new electronic bottle.
21.01.17	43-2	AWI250-1	64 min	230	Mooring found and hooked but not recovered.
26.01.17	58-2	AWI207-8	35 min	150	Mooring found, hooked and recovered.
27.01.17	63-2	AWI206-7	21 min	150	Mooring found, hooked and recovered.

To setup the ROV for the operation approximately 1 hour is required on the ROV's side, with a concurrent 45 min needed to install the GAPS transponder in the ship's well. Required personnel setup is as follows

- 1 person deploying / control of tether
- 1 persons unwinding tether / 2 persons winding tether
- 2 ROV pilots
- 1 chief scientist
- 1 chief mate
- 2-3 persons feeding recovery rope (setup dependent)
- 1 person controlling lifting gears

The following sequence of images show the successful hooking of the mooring on stations 43-2 (Fig. 3.1.1.7) and 63-2 (Fig. 3.1.1.8).

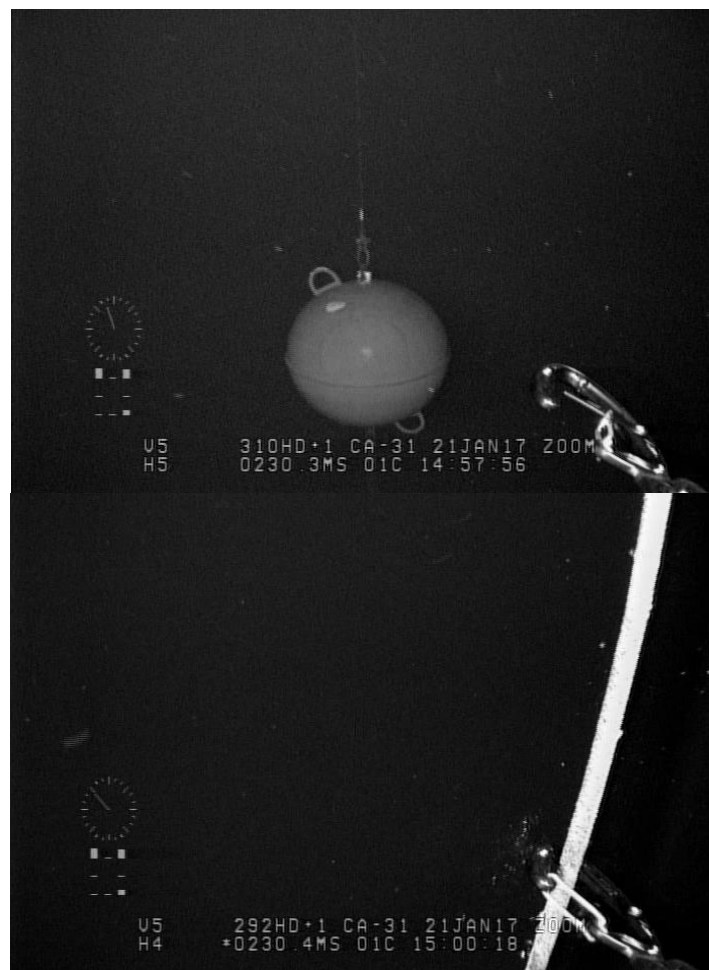
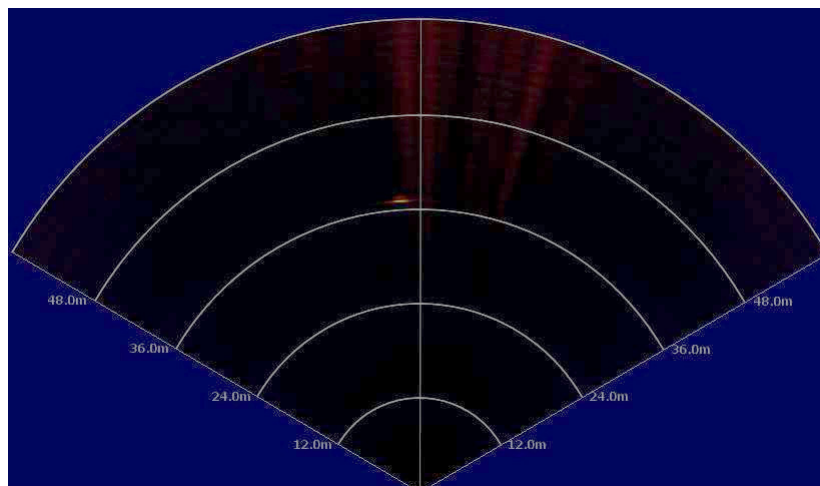


Fig. 3.1.1.7: Station 43-2. Top: mooring float on sonar image at 36 m of distance. Middle: Float on video at 4 m of distance. Bottom: Mooring rope hooked.

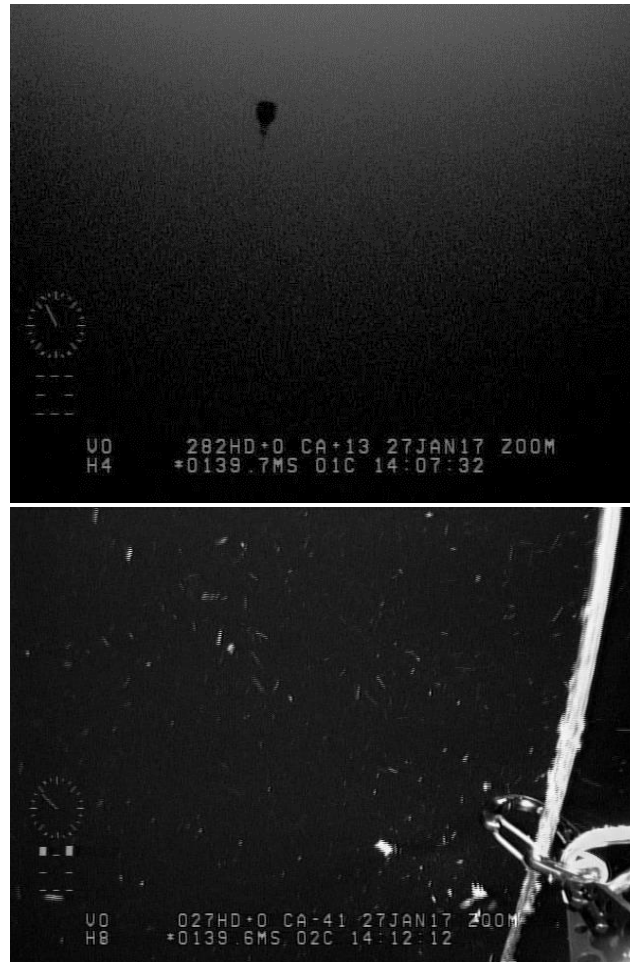


Fig. 3.1.1.8: Station 63-2. Top: Mooring's USBL on video at 24 m of (horizontal) distance. Bottom: Mooring rope hooked.

Issues during deployment and lessons learnt:

- We experienced software issues with the integration of the GAPS telegram HRP400 in the ROV's software SeanetPro with various software updates provided by the manufacturer during the expedition. For stations 24-1, 25-1, 29-1, 43-2 and 58-2 the GAPS' native graphical user interface was used directly for navigation purposes. For station 63-2 the navigation on SeanetPro was working fine.
- The video log options on SeanetPro shall be configured to use the default codec. This saves drive space and permits to log continuously. A log frame rate of 25 was sufficient for mooring recovery purposes.
- On stations 58-2 and 63-2 the sonar application on SeanetPro froze after a few seconds in water. Gemini's SW was used instead. This issue remains unresolved for the time being and is investigated by AWI and the SeanetPro manufacturer Tritech International Limited.
- During station 43-2 at 230 m of depth we experienced the ROV moving forward only very slowly in spite of full forward thrust being applied. Presumably this is due to the tether's drag or too little tether line having been paid out. To get a better control of the

3.1.1 Physical oceanography

length of the tether paid out, 20 m intervals were marked and labelled on the tether. Additionally, a clump weight behind the ROV may be used to reduce the effect of tether's drag. This was not tested on this cruise.

- On station 58-2, after completion of the carabiner attachment, the ROV was pulled back by its tether while applying slight forward thrust. However, at a depth of 69 m it ceased to ascend. Shortly after, it performed 6 turns around its vertical axis as indicated by its compass. Inspection by the upward directed camera, showed that the tether was turned around a rather tight recovery rope (Fig. 3.1.1.9). So far we lack an understanding of what led to this situation, but will investigate the incident further on basis of the ROV's data logs. Recovery was nevertheless achieved by slackening of the tether and the recovery rope, followed by active ascent of the ROV.



Fig. 3.1.1.9: Entangled ROV tether and recovery rope

- On station 58-2 the grabber was holding the carabiner together with part of the recovery rope. The grabber's jaws grabbed outside the carabiner's holes in the attachment base. This is believed to have caused a weakened grip and subsequently some movement of the carabiner during operation, allowing it to rotate within the grabber (Fig. 3.1.1.10) and causing it being stuck when released. While the carabiner closed on the first attempt without securing the mooring rope, it was nevertheless possible to get the rope inside the carabiner, in spite of it being "closed".
- On stations 58-2 and 63-2 the carabiner did not close when the mooring rope snapped in for the first time. Comparing the tilt angles of the carabiner in the grabber of station 43-2 with station 63-2 (Fig. 3.1.1.11), we can observe that the carabiner was more rotated upward during the successful try (43-2) than on the other stations (63-2 and 58-2 (not shown)). However, whether this was the ultimate reason for the malfunction is remains only a hypothesis, which needs to be tested. Fig. 3.1.1.12 shows the trajectories of ship, ROV and mooring during ROV dive #3 at station 63-2.



Fig. 3.10: Sequence showing the carabiner's behaviour. Left: original position of open carabiner, middle: "closed" carabiner after mooring rope snapped in and out of it, slightly tilted to right; right: carabiner tilted to left after slight pull on recovery rope.

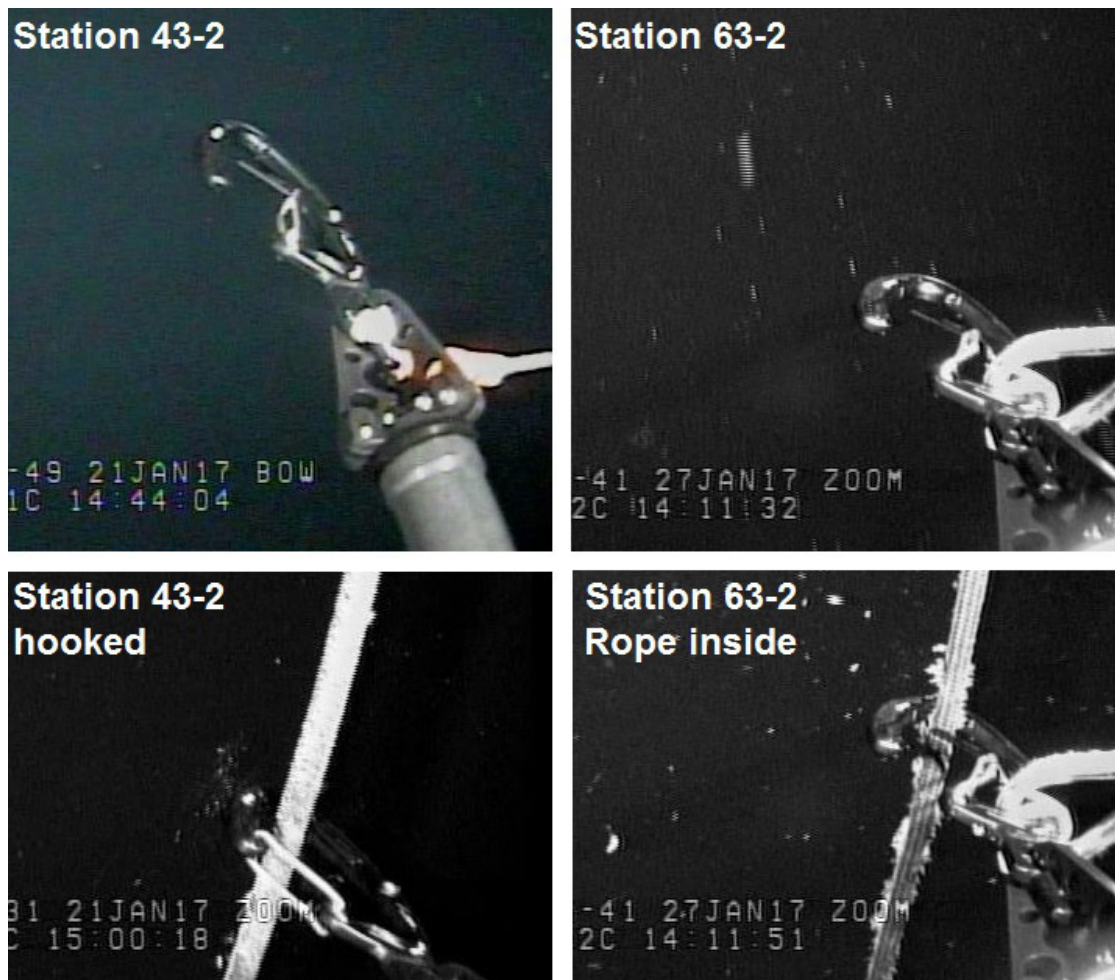


Fig. 3.11: Sequence showing carabiner before snapping the rope and shortly after. Upper left: Carabiner fixed in the grabber during station 43-2. Bottom left: Carabiner with mooring rope snapped in during station 43-2. Upper right: Carabiner fixed in the grabber during station 63-2. Bottom right: Mooring rope snapped in open carabiner during station 63-2.

3.1.1 Physical oceanography

- For hooking the mooring rope, it is advisable to observe both the sonar and the video image. The sonar depicts the manipulator arm and the echo from the mooring rope, providing a good estimate of the distance to the rope. The video provides overall orientation of the mooring rope and the carabiner, allowing a precise targeting of the rope.
- In open waters, diving with lights off to a depth below the top floatation and pointing the camera upwards seems to provide a good chance to detect the floatation against the lighter sea surface, and avoids backscatter from marine snow limiting the visibility. Prior to hooking, switching on 2 lights provides a clear view of the target.
- The black and white camera seems to provide a much better range and resolution than the colour camera.
- Piloting the ROV was improved with each dive. For the time being, it seems to be best, to dive as soon as the ROV is in the water and simultaneously approach the target, based on information from the MicronNav application. As soon as an echo from the mooring is received in the sonars image, navigation is sonar based, once visible in the video, by visual guidance.

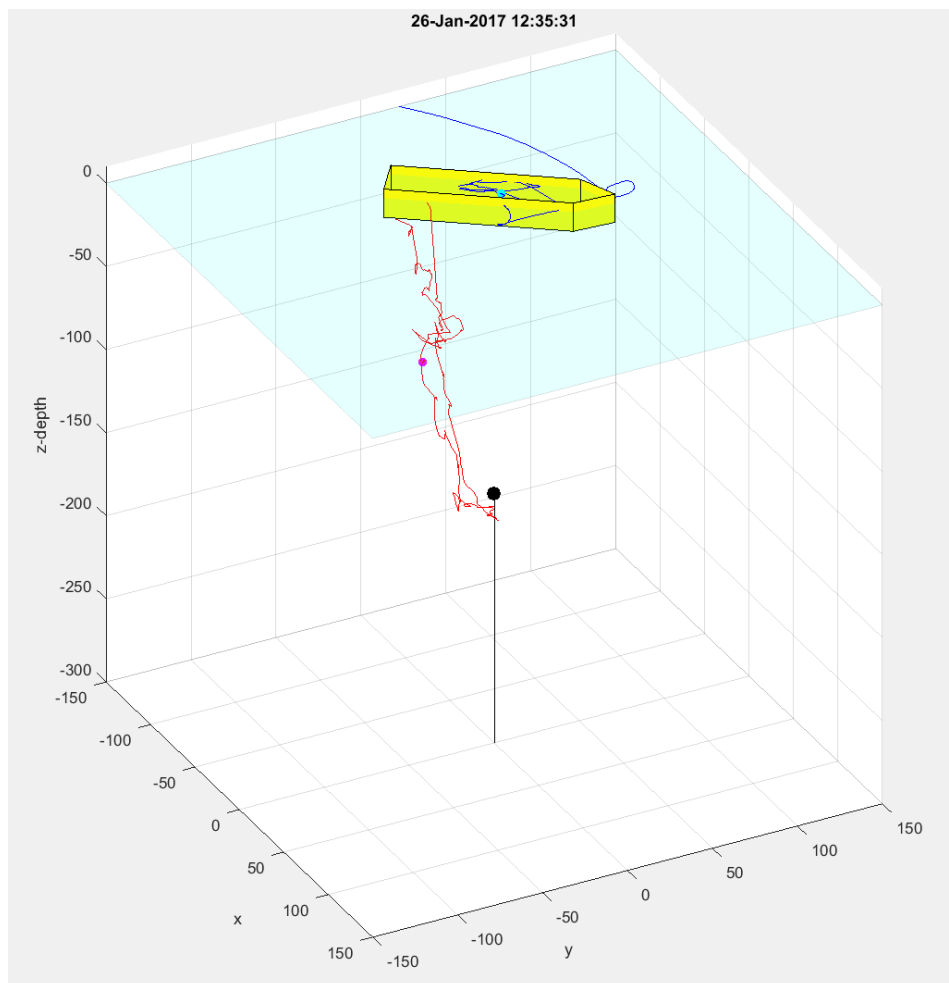


Fig. 3.1.1.12: 3-D illustration of trajectories of ship (blue/cyan), ROV (red/magenta) and mooring (black) during ROV dive #3 at station 63-2. Note that trajectory data is subject to GAPS and Posidonia positioning accuracy, possibly giving rise to the small scale jitter of trajectory data. Units are in metres.

Preliminary scientific results

CTD Observations

While the CTD section along the Greenwich Meridian could not be repeated completely (Fig. 3.1.1.3) due to time constraints, the temperature profile at 61°S shows the near-linear continuation of the warming in the aged Weddell Sea Bottom Water (WSBW, Fig. 3.1.1.13). Within the 50 m thick bottom layer of the WSBW, the temperature increased from -0.8435°C (1992) to -0.7825°C during PS103, which corresponds an increase of 0.024°C per decade.

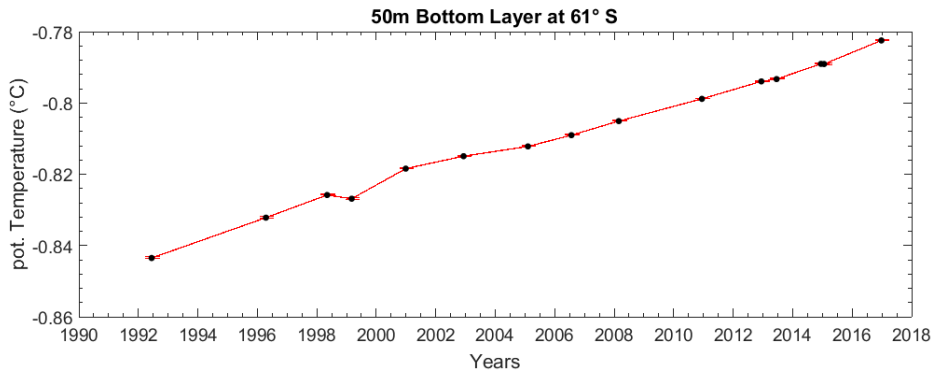


Fig. 3.1.1.13: Temperature records from past and current CTD casts at 61°S, 0°E

Towards the tip of the Antarctic Peninsula 19 deep CTD casts were taken at high horizontal resolution between 46°W to 54°W, repeating a section being occupied since 1989. The thin cold bottom layer at the continental slope indicates newly formed Weddell Sea Bottom Water flowing northward along the slope, see Fig. 3.1.1.14. During this expedition, it was the first time that a temperature below -1.0°C was observed in the deep basin at 46°W.

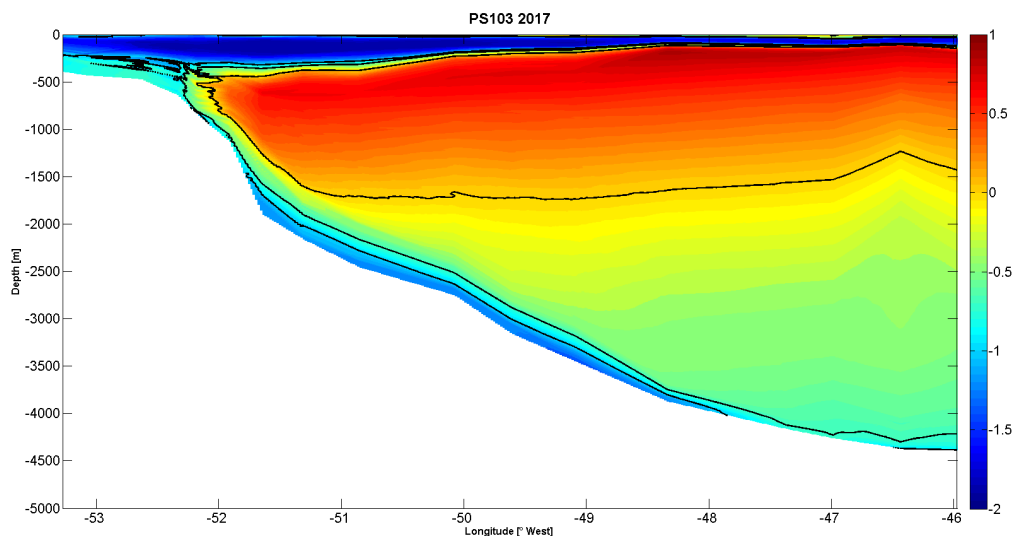


Fig. 3.1.1.14: Temperature section towards the tip of the Antarctic Peninsula taken at high horizontal resolution between 46°W to 54°W

Data management

The final records from moored instruments (CTD-recorders and current meters) have been post calibrated and are accessible through the PANGAEA data base via <https://doi.pangaea.de/10.1594/PANGAEA.875123> through *.875139. The final processing of CTD-data will be conducted after post-expedition calibrations are available. All data will be stored and available through PANGAEA. P.I.: Olaf Boebel and Gerd Rohardt.

References

- Boebel O (2013) The expedition of the research vessel POLARSTERN to the Antarctic in 2012/2013 (ANT-XXIX/2) , Berichte zur Polar- und Meeresforschung = Reports on polar and marine research, Bremerhaven, Alfred Wegener Institute for Polar and Marine Research, 671, 99 p. hdl:10013/epic.42735.
- Boebel O (2015) The Expedition PS89 of the Research Vessel POLARSTERN to the Weddell Sea in 2014/2015, Berichte zur Polar- und Meeresforschung = Reports on polar and marine research, Bremerhaven, Alfred Wegener Institute for Polar and Marine Research, 689, 151 p. hdl:10013/epic.45857.
- Klatt O, Boebel O, Fahrbach E (2007) A Profiling Float's Sense of Ice. J. Atmos. Oceanic Technol., 24, 1301–1308, hdl:10013/epic.28318.
- Rosby T, Dorson D, Fontaine J (1986) The RAFOS System, J. Atmos. Oceanic Technol., 3, 672-679.

3.1.2 Ocean acoustics

Stefanie Spiesecke¹, Ramona Mattmüller^{1,2},
Sarah Zwicker¹, Matthias Monsees¹, Rainer
Graupner¹, Olaf Boebel¹;
not on board: Karolin Thomisch¹, Ilse van
Opzeeland¹

¹AWI

²Uni Bremen

Grant No: AWI_PS103_01

Objectives

The restricted accessibility of the Southern Ocean throughout most of the year confines our knowledge of the distribution patterns, habitat use and behaviour of the marine mammals in this area. Most of the Antarctic marine mammals produce species-specific vocalizations during a variety of behavioral contexts. Hence, passive acoustic monitoring (PAM) offers a valuable tool for research on these species, capable of covering large temporal and spatial scales. Especially in remote areas such as the Southern Ocean, moored PAM recorders are the tool of choice as data can be collected year-round, under poor weather conditions, during darkness and in areas with dense ice cover.

The HAFOS observing system is a large scale oceanographic observatory, the backbone of which consists of moorings deployed throughout the Weddell Sea. Passive acoustic recorders are part of the moored instrumentation, which was recovered, refurbished and redeployed during PS103 to continue the long-term data collection. The basin-wide design of the HAFOS observatory and the multi-year scale of data collection enables an unprecedented investigation of the spatio-temporal patterns in marine mammal biodiversity at the different mooring locations. The HAFOS array set-up and design also allow collecting information on the detection range of the various marine mammal sounds. Information on the distance over which marine mammal sounds can be detected by passive acoustic sensors is of vital importance when acoustic presence data are linked to information on environmental parameters in the context of studies of species-specific habitat usage. Detailed knowledge on detection ranges is key to ascertaining that the spatial scale of environmental variables, such as depth or sea ice coverage, matches with the range over which calling marine mammals can be detected by the recorders.

Work at sea

Recovery of moored acoustic recorders

In total, 20 passive acoustic recorders, moored at 13 different positions were recovered during PS103 (Fig. 3.1.2.1, Tab. 3.1.2.1). These comprised 19 SonoVaults (manufactured by Develogic GmbH, Hamburg) and one AURAL (manufactured by MultiElectronique). Six of these recorders had been deployed during *Polarstern* expedition PS89, 11 recorders had been deployed during *Polarstern* expedition ANT-XXIX/2 and 2 had been deployed during ANT-XXVII/2. Double locations with recorders recovered from the same mooring position but from different servicing cycles were counted only once. This applies to moorings AWI207, AWI229 and AWI232. See also Tab. 3.1.2.1.

Unfortunately, two further moorings could not be recovered. Mooring AWI250-01 with SV1031 could not be recovered this time but will be attempted for retrieval in 2018/2019. Furthermore, mooring AWI206-08 (containing recorders AU0232 and SV0002) could not be recovered because it could not be found at its position. This mooring is believed to be lost.

An overview of the recovery information of all recovered acoustic recorders is provided in Tab. 3.1.2.1. Deployment positions of the recorders are marked in Fig. 3.1.2.1. After recovery, the

3.1.2 Ocean acoustics

acoustic recorders were rinsed with freshwater and cleaned from biological fouling. The mooring frame which facilitates the integration of the acoustic recorders in line with the oceanographic moorings was removed for easy handling and opening of the recorder for data recovery. To check the status of the recovered recorder, it was connected to a laptop through a serial connection and accessed using a custom-made software for the SonoVaults and a software provided by Multi-Electronique for the AURAL (see section “Operational Results” for technical evaluation results). The recorders were then left to dry overnight to prevent damage to the electronics from water that retained in the threading of the recorder housing. After opening the recorder housing, the internal power supply was disconnected. All SD-cards, which had been labeled with the recorder’s serial number, the recording module number and the SD card-slot prior to recorder deployment, were removed and backed up (see below).

Each recovered recorder was calibrated post-recovery to allow calculations of received sound/signal levels. For the calibration a Brüel & Kjaer calibrator (Type 4229) with the custom made adapter (SV.PA manufactured by Develogic) for the TC 4037 hydrophones was used. The calibration frequency is $251.2 \text{ Hz} \pm 0.1\%$ (ISO 266) and the amplitude (at 1013 hPa) is 153.95 dB SPL. For the calibration measurement the recorder was set to the deployment sampling rate and a file size of 1 minute. Every minute the gain setting was changed successively from 0 – 7 (system gain settings representing 6 dB to 48 dB amplification). All recordings were stored and signal levels were calculated.

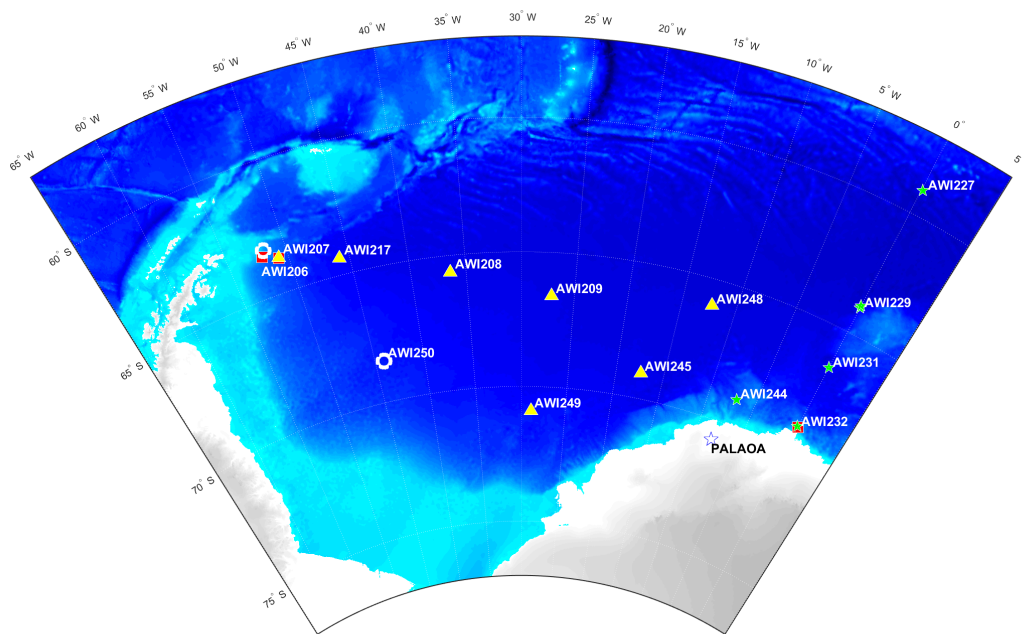


Fig. 3.1.2.1 Map showing the 13 locations of acoustic recorders that were recovered during PS103 and the two locations where moorings with acoustic recorders could not be recovered during PS103 (empty circles). The red squares indicate recovered recorders which were deployed on ANT-27/2, triangles indicate locations with recorders which were deployed on ANT-29/2, stars mark recorders deployed on PS89. (The blue star represents the position of the PALAOA observatory.)

Tab. 3.1.2.1: Overview of SonoVault and AURAL recorders recovered (white background) during PS103. Recorders shaded grey could not be retrieved during PS103. Mooring ID given in the format AWXXX-ZZ, with X representing the IDs of the respective mooring and Z indicating the consecutive numbering of this mooring (i.e., the number of the current servicing cycle).

Mooring	Device SN	Position LAT LON	Deployment depth /m	Deployment date	Recovery date	Gain /dB *)	Setup	Condition	Data availability
AWI 227-13	SV1056	59°02.67' S 000°05.37' E	1020	2014-12-13	2016-12-24	-/-	6.9 KHz/24bit; continuous recording; file duration: 600 s	Housing: good; electronics: no data, error: watchdog	no data
AWI 229-12	SV1055	63°54.94' S 000°00.17' W	1001	2015-01-20	2016-12-26	44.7/-	Scheduled Start: 01.01.16; 6.9 KHz/24bit; continuous recording; file duration: 600 s	electronics: batteries burned out error: watchdog, schedule from 01.01.2016 could not be started	no data
AWI 229-11	SV1057	64°00.32' S 000°00.22' W	970	2014-12-17	2016-12-26	44.7/45	6.9 KHz/24bit; continuous recording; file duration: 600 s	Housing and electronics: good	data available
AWI 231-11	SV1058	66°30.41' S 000°00.66' W	973	2014-12-19	2016-12-28	44.5/44.9	6.9 KHz/24bit; continuous recording; file duration: 600 s	Housing and electronics: good	data available
AWI 232-10	SV1003	69°00.11' S 000°00.11' W	987	2010-12-19	2016-12-31	-/45.7	5.3 KHz/24 bit, continuous recording; file duration: 600 s	Housing and electronics: good	data available

3.1.2 Ocean acoustics

Mooring	Device SN	Position LAT LON	Deployment depth /m	Deployment date	Recovery date	Gain /dB (*)	Setup	Condition	Data availability
AWI 232-12	SV1059	68°58.89' S 000°05.00' W	999	2014-12-23	2016-12-30	44.7/-	6.9 kHz/24bit; continuous recording; file duration: 600 s	electronics: batteries burned out	data available
AWI 244-04	SV1061	69°00.34' S 006°58.95' W	998	2015-01-16	2017-01-01	44.7/31.6	6.9 kHz/24bit; continuous recording; file duration: 600 s	Housing and electronics: good	data available
AWI 248-01	SV1013	65° 58.09' S 012° 15.12' W	1081	2012-12-27	2017-01-02	-/28	5.3 kHz/24 bit, continuous recording; file duration: 600 s, No Precision Clock	Housing and electronics: good	data available
AWI 245-03	SV1012	69° 03.48' S 017° 23.32' W	1065	2012-12-28	2017-01-11	-/30.8	5.3 kHz/24 bit, continuous recording; file duration: 600 s No Precision Clock	Housing and electronics: good	data available
AWI 249-01	SV1014	70° 53.55' S 028° 53.47' W	1085	2012-12-30	2017-01-13	-/44.7	5.3 kHz/24 bit, continuous recording; file duration: 600 s No Precision Clock	Housing and electronics: good	data available

3.1 HAFOS: Maintaining the AWI's long term ocean observatory in the Weddell Sea

Mooring	Device SN	Position LAT LON	Deployment depth /m	Deployment date	Recovery date	Gain /dB (*)	Setup	Condition	Data availability
AWI 209-07	SV1027	66° 36.45' S 027° 07.26' W	226	2013-01-01	2017-01-15	-/26.5	5.3 kHz/24 bit, continuous recording; file duration: 600 s No Precision Clock	Housing and electronics: good	data available
	SV1028	66° 36.45' S 027° 07.26' W	1007	2013-01-01	2017-01-15	-/45.3	5.3 kHz/24 bit, continuous recording; file duration: 600 s No Precision Clock	Housing and electronics: good	data available
	SV1029	66° 36.45' S 027° 07.26' W	2516	2013-01-01	2017-01-15	-/44.2	5.3 kHz/24 bit, continuous recording; file duration: 600 s No Precision Clock	Housing and electronics: good	data available
AWI 208-07	SV1030	65° 37.23' S 036° 25.32' W	956	2013-01-03	2017-01-19	-/44.6	5.3 kHz/24 bit, continuous recording; file duration: 600 s No Precision Clock	Housing and electronics: good	data available
AWI 250-01	SV1031	68° 28.95' S 044° 06.67' W	1041	2013-01-05	postponed	-/48	5.3 kHz/24 bit, continuous recording; file duration: 600 s No Precision Clock	--	

3.1.2 Ocean acoustics

Mooring	Device SN	Position LAT LON	Deployment depth /m	Deployment date	Recovery date	Gain /dB *)	Setup	Condition	Data availability
AWI 217-05	SV1020	64° 22.94' S 045° 52.12' W	960	2013-01-09	2017-01-23	-26.4	5.3 kHz/24 bit, continuous recording; file duration: 600 s No Precision Clock	Housing and electronics: good	data available
AWI 207-08	AU085LF	63° 43.07' S 050° 49.91' W	219	2011-01-06	2017-01-26	221)	32 kHz/16 bit, subsampling: 5 minutes every hour file duration: 300 s	Housing and electronics: good	data available
AWI 207-09	SV1032	63° 42.09' S 050° 49.61' W	219	2013-01-12	2017-01-25	-37.6	9.6 kHz/24 bit, continuous recording; file duration: 600 s; No Precision Clock	Housing and electronics: good	data available
	SV1033	63° 42.09' S 050° 49.61' W	1012	2013-01-12	2017-01-25	-45.2	9.6 kHz/24 bit, continuous recording; file duration: 600 s; No Precision Clock	Housing and electronics: good	data available
	SV1034	63° 42.09' S 050° 49.61' W	2489	2013-01-12	2017-01-25	-39.7	9.6 kHz/24 bit, continuous recording; file duration: 600 s; No Precision Clock	Housing and electronics: good	data available

3.1 HAFOS: Maintaining the AWI's long term ocean observatory in the Weddell Sea

Mooring	Device SN	Position LAT LON	Deployment depth /m	Deployment date	Recovery date	Gain /dB *)	Setup	Condition	Data availability
AWI 206-7	SV1006	63° 28.84' S 052° 05.77' W	909	2011-01-06	2017-01-27	-/-	5.3 kHz/24 bit, continuous recording; file duration: 600 s, No Precision Clock	Housing and electronics: good	data available
AWI 206-08	AU0232	63° 15.51' S 051° 49.59' W	277	2013-01-14	lost	221)	32 kHz/16 bit, subsampling: 5 minutes every hour, file duration: 300 s	--	
	SV0002	63° 15.51' S 051° 49.59' W	907	2013-01-14	lost	-/48	96 kHz/24 bit, Subsampling: 5 minutes every 2 hours, file duration: 300 s	--	

*) Calibration before/after recovery, using a B&K Pistonphone at 251.2 Hz ± 0.1% (ISO 266) and the amplitude (at 1013 hPa) is 153.95 dB SPL

1) Not calibrated

Data retrieval and backup

18 of the 20 recovered passive acoustic devices recorded for a part of their deployment period with recording periods ranging between 117 days and 635 days (Fig. 3.1.2.2 and Fig. 3.1.2.3); further details are discussed in section Operational results. A total of 7 TB and 123867 h (5963 days) of passive acoustic data were obtained. For the remaining two recorders, SV1055 and SV1056, no recordings could be retrieved due to technical problems during recorder operation (Tab. 3.1.2.2).

The SonoVault recorders store data on 35 SD cards (allowing a maximum of currently 2.2 TB of data storage per recorder). After recovery, the SD cards were removed from the recorders and the acoustic data were copied using a custom-written shell script. Up to eight SD cards were copied simultaneously, with data initially saved with original filenames sorted into daily folders to one HDD (6 TB) drive. In a next step, the data were synchronized with a second HDD (6 TB) after copying was completed. The backup process included the renaming of files based on each files' internal time stamp (WAV-header) to the file name format 'YYYYMMDD-HHMMSS_AWIXXX-ZZ_SVXXXX.wav' (with X representing the IDs of mooring and SonoVault recorder, respectively and Z indicating the consecutive numbering of this mooring (i.e., the number of the current servicing cycle at a respective mooring)). These data were used for the preliminary analyses, see *Preliminary Scientific Results*.

18 SD cards that presumably contain acoustic data were inaccessible during the data backup process (Tab. 3.1.2.2). Recovery of those data using professional recovery software will be attempted at AWI Bremerhaven in 2017.

3.1 HAFOS: Maintaining the AWI's long term ocean observatory in the Weddell Sea

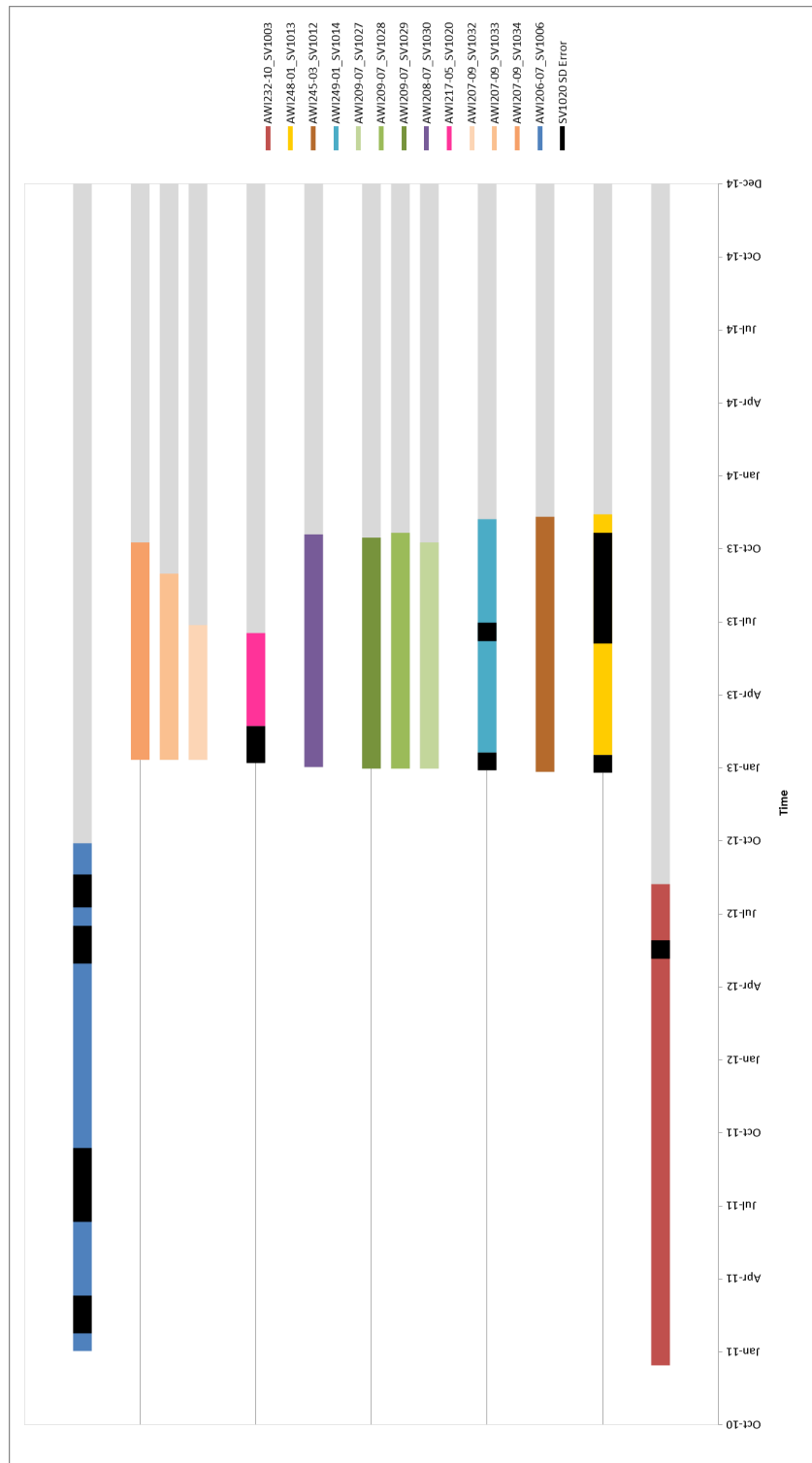


Fig. 3.1.2.2: Overview of deployment and operational period of acoustic recorders deployed during ANT-XXVII/2 and ANT-XXIX/2 and recovered during PS103. Grey bars indicate the deployment periods, while coloured bars are indicative for actual recording periods of the recorders. Black bars represent periods during which recorders presumably operated but collected data have not yet been retrieved or backed up due to damaged SD cards.

Tab. 3.1.2.2: Overview of the SD card status of all 20 recorders that were recovered during PS103

Mooring #	Device SN	Position	Deployment period	Deployment Cruise	Recording period	Recording period (days)	SD Error	missing period
AWI227-13	SV1056	59° 02.67' S 00° 05.37' E	13.12.2014 - 24.12.2016	PS89	no recordings	no recordings	no recordings	no recordings
	SV1057	64° 00.31' S 00° 00.22' W	17.12.2014 - 26.12.2016	PS89	16.12.2014 - 19.05.2016	521	none	none
AWI229-12	SV1055	63° 54.94' S 00° 00.16' E	20.01.2015 - 26.12.2016	PS89	no recordings	no recordings	destroyed	no recordings
AWI231-11	SV1058	66° 30.41' S 00° 00.66' W	19.12.2014 - 28.12.2016	PS89	18.12.2014 - 28.05.2016	528	none	none
AWI232-12	SV1059	68° 58.89' S 00° 05.00' W	13.12.2014 - 30.12.2016	PS89	08.01.2015 - 25.08.2015	230	unknown	13.12.2014 - 08.01.2015
	SV1003	69° 00.11' S 00° 00.11' W	19.12.2010 - 29.12.2016	ANT-XXVII/2	18.12.2010 - 10.08.2012	602	unknown	27.01.2015 - 14.02.2015
AWI244-04	SV1061	69° 00.34' S 06° 58.94' W	16.01.2015 - 01.01.2017	PS89	15.01.2015 - 18.07.2016	552	none	22.02.2015 - 04.03.2015
	SV1013	65° 58.09' S 12° 15.12' W	27.12.2012 - 02.01.2017	ANT-XXVIX/2	18.01.2013 - 14.11.2013	301	M0S0	08.05.2012 - 01.06.2012
AWI245-03	SV1012	69° 03.47' S 17° 23.32' W	28.12.2012 - 11.01.2017	ANT-XXVIX/2	28.12.2012 - 11.11.2013	319	none	27.12.2012 - 18.01.2013
	SV1014	70° 53.55' S 28° 53.47' W	30.12.2012 - 13.01.2017	ANT-XXVIX/2	21.01.2013 - 08.11.2013	292	M1S0	06.06.2013 - 22.06.2013
AWI209-07	SV1027	66° 36.45' S	01.01.2013 - 15.01.2017	ANT-XXVIX/2	31.12.2012 - 10.10.2013	284	none	none
	SV1028	27° 07.26' W						
	SV1029				31.12.2012 - 16.10.2013	290		8.11.2013 - 12/2013

3.1 HAFOS: Maintaining the AWI's long term ocean observatory in the Weddell Sea

Mooring #	Device SN	Position	Deployment period	Deployment Cruise	Recording period	Recording period (days)	SD Error	missing period
AWI208-07	SV1030	65° 37.23' S 036° 25.32' W	03.01.2013 - 19.01.2017	ANT-XXXVIX/2	02.01.2013 - 20.10.2013	292	none	none
AWI217-05	SV1020	64° 22.94' S 45° 52.12' W	09.01.2013 - 24.01.2017	ANT-XXXVIX/2	08.01.2013 - 19.06.2013	117	M0S0/M0S1 M1S0	08.01.2013 - 23.02.2013 19.06.2013 - 07/2013
AWI207-09	SV1032	63° 43.57' S 50° 51.64' W	12.01.2013 - 25.01.2017	ANT-XXXVIX/2	11.01.2013 - 29.06.2016 11.01.2013 - 01.09.2013 11.01.2013 - 10.10.2013	170 234 273	none	none
AWI207-08	AU0085	63° 43.20' S 50° 49.54' W	06.01.2011 - 26.01.2017	ANT-XXXVII/2	data yet to be analyzed		none	none
AWI206-07	SV1006	63° 28.93' S 52° 05.87' W	06.01.2011 - 27.01.2017	ANT-XXXVIX/2	05.01.2011 - 30.09.2012	635	M0S1/M0S2 M1S0/M1S2/ M1S3 M3S0/M3S1 M4S0	28.01.2011 – 16.03.2011 16.06.2011 – 16.09.2011 03.05.2012 – 19.06.2012 30.09.2012 - 10/2012

3.1.2 Ocean acoustics

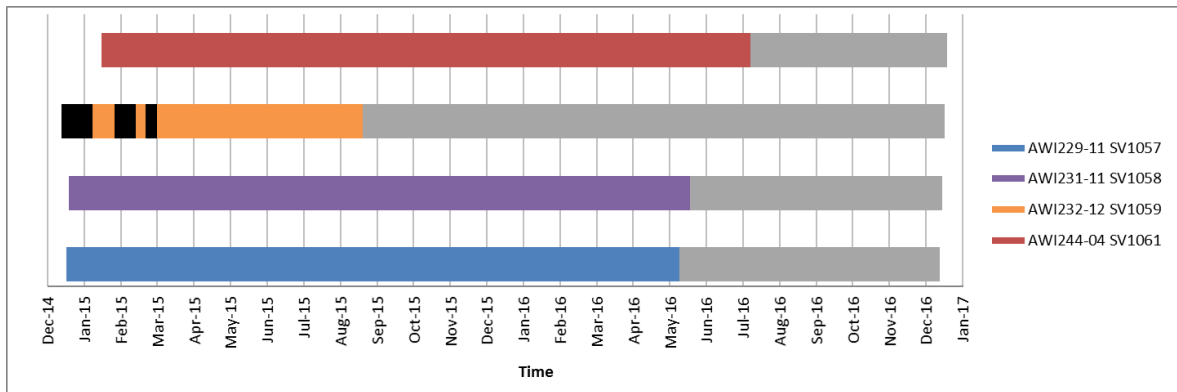


Fig. 3.1.2.3: Overview of deployment and operational period of acoustic recorders deployed during PS89 and recovered during PS103. Grey bars indicate the deployment periods, while coloured bars are indicative for actual recording periods of the recorders. Black bars represent periods during which recorders presumably operated but the collected data have not yet been retrieved and backed up due to damaged SD cards. SV1059 was burned out, most SD cards were nevertheless still readable.

Deployment of moored acoustic recorders

A total of 17 SonoVault recorders were deployed in 13 moorings during PS103 (Fig. 3.1.2.4 Tab. 3.1.2.3). These recorders are equipped with the latest electronics version V4.1. All recorders use the firmware version V4.12a. Additionally, one AURAL recorder (Multi-Electronique, Canada) was deployed in one mooring alongside the SonoVault recorder in mooring AWI251-02.

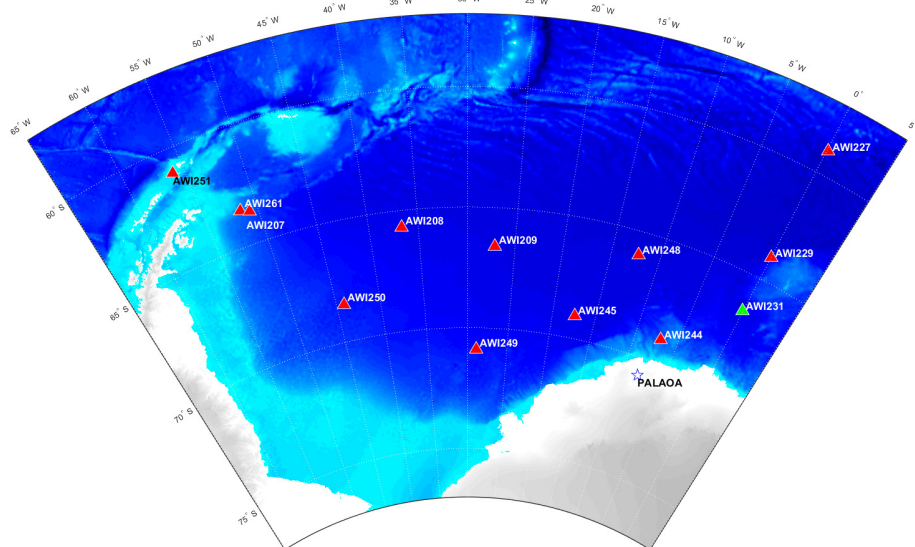


Fig. 3.1.2.4: Map showing the positions of acoustic recorders deployed during PS103. Red triangles indicate new recorder positions. The green triangle indicates a mooring with 5 recorders in different depths (Tab. 3.1.2.3). PALAOA is indicated with a blue star.

In devices with hardware and firmware versions older than 4.1 and 4.08, respectively, power consumption was higher than expected, causing the recorders to stop recording after approximately 6 to 9 months. It turned out that this was caused by the electronics being in the high-resolution mode of the analog-to-digital converter by default. The power consumption however was calculated based on the low power mode. The current firmware (V4.12) now features the possibility to choose between these modes. All SonoVaults now deployed exhibit this feature and comprise five recording modules (SVR) with either the hardware Recording Module Version V1.2 or V1.5, and firmware version V5.12. Depending on the SVR hardware version, a slightly modified firmware version was used to flash the modules. All implemented functions (e.g., changing parameter settings, downloading the configuration and retrieval of the system information) were tested prior to deployment. Subsequently, a test recording was started in the laboratory on board. For all recorders with V1.5, the electronics proved operational. After initial problems with SVR version V1.2, a firmware update for these modules was received from the manufacturer and flashed onto the modules microprocessor. After this, the modules were working.

A calibration, identical to the one performed with the recovered electronics, was performed using the Brüel & Kjaer calibrator (Type 4229). For further details on calibration procedure see section 'Recovery of moored acoustic recorders'.

Prior to the deployment, newly formatted SD cards were placed into the SD card slots on each recording module. 12 recorders now contain 35 SD cards with a capacity of 64 GB, resulting in a total storage capacity of 2.2 TB per recorder. Furthermore, 5 recorders were equipped with a combination of 32GB, 64GB and 128GB SD cards, also totalling about 2 TB per recorder. All SD cards were formatted to FAT32. 64 and 128 GB SDXC cards needed to be formatted using the freeware tool 'SDXCformatterFAT32'. On the first SD card (S0) of the first of five recording modules (M0-M4), the recording configuration (e.g., gain setting, sample rate) was stored. Additionally, the module number was copied onto S0 of every recording module to make the set of seven SD cards of this module available for storage.

The recorders were equipped with batteries (LS33600) and the O-rings were carefully cleaned and greased before closing the housing. All SonoVaults were programmed to record at a sampling rate of 6857 Hz with 24 bit and to store data in files of 600 s duration (Tab. 3.1.2.3). Internal data storage was structured to store data in daily folders. Gain was set to level 7 which in this hardware/firmware release corresponds to about 42dB in all deployed recorders (Tab. 3.1.2.3).

SonoVaults were deployed employing new mounts to attach the instrument to the mooring rope, consisting of two plastic clamps mounted in the upper and lower parts of the housing. The clamps were then attached to a 5 m Dyneema rope. All metal parts are titanium grade 2. Screws were secured using punch-marks and thread locker. A second Dyneema rope was attached to the top of the SonoVault as a backup line.

3.1.2 Ocean acoustics

Tab. 3.1.2.3: Overview of acoustic recorders that were deployed during PS103

Mooring	Acoustic Recorder SN	Corr. water depth /m EK60	Position LAT LON	Deployment depth /m	Deployment date /time (UTC)	Gain / dB ¹⁾	SoSo Time Signal (GPS time)	Setup
AWI 227-14	SV1004	4641	59° 03.03' S 000° 06.43' E	1070	2016-12-24 13:39	41.4	--	6857 Hz; 24bit; Low Power mode
AWI 229-13	SV1053	5197	64°00,49' S 000°00,84' E	1025	2016-12-26 16:02	41.3	--	6857 Hz; 24bit; Low Power mode
AWI 231-12	SV1021	4577	66°31,03' S 000°04,49' W	223	2016-12-28 12:34	41.9	--	6858 Hz; 24bit; Low Power mode
	SV1022	4577	66°31,03' S 000°04,49' W	570	2016-12-28 12:45	42.5	--	6859 Hz; 24bit; Low Power mode
	SV1023	4577	66°31,03' S 000°04,49' W	859	2016-12-18 13:05	42.5	--	6860 Hz; 24bit; Low Power mode
	SV1024	4577	66°31,03' S 000°04,49' W	1064	2016-12-18 13:12	42.3	--	6861 Hz; 24bit; Low Power mode
	SV1026	4577	66°31,03' S 000°04,49' W	2074	2016-12-18 13:41	41.6	--	6862 Hz; 24bit; Low Power mode
AWI 244-05	SV1057	2946	69°00,32' S 006°59,56' W	1044	2017-01-01 14:33	41.7	12:40	6863 Hz; 24bit; Low Power mode
AWI 248-02	SV1058	5047	65°58,12' S 012°13,87' W	1035	2017-01-02 14:35	41.6	14:00	6864 Hz; 24bit; Low Power mode
AWI 245-04	SV1005	4736	69°03.64' S 17°23.45' W	1004	2017-01-11 16:32	41.6	13:10	6865 Hz; 24bit; Low Power mode
AWI 249-02	SV1061	4401	70°53.54' S 28°53.47' W	1040	2017-01-13 15:55	29.9 ¹⁾	13:50	6866 Hz; 24bit; Low Power mode
AWI 209-08	SV1008	4872	66°36.45' S 27°07.29' W	1053	2017-01-18 14:42	41.2	13:30	6867 Hz; 24bit; Low Power mode
AWI 208-08	SV1009	4766	65°41.79' S 36°41.012' W	1032	2017-01-19 20:15	41.3	12:40	6868 Hz; 24bit; Low Power mode
AWI 250-02	SV1003	4737	68°27.84' S 44°08.71' W	1036	2017-01-21 18:26	41.5	13:30	6869 Hz; 24bit; Low Power mode

3.1 HAFOS: Maintaining the AWI's long term ocean observatory in the Weddell Sea

Mooring	Acoustic Recorder SN	Corr. water depth /m EK60	Position LAT LON	Deployment depth /m	Deployment date /time (UTC)	Gain / dB ¹⁾	SoSo Time Signal (GPS time)	Setup
AWI 261-01	SV1011	1700	63°30.87'S 51°38.14' W	842	2017-01-26 18:35	41.6	--	6870 Hz; 24bit; Low Power mode
AWI 207-10	SV1029	2555	63°39.36' S 50° 48.68 'W	1061	2017-01-26 09:28	35.2 ¹⁾	14:10	6871 Hz; 24bit; Low Power mode
AWI 251-02	SV1013	330	61°01.26' S 55°58.84' W	216	2017-01-29 15:30	41.2	--	6872 Hz; 24bit; Low Power mode
	AU0231	330	61°01.26' S 55°58.84' W	212	2017-01-29 15:30	22 ²⁾	--	32 kHz; 16bit; subsampling: 7 min every hour

*) Calibration before recovery, using a B&K Pistonphone at 251.2 Hz \pm 0.1% (ISO 266) and the amplitude (at 1013 hPa) is 153.95 dB SPL

1) Needs to be checked after recovery. Nominal Gain was set to Level 7 (42 dB)

2) No calibration was performed for this recorder type

Change in hardware setup of the PALAOA observatory

Since 2005, PALAOA (**P**erennial **A**coustic **O**bservatory in the **A**ntarctic Ocean) is located on the Ekström Ice Shelf (70° 31' S, 8° 13' W) and collects continuous underwater recordings from a coastal Antarctic environment using a hydrophone deployed at ca. 160 m depths.

During the supply of the *Neumayer Station III* from 28 Dec 2014 until 31 Dec 2014, an aluminum box, containing modified SonoVault electronics, was installed at the position of the former PALAOA container. It was recessed into the snow and is covered with a wooden board and some snow. The box (80cm x 60cm x 60cm) includes a Reson input module EC6073 for the active hydrophone (Reson TC4032) and a SonoVault electronics module, similar to those used in the moored recorders. For power supply, four 90 Ah, 12V batteries were included, two connected in row for each, the active hydrophone and the recording electronics. The battery setup was later in 2015 changed to batteries two in row and those in parallel for both, the hydrophone and the recording electronics. Storage capacity is 4.4 TB (35 x 128 GB SDXC). With a sampling rate of 80 kHz at 24bit and a file size of 600s the PALAOA system was expected to run up to 6 months. Servicing is provided by the overwintering team of Neumayer III. A servicing interval of 3-4 months showed to be necessary based on the experience from the Neumayer staff. On 5 January 2017 the box was maintained and a calibration of the hydrophone was performed. Additionally, a start plug with an LED as indicator for the start-up and file change was successfully tested alongside with a GPS.sync box, which allows the setting of the internal clock of the recorder to the GPS time.

Operational results

Three acoustic recorders, deployed in 2010 on ANT-XXVII/2, 11 acoustic recorders deployed during ANT-XXIX/2 in 2012 and 6 recorders deployed on PS89 in 2014 were recovered during PS103.

Mechanical status

None of the recovered recorders exhibited signs of corrosion on the device. However, one of the steel mooring frames, which was deployed with recorder SV1006 on ANT-XXVII/2 was heavily corroded. At the threads and at the edge of the plastic bars strong gap corrosion was evident. One steel bar was broken and as this mooring was recovered with the anchor still attached to the line, the second bar was heavily bent. None of the anodes was still in place. All other recovered frames were in good condition. The zinc anodes however were heavily corroded and their residue had in large parts clustered near and on the hydrophone, possibly impeding sound reception.

Communication with recovered instruments

Communication efforts after recovery were only successful with four recorders, including the AURAL. The instruments were connected via RS232 to a computer. With a custom built software a connection was tried to be established and status information on the system was queried. Success of communication efforts and information retrieved from the recorders are listed in Tab. 3.1.2.4.

Tab. 3.1.2.4: Overview of results of preliminary technical and data quality evaluation of recorders recovered during PS103

Mooring	Device SN	Position LAT LON	Data availability	Remaining Battery Voltage in V (initial Battery Voltage /V)	Communication established	Status	Total clock drift in s	Electronic noise present in recordings (preliminary results)
AWI 227-13	SV1056	59°02.67' S 000°05.37' E	no data	46.3 (47)	Yes	, Stopped'	-12	No data
AWI 229-12	SV1055	63°54.94' S 000°00.17' W	no data	nn	No	Not available	nn	No data
AWI 229-11	SV1057	64°00.32' S 000°00.22' W	data available	40.2 (47)	Yes	, Stopped'	-651	Yes, broadband electronic noise pulse at beginning of 10-minute file (detected in three of the analyzed files)
AWI 231-11	SV1058	66°30.41' S 000°00.66' W	data available	nn	No	Not available	nn	No
AWI 232-10	SV1003	69°00.11' S 000°00.11' W	data available	nn	No	Not available	nn	Yes, < 30Hz
AWI 232-12	SV1059	68°58.89' S 000°05.00' W	data available	nn	No	Not available	nn	Yes, pulsed and monotonous, not restricted to end of operation
AWI 244-04	SV1061	69°00.34' S 006°58.95' W	data available	nn	No	Not available	nn	Yes, pulsed and monotonous, after 22nd day of operation
AWI 248-01	SV1013	65°58.09' S 012°15.12' W	data available	nn	No	Not available	nn	Yes, low volume pulsed electronic noise between ca. 250 to 750 Hz in the last two recording months
AWI 245-03	SV1012	69°03.48' S 017°23.32' W	data available	nn	Yes	, Full'	+408	Yes, pulsed and monotonous, not restricted to end of operation
AWI 249-01	SV1014	70°53.55' S 028°53.47' W	data available	nn	No	Not available	nn	Yes, pulsed and monotonous, not restricted to end of operation
AWI 209-07	SV1027	66°36.45' S 027°07.26' W	data available	nn	No	Not available	nn	Yes, pulsed, only prior to operation end, possible cause: related to power supply issues
	SV1028	66°36.45' S 027°07.26' W	data available	nn	No	Not available	nn	Yes, pulsed, only prior to operation end, possible cause: related to power supply issues

3.1.2 Ocean acoustics

Mooring	Device SN	Position LAT LON	Data availability	Remaining Battery Voltage in V (initial Battery Voltage /V)	Communication established	Status	Total clock drift in s	Electronic noise present in recordings (preliminary results)
	SV1029	66° 36.45' S 027° 07.26' W	data available	nn	No	Not available	nn	Yes, pulsed and monotonous, not restricted to end of operation
AWI 208-07	SV1030	65° 37.23' S 036° 25.32' W	data available	nn	No	Not available	nn	No
AWI 217-05	SV1020	64° 22.94' S 045° 52.12' W	data available	nn	No	Not available	nn	No
AWI 207-8	AU085LF	63° 43.07' S 050° 49.91' W	data available	6.7 (12)	Yes	, Full'	+998	No
AWI 207-09	SV1032	63° 42.09' S 050° 49.61' W	data available	nn	No	Not available	nn	No
	SV1033	63° 42.09' S 050° 49.61' W	data available	nn	No	Not available	nn	No
	SV1034	63° 42.09' S 050° 49.61' W	data available	nn	No	Not available	nn	No
AWI 206-7	SV1006	63° 28.84' S 052° 05.77' W	data available	nn	No	Not available	nn	No

Evaluation of recorder performance

However, all SonoVaults had ceased recording prior to recovery. All devices were equipped with sufficient power supply and storage capacity to bridge the entire deployment period with recordings. Most of the recovered SonoVaults still used the hardware version 3.3, with firmware version 3.11, which are now known to use the high-resolution mode as default sampling mode. This led to a higher power consumption and thus to shorter recording periods.

Two recorders (AWI229-12 SV1055 and AWI232-12 SV1059) appear to have suffered a burn out of the batteries for unknown reasons. Recorder SV1055 also contained water, which was observed upon opening the housing. Possibly this water short-circuited the batteries, leading to a fire, although evidence in support of this scenario is missing. Alternatively (and with higher probability), and consistent with the small amount of water observed, excess internal pressure, caused by the burning batteries might have been released through the pressure valve integrated in the top lid of the SonoVault while ascending after the release of the mooring. Upon closing after internal pressure release, the water might have entered through this valve. According to the manufacturer, an exhaustive discharge of the batteries might have caused the batteries to start burning. The same might apply for recorder SV1059.

SV1055 was set to start on the 1 January 2016. In the logfile contained on the first SD card a reboot in August 2015, initiated by the watchdog, was logged. The reason is yet unclear, but it seems to correspond with the time the batteries failed.

Recorder AWI227-13 SV1056 only recorded for a few hours before a software error occurred. The reason for the software error is unknown.

Clock drift and post calibration

To check the clock drift, the hardware and to post-calibrate the hardware in combination with the hydrophone, a 16V laboratory power supply was connected to the hardware. The time drift of the real-time-clock, which is powered independently by a lithium cell embedded on the electronics module, was determined (Tab. 3.1.2.4).

A post calibration of each recovered recorder was performed to ensure the correct calculation of signal levels after recovery. This calculation is still pending and will be completed in Bremerhaven. As mentioned above, the residue of the anodes, might have had an effect on the sound perception in the water for this device. However, with the recorders having been deployed for a significant longer time than the recording period, this residue was likely less at the time of the recordings.

Data quality

In general, the SonoVault recordings were of good quality. Some recordings contained low-frequency noise within the frequency range from 3 to 10 Hz which likely represented internal noise caused by the electronics. Additionally, some recorders (e.g. AWI232-10 SV1003) contained low-frequency noise below 30 Hz. This low-frequent noise occurred throughout the recordings without a clear pattern, hence it is unlikely to be related to transitions between SD cards or modules during data storage. Regularly pulsed electronic noise, as observed in an earlier generation of the recorders, was also noted. In AWI2013-01 SV1030, AWI209-07 SV1028/SV1027, the pulsed noise was only evident a few days before the recorder stopped operating. Therefore, battery voltage related issues might have caused its occurrence. However, for AWI244-04 SV1061, AWI209-07 SV1029, AWI232-12 SV1059, AWI245-03 SV1012 and AWI249-01 SV1014 the presence of monotonous electronic noise and pulses were not restricted to the end of the recording period. The recordings of AWI244-04 SV1061

contained monotonous electronic noise throughout the entire operational period after the 22nd day and the recorded sound levels dropped. The recorder AWI229-11 SV1057 contained broadband electronic noise pulse after a new 10-minute file started (detected three times). In recorder AWI248-01 SV1013 low volume pulsed electronic noise between ca. 750 to 250 Hz in the last two recording months was noted (Tab. 3.1.2.4).

Preliminary scientific results

Monthly long-term spectrograms (LTS, Fig. 3.1.2.5) were calculated for all acoustic data retrieved during PS103 using MATLABM. For calculation speed and memory space reasons, only every fifth 10-min long data file was used for the spectrogram calculation.

These long-term spectrogram (totaling approx. 151,056 hours of recordings) provided the basis for a preliminary analysis investigating acoustic data quality of the recordings as well to determine the presence of distinct acoustic events (e.g., temporally dominant frequency bands, repetitive loud events, etc.) during the recording period (Fig. 3.1.2.5).

Visual and aural inspection of single files (i.e., 10 minute wav files) was conducted using Raven Pro 1.5 Beta Version in order to provide more detailed information on the acoustic presence of different marine mammals. To this end, evaluation was performed using a fifteen day resolution. Furthermore, single files showing conspicuous structures in the long-term spectrogram were additionally chosen for analysis. For each recorder, the audible marine mammal species were depicted in preliminary biodiversity maps (Fig. 3.1.2.6) to obtain a first overview of spatial differences in species composition.

The recordings of recorders AWI217-05 SV1020, AWI207-09 SV1032/SV1033/SV1034, AWI207-08 AU0085LF and AWI206-07 SV1006 (smaller grey shaded species composition squares in Fig. 3.2.1.6) were only superficially screened due to time constraints, choosing days with conspicuous structures in the LT-spectrogram, i.e. not with a fifteen-day resolution. For these coarser scanned data, the information on acoustic biodiversity from recorders from the same mooring site was merged for each recording position (therefore hereinafter indicated by mooring ID only).

Pinnipeds

All recorders deployed in the Southern Ocean recorded vocalizations of leopard seals (*Hydrurga leptonyx*) and crabeater seals (*Lobodon carcinophaga*), except for the recorder at AWI217. The absence of these species at this recording position will be further investigated. Calls of Ross seals (*Ommatophoca rossii*) were not detected in data from recorders at AWI229-11 (SV1057), AWI248-01 (SV1013) and AWI245-03 (SV1012), as well as in data from AWI207 and AWI206. Spatio-temporal patterns in acoustic presence of this species are still relatively unknown given the offshore, pack-ice habitat that this elusive species prefers. Calls are thought to be exclusively produced during the mating season and these data may therefore provide valuable new insights into Ross seal mating behavior and habitat preferences. Weddell seal (*Leptonychotes weddellii*) calls were detected in most recorders that were closest to the continent, likely reflecting their breeding habitat preferences for fast-ice(-associated) areas. The data from AWI245-03 (SV1012) nevertheless, did not contain Weddell seal acoustic signatures. Furthermore, data from AWI208-07 unexpectedly did comprise Weddell seal vocalizations, the exact timing and type of which will be further explored.

Cetaceans

The choruses of Antarctic blue whales (*Balaenoptera musculus intermedia*), fin whales (*B. physalus*) and Antarctic minke whales (*B. bonaerensis*) were present at all recording positions. In contrast, humpback whale (*Megaptera novaeangliae*) calls were recorded at most positions along the Greenwich meridian and across the Weddell Sea north of 65° S. The absence of humpback whale signatures at positions AWI207, AWI217 and AWI206 is likely an artifact of the coarser sampling method with which these recordings were explored, but warrants further investigation. Clicks of sperm whales (*Physeter macrocephalus*) were recorded as well along the Greenwich meridian and at most offshore recording positions across the Weddell Sea north of 65°S. Sperm whale clicks, too, are difficult to detect from LTS's alone, and the absence of clicks in the recordings from AWI207, AWI217 and AWI206 therefore should be interpreted with caution.

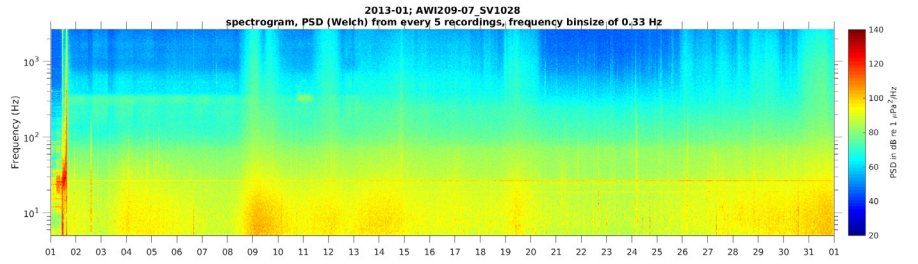
Calls of killer whales (*Orcinus orca*) were recorded in AWI209-07 SV1027/1028 and AWI232-12 SV1059. However, since much of their main vocalization frequencies are higher than the maximum frequency that the SonoVaults can record (i.e., Nyquist frequency 2500 Hz), it is difficult to assess their vocal presence with certainty. Given this uncertainty, killer whale acoustic presence is therefore not included in Fig 3.2.1.5.

Other sound sources

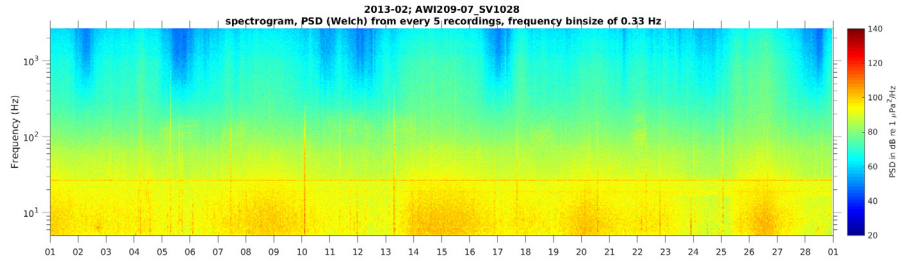
Furthermore, some of the recordings contained occasional air gun signals (e.g., AWI232-10 SV1003 16.02.2011 and 17.02.2011) and broadband noise, the latter presumably originating from distant ships. On 16.07.2013 and 17.07.2013, the recordings from mooring AWI209-07 contained clear ship acoustic signatures.

3.1.2 Ocean acoustics

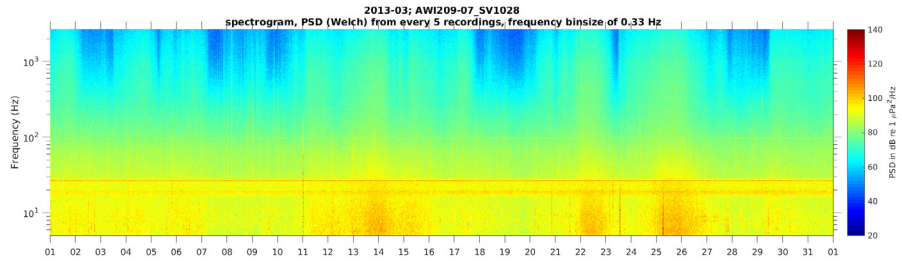
January
2013



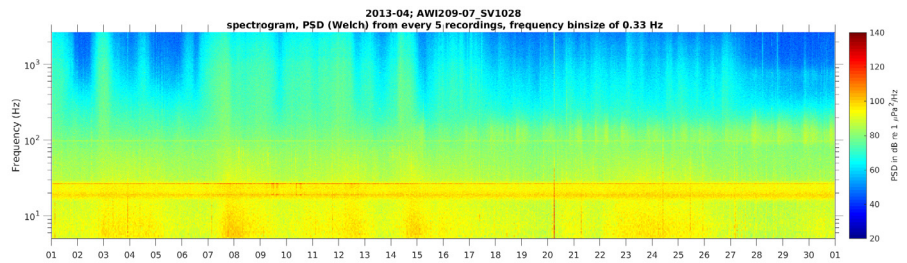
February
2013



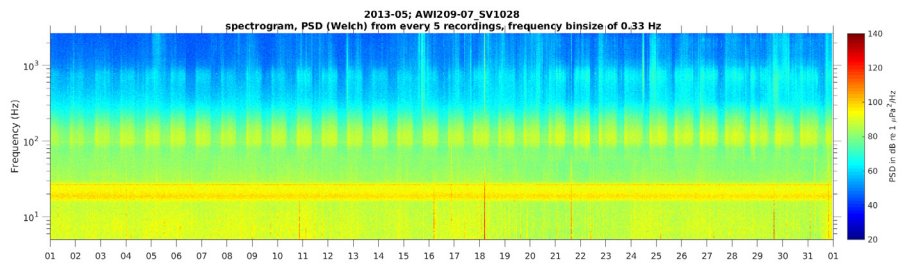
March
2013



April 2013

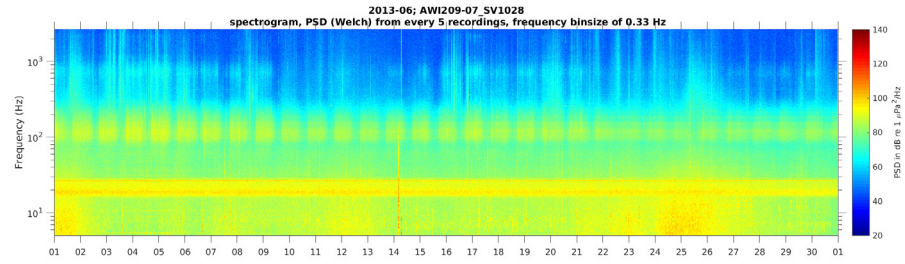


May 2013

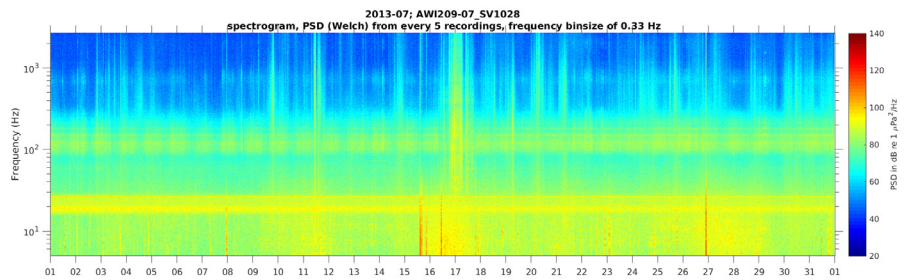


3.1 HAFOS: Maintaining the AWI's long term ocean observatory in the Weddell Sea

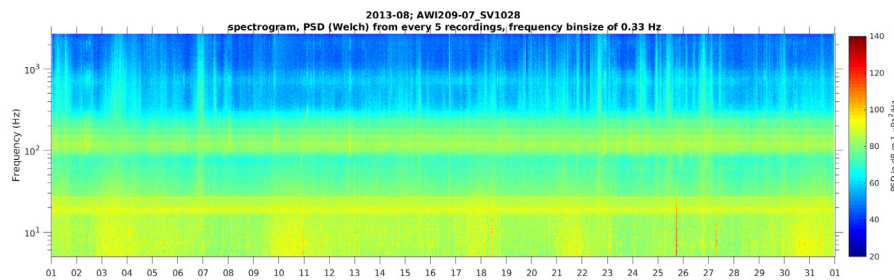
June
2013



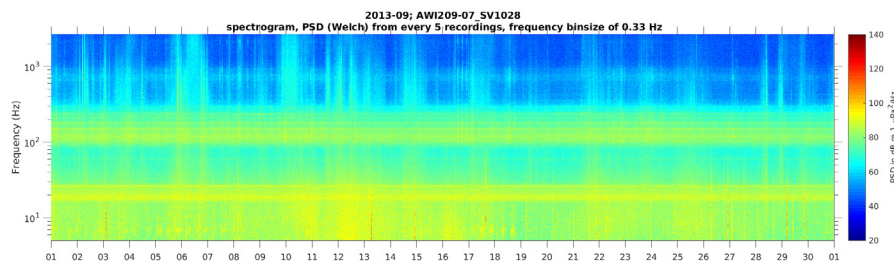
July 2013



August
2013



September
2013



October
2013

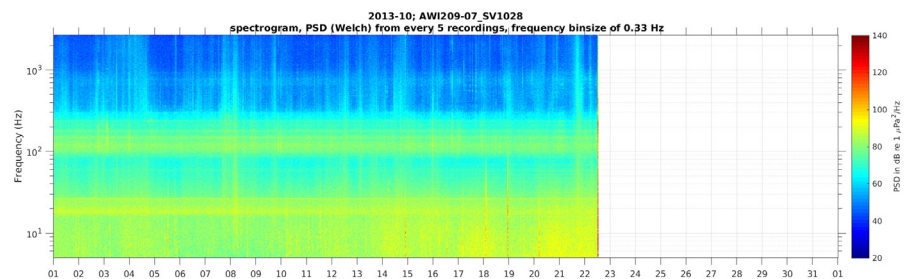


Fig. 3.1.2.5: Example of the 10 monthly long-term-spectrograms of recorder AWI209-07 SV1028 showing the temporal variability in intensity (colour coding) and events, with e.g. in May clear periodic acoustic presences of Antarctic minke whale calling activity

3.1.2 Ocean acoustics

We emphasize that these results base on a first very coarse screening of the passive acoustic data and that it cannot be excluded that the maps presented here do not reflect the full local marine mammal biodiversity.

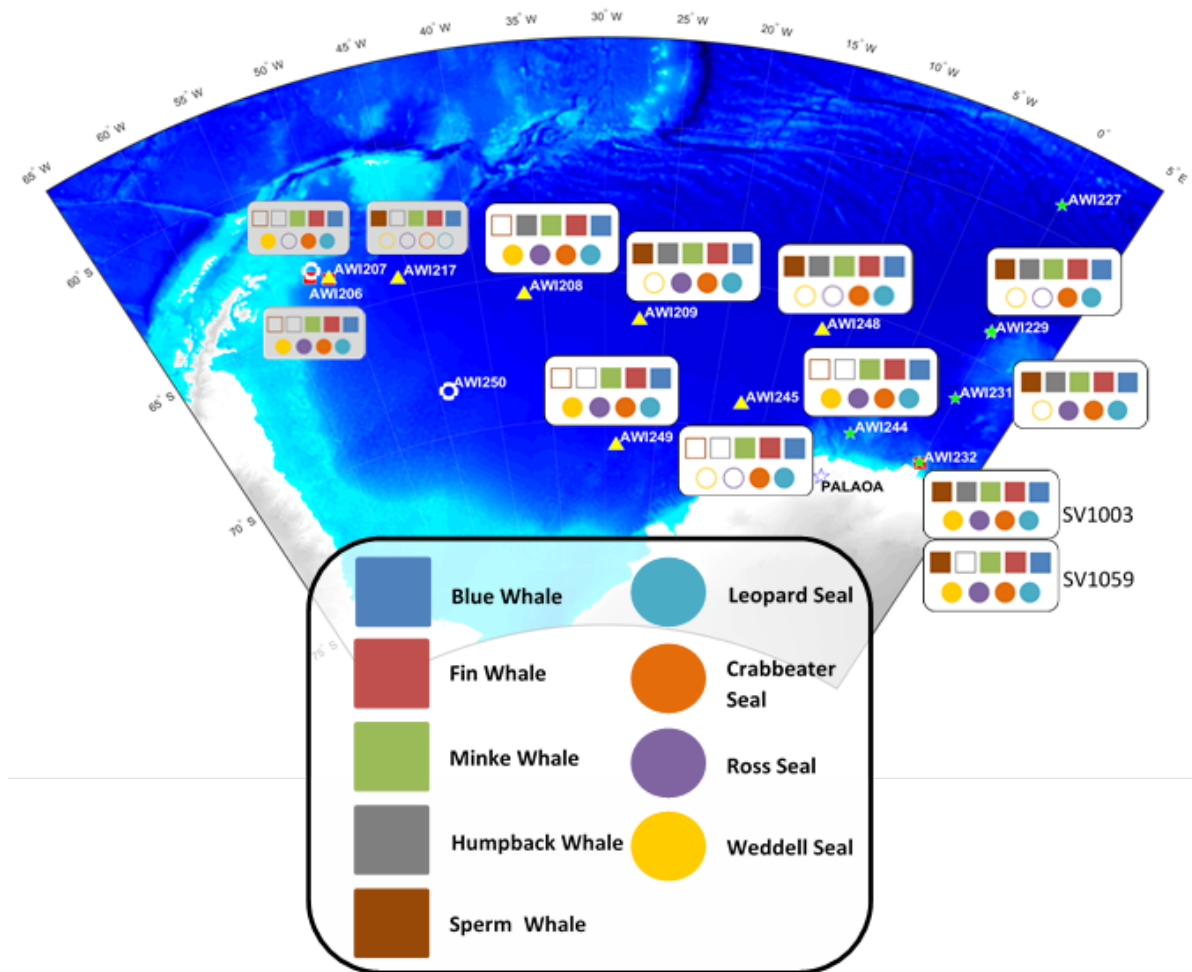


Fig. 3.1.2.6: Preliminary results on acoustic presence of marine mammal species in passive acoustic data recorded at 13 recorder positions from recoveries on PS103 SV1003 and SV1059 were recovered from the same mooring position (AWI232), but were deployed in different years (see Tab. 3.1.2.1). Smaller grey shaded species composition squares (AWI217, AWI207, AWI206) were only superficially screened choosing days with conspicuous structures in the LT-spectrogram but no fifteen-day resolution.

Data management

All passive acoustic data will be transferred to the AWI silo and made accessible through the PANGAEA database. P.I.: Ilse van Opzeeland.

3.1.3 Transport variations of the Antarctic Circumpolar Current

Olaf Boebel¹, Ioana Ivanciu^{1,2}, Gerd Rohard¹,
Matthias Monsees¹
not on board: Andreas Macranders³

¹AWI
²IfM-GEOMAR
³HAFRO

Grant No: AWI_PS103_01

Objectives

Pressure Inverted Echo Sounders (PIES) deliver bottom pressure, bottom temperature and travel times of sound signals from the bottom to the sea-surface, effectively providing a measure of average temperature of the water column and sea surface height (SSH). C-PIES additionally provide local current speed 50 m above the bottom by an acoustic DCS current meter. These data are used to evaluate variations of both barotropic and baroclinic geostrophic transport of the Antarctic Circumpolar Current (ACC) as part of the AWI programme to observe the decadal variability of the ACC. The PIES are placed along the GoodHope section between South Africa and Antarctica (Fig. 3.1.3.1), which in large parts coincides with ground track #133 of the Jason (previously TOPEX/Poseidon) satellite mission to allow direct comparison with altimetry SSH. PIES-to-PIES distances are chosen to resolve the major oceanic fronts of this region.

Work at sea

During PS89, 13 out of 14 PIES were recovered. One PIES (ANT 10 at 49°S) was left on the bottom on the ocean due to severe weather. During PS103, this last C-PIES was successfully recovered, after a record 6 years from deployment, completing the data set from this PIES deployment (Tab. 3.1.3.1).

The PIES was acoustically released by a mobile Teledyne UDB9000 unit connected to a hydrophone lowered over the side of the vessel. Release commands were repeated 6 times with 2-4 minutes spacing to ensure that the PIES is not blocked during its own measurement schedule, and to re-trigger release execution after possible resets. Due to the high underwater noise level of *Polarstern*, acknowledge pings of the PIES were never detected. The PIES mooring featured an Ixsea ET861 Transponder, which was used to establish the underwater location and aid the recovery with the ship's Posidonia device. Monitoring the PIES/transponders ascent, the ship was positioned for the PIES to surface at a bearing of 15° and 2 cables distance from the bow, allowing a speedy recovery from the ship.

3.1.3 Transport variations of the Antarctic Circumpolar Current

Tab. 3.1.3.1: Summary of deployment and recovery information regarding the GoodHope PIES array 2010-2016. Only C-PIES #250 (ANT 10.2) (printed in bold) was recovered during this expedition, the remainder of instruments was recovered during PS89.

PIES SN DCS SN Posidonia SN	Deployment				Recovery				
	Mooring ID Station book	Date time (UTC)	Position (GPS) Depth (DWS)	Deployment CTD	Mooring ID Station book	Release date Release time (UTC)	Position Depth (Posidonia)	Time offset	Recovery CTD
PIES #058	ANT 3-3	30.11.2010	37° 5.84' S 12° 45.23' E 4904 m	PS77/013-1	ANT 3-3	04.12.2014	37° 5.90' S 12° 45.56' E 4983 m	PIES:09:45:12 GMT 09:47:20	PS89/001-1
no DCS ET861 #637	PS77/013-3	06:31			PS89/001-2	07:08			
C-PIES #184	ANT 4-3	05.12.2011	39° 13.07' S 11° 20.04' E 5122	PS79/035-3	ANT 4-2	05.12.2014	39° 13.67' S 11° 20.05' E 5076 m	PIES 13:32:48 GMT 13:34:00	PS89/002-1
DCS #752 ET861 #726	PS79/035-2	12:07			PS89/002-2	01:20			
C-PIES #182	ANT 5-3	02.12.2010	41° 9.77' S 9° 55.31' E 4624 m	PS77/015-1	ANT 5-3	05.12.2014	41° 9.87' S 9° 55.61' E 4605 m	PIES 20:47:00 GMT 20:48:00	PS89/003-1
no DCS ET861 #469	PS77/015-3	08:05			PS89/003-2	18:32			
PIES #069	ANT 6-1	02.12.2010	42° 58.80' S 8° 30.15' E 3930 m	PS77/016-2	ANT 6-1	06.12.2014	42° 58.46' S 8° 30.67' E 3882 m	unavailable	PS89/004-2
no DCS ET861 #384	PS77/016-1	22:17			PS89/004-3	11:23			
C-PIES #181	ANT 7-4	03.12.2010	44° 39.73' S 7° 5.15' E 4593 m	PS77/017-3	ANT 7-4	07.12.2014	44° 39.46' S 7° 5.60' E 4540 m	PIES 06:18:48 GMT 06:18:30	PS89/005-1
DCS #750 ET861 #639	PS77/017-2	18:37			PS89/005-2	04:00			
C-PIES #183	ANT 8-1	04.12.2010	46° 12.97' S 5° 40.23' E 4786 m	PS77/018-2	ANT 8-1	07.12.2014	46° 12.91' S 5° 40.51' E 4767 m	PIES 20:28:56 GMT 20:29:40	PS89/006-1
DCS #751 ET861 #616	PS77/018-1	14:55			PS89/006-2	18:24			

3.1 HAFOS: Maintaining the AWI's long term ocean observatory in the Weddell Sea

PIES SN DCS SN Posidonia SN	Deployment				Recovery				
	Mooring ID Station book	Date time (UTC)	Position (GPS) Depth (DWS)	Deployment CTD	Mooring ID Station book	Release date Release time (UTC)	Position Depth (Posidonia)	Time offset	Recovery CTD
C-PIES #251	Ant 9-3	05.12.2010	47° 39.87' S 4° 15.22' E 4541 m	PS77/019-3	ANT 9-3	08.12.2014	47° 40.34' S 4° 15.03' E 4504 m	PIES 11:12:32 GMT 11:17:10	PS89/007-1
DCS #26	PS77/019-2	10:20			PS89/007-2	08:31			
ET861 #602									
C-PIES #250	ANT 10-2	06.12.2010	49° 0.77' S	PS77/020-3	PS103/002-1	21.12.2016	49° 00.74' S	unavailable due to deple- ted batteries	PS103/02-4
DCS #031	PS77/020-2	03:58	2° 50.05' E			14:09	2° 50.85' E		
ET861 #617			4056 m				4081 m		
C-PIES #249	ANT 11-4	07.12.2010	50° 15.45' S 1° 25.18' E 3901 m	PS77/021-2	ANT 11-4	09.12.2014	50° 15.40' S 1° 25.48' E 3842 m	PIES 16:54:01 GMT 16:59:00	PS89/009-1
DCS # 24	PS77/021-3	00:13			PS89/009-2	15:11			
ET861 #385									
PIES #062	ANT 12-1	07.12.2010	51° 25.15' S 0° 0.24' E 2713 m	PS77/022-2	ANT 12-1	10.12.2014	51° 25.37' S 0° 0.63' E 2638 m	PIES 02:47:03 GMT 02:48:10	PS89/010-2
no DCS	PS77/022-1	10:52			PS89/010-1	01:08			
ET861 #612									
C-PIES # 252	ANT 13-3	08.12.2010	53° 31.22' S 0° 0.13' E 2642 m	PS77/026-3	ANT 13-1	10.12.2014	53° 31.35' S 0° 0.36' E 2570 m	PIES 20:21:12 GMT 20:26:00	PS89/012-2
DCS # 32	PS77/026-2	11:23			PS89/012-1	18:53			
ET861 #391									
PIES # 191	ANT 14-1	10.12.2010	56° 55.71' S 0° 0.01' W 3673 m	PS77/034-2	ANT 14-1	12.12.2014	56° 55.65' S 0° 0.36' E 3714 m	PIES 11:12:51 GMT 11:15:00	PS89/016-1
no DCS	PS77/034-1	04:15			PS89/016-2	08:43			
ET861 #638									
PIES #189	ANT 15-2	11.12.2010	59° 2.37' S 0° 5.29' E 4647 m	PS77/042-2	ANT 15-2	13.12.2014	59° 2.27' S 0° 5.86' E 4594 m	PIES 14:12:52 GMT 14:14:15	PS89/020-2
no DCS	PS77/042-2	18:51			PS89/020-3	11:48			
ET861 #614									

3.1.3 Transport variations of the Antarctic Circumpolar Current

		Deployment				Recovery			
PIES SN	Mooring ID Station book	Date time (UTC)	Position (GPS) Depth (DWS)	Deployment CTD	Mooring ID Station book	Release date Release time (UTC)	Position Depth (Posidonia)	Time offset	Recovery CTD
DCS SN	ANT 17-1	14.12.2010	64° 0.70' S	PS77/053-2	ANT 17-1	17.12.2014	64° 0.55' S	PIES 14:55:02	PS89/027-1
Posidonia SN	PS77/053-1	23:45	0° 2.72' W		PS89/027-4	12:50	0° 3.03' W	GMT 14:57:00	
PIES #125			5201 m				5164 m		
no DCS									
ET861 #601									

GMT+16 s=GPS

Remarks

ANT 4-3 - Only three years of record

ANT 6-1 - Connection through thin wire broken, PIES took approximately 3 h to release; no response on "switch on" – PIES opened, memory card removed.

ANT 10-2 – Low battery at recovery - PIES opened, memory card removed.

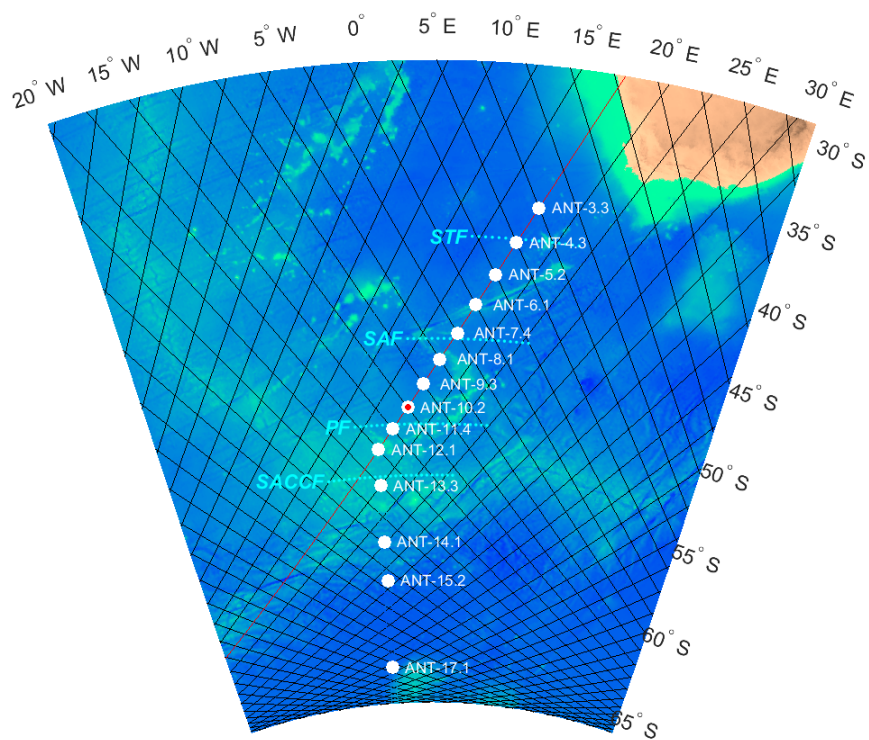


Fig. 3.1.3.1: Summary of deployment and recovery information regarding the GoodHope PIES array 2010-2016. Only C-PIES #250 (ANT 10.2) (printed in bold) was recovered during this expedition, the remainder of instruments was recovered during PS89.

Preliminary results

The PIES was opened after recovery and the memory card was removed for the data to be downloaded and saved to the ship's network drive. Data was processed according to GSO Technical Report No. 2007-02 (Fig. 3.1.3.2, Fig. 3.1.3.3). Travel time data was derived according to the quartile period and the pressure was detided and de-drifted. The average of the differences between the CTD and the PIES temperature at deployment and on 8 December 2014 (when a CTD was casts near the PIES on expedition PS89, Tab. 3.1.3.2) was used to shift the PIES temperature such that it better agrees with the CTD measurements. A fourth order Butterworth filter with a cut-off period of 3 days was applied to the data.

The recovered PIES operated flawlessly over a time period of 5 and a half years, but stopped taking measurements on 8 June 2015 when it detected that its battery was running low. Pressure accuracy and drift is within accepted range of the sensor; also acoustic travel time yields plausible results (Tab. 3.1.3.3).

3.1.3 Transport variations of the Antarctic Circumpolar Current

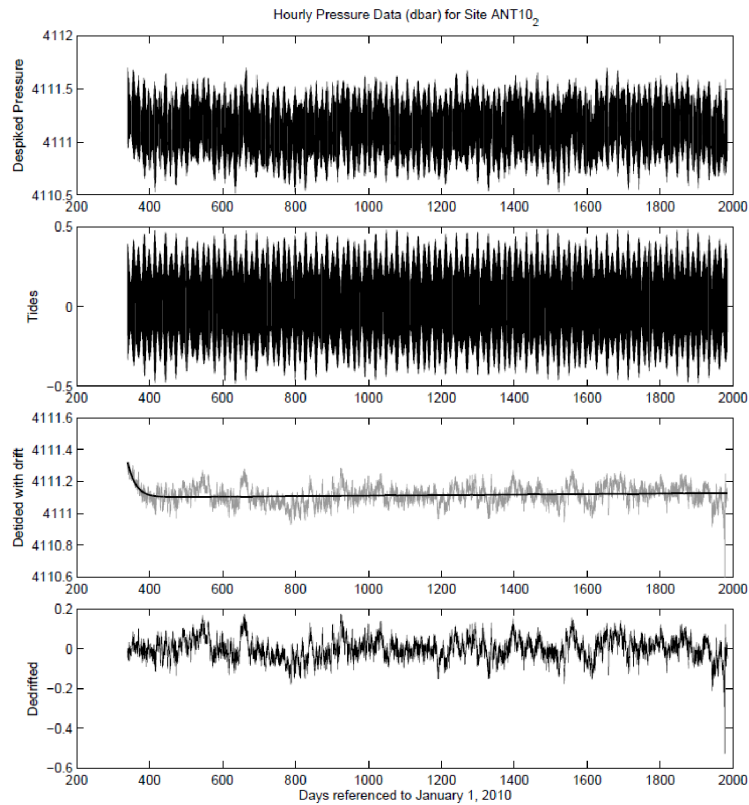


Fig. 3.1.3.2: ANT 10-2 hourly values of raw pressure data, fitted tides, detided pressure data, and detided and de-drifted pressure data (top to bottom). Note the unusual pressure event near the end of the record.

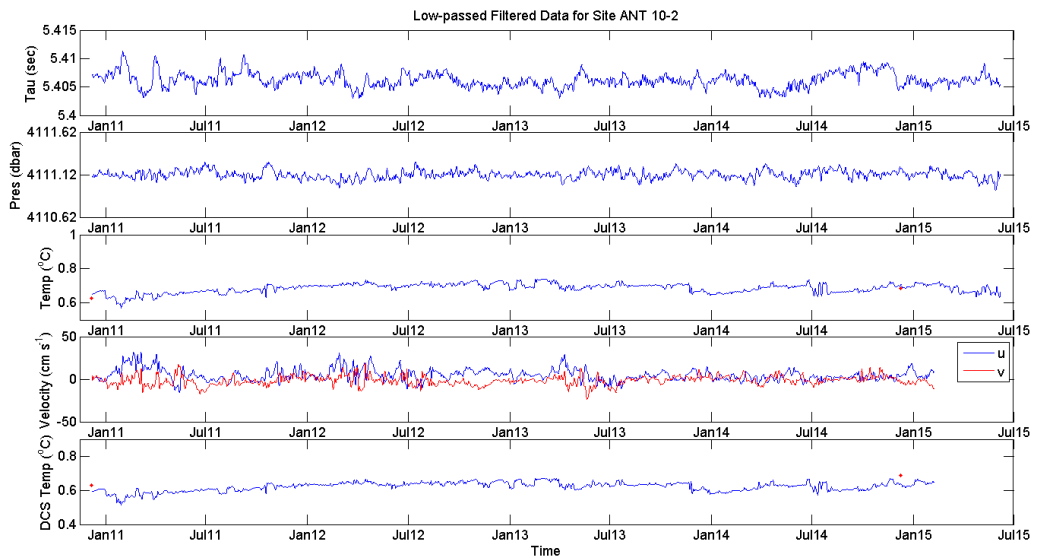


Fig. 3.1.3.3: ANT 10-2 travel time (τ), pressure, temperature, velocity and DCS temperature data after final processing (incl. filtering and shift of PIES temperatures (but not DCS)). The red dots in the temperature time series indicate the CTD's bottom temperatures.

Tab. 3.1.3.2: Temperature offsets between recovered PIES and deep CTD bottom temperatures. Note that the date of the “recovery” data for location Ant 10-2 corresponds to a CTD cast during PS89, when the PIES was not released. As data acquisition had stopped when releasing during PS103, the (existing) CTD cast cannot be matched with corresponding PIES data.

PIES ID Station book	Deployment				Recovery				
	Bottom T [°C]	CTD Pres. [dbar]	CTD Date & Time	CTD Position	Bottom T [°C]	CTD Pres. [dbar]	CTD Date & Time	CTD Position	PIES Pres. [dbar]
ANT 3-3	1.0263	4933	30-Nov- 2010 03:38:00	37.0957 S 12.7702 E	1.1279	4904	04-Dec- 2014 04:57:00	37.1028 S 12.7603 E	5176
ANT 4-3					1.0207	5226	05-Dec- 2014 00:56:00	39.2277 S 11.3338 E	5258
ANT 5-3	0.9921	4778	02-Dec- 2010 05:07:00	41.1247 S 9.9623 E	1.0258	4702	05-Dec- 2014 18:12:00	41.1647 S 9.9267 E	4750
ANT 6-1	1.2557	3968	03-Dec- 2010 00:04:00	42.9823 S 8.5013 E	1.2055	3969	06-Dec- 2014 10:59:00	42.9798 S 8.5058 E	3986
ANT 7-4	0.8495	4654	03-Dec- 2010 20:36:00	44.6693 S 7.0920 E	0.7508	4655	07-Dec- 2014 03:44:00	44.6578 S 7.0923 E	4679
ANT 8-1	0.8419	4889	04-Dec- 2010 16:55:00	46.2195 S 5.6831 E	0.8067	4877	07-Dec- 2014 18:04:00	46.2150 S 5.6750 E	4901
ANT 9-3	0.7160	4604	05-Dec- 2010 12:26:00	47.6605 S 4.2555 E	0.8031	4587	08-Dec- 2014 07:43:00	47.6713 S 4.2537 E	4623
ANT 10-2	0.6282	4079	06-Dec- 2010 05:56:00	49.0145 S 2.8302 E	0.6864	4239	08-Dec- 2014 23:19:00	49.0353 S 2.8600 E	4111
ANT 11-4	0.6060	3889	06-Dec- 2010 22:28:00	50.2602 S 1.4440 E	0.6343	3902	09-Dec- 2014 14:51:00	50.2550 S 1.4255 E	3948
ANT 12-1	0.5443	2698	07-Dec- 2010 12:28:00	51.4195 S 0.0055 E	0.5348	2678	10-Dec- 2014 03:41:00	51.4218 S 0.0097 E	2717
ANT 13-3	0.3843	2619	08-Dec- 2010 12:57:00	53.5200 S 0.0008 W	0.4067	2596	10-Dec- 2014 21:21:00	53.5243 S 0.0030 E	2645
ANT 14-1	-0.2869	3696	10-Dec- 2010 06:04:00	56.9330 S 0.0030 W	-0.2796	3670	12-Dec- 2014 08:11:00	56.9270 S 0.0058 E	3686
ANT 15-2	-0.4026	4677	11-Dec- 2010 20:48:00	59.0387 S 0.1057 E	-0.4029	4683	13-Dec- 2014 11:25:00	59.0373 S 0.0938 E	4701
ANT 17-1	-0.3957	5267	15-Dec- 2010 02:01:00	64.0405 S 0.0030 W	-0.3848	5271	16-Dec- 2014 11:06:00	64.0263 S 0.0173 E	5291

3.1.3 Transport variations of the Antarctic Circumpolar Current

Tab. 3.1.3.3: Overview of data quality from recovered PIES

PIES ID Station book	C-option	Duration	Data quality	Comment	Depth
ANT 3-3		4 years	all good		
ANT 4-3	yes	3 years	all good		
ANT 5-3		4 years	all good		
ANT 6-1		3.5 years	TT gap in 2012		
ANT 7-4	yes	4 years	all good		
ANT 8-1	yes	4 years	all good		
ANT 9-3	yes	4 years	all good	warming 0.1°C	4624 dbar
ANT 10-2	yes	5.5 years (PIES) 5 years (DCS)	all good	-0.5 dbar pressure spike near end of record	
ANT 11-4	yes	4 years	all good		
ANT 12-1		4 years	all good		
ANT 13-3	yes	4 years	all good	warming 0.02°C	2645 dbar
ANT 14-1		4 years	all good		
ANT 15-2		4 years	all good		
ANT 17-1		4 years	all good	warming 0.02°C	5291 dbar

Data management

PIES data will be validated and made available through the Pangaea database at AWI within one year of this cruise. P.I.: Olaf Boebel (AWI) and Andreas Macrander (HAFRO)

References

Fahrbach E (2011) The Expedition of the Research Vessel "Polarstern" to the Antarctic in 2010/11 (ANT-XXVII/2), Berichte zur Polar- und Meeresforschung (Reports on Polar and Marine Research), Bremerhaven, Alfred Wegener Institute for Polar and Marine Research, 634, 242 p. hdl: <http://epic.awi.de/29981/>.

Boebel O (2015) The Expedition PS89 of the Research Vessel POLARSTERN to the Weddell Sea in 2014/2015, Berichte zur Polar- und Meeresforschung = Reports on polar and marine research, Bremerhaven, Alfred Wegener Institute for Polar and Marine Research, 689, 151 p. [10013/epic.45857.d001](http://epic.awi.de/45857.d001)

3.2 EK80 Acoustic Signal Emission Measurements

Maria Pia Falla Ramirez, Stefanie Spiesecke, AWI
 Sarah Zwicker, Olaf Boebel
 Sören Krägefsky (not on board)

Grant No: AWI_PS103_00

Objectives

The purpose of the measurements was to derive the specific characteristics of the acoustic signals emitted by the multi-frequency echo-sounder EK80 system from SIMRAD using different operation modes. The EK80 system on the *Polarstern* consists of the two transducers ES70-7C and ES120-7C mounted behind ice protection windows in the “Kastenkiel” of the vessel. The ES70-7C operates in the frequencies between 45 and 90 kHz and the ES120-7C in the frequencies between 90 and 170 kHz.

Work at sea

The measurements of the EK80 acoustic signal were performed during part of a deep CTD cast. Two hydrophones were used to record the sound signals emitted by the two EK80 transducers. A Posidonia transponder was used to determine the position of the hydrophone ensemble relative to the EK80 transducers. The EK80 transducers are located in the Kastenkiel.

The CTD cast was the PS103-2/4 performed 21 December 2016 with a bottom depth of 4,056 m (Tab. 3.2.1). The CTD winch was stopped after spooling out 1,500 m of winch cable. At this point the recording ensemble was attached and secured to the winch cable. The recording ensemble consisted of the two hydrophones Iclisten 1414 and 1413, passive acoustic recorders manufactured by OceanSonics, Canada, which sampled at a rate of 512,000 samples per second; and the Posidonia acoustic transducer A008 operating at a frequency of 9,5 kHz manufactured by Ixsea. The CTD downcast continued at 17:26 until the maximum CTD depth of 4,022m was reached at 18:17. The recording ensemble was back on deck at 19:16.

Tab. 3.2.1: CTD PS103-2/4 logged activities from DAVIS-Ship on *Polarstern*

Timestamp	Action	Latitude	Longitude	Comment
16:42	in the water	49° 00,825' S	002° 50,189' E	CTD Responsible: I Ivanciu
17:26	information	49° 00,794' S	002° 50,151' E	Hydrophones fixed to cable
18:17	max depth/ on ground	49° 00,831' S	002° 50,227' E	Cable length=4104m
18:17	hoisting	49° 00,830' S	002° 50,226' E	
19:16	information	49° 00,824' S	002° 50,083' E	Hydrophones on deck
19:52	on deck	49° 00,775' S	002° 50,262' E	

During the 110 minutes between 17:26 and 19:16 for which the recording ensemble was in the water, the acoustic signals emitted by the EK80 transducers were recorded. The EK80 transducer ES70-C was active during the downcast (Tab. 3.2.2) and the EK80 transducer ES120-7C was active during the upcast (Tab. 3.2.3). For each EK80 transducer the ramping modus was switched once during the cast between fast and slow. The EK80 transducers sent a FM pulse with a duration of 2.048 ms and were configured during the measurements as registered in the tables below.

Tab. 3.2.2: EK80 ES70-7C Transducer's configuration during the measurements

Power	Frequency range [kHz]	Ramping	Ping & Recording		EK80 SIMRAD data file prefix
			On	Off	
750	45 - 90	fast	17:22:22	17:46:00	PS103_2_4_ES70fast
750	45 - 90	slow	17:46:30	18:16:00	PS103_2_4_ES70slow

Tab. 3.2.3: EK80 ES120-7C Transducer's configuration during the measurements

Power	Frequency range [kHz]	Ramping	Ping & Recording		EK80 SIMRAD data file prefix
			On	Off	
250	90 - 160	slow	18:18:22	18:45:12	PS103_2_4_ES120fast
250	90 - 160	fast	18:45:50	19:14:32	PS103_2_4_ES120slow

The vessel's DOLOG (70 kHz) and ADCP (150 kHz) were turned off at 15:32 and 15:35 respectively. Therefore the data before 15:35 in the IcListen recordings and especially in the EK80 data files show a these signals. Additionally, the IcListen 1413 stopped recording at 18:14.

The Posidonia system delivered the geographical position of the transponder during the measurements, starting the recording at 17:30 until 19:12.

Preliminary and expected results

Measurements were carried out successfully. Detailed data analysis will be performed at AWI.

Data management

Data will be stored in the AWI's permanently storage facility PANGAEA.

3.3 Sea Ice Physics

3.3.1 Deployments of autonomous ice tethered platforms (buoys)

Mathias van Caspel¹, Hendrik Hampe¹ ¹AWI
 Stefanie Arndt¹, Marcel Nicolaus¹ (not on board)

Grant No: AWI_PS103_02

Objectives

The sea ice physics programme during PS103 was mainly designed to renew the network of autonomous measurement platforms (buoys) in the Weddell Sea. Here, we continue and extend the successful deployments of buoys in the same region over previous years (PS89 and PS96), as well as earlier programmes in the Weddell Sea. The main goal of these deployments is to obtain time series measurements of key parameters of the atmosphere, ice, ocean system, which are urgently needed for manifold projects. Based on the combined data sets from the many platforms, we aim to describe the state of sea ice coverage in the observation area. This will improve our knowledge concerning the determination of sea ice thicknesses from other methods like autonomous *in-situ* techniques or remote sensing products. Data that will be obtained during the cruise will additionally be used for the validation of sea ice and snow parameters derived from satellite data (e.g. CryoSat-2, SMOS, AMSR-E) and numerical models (e.g. FESOM), which in turn are used to identify the variability and trends in the sea ice cover. The deployments are a direct contribution to the International Program for Antarctic Buoys (IPAB).

Work at sea

Three different types of buoys were deployed on the sea ice. The different buoy types are: (1) Thermistor string buoys (ice mass-balance buoys, IMBs) will help to detect the temporal evolution of snow and sea ice thickness as they measure the sea ice surface and bottom accumulation and melt. Complementary, sensors allow for measurements of air, snow, and sea ice temperature. The thermistor string length is 5 m long with sensors every 2 cm. (2) Snow Buoys (SB) will serve small-scale regional variability of snow accumulation. They measure snow depth, air temperature and barometric pressure. (3) GPS buoys (surface velocity profilers, SVPs) in an array around the station, the evolution of sea ice and snow thickness can also be related to dynamical processes.

Ideally, one IMB and one SB should be deployed in the center of an ice floe surrounded by three SVPs with ~10 m distance (Fig. 3.3.1.1), so that the relative movement of the buoys would allow additional analysis of dynamic sea ice processes, as ridging and lead opening. Nevertheless, due to the unusual small amount of sea ice cover in the Weddell Sea during the summer 2016/2017 an alternative plan was designed using high resolution satellite images.

One pair IMB, SB was deployed on fast ice in Atka Bay (Fig. 3.3.1.2) bay during the time that the *Neumayer Station III* was serviced. The buoys, all equipment needed, and two scientists (M. van Caspel and H. Hampe) were taken to the ice by helicopter and left there to perform the work. The lower part of the SB, where the battery and electronics are, was carefully dropped in a hole with ~20 cm radius and 1 m depth. The sticking out mast, where the sensors and GPS antenna are attached, was stabilized by four cables fixed to the ice with ice bolts. A thinner hole, ~5 cm radius, was drilled complete through the ice to measure the sea ice thickness and insert the thermistor string from the IMB; the string is hanged on a small tripod placed over the hole.

3.3.1 Deployments of autonomous ice tethered platforms (buoys)

The second hole was immediately filled with ice platelets probably formed due to the presence of super cold water coming from underneath the surrounding ice shelves. The platelets turned the measurement of sea ice thickness and dropping of the thermistor string more difficult than usual since they obstructed the 'free fall' from the equipment. Only one of three SVPs (cf. Fig. 3.3.1.1) was deployed in the first area since we do not expect much dynamical movements over a fast ice area, the SVP was placed near open water approximately 2.7 nm away from the IMB SB pair. Position, ice thickness and snow thickness of all deployments are showed in Tab. 3.3.1.1.

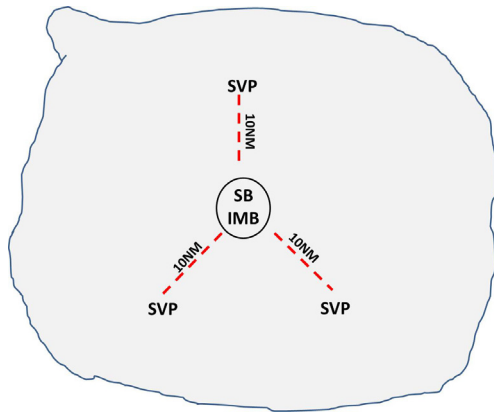


Fig. 3.3.1.1: Schematic of ideal deployment configuration

For the second deployment the ship made a small detour from its planned route into the region off Kapp Norvegia. Sea ice there was formed by several small floes with variable size and thickness, between ~5 m and ~100 m radius, and between 5 cm and 200 cm thickness. After a recognition flight the biggest floe found had a radius of ~500 m. It was decided to place the second IMB SB pair on this floe instead of placing it on fast ice with the hope that the floe would survive the summer and drift into the southwest Weddell Sea. Again the equipment and scientists were deployed by the helicopter, the ship steamed to the floe to guaranty the safe recovery of the researches in case of possible changes in the weather conditions. The second deployment was serviced by three scientists, J. Allerholt joined, which

sped up the procedure. The floe had some small ridges and some melt ponds hidden beneath the snow could be identified. Three SVPs were placed on floes surrounding the central buoys, the biggest available floes near to the desired position were picked for these deployments but all of them had a radius smaller than 100 m.

Fig. 3.3.1.2: GPS buoy (surface velocity profilers, SVP) on the first deployment site. Picture credits H. Hampe.



Tab. 3.3.1.1: Sea ice Buoys deployment information. SB: Snow Buoy, IMB: Sea Ice Mass-balance Buoy, SVP: Surface Velocity Profiler

Date Time (UTC)	Buoy type	IMEI	Latitude (°S)	Longitude (°W)	Ice thickness (cm)	Snow thickness (cm)
First Deployment						
05.01.2017 10:55	SB	300334064116480 under Sensor 1 under Sensor 2 under Sensor 3 under Sensor 4	70.58255	008.02857	240	9 15 14 11 9
05.01.2017 10:55	IMB	034 Sensor numbers at interfaces: •Air-snow: 37 •Snow-ice: 44 •Sea surface: ? •Ice-water: ?	70.58255	008.02857	240	9
05.01.2017 12:00	SVP	300234062783540	70.5678	007.9003		
Second Deployment						
10.01.2017 11:55	SB	3003340640161010 under Sensor 1 under Sensor 2 under Sensor 3 under Sensor 4	71.37068	013.97976	39	6 6 3 3 3
10.01.2017 11:55	IMB	033 Sensor numbers at interfaces: •Air-snow: 29 •Snow-ice: 30 •Sea surface: 33 •Ice-water: ?	71.37068	013.97976	39	6

3.3.1 Deployments of autonomous ice tethered platforms (buoys)

Date Time (UTC)	Buoy type	IMEI	Latitude (°S)	Longitude (°W)	Ice thickness (cm)	Snow thickness (cm)
10.01.2017 11:30	SVP	300234062889930	71.30266	013.87		
10.01.2017 12:30	SVP	300234062880940	71.46033	014.005		6
10.01.2017 12:35	SVP	300234062887950	71.39033	014.27083		4

Preliminary (expected) results

All buoys of the first deployment are stable and sending the data. The SB from the second deployment got a strong tilt after we left. One of the SVPs from the second deployment (IMEI: 300234062889930) is, not sending data. Since the buoy was working during tests performed on deck days before deployment, the most likely cause for the failure is human error, i.e. buoy was not activated.

The buoys of the first deployment will improve the knowledge about the dynamics and thermodynamics of fast ice. With the other buoys one can investigate the relative motion of different ice floes under the same current regime, i.e. do they drift together as an ice aggregate or the floes closer to the open ocean drift away first (faster) then the floes located closer to fast ice. If these floes survive the summer without melting they can drift into the southwestern Weddell Sea and send information about this under sampled region.

The most immediate results are high-resolution time series of essential climate variables from the autonomous measurements and thus directly contribute to various sea-ice related projects and research programmes. Further analysis will enable quantifications of energy and mass budgets of the Weddell Sea and thus help to improve satellite data interpretation and the improvement of numerical models, e.g. towards coupled bio-physical sea ice-ocean models.

Data management

All buoy data contribute to the International Program on Antarctic Buoys (IPAB) and are available online in real time through www.meereisportal.de (and data.seaiceportal.de). Metadata of recorded data will be made available through the cruise report. All data will be published after processing in the PANGAEA database and publishing system. Final results and analyses will be published in international journals.

3.3.2 Along track observations of sea ice conditions

Ioana Ivanciu¹, Katrin Latarius¹, Maria Falla¹,¹AWI
 Mathias Rucker¹, Sandra Tippenhauer¹, Nicolas
 Le Paih¹
 Stefanie Arndt¹, Marcel Nicolaus¹ (not on board)

Grant No: AWI_PS103_02

Objectives

Throughout the last three decades, ship-based visual observations of the state of the sea ice and its snow cover have been conducted during all seasons, serving as the best-available observational data set of Antarctic sea ice. The recordings follow the Scientific Committee on Antarctic Research (SCAR) Antarctic Sea Ice Processes and Climate (ASPeCt) protocol and include information on sea-ice concentration, sea-ice thickness and snow depth as well as sea-ice type, surface topography and floe size. These data are combined with information about meteorologic conditions like air temperature, wind speed and cloud coverage. This protocol is considered a useful method to obtain a broad range of characterization and documentation of different stages of sea-ice and its specific features as encountered during the cruise.

Work at sea

During PS103 the sea-ice observations were carried out at the top of every odd hour during steaming (01:00, 03:00, ..., 23:00 UTC). The observations follow the ASPeCt protocol (Worby, 1999), with a newly developed software observing the ASPeCt standard. The software is installed on a notebook located on the ship's bridge. For every observation, pictures were taken in three different directions, portside, forward, and starboard.

Date, time and position of the observation were obtained from the DSHIP system, along with standard meteorological data (current sea temperature, air temperature, true wind speed, true wind direction, visibility). The recorded sea ice conditions were estimated by taking the average between observations to portside, ahead and to starboard side. Ice thicknesses of tilted floes were estimated by observing a stick attached to the ships starboard side (Fig. 3.3.2.1).



Fig. 3.3.2.1: Example of pictures made to the portside, ahead and starboard showing different sea ice and weather conditions

Sea-ice observations were performed on the top of every odd hour, once we passed the first sea ice on 29 December 2016 at 69° 24.0' S and 0° 01.3' W. The ship left the sea-ice zone on 29 of January 2017 at 61° 13.6' S and 55° 39.6' W. Fig. 3.3.2.2 shows the expedition track with the segments along which the sea-ice observations were performed superposed. Within the 32 days of observations, we obtained 113 individual observations. Sea-ice observations were skipped when the ship was stopped, for example at CTD stations. During the provisioning of *Neumayer Station III*, i.e. while berthed on the shelf ice edge, observations were taken once a day in order to track the time evolution of sea ice at this location.

3.3.2 Along track observations of sea ice conditions

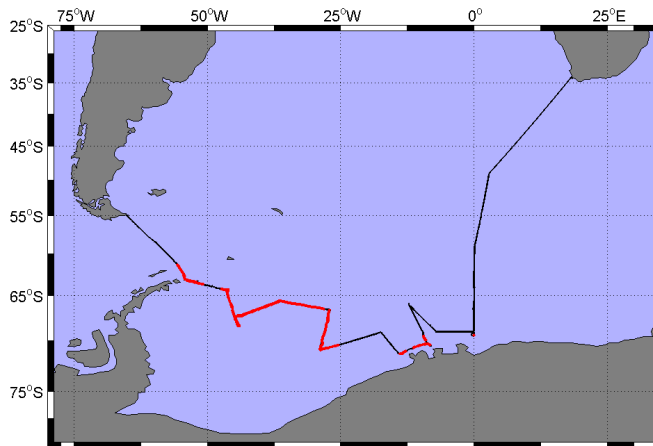


Fig. 3.3.2.2: PS103 expedition track from Cape Town to Tierra del Fuego (black line) and stretches over which sea-ice observations were conducted (red). No observations were taken in regions far from any ice as indicated by AMSRI where sea-ice concentration may be safely assumed to be 0.

Preliminary results

The mean sea-ice concentration (averaged over all observations) was calculated to be 20 % and the level sea-ice thickness 1.4 m. Fig. 3.3.2.3 shows the variation of the sea-ice concentration and the sea-ice thickness along the cruise track. The sea-ice concentration varied between fully covered in the region close to the shelf ice edge near Neumayer III station and open water along large sections of our track. Sea-ice thicknesses of up to 6 m were observed, but mostly it was between 0.7 m and 1.5 m. on average.

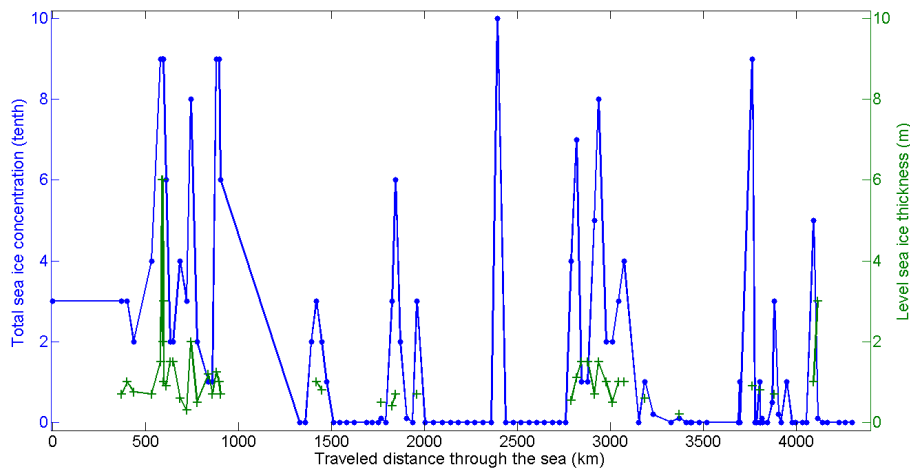


Fig. 3.3.2.3: Total sea-ice concentration and total level sea-ice thickness from of ASPeCt observations over travelled distance within the area where sea-ice was present.

Data management

The visual sea-ice observations will be post-processed after the cruise and will be published together with the taken pictures in PANGAEA within two months after the cruise.

References

Worby AP (1999) Observing operating in the Antarctic sea ice: A practical guide for conducting sea ice observations from vessels operating in the Antarctic pack ice.

3.4 INTERPELAGIC: Interactions between Key Players of the Southern Ocean Zooplankton: Amphipods, Copepods, Krill and Salps

Charlotte Havermans¹, Simon Schöbinger¹, Franz Schröter¹

¹University of Bremen

Grant-No. AWI_PS103_03

Objectives

The Southern Ocean is experiencing rapid environmental change in the form of raising surface water temperatures and sea ice retreat, which result in density changes and distributional shifts of key players during the last decades. Since the 1970s, Antarctic krill (*Euphausia superba*) has experienced a major decline, whilst salps (mainly *Salpa thompsoni*) are on the rise, particularly in the Southwest Atlantic sector where changes have been most drastic (Loeb et al. 1997, Atkinson et al. 2004). These density changes have been mainly attributed to bottom-up factors such as alterations in summer phytoplankton blooms and winter sea-ice extent (Loeb et al. 1997, Atkinson et al. 2004). Salps indeed thrive in less productive and warmer waters, whilst Antarctic krill is dependent on sea ice for feeding of the larvae during winter. Hence, it is likely that salps outcompete krill under the predicted climate change scenario of less sea ice and warmer surface waters, implying the substitution of an essential component of the Antarctic pelagic food web. This will have negative consequences for higher trophic levels (e.g. for the ice-associated and krill-feeding blue whale and minke whale) and for the fishing industries, as well as major biogeochemical implications. For example, the production of large faecal pellets by salps may enhance the sinking rate of biogenic carbon (Alcaraz et al. 2014) whilst krill concentrate iron in their faeces and hence play a major role in the recycling of this nutrient constraining productivity in the Southern Ocean (Smith et al. 2016).

These past and ongoing changes in krill and salp densities - most likely to be intensified due to the rising water temperatures - are however not the only changes that the Antarctic and sub-Antarctic pelagic will experience. Known as the most common pelagic amphipod in the Southern Ocean, the predominantly carnivorous amphipod *Themisto gaudichaudii* occurs in high densities in waters at sub-zero temperatures to as far north as the Subtropical Front (Kane 1966, Auel and Ekau 2009). It has its core distribution centre in the more productive eastern Scotia Sea, near South Georgia (Mackey et al. 2012). In the northern ice-free zones of the Scotia Sea, the more widespread species *T. gaudichaudii* is dominant, whilst the southern fauna, influenced by a seasonal sea ice cover, is composed of a more cold-adapted fauna such as Antarctic krill (Ward et al. 2012). Unlike krill that is more closely associated with colder waters, *T. gaudichaudii* has a much broader temperature tolerance and hence may be better equipped to cope with change. In a current and a predicted scenario of a decreasing winter sea-ice extent (e.g. Parkinson 2002), *T. gaudichaudii* could simply extend its range southward. Indeed, Mackey et al. (2012) predicted that, when considering pelagic species' distributions in relation to temperature, with a 1°C increase in winter water temperature, *T. gaudichaudii* will become much more widespread and abundant across the Scotia Sea, which may widen its predation impact on mesozooplankton and recruiting stages of Antarctic krill and mackerel icefish.

As krill abundance is known to fluctuate locally and regionally from year to year (e.g. Brierly et al. 1997, Murphy & Reid 2001), one can already deduct the ramifications of these ongoing and predicted range shifts on top predators from present-day observations. Even though some krill consumers can efficiently switch from a krill-based to an amphipod-based diet in years of low krill availability (e.g. Macaroni penguins), most species seem to be truly krill-dependent for their breeding success and even adult survival, which was shown to be the case for the black-browed

and grey-headed albatrosses, the Gentoo penguin and the Antarctic fur seal (e.g. Croxall et al. 1999, Forcada et al. 2005). However, these effects can only be evaluated when there is sufficient knowledge for the functioning and roles of the different components representing the lower trophic levels. The distributional ranges of the three key players, *Themisto*, salps and Antarctic krill, will be undergoing an increasing overlap (documented in Mackey et al. 2012). Whilst Antarctic krill has been thoroughly studied, hyperiid amphipods in general, and *T. gaudichaudii* in particular, have been neglected so far and the lack of a solid baseline knowledge of their ecology, diversity and connectivity severely hampers the evaluation of potential distributional and ecological shifts in the light of climate change. Due to the knowledge gap on the role of top-down processes in the pelagial, in particular the predator-prey relationships between its key players, ongoing changes may remain unnoticed. The feeding ecology of *Themisto* has only been studied locally (e.g. around South Georgia, Pakhomov & Perissinotto 1996, and around the Prince Edward Islands, Froneman et al. 2000), and based on these studies this species is believed to be an opportunistic carnivore. However, recent results pinpointed uncertainties regarding the prevalence of omnivorous habits and a high degree of herbivory was revealed (Stowasser et al. 2012). Hence, characterisation of regional variation in the diet of *Themisto* is needed in terms of competition for resources or predation in order to predict the consequences of these distributional and ecological shifts, i.e. the poleward range expansion of *Themisto* and salps and the range retraction of krill. Finally, the genetic connectivity and potential for local adaptation has not yet been studied with recent molecular tools or on a large geographic scale. Preliminary genetic studies based on the COI gene (or barcode marker) has pointed out the existence of three lineages within *T. gaudichaudii* in the Atlantic sector of the Southern Ocean (Havermans 2015), however, more specimens from other localities need to be investigated to test whether gene flow occurs between temperate, sub-Antarctic and Antarctic populations, as well as between coastal (Antarctic Peninsula) and oceanic regions (Antarctic Polar frontal zone).

With this project, we aimed to gain a better understanding of the trophic interactions between the main key players in the Southern Ocean pelagic realm, as well as their genetic connectivity and resilience to change. Our main focus was the biology and ecology of *Themisto* and other hyperiid amphipods as well as detailed studies on their trophic and genetic connectivity. Thus, the objectives of this project were to:

- Quantify abundance, biomass and biodiversity of the different zooplankton components (copepods, hyperiid amphipods, chaetognaths, gelatinous zooplankton);
- Study trophic interactions (predator-prey relationships) in order to delimit the roles of the different components of the Southern Ocean pelagic food web. For this purpose, classic approaches (feeding experiments, morphological gut content analysis) will be combined with state-of-the-art trophic biomarker studies (fatty acid biomarkers, stable isotopes) and molecular diet analyses.
- Investigate comparative gene expression responses and transcriptional regulation of the different key zooplankton species under varying thermal regimes in the light of the different scenarios of predicted range extensions or retractions. Together with the results of the population genetic analyses, these data may be crucial for studying potential adaptation under climate change scenarios.
- Gain insights into the general ecology and biology of *Themisto gaudichaudii* by means of life history analyses and behavioural observations;
- Study the genetic structure of pelagic hyperiid amphipods in general, and *T. gaudichaudii*

in particular, throughout the sampling region, and in a later stage, between the sampling region and other localities in the Antarctic, sub-Antarctic and temperate shelf ecosystems where *T. gaudichaudii* represents a key species (e.g. Patagonian shelf, Benguela Upwelling system). This will allow us to clarify its adaptation and spreading potential and interspecific evolutionary relationships amongst hyperiid amphipod taxa.

Work at sea

At three stations stratified mesozooplankton samples were collected with a HydroBios Multinet Midi (mouth opening 0.25 m²) equipped with five nets of 150 µm mesh size. Sampling at each of these stations (St 001 – St 003) was carried out to a maximum depth of 350 m. Standard depth intervals were: 350 m to 150 m, 150 m to 100 m, 100 m to 50 m, 50 m to 20 m and 20 m to the surface. More mobile macrozooplankton species, such as our target taxa (hyperiid amphipods), can avoid slower nets and hence were clearly underestimated in these vertical net hauls. Therefore, most samples for further analyses and experimental work on board were collected from the epipelagic layer (max. 450 m to 0 m) using oblique hauls with 50 towed Bongo nets (mesh size 500 µm, max. towing speed 1.5 knots) equipped with a large non-filtering cod end. At the three first stations (St 001 – St 003), oblique tows were carried out from the side of the ship, whilst from station 004 onwards, the nets were towed from the aft of the ship, allowing a better positioning of the gear as well as monitoring of the speed of the vessel. A video survey was carried out at every station by deploying the nets with a GoPro® camera attached to the frame, and deploying it to a maximum depth of 60 m. This approach has been shown useful for obtaining a semi-quantitative estimate of net avoidance by particular groups, a better characterization of soft-bodied zooplankton such as jellyfish and salps, and a rough impression of the depth distribution of particular taxa. Details of each net deployment are given in Tab. 3.4.1.

Tab. 3.4.1: Deployment details and most abundant taxa found at each zooplankton sampling station

Date	Station	Net	Deployment details	Dominant taxa
20.12.16	001/3	MN	closures: 20, 50, 100, 150, 350 m	Copepods, <i>T. gaudichaudii</i>
20.12.16	001/4	Bongo	60 m, oblique tow (10'), Video	Copepods, <i>T. gaudichaudii</i>
20.12.16	001/5	Bongo	450 m, oblique tow (5')	Copepods, <i>T. gaudichaudii</i>
21.12.16	002/2	MN	closures: 20, 50, 100, 150, 350 m	Copepods, <i>T. gaudichaudii</i>
21.12.16	002/5	Bongo	60 m, oblique tow (10'), Video	<i>T. gaudichaudii</i> , salps, euphausiids
21.12.16	002/6	Bongo	60 m, oblique tow (5')	<i>T. gaudichaudii</i> , salps, euphausiids
22.12.16	003/3	MN	closures: 20, 50, 100, 150, 350 m	Copepods, tintinnids, <i>T. gaudichaudii</i>
22.12.16	003/4	Bongo	60 m, oblique tow (10')	Copepods, <i>T. gaudichaudii</i>
22.12.16	003/5	Bongo	150 m, oblique tow	Copepods, <i>T. gaudichaudii</i>
22.12.16	003/6	Bongo	60 m, vertical haul	Copepods, <i>T. gaudichaudii</i> , <i>Limacina</i>
23.12.16	004/3	Bongo	60 m, oblique tow (10') from aft, video survey	Copepods, polychaetes, pteropods, krill

Date	Station	Net	Deployment details	Dominant taxa
23.12.16	004/4	Bongo	150 m, oblique tow (5') from aft	Copepods, polychaetes, pteropods, krill
24.12.16	005/6	Bongo	60 m, oblique tow (10') from aft, video survey	Copepods, Clio, appendicularians, salps
24.12.16	005/7	Bongo	200 m, oblique tow (5') from aft	Copepods, Clio, polychaetes, salps
25.12.16	006/4	Bongo	60 m, oblique tow (10') from aft, video survey	Copepods, salps
25.12.16	006/5	Bongo	200 m, oblique tow (5') from aft	Copepods, salps, euphausiids
27.12.16	008/1	Bongo	60 m, oblique tow (10') from aft, video survey	Copepods, polychaetes, <i>Limacina</i> , <i>Hyperia</i>
27.12.16	008/2	Bongo	200 m, oblique tow (5') from aft	Copepods, polychaetes, <i>Limacina</i> , <i>Hyperia</i>
28.12.16	010/2	Bongo	60 m, oblique tow (10') from aft, video survey	Copepods, appendicularia, Clione, <i>Limacina</i>
28.12.16	010/3	Bongo	150 m, oblique tow (5') from aft	Copepods, Clione, <i>Limacina</i> , jellyfish
28.12.16	012/2	Bongo	surface tow from aft, video survey	<i>Euphausia superba</i> , <i>Limacina</i>
28.12.16	012/3	Bongo	surface tow from aft, video survey	<i>Euphausia superba</i> , <i>Limacina</i>
01.01.17	022/6	Bongo	60 m, oblique tow (10') from aft, video survey	Copepods, euphausiids, pteropod spp.
01.01.17	022/7	Bongo	300 m, oblique tow (5') from aft	Copepods, polychaetes, pteropod spp.
02.01.17	023/3	Bongo	60 m, oblique tow (10') from aft, video survey	Copepods, appendicularians, amphipods
02.01.17	023/4	Bongo	350 m, oblique tow (5') from aft	Copepods, chaetognaths, <i>Hyperia</i>
09.01.17	027/1	Bongo	60 m, tow interrupted (ice floes), video survey	Calanoid copepods, euphausiids, <i>Limacina</i>
10.01.17	030/1	Bongo	60 m, oblique tow (10') from aft, video survey	Calanoid copepods, ctenophores, krill
10.01.17	030/2	Bongo	350 m, oblique tow (5') from aft	Calanoid copepods, krill, <i>Hyperia</i>
11.01.17	031/5	Bongo	60 m, oblique tow (10') from aft, video survey	Copepods, chaetognaths, <i>Hyperia</i> , <i>Limacina</i>
11.01.17	031/6	Bongo	350 m, oblique tow (5') from aft	Copepods, chaetognaths, <i>Hyperia</i> , <i>Limacina</i>
20.01.17	040/6	Bongo	60 m, oblique tow (10') from aft, video survey	Copepods, jellyfish, Clio, appendicularians
20.01.17	040/7	Bongo	350 m, oblique tow (5') from aft	Copepods incl. predatory ones, jellyfish, Clio,
23.01.17	045/1	Bongo	60 m, oblique tow (10') from aft, video survey	Copepods, salps, <i>Vibilia</i> , appendicularians
23.01.17	045/2	Bongo	350 m, oblique tow (5') from aft	Predatory copepods, salps, jellyfish, <i>Vibilia</i>

3.4 INTERPELAGIC: Interactions between Key Players of the Southern Ocean Zooplankton

Date	Station	Net	Deployment details	Dominant taxa
24.01.17	048/3	Bongo	60 m, oblique tow (10') from aft, video survey	Salp chains, calanoid copepods, <i>Vibilia</i>
24.01.17	048/4	Bongo	350 m, oblique tow (5') from aft	Salp chains, calanoid copepods, <i>Vibilia</i>
25.01.17	053/2	Bongo	60 m, oblique tow (10') from aft, video survey	Copepods, <i>Limacina</i> , appendicularians
25.01.17	053/3	Bongo	350 m, oblique tow (5') from aft	Copepods, <i>Limacina</i> , chaetognaths
26.01.17	056/2	Bongo	60 m, oblique tow (10') from aft, video survey	Copepods, euphausiids, pteropods
26.01.17	056/3	Bongo	350 m, oblique tow (5') from aft	Copepod nauplii, copepods, euphausiids
27.01.17	061/2	Bongo	60 m, oblique tow (10') from aft, video survey	Clio pteropods, copepods
27.01.17	061/3	Bongo	350 m, oblique tow (5') from aft	Chaetognaths, euphausiids, ctenophores
28.01.17	067/3	Bongo	60 m, oblique tow (10') from aft	<i>Euphausia superba</i> , copepods
28.01.17	067/4	Bongo	150 m, oblique tow (5') from aft	<i>Euphausia superba</i> , copepods
28.01.17	070/2	Bongo	60 m, oblique tow (10') from aft, video survey	<i>Euphausia superba</i> , copepods
28.01.17	070/3	Bongo	200 m, oblique tow (5') from aft	Copepods, <i>Euphausia superba</i>
29.01.17	071/4	Bongo	60 m, oblique tow (10') from aft, video survey	Salps, <i>Vibilia</i>
29.01.17	071/5	Bongo	350 m, oblique tow (5') from aft	Salps, <i>Vibilia</i>
30.01.17	072/3	Bongo	60 m, oblique tow (10') from aft, video survey	Salps, <i>Euphausia superba</i>
30.01.17	072/4	Bongo	350 m, oblique tow (5') from aft	Salps, <i>Euphausia superba</i>
30.01.17	073/3	Bongo	60 m, oblique tow (10') from aft, video survey	<i>Euphausia superba</i>
30.01.17	073/4	Bongo	350 m, oblique tow (5') from aft	Salps, <i>Euphausia superba</i> , <i>Cylopus</i> , <i>Vibilia</i>

Zooplankton samples were sorted alive in a temperature-controlled laboratory container immediately after the catch in order to collect frozen and ethanol-preserved samples for trophic biomarker studies and genetic analyses. Ethanol-preserved samples of *T. gaudichaudii* and other hyperiid amphipods were taken for various purposes, including taxonomic, life history, phylogeographic and molecular diet analyses. For other zooplankton samples, frozen and ethanol-preserved samples were prepared for biomarker and genetic studies, respectively. The biomarker samples have been prepared for fatty acid and stable isotope analyses as well as dry weight calculations to be carried out in the home laboratory, in order to reveal the role of the different taxa in the Southern Ocean pelagic food web. Ethanol-preserved samples of

all zooplankton taxa encountered will serve for genetics, in order to establish a DNA-sequence library of COI-“barcodes” that will serve as reference for detecting the prey in the stomachs of hyperiid amphipods investigated with molecular diet analyses. RNAlater-preserved samples were taken for some taxa for *in-situ* gene expression profiles and for the different animals with which temperature-change experiments were carried out.

Alive specimens of copepods, euphausiids, salps and amphipods were isolated and used for starvation, interaction (IA), feeding (Fexp) or temperature-change (Texp) experiments. All experiments were conducted in aquaria containing 0.2 µl-filtered seawater and details can be found in Tab. 3.4.2. One starvation experiment was conducted where 50 juvenile *Themisto* were kept in individual beakers (to avoid cannibalism): 25 juveniles at 0°C and 25 at 11°C (progressive warming from 5°C to 11°C). Several different feeding experiments were carried out, including prey preference experiments where *Themisto* amphipods were placed with potential prey taxa in small individual aquaria. Depending on the sampled number of individuals and their condition, the experiments consisted of at least 5 replicates (5 for Fexp 1 and 8-10 for the other experiments) and one or more control consisting of an aquarium without *Themisto* but with all prey taxa. One feeding experiment was carried out where one *Themisto* has been exposed to three large krill in order to find out whether the amphipods feed on adult krill much larger than themselves. Furthermore, three interaction experiments were designed in order to reveal the relationship between hyperiids and soft-bodied zooplankton. In the first one, five juvenile *Themisto* were exposed to a small salp in a small container (10 replicates) and their visits on salps as a substrate or for feeding were noted every 5-10 minutes during two hours. The same was done in the second interaction experiment with adult *Themisto*: 5 adults and 1 salp were placed together in all 5 different aquaria. Finally, an interaction experiment was also carried out with the species *Vibilia antarctica* (Crustacea: Amphipoda: Hyperieida), that are suspected to use salps not only as a host but also for feeding. These amphipods were very abundant at one station (St 048) where both salps and a jellyfish species were found in very high numbers. Hence, to find out whether they are specialized exclusively on salps as host or food, we tested the amphipods' affinity for either salps or jellyfish by exposing them to either salps (*Salpa thompsoni*, 5 replicates) or jellyfish (5 replicates) or to both (5 replicates).

For the temperature-change experiments carried out on board, animals were incubated for particular time intervals at increasing or decreasing temperatures compared to the temperature recorded *in-situ*. Details are given in Tab. 3.4.2. Molecular genetic analyses of gene expression (transcriptomics) in the home lab will show which genes are most important for temperature acclimation in zooplankton species and whether gene expression differs between regional populations. These experiments were conducted with (1) *T. gaudichaudii* (both adults and juveniles) (2) Antarctic krill, (3) *Salpa thompsoni*, (4) *Calanus propinquus* and (5) *Calanus similimus*. Several individuals were gently picked out of the sample, representing natural *in-situ* conditions, and immediately frozen in RNAlater and stored at -80°C. The remaining groups of individuals were placed in 300 ml flasks filled with filtered seawater (for copepods) or larger aquaria (for other taxa) and placed in a temperature-controlled laboratory container at 0-1°C, 6-8°C or 11-12°C, depending on the experiment. After 24h of acclimation (t₀), a subsample of 1-21 individuals was preserved in RNAlater and stored at -80 °C and all other individuals were transferred to different flasks or aquaria with water at higher temperatures (heat shock) or transferred to a laboratory container at a different temperature (for a gradual temperature decrease or increase). Then, subsamples were preserved in RNAlater and frozen after different time intervals (1h, 2h, 4h, 8h, 16h, 32h).

3.4 INTERPELAGIC: Interactions between Key Players of the Southern Ocean Zooplankton

Tab. 3.4.2: Description of the experimental work conducted on board. For each feeding (Fexp) or interaction experiment, there were at least 8-10 replicates. Different temperatures to which the animals have been exposed during the temperature-change (Texp) experiments are shown as well as the intervals at which individuals have been sampled for gene expression profiles.

Experiment	Taxon	Description
Starvation	<i>T. gaudichaudii</i> (juveniles)	Starving 2x 25 individuals at 9°C and 0°C
Fexp1: prey preference	<i>T. gaudichaudii</i> (adults)	1 <i>Themisto</i> and 5 copepods, 1 chaetognath, 1 salp, 1 <i>Limacina</i>
Fexp2: prey preference	<i>T. gaudichaudii</i> (adults)	Krill vs salps: 1 <i>Themisto</i> , 3 euphausiids, 3 small salps
Fexp3: krill as prey	<i>T. gaudichaudii</i> (adults)	1 <i>Themisto</i> and 3 large euphausiids (> 5 cm)
Fexp4: prey preference	<i>T. gaudichaudii</i> (adults)	1 <i>Themisto</i> , 10 copepods, 2 euphausiids
Fexp5: prey preference	<i>T. gaudichaudii</i> (adults)	1 <i>Themisto</i> , 1 <i>Clio</i> pteropod, 1 <i>Hyperietta</i> amphipod
Fexp6: prey preference	<i>T. gaudichaudii</i> (adults)	1 <i>Themisto</i> , 10 copepods, 5 euphausiids
Interaction 1: <i>Themisto</i> /salps	<i>T. gaudichaudii</i> (juveniles)	5 juvenile <i>Themisto</i> with 1 salp
Interaction 2: <i>Themisto</i> /salps	<i>T. gaudichaudii</i> (adults)	1 adult <i>Themisto</i> with 1 salp
Interaction 3: host preference	<i>Vibilia antarctica</i> (adults)	1 <i>Vibilia</i> with 1 salp or 1 jellyfish, or both
Texp 1: increase vs. decrease	<i>T. gaudichaudii</i> (adults)	N=55; 5°C (<i>in-situ</i>) à 13.5°C, 5°C à 1.5°C
Texp 2: heat shock	<i>T. gaudichaudii</i> (juveniles)	N=105; 0°C (<i>in-situ</i>) à 11°C, after 1h, 2h, 4h, 8h, 16h, 32h
Texp 3: heat shock	<i>T. gaudichaudii</i> (adults)	N=105; 0°C (<i>in-situ</i>) à 11°C, after 1h, 2h, 4h, 8h, 16h, 32h
Texp4: gradual decrease	<i>Salpa thompsoni</i>	N=10; 5°C (<i>in-situ</i>) à 1°C, after 24h
Texp5: gradual increase	<i>Euphausia superba</i>	N=75, 0°C (<i>in-situ</i>) à 8°C, after 1h, 2h, 4h, 6h
Texp6: heat shock	<i>Calanus simillimus</i>	N=105; 0°C (<i>in-situ</i>) à 11.5°C, after 1h, 2h, 4h, 8h, 16h, 32h
Texp7: heat shock	<i>Calanus simillimus</i>	N=105; 0°C (<i>in-situ</i>) à 8°C, after 1h, 2h, 4h, 8h, 16h, 32h
Texp8: heat shock	<i>Calanus propinquus</i>	N=105; 0°C (<i>in-situ</i>) à 11°C, after 1h, 2h, 4h, 8h, 16h, 32h

Finally, during the feeding experiments, as well as while keeping the animals alive from the different catches, we documented and photographed feeding interactions and other behavioural observations. Brood size was measured for female *Themisto* amphipods bearing juveniles in their brood pouch and faecal pellets of amphipods have been documented. Sinking speeds of dead *Themisto* individuals of different size classes were measured with video recordings and time measurements and will be compared with similar size classes of other types of organisms such as chaetognaths and copepods, as well as with different *Themisto* species measured during a previous Arctic expedition.

Preliminary and expected results

Stations and sampling

At the first three stations, *T. gaudichaudii* was recovered both in the Multinet as in the Bongo net samples, however in much higher numbers with the latter sampling gear. These three stations (45° to 51°S) varied in sea surface temperature from 6°C (St 001) to 1°C (St 003) and were all characterized by a high phytoplankton biomass. South of these stations, no more *Themisto* amphipods were found in the nets. At the first station, several hundreds of juveniles were found (around 2 mm) as well as some larger specimens, whilst at the second station, mostly adults were recovered. At the third station, many *Themisto* individuals were found dead in the nets and could hence not be used for experimental work. The size distributions of a subsample of the catches at these two stations are documented in Fig. 3.4.1.

A description of the dominant taxa in each net tow can be found in Tab. 3.4.1. From station 4 onwards, every station (except for station 12) had a sequence of two bongo tows, a shallow one (60 m), with a video survey using a camera attached to the frame, followed by a deeper tow (from 150 – 300 m). At station 4, characterized by a high phytoplankton biomass, the zooplankton assemblage was dominated by copepods, polychaetes, *Limacina* pteropods, as well as other hyperiid amphipod species such as *Hyperial/Hyperielliella* sp. and *Primno macropa*. These hyperiids were not present in the stations where *T. gaudichaudii* occurred. Euphausiids from this station had been feeding recently, as their stomachs were filled with phytoplankton. At station 5, the assemblage was diverse and included copepods (including the bioluminescent *Metridia*), *Hyperial/Hyperielliella* species as well as *Clio* pteropods, appendicularians, salps and polychaetes. The deeper tow (200 m) comprised almost no appendicularians. At station 6, the deeper tow was dominated by euphausiids and copepods with green stomachs, as well as appendicularians, whilst in the nets of the 60 m tow there was much less krill but some salps. The assemblage of station 8 (60 m tow) consisted of copepods, polychaetes, many *Hyperial/Hyperielliella*, *Primno macropa*, and pteropods (many *Limacina* but only one *Clio*). In the deeper tow (200 m), euphausiids and salps were more abundant. The video survey showed that *Limacina* is concentrated at the water surface. At station 10, phytoplankton aggregates were found in the nets, and the zooplankton assemblage consisted of copepods, several of which were predatory ones, as well as appendicularians, *Hyperial/Hyperielliella*, *Limacina*, *Clione* and polychaetes. In the evening of the same day, a brown patch was observed on the water surface, and at that locality a station was set up. Two surface bongo tows were carried out and the first one crossed the patch. The first Bongo nets were dominated by adult krill (*Euphausia superba*), and as second most dominant taxon, *Limacina* pteropods. The second tow still comprised a lot of krill but less than the previous tow. Video surveys were carried out for both tows and confirmed the passage through a krill swarm for the first tow. Comparatively with station 6, the other station where euphausiids were the most abundant taxon in the catch, the size distribution of krill at station 12 was clearly skewed towards larger, adult specimens (Fig. 3.4.2).

3.4 INTERPELAGIC: Interactions between Key Players of the Southern Ocean Zooplankton

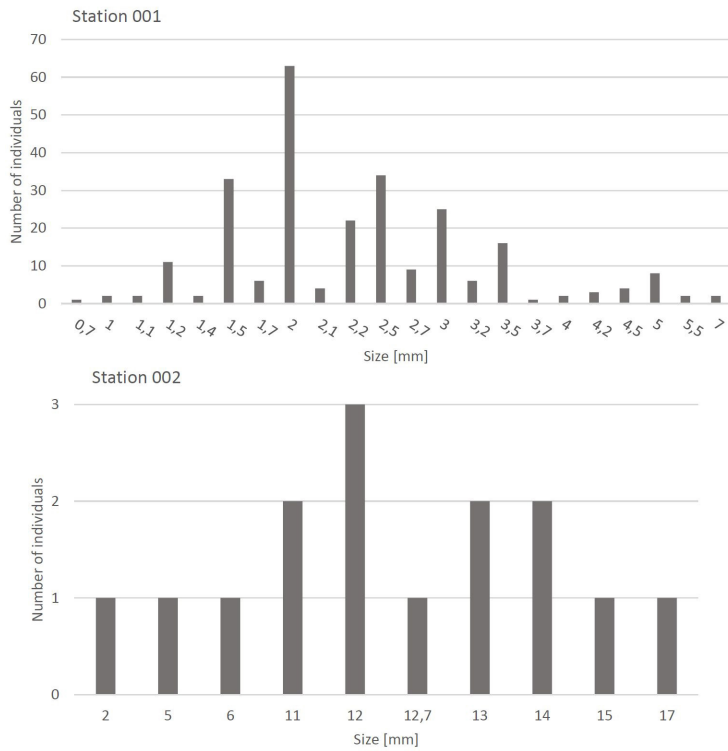


Fig. 3.4.1: Size distribution plots of *Themisto gaudichaudii* collected at station 001 (upper graph) and station 002 (lower graph).

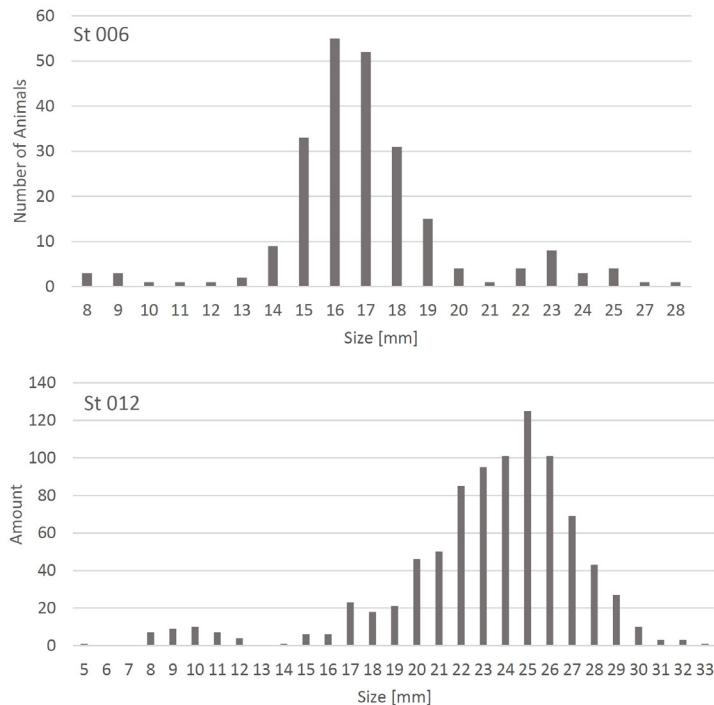


Fig. 3.4.2: Size distribution plots of *Euphausia superba* collected at station 006 (upper graph) and station 012 (lower graph). Station 012 represents the krill patch seen at the water surface. The distribution of the individuals sampled here was clearly skewed towards larger, adult krill.

For station 22 the algal biomass recovered in the nets was comparatively low; zooplankton consisted of copepods, large and smaller euphausiids and different pteropod species (*Clione*, *Clio* and *Limacina*). The deep tow (300 m) sample was composed of copepods (mainly *Calanus propinquus*), ostracods, different species of polychaetes, as well as *Limacina* pteropods. Station 23 (60 m tow) was characterized by a higher algal biomass again, and the zooplankton

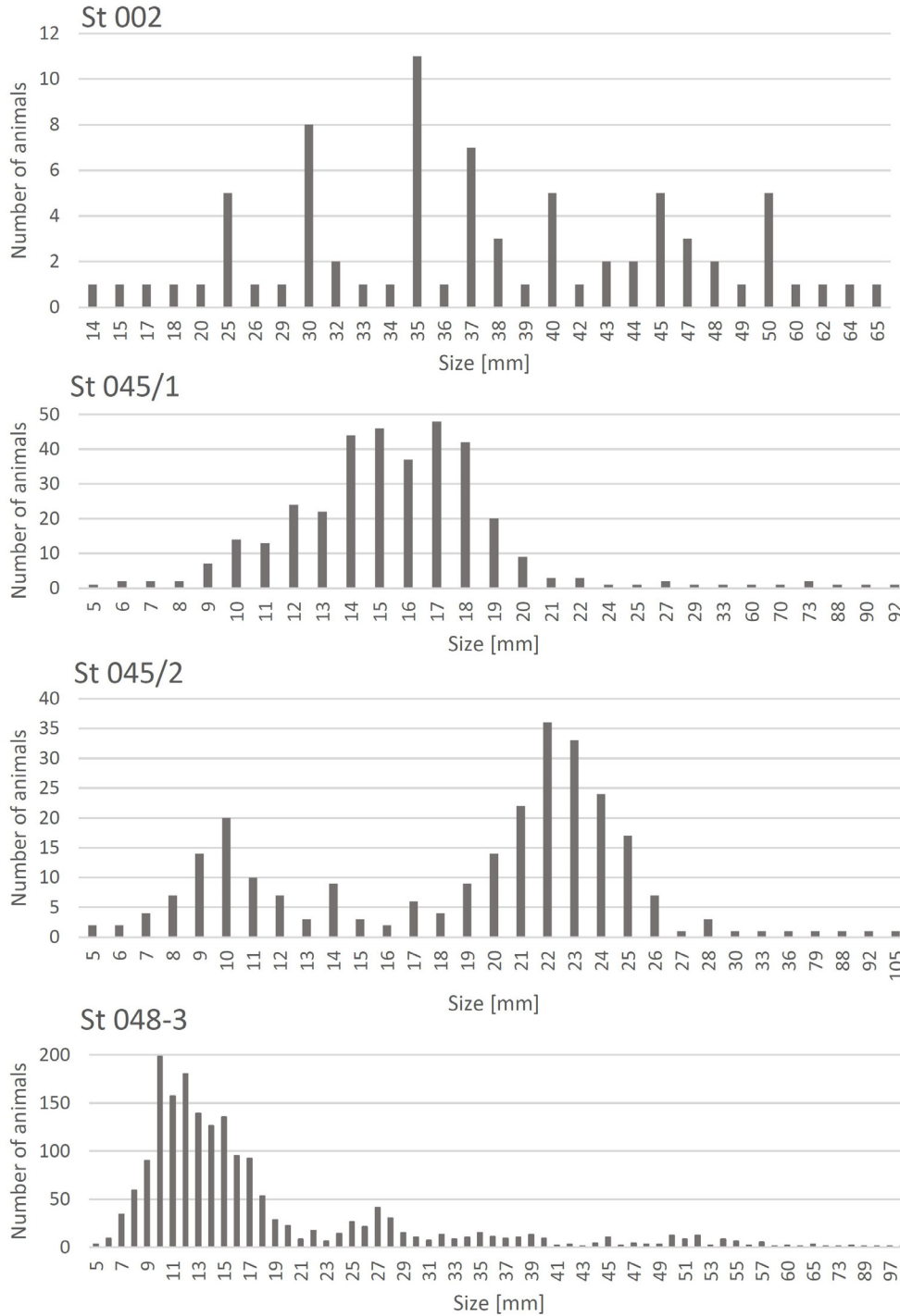


Fig. 3.4.3: Size distribution plots of *Salpa thompsoni* collected at station 002, station 045/1, station 045/2, station 048/3. At station 045, the shallow (60 m wire) and deep tow (350 m wire) yielded a set of different sized individuals: in the latter larger individuals were recovered.

was dominated by copepods and appendicularians. For the deep tow, calanoid copepods, much less appendicularians, some chaetognaths and a high number of *Hyperia/Hyperielli* amphipods were found in the nets. For both the shallow and the deeper tow, several eusirid amphipods were also found in the nets. At station 27, the shallow tow was interrupted due to the ice conditions obstructing the wire as well as the frame when pulled out of the water. Large pieces of ice entered the nets and within these, calanoid copepods appeared to be the most abundant zooplankton taxon, followed by euphausiids and *Limacina* pteropods. At station 30, calanoid copepods with green stomachs were, together with ctenophores and other soft-bodied zooplankton species, the most abundant groups, followed by euphausiids, *Hyperia/Hyperielli* amphipods as well as appendicularians, the latter being much less abundant in the deeper tow (350 m). At station 31, the zooplankton assemblage was mainly composed of copepods, chaetognaths, *Limacina* pteropods, *Hyperia/Hyperielli* amphipods and appendicularians. Several individuals of the hyperiid species *Cylopus lucasii* were also recovered with both tows. Station 40 was characterized by a high phytoplankton biomass, and the zooplankton assemblage was composed of copepods, several very large jellyfish, *Clio* pteropods as well as appendicularians, which were less abundant in the deeper tow that caught many large, predatory copepods. Station 45 was characterized by an assemblage composed of salps, copepods (bioluminescent *Metridia*), the hyperiid amphipod *Vibilia antarctica* and appendicularians. The deep tow also sampled jellyfish, two myctophid fishes as well as large, predatory copepods. At station 48, thousands of salps were recovered in the nets of both the shallow (60 m) and deeper tow (350 m). On the video survey many salps were observed to occur in long chains instead of the small individual salps recovered in the nets, which probably broke off from the chains during the towing. Larger reproductive individuals could also be observed, both on the video as in the net sample. The size distribution of the salps at this station is shown on Fig. 3.4.3 and compared with the salps at station 2. The other dominant taxa at station 48 were calanoid copepods and *Vibilia* amphipods. The latter species is known for its association with salps, which explains their presence in high numbers at this station.

The subsequent stations 53, 56 and 61 were all characterized by remarkably low zooplanktonic biomass and abundances. The most common taxa observed at these stations were copepods, appendicularians, *Limacina*, eusirid amphipods and chaetognaths (deeper tows) for station 53. The sample from the deeper tow (350 m) carried out at station 56 comprised a high number of copepod nauplii, responsible for the foamy aspect of the entire sample. They were also observed – but in much lower numbers – in the sample of station 53. The shallow tow of station 61 as composed of *Clio* pteropods, and phytoplankton aggregates. The deeper tow consisted of a much more diverse fauna, comprising chaetognaths, large euphausiids (with green stomachs) and ctenophores. At stations 67 and 70, the most dominant zooplankton was *Euphausia superba*, outnumbering by thousands the other taxa except copepods. All krill had their stomachs filled with phytoplankton. The tows clearly traversed some krill schools; brown krill patches had also been observed from the bridge whilst steaming through the area. At station 71, the two dominant taxa found in both net tows were salps followed by small-sized Antarctic krill, and the hyperiid amphipods *Cylopus* and *Vibilia*. The deeper tow yielded thousands of salps ranging in size from 3 to 7 cm. At this station, several flocks of cape petrels were observed feeding at the surface on plankton. At station 72, high numbers of salps were collected together with larger Antarctic krill; one specimen of *T. gaudichaudii* was found in the shallow towed net (60 m). At the last station, the 60 m tow yielded the lowest biomass encountered during this cruise, less than five small euphausiids were caught, in contrast with the deep tow (350 m) that yielded again hundreds of salps, as well as smaller (+/- 1 cm) and larger-sized (> 5 cm) Antarctic krill, as well as *Cylopus* and *Vibilia* amphipods, and one single *T. gaudichaudii*.

A huge number of individually sorted frozen samples was collected from all dominant components of the Southern Ocean food web, covering all sampling stations. The collection

includes 894 individual zooplankton samples for trophic biomarker analyses (fatty acids and stable isotopes) including the full range of zooplankton species encountered during the cruise (e.g. copepods, amphipods, euphausiids, chaetognaths, pteropods, ctenophores, jellyfish, appendicularians, larvaceans, salps, myctophids, fish larvae and juveniles, and squids). Approximately 450 separate samples comprising one or more specimens per species and per station have been collected and preserved in absolute ethanol. These will be used for genetic analyses such as population genetics of target taxa as well as establishment of a DNA barcode library for all zooplankton taxa encountered. Quantitative subsamples of the multinet and bongonet hauls have been collected and preserved in absolute ethanol and will serve for determining species abundance and biomass data. Finally, to examine the resilience of the different key pelagic species (copepods, amphipods, euphausiids and salps) to climate change and to investigate the gene expression profiles at different sampling localities across a water temperature gradient, *in-situ* samples of these species at several stations along the expedition track were preserved in RNAlater and kept at -80°C. When comparing these transcriptomic profiles with samples from the temperature-change experiments, the differentially down- or upregulated genes can be identified according to the treatments/species as well as the processes involved in thermal adaptation as well as regulatory controls.

Feeding ecology of T. gaudichaudii

Prey preference experiments have shown that *Themisto* consumes both copepods and krill when having the choice (Fexp 1, 4 and 6) and the same holds true when the amphipods are exposed to salps and euphausiids. *Themisto* did not feed on any pteropod species: in the first prey preference experiment (Fexp 1) individuals have been feeding on chaetognaths, salps and copepods but not *Limacina*, and in the experiment where *Themisto* was placed together with *Clio* pteropod and a smaller *Hyperia* amphipod (Fexp 5) it did not touch the *Clio* specimen. *Themisto* amphipods were observed at several instances to feed directly on the salps stomach (Fig. 3.4.4). The fact that it then utilizes the pre-digested phytoplankton as food may have led to a bias in studies that determined *Themisto*'s trophic level since biomarker analyses would have indicated a predominance of herbivory. When *Themisto* was placed in an aquarium together with large individuals of Antarctic krill (> 5 cm), it predominantly fed on the head, in particular the eyes, as well as on the stomach region. Again, when emptying the stomach of its prey, the amphipod also ingests pre-digested phytoplankton and this may explain the high degree of herbivory revealed by stable isotope analyses as shown in a previous study (Stowasser et al. 2012). Behavioural observations also confirmed the occurrence of cannibalism: *Themisto* adults were observed attacking other individuals of a similar size class and starting to feed on them.

Based on the collected samples during this expedition, the food spectrum of *Themisto* will be investigated using light microscopy and molecular diet analyses. The results will be compared with those of other populations sampled during other expeditions across *Themisto*'s distributional range (e.g. the Argentine Sea or the South Georgia region). Semi-quantitative identification of food items will be carried out by molecular methods on gut content and faecal pellet samples. For this, we will carry out (i) prey-specific PCR tests using highly-specific primers designed for determining the presence/absence of single species (potential prey items, e.g. salps) (Harper et al. 2005, Passmore et al. 2006), (ii) amplification and high-throughput pyrosequencing of DNA using conserved primers targeting a broad array of eukaryotes (e.g. for COI, 16S and 18S rDNA, Blankenship & Yyanos 2005, Deagle et al. 2009) by comparison with the molecular reference database that will be established based on the collected samples for genetic analyses of the major zooplankton taxa encountered.

Feeding ecology and trophic position of other hyperiid species

Biomarker analyses (stable isotopes, fatty acids) will be carried out on the main species encountered at the different stations, and the trophic position of the different species in the food web will be compared along the environmental gradient across the Southern Ocean. Since many hyperiid species have co-evolved with species of soft-bodied plankton, in the shape of parasite-host relationships with salps, jellyfish and ctenophores (e.g. Laval 1980), the distribution and abundances of both groups can often be linked (e.g. Burrige et al. 2016). In order to elucidate the role of soft-bodied plankton for the different hyperiid species, we will compare the abundance data of both hyperiid amphipods with those of jellyfish, salps and ctenophores. As an example, it was clear from the sampling results that *Vibilia antarctica* occurred in high numbers in the catches dominated by salps. Furthermore, the abundance data of soft-bodied zooplankton in the nets will be compared with the occurrence of these species from the video surveys.

Notes on the biology of hyperiid amphipods

At stations 001, 003, 22/7 and 30/1, a hyperiid (*Hyperial/Hyperiella*) amphipod was found carrying a *Clione* pteropod on its back (Fig. 3.4.4), holding it between its sixth and seventh pereopod and swimming around with it. This has been reported previously for the Antarctic species *Hyperiella dilatata* where the pteropod acts as an efficient chemical defence against visual predators including notothenioid fishes in the clear shallow waters of the Antarctic shelf (McClintock and Janssen 1990). Whether this represents also a predation escape mechanism to deter certain 'engulfing' predators present in the oceanic zones, such as myctophids or squid, or whether this is still a relict behaviour that evolved in the clear shelf waters, needs to be confirmed. A feeding experiment was set up to determine whether *Themisto* may be one of the predators feeding on the smaller hyperiids. Since all remained untouched, it can be concluded that *Themisto* does not feed on this species.

Comparative studies on sinking speeds of dead specimens will allow us to improve our understanding of the contribution of *Themisto* biomass to the downward carbon flux. The characterization of faecal pellets of *Themisto* revealed a variety of rather loose faecal material depending on the food ingested, in contrast with the compact faecal material from salps or the pellets produced by krill. Finally, *T. gaudichaudii* brooding females have been observed releasing their juveniles from the brood pouch. This was achieved by beating their pleopods extensively. Brood size varied from 45 to 237 juveniles per female. A number of *Themisto* juveniles survived longer than a month without food during the starvation experiments.

The results of the interaction experiments showed that *T. gaudichaudii* juveniles only rarely use the salps as substrate and not for feeding. Adults did not colonize or feed on the salp offered. However, the salps were either dead or in a bad state, hence, this may indicate that *Themisto* does not scavenge on dead material but needs alive specimens for feeding, in contrast to many other amphipods that are opportunistic scavengers. Dead or weak salps may not be used as a host, so caution must be taken in interpreting these observations. *Themisto* was observed to hang onto a salp in one of the feeding experiments (Fig. 3.4.4). The same was true for *Vibilia antarctica*, a species that is believed to use salps not only as a host but also for feeding. However, all but one individual was not found on any of the soft-bodied zooplankton offered, probably because they also need the host to be alive. This was observed in the net catches where several individuals colonized freshly caught salps immediately (Fig. 3.4.4). Finally, behavioural observations on hyperiids in the aquaria revealed a *Hyperoche* individual feeding on an appendicularian as well as a specimen of *Hyperial/Hyperiella* colonizing a *Clio* pteropod and feeding on its soft parts (Fig. 3.4.4).

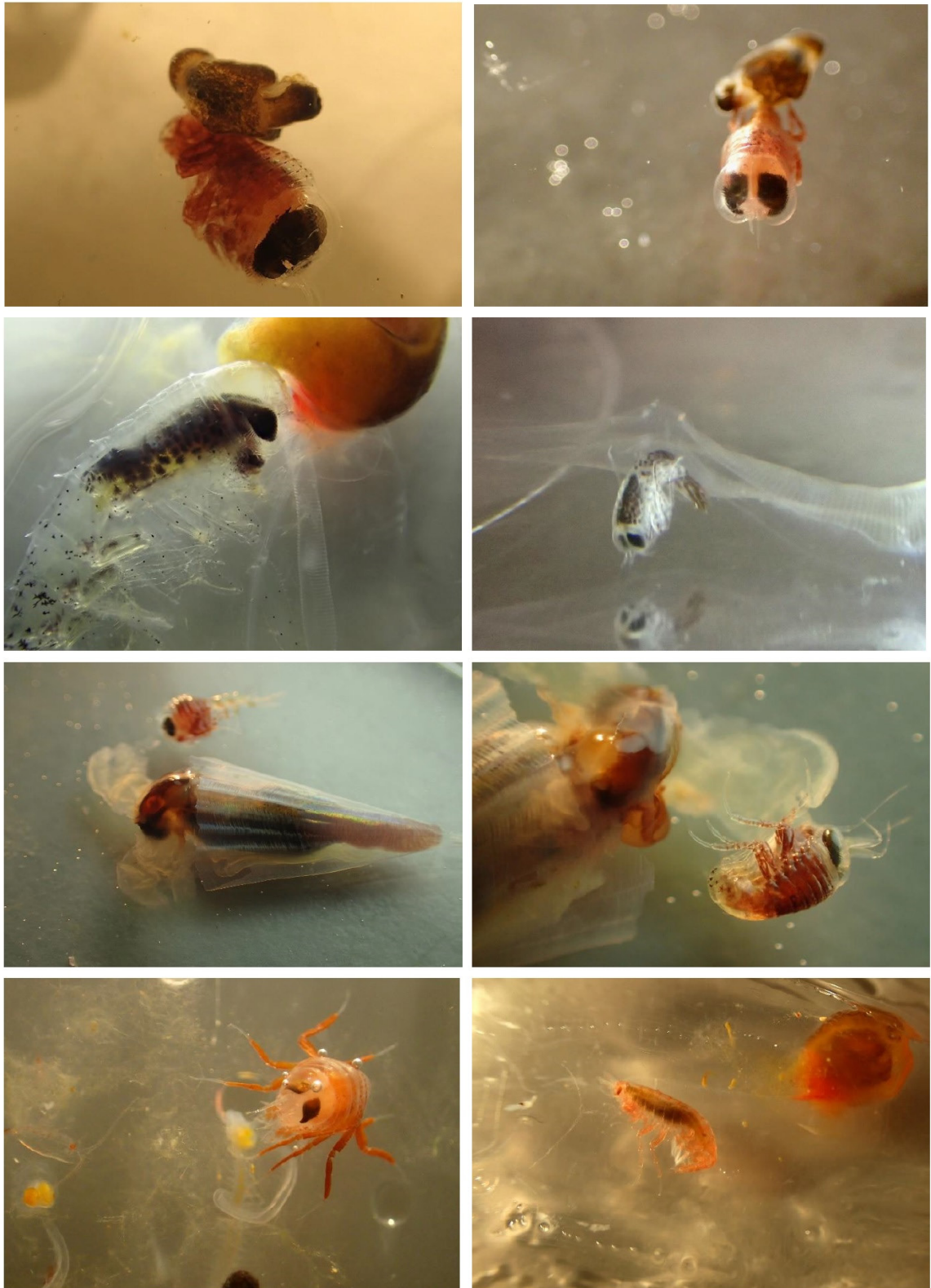


Fig. 3.4.4: Illustrations on the behavioural observations on hyperiid amphipods. The upper two pictures show the species *Hyperia*/*Hyperiella* carrying a *Clione* on its back. On the second row, *T. gaudichaudii* is feeding on the stomach of a salp (left) and hanging onto a salp (right). The third row shows a hyperiid detecting (left) and feeding (right) on a *Clio pteropod*. The lower left picture shows a *Hyperoche* feeding on an appendicularian, and the lower right picture shows the species *Vibilia antarctica* colonizing a salp.

Resilience and local adaptation to temperature of the key pelagic players

In order to investigate whether the gene expression under thermal stress varies between the key pelagic players and within each species across its geographical range, we carried out experiments where specimens were exposed to either a gradual increase in temperature or a “heat or cold shock”. Additional molecular genetic analyses of gene expression (transcriptomics) in the home lab will show which genes are most important for temperature acclimation in zooplankton species and whether gene expression differs interspecifically, i.e. between sister species and/or intraspecifically, i.e. between different geographic populations of the same species. To do so, temperature experiments were carried out for five different taxa: *Themisto gaudichaudii*, *Euphausia superba* or Antarctic krill, *Salpa thompsoni*, as well as the copepod species *Calanus propinquus* and *Calanus simillimus*.

For each experiment, a high number of individuals per station were gently picked and randomly assigned to different groups. One of these, representing natural *in-situ* conditions, was immediately preserved in RNAlater and stored at -80°C . The remaining groups were placed in flasks or aquaria filled with filtered seawater and placed in a temperature-controlled laboratory container at $0-1^{\circ}\text{C}$, $6-8^{\circ}\text{C}$ or $11-12^{\circ}\text{C}$. Details on the experimental designs are given in Table 3.4.2. All these individuals were preserved in RNAlater, or frozen, at -80°C and for each, total RNA will be extracted in the home laboratory and prepared for Illumina sequencing. We expect to obtain high-quality reference transcriptome assemblies of each species and thus perform a large-scale analysis of transcriptional response to thermal stress. Differential expression analyses will allow us to compare the differentially down- or upregulated genes according to the treatments/species. We will characterize genes and processes involved in thermal adaptation as well as regulatory controls, signal transduction pathways and stress response networks, for all the taxa. We will also identify molecular markers for physiological stressors, namely thermal stressors. From these data, we will be able to identify proteins and pathways involved in temperature responses.

*Genetic connectivity of *T. gaudichaudii* and other hyperiid amphipods*

Investigating *Themisto*'s genetic connectivity across the Southwest Atlantic sector is crucial for evaluating potential range shifts or expansions with ongoing and future climate change. Covering an enormous temperature range, *T. gaudichaudii* is expected to extend its distribution southwards with warming waters. Depending on its future distribution and feeding habits, *Themisto* may be in the position to displace Antarctic krill. However, this scenario may only hold true if *Themisto* represents one (or more) panmictic lineage or species across its distributional range. A recent study showed the existence of three distinct but sympatric genetic lineages of *Themisto gaudichaudii*, all three occurring in almost all sampling localities situated along an environmental gradient ranging from the Antarctic Polar Front in the North to the Eastern Weddell Sea in the South (Havermans 2015). *T. gaudichaudii*'s status of a circumantarctic species has recently also been questioned on morphological grounds; when comparing specimens from Prydz Bay and from the Pacific sector of the Southern Ocean, substantial morphological differences were reported with the possibility of at least two distinct lineages or species in the Southern Ocean (Zeidler and De Broyer 2014). Hence, based on these and previously collected samples, the biogeographic limits of *Themisto* lineages/species will be investigated with an integrative approach combining phylogeographic analyses and population genetic methods for detecting the small-scale genetic structure and gene flow patterns, as well as morphological analyses to revise the taxonomy of the genus.

To do so, genetic analyses of *T. gaudichaudii*, as well as of other collected hyperiid amphipods, will be carried out using standard sequence markers such as the mitochondrial barcode gene COI, in order to characterize the phylogeography of the different species. Second, using

Next-Generation Sequencing techniques, complete genomes of *Themisto* specimens will be sequenced in order to pinpoint regions suitable for population genetics, which will shed light on the extent of gene flow between the different populations sampled throughout the voyage and compared with other previously sampled populations in the Argentine Sea, the South Georgia region and the Polar Frontal Zone. Population genetic analyses will be conducted on multiple single nucleotide polymorphisms (SNPs) or microsatellite markers amongst individuals from different localities in order to evaluate the fine-scale genetic structure and the extent of gene flow between these different populations. The study of the gene-linked variation in SNPs or candidate genes will allow us to find out to which extent the evolutionary history of the species has been influenced by selection and adaptation processes.

Data management

Results from the PS103 expedition will be published in peer-reviewed journals by the participating scientists in co-operation with other colleagues. The gathered samples will be analyzed for biomarker studies and contribute to the Master thesis of Simon Schöbinger at the University of Bremen. Zooplankton samples will be archived and stored at the BreMarE Centre of the University of Bremen. Geo-referenced data sets such as zooplankton abundance and biomass will be archived and made publicly available through the PANGAEA database during the publication process. By doing so, every dataset, as a supplement to publications or separately, can be identified, published, cited and shared using a Digital Object Identifier (DOI). Citations will be available through the German National Library of Science and Technology portal. Genetic data obtained throughout the project will be submitted to the GenBank database. Raw DNA and RNA sequence data will be deposited in the National Center for Biotechnology Information (NCBI) Sequence Read Archive (SRA). Transcriptomic data referred to in scientific publications will be made available as supplementary electronic file to the respective publications.

References

- Alcaraz M, Almeda R, Duarte CM, Horstkotte B, Lastemas S, Agusti S (2014) Changes in the C, N, and P cycles by the predicted salps-krill shift in the Southern Ocean. *Frontiers in Marine Science*, doi: 10.3389/fmars.2014.00045.
- Atkinson A, Siegel V, Pakhomov E, Rothery P (2004) Long-term decline in krill stocks and increase in salps within the Southern Ocean. *Nature*, 432, 100-103.
- Auel H, Ekau W (2009) Distribution and respiration of the high-latitude pelagic amphipod *Themisto gaudichaudii* in the Benguela Current in relation to upwelling intensity. *Progress in Oceanography*, 83, 237-241.
- Blankenship LE, Yayanos AA (2005) Universal primers and PCR of gut contents to study marine invertebrate diets. *Molecular Ecology*, 14, 891-899.
- Brierley AS, Watkins JL, Murray AWA (1997) Interannual variability in krill abundance at South Georgia. *Marine Ecology Progress Series*, 150, 87-98.
- Burridge AK, Tump M, Vonk R, Goetze E, Peijnenburg KTCA (2016) Diversity and distribution of hyperiid amphipods along a latitudinal transect in the Atlantic Ocean. *Progress in Oceanography*, in press.
- Croxall JP, Reid K, Prince PA (1999) Diet, provisioning and productivity responses of marine predators to differences in availability of Antarctic krill. *Marine Ecology Progress Series*, 177, 115-131.
- Deagle BE, Kirkwood R, Jarman SN (2009) Analysis of Australian fur seal diet by pyrosequencing prey DNA in faeces. *Marine Ecology*, 18, 2022-2038.
- Forcada J, Trathan PN, Reid K, Murphy EJ (2005) The effects of global climate variability in pup production of Antarctic fur seals. *Ecology*, 86, 2408-2417.

3.4 INTERPELAGIC: Interactions between Key Players of the Southern Ocean Zooplankton

- Froneman PW, Pakhomov EA, Treasure A (2000) Trophic importance of the hyperiid amphipod, *Themisto gaudichaudii* in the Prince Edward Archipelago (Southern Ocean) ecosystem. *Polar Biology*, 23, 429-436.
- Havermans C (2015) Report COMNAP fellowship 2013/2014: The impact of environmental changes on a key component of pelagic food webs in the Southern Ocean: the amphipod *Themisto gaudichaudii* (Crustacea: Hyperiidea). <https://www.comnap.aq/SiteAssets/SitePages/fellowships>.
- Harper GL, King RA, Dodd CS, Harwood D, Glen DM, Bruford MW, Symondson WOC (2005). Rapid screening of invertebrate predators for multiple prey DNA targets. *Molecular Ecology* 14: 819-827.
- Kane JE (1966) The distribution of *Parathemisto gaudichaudii* (Guerin) with observations on its life-history in the 0° to 20°E sector of the Southern Ocean. *Discovery Reports*, 34, 163-198.
- Laval P. (1980) Hyperiid amphipods as crustacean parasitoids associated with gelatinous zooplankton. *Oceanography and Marine Biology: An annual review*, 18, 11-56.
- Loeb V, Siegel V, Holm-Hansen O, Hewitt R, Fraser W, Trivelpiece W, Trivelpiece S (1997) Effects of sea-ice extent and krill or salp dominance on the Antarctic food web. *Nature*, 387, 897-900.
- Mackey AP, Atkinson A, Hill SL, Ward P, Cunningham NJ, Johnston NM, Murphy EJ (2012) Antarctic macrozooplankton of the southwest Atlantic sector and Bellingshausen Sea: Baseline historical distributions related to temperature and food, with projections for subsequent ocean warming. *Deep-Sea Research II*, 59-60, 130-146.
- McClintock JB, Janssen J (1990) Pteropod abduction as a chemical defence in a pelagic Antarctic amphipod. *Nature*, 346, 462-464.
- Murphy EJ, Reid K (2001) Modelling Southern Ocean krill population dynamics: biological processes generating fluctuations in the South Georgia ecosystem. *Marine Ecology Progress Series*, 217, 175-189.
- Pakhomov EA, Perissinotto R (1996) Trophodynamics of the hyperiid amphipod *Themisto gaudichaudii* in the South Georgia region during late austral summer. *Marine Ecology Progress Series*, 134, 91-100.
- Pakhomov EA, Froneman PW, Perissinotto R (2002). Salp/krill interactions in the Southern Ocean: spatial segregation and implications for the carbon flux. *Deep-Sea Research II*, 49, 1881-1907.
- Parkinson CI (2002) Trends in the length of the Southern Ocean sea-ice season 1979-99. *Annals of Glaciology*, 34, 435-440.
- Passmore AJ, Jarman SN, Swadling KM, Kawaguchi S, McMinn A, Nicol S (2006) DNA as a dietary biomarker in Antarctic krill, *Euphausia superba*. *Marine Biotechnology*, 8, 686-696.
- Smith K, Schlosser C, Atkinson A, Fielding S, Venables HJ, Waluda CM, Achterberg EP (2016) Zooplankton gut passage mobilizes lithogenic iron for ocean productivity. *Current Biology*, 26(19), 2667-2673.
- Stowasser G, Atkinson A, McGill RAR, Philips RA, Collins MA, Pond DW (2012) Food web dynamics in the Scotia Sea in summer: A stable isotope study. *Deep-Sea Research II*, 59-60, 208-221.
- Ward P, Atkinson A, Tarling G (2012) Mesozooplankton community structure and variability in the Scotia Sea: A seasonal comparison. *Deep-Sea Research II*, 59-60, 78-92.
- Watts J, Tarling GA (2012) Population dynamics and production of *Themisto gaudichaudii* (Amphipoda, Hyperiididae) at South Georgia, Antarctica. *Deep-Sea Research II*, 59-60, 117-129.
- Zeidler W, De Broyer C (2014) Amphipoda Hyperiidea. In: De Broyer C, Koubbi P, Griffiths HJ, Raymond B, Udekem d'Acoz C d' et al. (Eds.) *Biogeographic Atlas of the Southern Ocean*. Scientific Committee on Antarctic Research, Cambridge pp. 303-308.

3.5 Algenom: Molecular Ecology and Microevolutionary Genomics of Primary Producers

Bánk Beszteri¹, Fenina Buttler¹, Allison Fong¹
Not on board: Gernot Glöckner², Uwe John¹,
Klaus Valentin¹

¹AWI
²Uni Cologne

Grant-No. AWI_PS103_04

Objectives

Microalgae form the basis of open ocean food webs and are important drivers of the biological carbon and silicate pump in the Southern Ocean, like in other oceans as well. Our working group collected samples for different research projects addressing the diversity, ecology and evolution of these microscopic organisms in the pelagic of the Southern Ocean. Since project 2 samples not only phytoplankton but all (auto-, hetero- and mixotrophic) components of microscopic plankton, we will refer to the target organisms of this project as “protistan plankton” below.

*Project 1: Microevolutionary genomics of *Fragilariopsis kerguelensis**

The aim of this project is to characterize the amount of neutral and adaptive genomic variation among populations of one of the best studied diatom species of the Southern Ocean, *Fragilariopsis kerguelensis* (O’Meara) Hustedt; and to get insights into microevolutionary dynamics and their relation to main environmental regimes (Antarctic Circumpolar Current [ACC] vs. Weddel Sea) and gradients (latitudinal gradient across the ACC and associated physico-chemical gradients) in this species. For this, we aimed at isolating clonal cultures from at least 8-10 populations along the North-South transect from the Northern edge of the Antarctic Circumpolar Current and in the Weddel Sea.

Fragilariopsis kerguelensis (O’Meara) Hustedt is one of the ubiquitous diatom species of the Southern Ocean (Smetacek, Assmy et al. 2004). It occurs at moderate to high abundances throughout the ACC as well as south of it, although at lower abundances, but practically all the way to the Antarctic ice shelf (Pinkernell and Beszteri 2014). Although not always dominant at the surface, it is almost always present in ACC water samples and its thick frustules are among the main constituents of the siliceous ooze belt on the seafloor, due also to their good preservation (Cortese and Gersonde 2007, Cortese and Gersonde 2008). The species has received much attention not only for this reason but also because it has emerged as a model system for understanding the unique biological oceanographic properties of the high nutrient, low productivity open ocean water masses of the Southern Ocean, and the intriguing interactions between oceanic nutrient budgets and organismal adaptations (Assmy, Henjes et al. 2006, Cortese and Gersonde 2007, Hoffmann, Peeken et al. 2007, Timmermans and van der Wagt 2010, Cortese, Gersonde et al. 2012, Assmy, Smetacek et al. 2013, Fuchs, Scalco et al. 2013, Shukla, Crosta et al. 2013). For instance, the growth of thick-shelled diatoms like *F. kerguelensis* is responsible for decoupling surface silicate from nitrate consumption in surface ACC water masses (Assmy, Smetacek et al. 2013). Recently, a full genome sequencing project has also been initiated for *F. kerguelensis* (under the lead of Prof. Thomas Mock, Univ. East Anglia, Norwich, UK and with participation of members of our team), providing novel possibilities for molecular ecological/evolutionary investigations of this diatom species.

The predominant mode of reproduction in phytoplankton organisms is vegetative division. In spite of this, the traditional paradigm (which had probably not been based on anything else besides the lack of data) that phytoplankton blooms or non-bloom populations are largely clonal has by now largely been overturned. In practically every case investigated, populations of phytoplankters have turned out to be assemblages of highly diverse clonal lineages (Ryneckson and Armbrust 2000, Ryneckson and Armbrust 2005, Ryneckson, Lin et al. 2009). A single-cell genome sequencing study has recently demonstrated the coexistence of hundreds of differentiated “ecotypes” of the cyanobacterium *Prochlorococcus* within a single water sample (Kashtan, Roggensack et al. 2014). In the case of eukaryotic phytoplankton, comparative genome sequencing of the globally abundant haptophyte *Emiliania huxleyi* revealed a large variation in gene contents of individual isolates from diverse geographic origins which was hypothesized to have contributed to the ability of this species to adapt to varied environmental conditions (Read, Kegel et al. 2013, von Dassow, John et al. 2015). The emerging picture is that phytoplankton species and even individual populations are far from homogeneous, and that phytoplankton populations adapt in their genomic composition to local environmental factors. Hardly anything is known about the amount of such genomic diversity and its distribution along the genome, as well as in geographic space and in time in important phytoplankton taxa contributing substantially to biogeochemical cycles in high latitude regions. Regarding phytoplankton of the Southern Ocean, the only taxon that has been studied at some depth in this respect up to now is the Haptophyte *Phaeocystis* (Gäbler-Schwarz and Medlin 2011) for which microsatellite markers have been applied to study population diversity and differentiation revealing novel insights about genetic and functional differentiation (Gäbler-Schwarz et al. 2015). About the important diatom species of the region, however, no such data have been available so far.

Our first project on PS103 addresses this gap by pursuing the first in-depth investigation of genomic diversity within and among populations of a Southern Ocean diatom species. This requires isolation of individual strains of *F. kerguelensis* from several populations in different environmental regimes of the Southern Ocean. The aim of the work is to get insights into the amount of within and among-population genomic diversity and its patterns across the genome, to trace neutral and adaptive differentiation across genomic regions, and to identify genomic loci of potential relevance to adaptation different local environmental conditions in different regions of the ACC and the Weddell Sea. These parameters are relevant to assess the genetic cohesiveness of the species as a whole, as well as its micro-evolutionary potential to respond to quick environmental changes, particularly relevant in the face of ongoing ocean warming (Pinkernell & Beszteri 2014).

Project 2: Sea of Change – taxonomic and gene expressional trends in protistan plankton along temperature gradients

Temperature is one of the major drivers of biodiversity and ecosystem functioning. We recently used large scale community transcriptome sequencing to analyze the fundamental effect of temperature on protistan plankton biodiversity and metabolic function. The study was based on five samples from three temperature regimes, polar, subpolar, and equatorial. Along this rather rough temperature gradient we saw an increase of dinoflagellates at the cost of diatoms and a decrease of transcripts related to protein biosynthesis at higher temperatures. We postulated that this might reflect a general temperature related resource allocation trend in marine protistan plankton (Toseland et al. 2013). To test this hypothesis, to extend the geographic range sampled and to refine the picture obtained about temperature dependent shifts in transcriptional allocation to major cellular processes, we previously conducted sampling along two transects between Spitsbergen and Cape Town, covering a broad temperature range at a high resolution, and sequenced RNA samples with high coverage. The latter was made possible

through a grant coined “Sea of Change”, awarded to Thomas Mock, KV, and co-workers, by the Joint Genome Institute (<http://genome.jgi.doe.gov/SeaofArctiOcean/SeaofArctiOcean.info.html>.) The current expedition was meant to add to the previous sampling the yet missing Southern Ocean and collect surface seawater samples using the CTD rosette for immediate filtration and later DNA and RNA extraction back in the home laboratory for metatranscriptome sequencing of Antarctic samples equivalent to the existing “Sea of Change” dataset.

Project 3: Bacterioplankton and diatom microbiome composition and function

Prokaryotes are ubiquitous in both terrestrial and aquatic ecosystems and regulate a suite of complex biogeochemical and ecological processes. Historically, prokaryotes, specifically Bacteria, were studied in isolation through culturing methods, microbiological assays, and most recently via – omics approaches. However, recent discoveries have fueled a new paradigm in science about the connectivity between all things and microbes. The new frontier of microbiome research, especially in the world’s oceans, is pivotal to elucidating how microbes interact and shape ecosystems through associations. Diatom-prokaryote associations have been observed in a number of species, most often in cultured strains. These associations and interactions exist on the continuum from mutualism to parasitism, suggesting complex evolutionary pressure between diatoms and their microbiome. In oceanic environments, research on diatom-prokaryote associations has shown that bacteria can 1) control organic matter remineralization, and in turn, carbon and silicon export efficiency of diatoms, 2) protect against or suppress antagonistic attacks to diatom health, 3) provide essential micronutrients, such as vitamins. These examples illustrate the breadth of mechanisms by which diatom-bacteria associations can influence both biogeochemical and ecological processes. There are likely many yet-to-be discovered interactions between diatoms and prokaryotes, which will inform us on how the reciprocal nature of associations in the natural world governs ecosystem function.

This project is designed to integrate field-based environmental sampling and experiments of natural phytoplankton communities to laboratory-controlled experiments with specific diatom and prokaryote isolates to yield information that will connect microscale, population level, and community-wide activity to ecologically and biogeochemically relevant processes. Parallel incubations with a tracer dye to monitor silicate incorporation into diatom frustules and ¹³C-labeled bicarbonate for DNA-stable isotope probing (SIP) will yield relative diatom-specific growth rates and separate photosynthetically (non)active phytoplankton functional groups. These two independent methods to address phytoplankton activity will be used to place observed patterns in phytoplankton and prokaryote community structure into context.

Work at sea

Altogether, we sampled at 32 stations (27 of them south of 60° S; see details in Tab. 3.5.1). Sampling for all projects was performed at 25 common stations by both CTD casts with water collection at three resp. two depths (see Tab. 3.5.1), and a 20 µm mesh size phytoplankton hand net. Hand net samples were also taken at five additional locations. One sampling, at the shelf ice edge (during logistic work of the ship for supplying Neumayer station), was performed by obtaining seawater samples from the on-board seawater supply system; this sample was otherwise processed in an identical manner to all other samples, except that instead of an accompanying hand net, several liters of the seawater sample were concentrated by gravitational filtration through a 20 µm mesh size gauze. At one sea ice station, an ice basket, instead of a hand net, was used to obtain a chunk of diatom colonized brown sea ice; this sample could only be fixed for microscopy. After CTD/net hauls, samples were subdivided and processed by a combination of methods, as detailed in the following.

Community nucleic acid sampling.

Seawater subsamples were serially filtered onto 1.2 and 0.2 μm pore size membrane filters on an 8-channel peristaltic pump filtration system in a cold container tempered to 1-2 $^{\circ}\text{C}$. At each station/depth, three replicate filters were collected for eukaryotic (1.2 μm pore size) DNA and RNA, and prokaryotic (0.2 μm pore size) DNA samples. Filters for DNA extraction were frozen dry, and samples for RNA extraction were frozen after addition of 500 μl RNA extraction buffer, in liquid nitrogen. All filters for nucleic acid extraction are stored and being transported to the home laboratory at -80 $^{\circ}\text{C}$. The DNA samples will be used for marker gene amplification (small subunit ribosomal DNA) and sequencing for characterizing microbial (eukaryotic and prokaryotic fraction) community composition and its changes along our route. The RNA samples will be used for preparation and sequencing of community transcriptome libraries for assessing gene expression trends in protistan plankton along the North-to-South surface temperature gradient.

Contextual parameters

Further seawater subsamples (three replicates from each station/depth) were filtered for measuring contextual parameters. A subsample was filtered under dimmed light onto glass fiber filter and frozen at -80 $^{\circ}\text{C}$ for HPLC based pigment analysis. A further subsample was filtered upon pre-combusted glass fiber filters for measuring particulate organic carbon. 15 ml subsamples of the seawater filtered of organisms (i.e., 0.2 μm pore size) using the peristaltic system were stored for measurement of inorganic nutrient concentrations. A subsample was filtered on glass fiber filters for determination of biogenic silicate concentrations. A subsample was fixed with paraformaldehyde for flow cytometric analysis. Finally, quantitative subsamples from the Niskin bottles, as well as a subsample from the phytoplankton net, was fixed with formaldehyde for microscopic observation and counting of microphytoplankton.

Cultivation

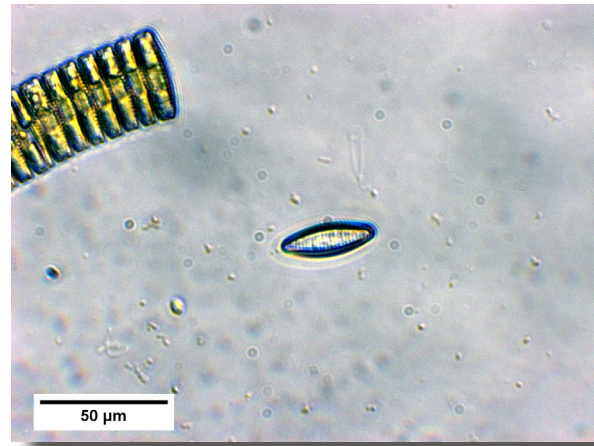
For population genomic analyses and for experimental work, clonal cultures of the diatom *Fragilariopsis kerguelensis* were isolated from 21 populations by picking single chains and repeatedly washing them in sterile filtered F/2 phytoplankton growth medium under the inverted microscope (Fig. 3.5.1). In living material, colonies of this species cannot be differentiated from colonies of all congeners with high certainty. For this reason, and also in order to have a representation of closely related species for comparative purposes, we initially sampled *Fragilariopsis* chains encountered randomly for cultivation. When observing our cultures after 2-4 weeks of growth, in several cases we were able to document differences in colony morphology, i.e., morphological differences also observable in living/fresh material, between individual species. The key to linking live colony morphology to valve morphology, the former of which has so far not been documented in the scientific literature for these taxa, indeed lies in the availability of clonal cultures: only the rare individual cells lying in valve view (among the majority of chains presenting cells in girdle view) allow a species level identification based on available literature (see Fig. 3.5.2). Detailed results from these observations will be published in a peer reviewed journal.

After inoculation, isolates were incubated in a laboratory container at 3-4 $^{\circ}\text{C}$ and an 18:6 hours daily light-dark cycle at total illumination intensities between 1,000-2,500 Lux. Strains were observed on a regular basis, re-isolated to clean of contaminants as necessary (and as time permitted; some strains will need to be cleaned of remaining contaminants in the home lab) and finally, transferred into 15 ml Falcon tubes or 2 ml Eppendorf tubes for transport. The isolates are being transported back to the home laboratory at 4 $^{\circ}\text{C}$ for experimental work and in depth genomic and population genomic characterization.



Fig. 3.5.1: Isolating a single *F. kerguelensis* chain for cultivation using a micropipette under the inverted microscope

Fig. 3.5.2: Precise identification of *Fragilariopsis* species has so far only been possible from oxidized material, due to a lack of documentation of live colony morphology in the scientific literature. In clonal cultures, both colony morphology (left, brown cells in a chain) and the fine scale morphology of valve faces (to the right, valve of a single detached cell) can be observed and matched together.



Tab. 3.5.1: Summary of sampling activities of our group during PS103. Under CTD depths sampled, numbers without parentheses represent depths sampled for the full set of parameters described in the text (eukaryotic and prokaryotic nucleic acids, microscopy, flow cytometry and contextual measurements). Numbers in parentheses denote depths sampled for microscopy and flow cytometry only. HN: hand net. Cultures: number of *Fragilariopsis* cultures isolated at the corresponding station. Experiment: marks if an incubation experiment was performed at the corresponding station.

Station number	Latitude	Longitude	CTD (depths sampled, m)	HN	Cultures	Experiment
1	-45,96	6,29	2, 35, 76 (95)	+	58	-
2	-49,02	2,84	4, 10, 50 (120, 150)	+	54	+
3	-51,99	2,10	5, 20, 50 (120, 150)	+	55	+
4	-55,88	1,06	3, 10, 24 (120, 151)	+	41	+
5	-59,05	0,08	2, 10, 25 (120,150)	+	62	+
6	-61,00	0,00	2, 15, 35 (120, 150)	+	61	+
7	-63,99	0,06	7, 25, 35 (120, 150)	+	43	+
9	-66,00	0,00	N.S.	+	19	-
11	-66,54	0,01	4, 15, 40 (120, 150)	+	14	+
12	-67,03	0,00	N.S.	+	-	-

3.5 Algenom: Molecular Ecology and Microevolutionary Genomics of Primary Producers

Station number	Latitude	Longitude	CTD (depths sampled, m)	HN	Cultures	Experiment
14	-68,01	0,01	3.5, 20, 33 (120, 150)	+	36	+
15	-69,20	-0,02	N.S.	+	23	-
16	-69,40	-0,02	N.S.	+	-	-
17	-69,40	-0,05	5, 10, 15 (120, 150)	+	55	+
19	-68,95	-0,09	N.S.	+	-	-
22	-69,01	-7,02	10, 15 (120, 150)	+	30	-
23	-66,00	-12,28	20, 40 (120, 150)	+	38	-
NM	-70,53	-8,14	*	*	36	-
26	-70,39	-8,19	N.S.	+**	-	-
27	-70,37	-8,27	10, 30 (120, 150)	+	-	-
29	-71,36	-13,98	10, 30 (120, 150)	+	-	-
31	-69,07	-17,37	10, 25 (120, 150)	+	-	-
34	-70,90	-28,98	35, 65 (120, 150)	+	36	+
39	-66,60	-27,23	20, 80 (120, 150)	+	35	+
40	-65,73	-36,73	50, 90 (120, 150)	+	27	-
43	-68,42	-44,10	30, 55 (120, 150)	+	39	+
45	-64,38	-45,92	20, 35 (120, 150)	+	-	-
59	-63,48	-52,60	20,40 (120, 150)	+	-	-
67	-62,22	-53,70	10, 25 (120, 150)	+	-	-
71	-61,00	-56,03	20, 45 (120,150)	+	-	-
72	-59,77	-57,82	25, 50 (120, 150)	+	24	-
73	-58,47	-59,64	30, 95 (120,150)	+	48	-

Preliminary and expected results

Fragilariopsis cultures

Upon arrival at the home laboratory, cultures of *Fragilariopsis* species isolated during the cruise will be transferred into fresh growth medium and kept under similar conditions as they were grown on board. After a thorough check for remaining eukaryotic contamination, a subset of the strains will be grown for DNA extraction in a medium supplied with an antibiotic cocktail in order to reduce bacterial growth. DNA extracts will be subjected to ddRAD-seq (double digestion restriction site associated DNA sequencing (Davey and Blaxter 2011, Peterson, Weber et al. 2012), a genotyping-by-sequencing method, to assess amounts of within vs. among-population diversity, gene flow among populations across the ACC and between the ACC and the Weddell Sea, and to screen for loci showing patterns of variation deviating from the genomic main trend (potentially representing loci under selective evolutionary pressure). In addition, for selected strains, low coverage comparative shotgun genome sequencing will be performed and the resulting sequence data mapped to the *F. kerguelensis* high coverage reference genome. A selection of strains for the Northern and Southern ACC, and from the Eastern and Western Weddell Sea, will be subjected to a common garden experiment under different temperature and silicate conditions in order to test for the presence of local adaptation at the phenotypic level. Accompanying these analyses, as far as the relative abundance of transcripts identifiable as belonging to our target species in the community transcriptome sequence data sets will allow, we hope to analyze protein coding sequence variation as well as gene expressional differences among individual populations using the community transcriptome sequence data to be obtained for the *Sea of Change* project (see below). After synthesizing the results, we hope to gain a first, but thorough glimpse into the microevolutionary dynamics and short-term

evolutionary potential of a phytoplankter with an extensive geographic range and playing an important role in the Southern Ocean silicate pump.

Isolates of other species of *Fragilariopsis* will allow us to continue and broaden our work started recently both with collection material (valve morphometrics using high throughput microscopy and image analyses) and now on board using live material aimed at clarifying species-level diversity and give a novel assessment of morphological and molecular variation among Southern Ocean species of this important polar diatom genus. Colony and valve morphology of clonal strains representing different *Fragilariopsis* species will be analyzed microscopically (observation of live cell and colony morphology by light microscopy; morphometric comparison using high throughput microscopy and our custom developed diatom image analysis methods, and frustule ultrastructure by scanning electron microscopy), and the strains will also be used for DNA extraction and amplification and sequencing of phylogenetic marker genes. This will be informative about species level diversity (species limits, presence of cryptic species) as well as about evolutionary history (phylogenetic relationships of individual species).

Sea of Change

The Sea of Change project has already processed several samples from the North and Equatorial Atlantic. Filtered plankton samples collected at this cruise will be processed similarly (DNA extraction followed by partial 18S ribosomal DNA amplification and sequencing; RNA extraction followed by preparation of cDNA libraries and their shotgun sequencing). The Southern Ocean samples collected at the present cruise are also accompanied by samples of the 0.2 – 1.2 μm size fraction, considered to represent bacterioplankton. DNA extracted from these samples will also be analysed by marker gene sequencing (partial 16S rDNA amplification and sequencing), as well as by shotgun metagenome sequencing.

The diatom microbiome project

This project will leverage the 18S and 16S amplicon sequence libraries generated by the *Sea of Change* project to develop a perspective of the protistan and prokaryotic community composition. Additionally, DNA samples generated from the incubation experiments to identify taxa-specific activity responses to the addition of vitamins will be extracted and separated by incorporation of “heavy” labeled ^{13}C -bicarbonate. This method, known as DNA-Stable Isotope Probing (SIP), connects a known function, in this case, photosynthesis, with the phylogeny of the (in)active organisms. Both the protistan and prokaryotic fractions will be examined to understand how interactions between these different organisms can support diatom-specific growth.

To provide environmental-oceanographic context to all above analyses, CTD data obtained by the HAFOS group during the present cruise will be used, alongside the samples collected by our group for determining concentrations of photosynthetic pigments, particulate organic carbon, inorganic nutrients and biogenic silica.

Data management

Measurement results of contextual parameters will be deposited in PANGAEA (www.pangaea.de). Permanent diatom slides and material will be deposited in the Hustedt Diatom Study Centre (herbarium code BRM). The main type of primary data to be obtained during the cruise is nucleotide sequence data which will be deposited in the corresponding databases of the International Nucleotide Sequence Database Cooperation (INSDC: <http://www.insdc.org/>).

References

- Assmy P, Henjes J, Smetacek V and Montresor M (2006) Auxospore formation by the silica-sinking, oceanic diatom *Fragilariopsis kerguelensis* (Bacillariophyceae), *Journal of Phycology*, 42, 1002-1006.
- Assmy P, Smetacek V, Montresor M, Klaas C, Henjes J, Strass VH, Arrieta JM, Bathmann U, Berg GM, Breitbarth E, Cisewski B, Friedrichs L, Fuchs N, Herndl GJ, Jansen S, Kragefsky S, Latasa M, Peeken I, Rottgers R, Scharek R, Schuller SE, Steigenberger S, Webb A, and Wolf-Gladrow D (2013) Thick-shelled, grazer-protected diatoms decouple ocean carbon and silicon cycles in the iron-limited Antarctic Circumpolar Current, *Proceedings of the National Academy of Sciences of the United States of America*, 110, 20633-20638.
- Cortese G and Gersonde R (2007) Morphometric variability in the diatom *Fragilariopsis kerguelensis*: Implications for Southern Ocean paleoceanography, *Earth and Planetary Science Letters*, 257, 526-544.
- Cortese G and Gersonde R (2008) Plio/Pleistocene changes in the main biogenic silica carrier in the Southern Ocean, Atlantic Sector, *Marine Geology*, 252, 100-110.
- Cortese G, Gersonde R, Maschner K and Medley P (2012) Glacial-interglacial size variability in the diatom *Fragilariopsis kerguelensis*: Possible iron/dust controls?, *Paleoceanography*, 27.
- Davey JW and Blaxter ML (2011) RADSeq: next-generation population genetics (vol 9, pg 416, 2010), *Briefings in Functional Genomics*, 10, 108-108.
- Fuchs N, Scalco E, Kooistra WHCF, Assmy P and Montresor M (2013) Genetic characterization and life cycle of the diatom *Fragilariopsis kerguelensis*, *European Journal of Phycology*, 48, 411-426.
- Gabler-Schwarz S and Medlin LK (2011) Microsatellite Markers for *Phaeocystis antarctica*: Assessment of Population Structure and Physiological Responses, *European Journal of Phycology*, 46, 91-91.
- Hoffmann LJ, Peeken I and Lochte K (2007) Effects of iron on the elemental stoichiometry during EIFEX and in the diatoms *Fragilariopsis kerguelensis* and *Chaetoceros dichaeta*, *Biogeosciences*, 4, 569-579.
- Kashtan N, Roggensack SE, Rodrigue S, Thompson JW, Biller SJ, Coe A, Ding HM, Marttinen P, Malmstrom RR, Stocker R, Follows MJ, Stepanauskas R and Chisholm SW (2014) Single-Cell Genomics Reveals Hundreds of Coexisting Subpopulations in Wild *Prochlorococcus*, *Science*, 344, 416-420.
- Peterson BK, Weber JN, Kay EH, Fisher HS and Hoekstra HE (2012) Double Digest RADseq: An Inexpensive Method for De Novo SNP Discovery and Genotyping in Model and Non-Model Species, *Plos One*, 7.
- Pinkernell S and Beszteri B (2014) Potential effects of climate change on the distribution range of the main silicate sinker of the Southern Ocean, *Ecology and Evolution*, 4, 3147-3161.
- Read BA, Kegel J, Klute MJ, Kuo A, Lefebvre SC, Maumus F, Mayer C, Miller J, Monier A, Salamov A, Young J, Aguilar M, Claverie JM, Frickenhaus S, Gonzalez K, Herman EK, Lin YC, Napier J, Ogata H, Sarno AF, Shmutz J, Schroeder D, de Vargas C, Verret F, von Dassow P, Valentin K, Van de Peer Y, Wheeler G, Dacks JB, Delwiche CF, Dyhrman ST, Glockner G, John U, Richards T, Worden AZ, Zhang XY, Grigoriev IV, Allen AE, Bidle K, Borodovsky M, Bowler C, Brownlee C, Cock JM, Elias M,

- Gladyshev VN, Groth M, Guda C, Hadaegh A, Iglesias-Rodriguez MD, Jenkins J, Jones BM, Lawson T, Leese F, Lindquist E, Lobanov A, Lomsadze A, Malik SB, Marsh ME, Mackinder L, Mock T, Mueller-Roeber B, Pagarete A, Parker M, Probert I, Quesneville H, Raines C, Rensing SA, Riano-Pachon DM, Richier S, Rokitta S, Shiraiwa Y, Soanes DM, van der Giezen M, Wahlund TM, Williams B, Wilson W, Wolfe G, Wurch LL and Annotation EH (2013) Pan genome of the phytoplankton *Emiliana* underpins its global distribution, *Nature*, 499, 209-213.
- Rynearson TA and Armbrust EV (2000) DNA fingerprinting reveals extensive genetic diversity in a field population of the centric diatom *Ditylum brightwellii*, *Limnology and Oceanography*, 45, 1329-1340.
- Rynearson TA and Armbrust EV (2005) Maintenance of clonal diversity during a spring bloom of the centric diatom *Ditylum brightwellii*, *Molecular Ecology*, 14, 1631-1640.
- Rynearson TA, Lin EO and Armbrust EV (2009) Metapopulation Structure in the Planktonic Diatom *Ditylum brightwellii* (Bacillariophyceae), *Protist*, 160, 111-121.
- Shukla SK, Crosta X, Cortese G and Nayak GN (2013) Climate mediated size variability of diatom *Fragilariopsis kerguelensis* in the Southern Ocean, *Quaternary Science Reviews*, 69, 49-58.
- Smetacek V, Assmy P and Henjes J (2004) The role of grazing in structuring Southern Ocean pelagic ecosystems and biogeochemical cycles, *Antarctic Science*, 16, 541-558.
- Timmermans KR and van der Wag, B (2010) Variability in Cell Size, Nutrient Depletion, and Growth Rates of the Southern Ocean Diatom *Fragilariopsis kerguelensis* (Bacillariophyceae) after Prolonged Iron Limitation, *Journal of Phycology*, 46, 497-506.
- von Dassow P, John U, Ogata H, Probert I, Bendif E, Kegel JU, Audic S, Wincker P, Da Silva C, Claverie JM, Doney S, Glover DM, Flores DM, Herrera Y, Lescot M, Garet-Delmas MJ and de Vargas C (2015) Life-cycle modification in open oceans accounts for genome variability in a cosmopolitan phytoplankton, *ISME Journal*, 9, 1365-1377.

3.6 **MicroPath: Effects of Environmental Changes on Microbial Pathways Relevant for the Production of Climate-Active Gases**

Sonja Endres¹, Anna-Adriana Anschutz^{1,2}, Moritz Krusenbaum^{1,2}
Judith Piontek¹, Anja Engel¹ (not on board)

¹GEOMAR
²CAU

Grant-No. AWI_PS103_05

Objectives

Physical, chemical and biological processes in the ocean drive the exchange of climate-active gases between atmosphere and ocean. The Southern Ocean is a net sink for atmospheric CO₂, which is strongly controlled by biological processes (Orr et al., 2001; Takahashi et al., 2002). Phytoplankton primary production and the subsequent export of organic carbon towards long-term storage in the deep ocean primarily drive the biological drawdown of CO₂ in the ocean. Photosynthetic products (polysaccharides, proteins, and nucleic acids chains) coagulate and aggregate forming eventually gel particles (Alldredge et al. 1993; Passow 2002a, 2002b) which play an important role in sedimentation processes and thus in the carbon export (Bhaskar et al., 2005). However, heterotrophic bacterial activity can remineralize about 50 % of primary production in surface waters of coastal and low-latitude oceans. As a result, they produce CO₂ that is released back to the atmosphere on short time scales (Robinson 2008, Fig. 3.6.1). Hence, environmental changes that tip the balance between autotrophic CO₂ fixation and heterotrophic CO₂ production have a high potential to affect carbon budgets and the storage of CO₂ in marine systems. Temperature has a stronger impact on bacterial heterotrophic metabolism than on autotrophic CO₂ fixation, implying the decoupling of phytoplankton production and bacterial growth in cold oceans (Pomeroy and Deibel, 1986). An increasing number of studies revealed the high potential of temperature and organic matter for synergistic effects on bacterial activity in polar oceans (Kritzberg et al., 2010; Piontek et al., 2015). Temperature sensitivities of enzymatic degradation processes increase with molecular complexity of substrates. Several studies in soil science show that the temperature sensitivity of bacterial litter degradation can be linked directly to the chemical complexity of the material (Fierer et al., 2005; Steinweg et al., 2013). Whether the structural complexity of substrates affects the temperature sensitivity of bacterial organic matter turnover and, thereby, the biological CO₂ production in the ocean is currently unknown.

In addition to CO₂ production by heterotrophic bacteria, marine microbes also influence the production of halocarbons. They are climate-active trace gases, which play an important role in atmospheric composition and chemistry (Salawitch et al., 2005; Liss et al., 2007). The importance of halocarbons in the degradation of the stratospheric ozone layer is increasing as the anthropogenic emission of chlorofluorocarbons is ceasing (Montzka & Reimann, 2011). Biological production of bromoform is currently hypothesized as the main source for oceanic bromocarbons, but with little knowledge of the detailed mechanisms.

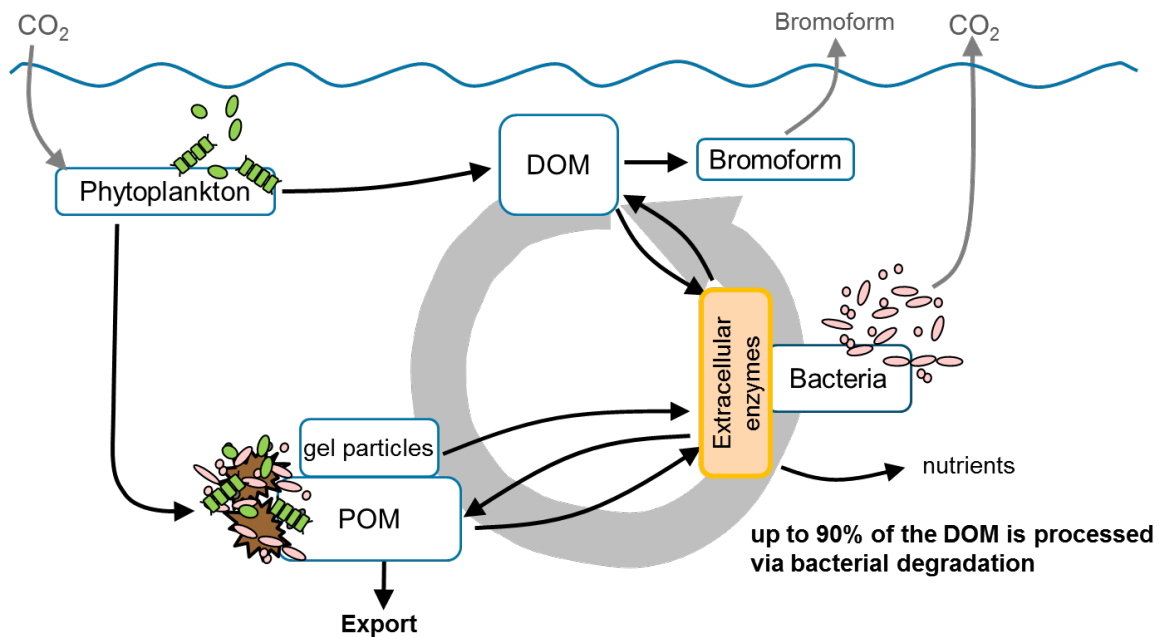


Fig. 3.6.1: Microbial cycling of dissolved and particulate organic matter (DOM, POM) relevant for the production of the climate-active gases CO₂ and bromoform

During austral summer, high bromoform surface ocean concentrations can be found in the Southern Ocean (Stemmler et al. 2014). Measurements at the RaTS time series site (western Antarctic Peninsula) show a correlation between the melting of sea-ice in spring and an increase in chlorophyll *a* and bromoform concentrations (Hughes et al. 2009) in the seawater. It has been suggested that reactive halogen species in seawater halogenate dissolved organic matter (DOM) with the help of the enzyme bromoperoxidase releasing halogenated trace gases (Liu et al. 2015, Fig. 3.6.1). Marine cold-water diatoms (e.g. *Porosira glacialis* and *Thalassiosira antarctica*) as well as mixed natural assemblages of ice-algae were positively tested for bromoperoxidase activity in laboratory studies (Hughes et al. 2013, Hughes et al. 2016). However, so far we lack any data on bromoperoxidase activities in natural plankton communities. According to tests with single substrate additions, the composition of DOM drives the production of bromoform. Several DOM compounds, such as glycolic acid, alginic acid, citric acid, humic acid and urea, enhance bromoform production. Currently we lack even basic knowledge of how DOM release and composition as well as microbial turnover are contributing to oceanic bromoform production and how environmental parameters such as temperature will affect bromocarbon formation in the future.

The Weddell Sea is characterized by highly efficient remineralisation of biogenic detritus and organic carbon at shallow depth (above 200 m) (Usbeck et al., 2002). Previous microbiological studies revealed high shares of psychrotolerant bacterial isolates, suggesting a high responsiveness of bacterioplankton in the Weddell Sea to rising temperature (Delille, 1992, Helmke and Weyland, 1995). However, the temperature sensitivity of natural communities, its spatial variability and the potential of temperature effects to alter organic matter cycling have not been investigated so far. Results of this project will provide new rate estimates to evaluate and improve existing models. In the context of ocean change, this will help to improve our process understanding of climate feedback cycles.

Work at sea

The working programme in the Weddell Sea consisted of three work packages (WP) consisting of field studies (WP 1) and on-board experiments (WP 2+3).

WP 1: Field studies

22 stations were sampled along the Greenwich (0°-)meridian and in the Weddell Sea resulting in a north-south and an east-west transect that includes coastal and open ocean as well as ice covered sites. Hence, gradients in phytoplankton production and ice coverage provided the chance to sample for phyto- and bacterioplankton communities exposed to different supplies of organic matter. Stations were sampled each with seven depths from the surface to 150 m and at 1,000 m depth. At four selected stations, deep-water masses (500 m until bottom) were characterized in more detail (Tab. 3.6.1). Rates of three extracellular enzymes were determined for each depth to characterize heterotrophic bacterial activity. Rate measurements were combined with sampling for bacterial cell abundances, nutrients, dissolved organic carbon (DOC) concentrations, and carbohydrate- and protein-rich gel particles. Additionally, bromoperoxidase activity was determined from the deep chlorophyll a maximum depth at each station. At selected stations, also samples for bromoform concentration, phytoplankton and DOM composition (combined carbohydrates and amino acids, see also WP3) were taken for further analysis at GEOMAR.

Tab. 3.6.1: Sampled CTD stations and depths during PS103 including parameters that will be analysed from each sample

#	Station	Latitude	Longitude	Sampled depth	Extracellular enzyme activities	Gel particles	DOC, Nutrients	Bacterial abundance	DOM composition	Bromoform	Phytoplankton composition
1	PS103_1	45° 57.293' S	6° 17.236' E	2, 35	x	x	x	x			
2	PS103_4	55° 52.571' S	1° 03.292' E	3, 10, 20, 60, 120, 150	x	x	x	x			
3	PS103_5	59° 02.984' S	0° 04.783' E	2.2, 10, 25, 76, 120, 150, 1000	x	x	x	x			
4	PS103_6	61° 00.016' S	0° 00.091' W	2, 15, 35, 110, 120, 150, 1000	x	x	x	x	x	x	x
5	PS103_7	63° 59.582' S	0° 03.853' E	7, 25, 35, 60, 120, 150, 997	x	x	x	x			
6	PS103_8	65° 00.052' S	0° 01.486' E	5, 26, 35, 60, 120, 150, 1000	x	x	x	x			
7	PS103_9	66° 00.018' S	0° 00.031' W	5, 30, 45, 65, 120, 150, 1000	x	x	x	x			
8	PS103_10	67° 00.018' S	0° 00.093' E	3, 20, 40, 70, 120, 150, 1000	x	x	x	x			
9	PS103_14	68° 00.061' S	0° 00.240' W	3.5, 20, 33, 48, 120, 150, 500, 1000, 2000, 4406	x	x	x	x			

#	Station	Latitude	Longitude	Sampled depth	Extracellular enzyme activities	Gel particles	DOC, Nutrients	Bacterial abundance	DOM composition	Bromoform	Phytoplankton composition
10	PS103_17	69° 24.249' S	0° 03.105' W	5, 10, 15, 48, 120, 150, 1000	X	X	X	X			
11	PS103_22	69° 00.705' S	7° 01.326' W	3.3, 20, 45, 70, 120, 150, 1000	X	X	X	X	X	X	X
12	PS103_23	65° 59.752' S	12° 16.250' W	4, 20, 40, 80, 120, 150, 1000	X	X	X	X			
13	PS103_29	71° 21.907' S	13° 58.591' W	1.5, 10, 30, 45, 120, 150, 379	X	X	X	X	X		
14	PS103_31	69° 03.931' S	17° 22.528' W	3.4, 10, 25, 55, 120, 150, 1000	X	X	X	X			
15	PS103_34	70° 54.010' S	28° 59.079' W	4.1, 35, 65, 90, 120, 150, 1000	X	X	X	X	X	X	X
16	PS103_39	66° 36.041' S	27° 14.003' W	3, 20, 40, 80, 120, 150, 500, 1000, 2000, 4821	X	X	X	X	X		
17	PS103_40	65° 43.533' S	36° 43.989' W	3, 20, 50, 90, 120, 150, 1000	X	X	X	X			
18	PS103_43	68° 25.294' S	44° 05.989' W	1.9, 30, 55, 75, 120, 150, 500, 1000, 2000, 4050	X	X	X	X	X		
19	PS103_45	64° 22.814' S	45° 56.411' W	2.4, 20, 35, 80, 120, 150, 1000	X	X	X	X			
20	PS103_48	64° 04.04' S	48° 22.37' W	2.5, 10, 45, 120, 150, 500, 1000, 2000, 3877	X	X	X	X	X		
21	PS103_59	63° 28,96' S	51° 35,53' W	3, 20, 39, 70, 120, 150, 1000	X	X	X	X	X	X	
22	PS103_67	63° 13,32' S	53° 42,15' W	2, 10, 25, 55, 120, 150, 297	X	X	X	X	X	X	

WP 2: On-board experiments on temperature effects on hydrolytic extracellular enzymes

From every CTD sample, rates of three extracellular enzymes (alkaline phosphatase, beta-glucosidase, and leucine aminopeptidase) were determined at *in-situ* temperature (1.8 °C) and at elevated temperature (5.8 °C) to estimate the activation energy for enzymatic reactions driven by natural bacterioplankton communities of the Weddell Sea.

WP 3: On-board experiments on halocarbon cycling

In order to elucidate the link between photosynthetic and bromocarbon production, and if this might change with future climate change, seawater samples were incubated for 10 days in gas tight bottles under *in-situ* and altered temperature conditions (1.8°C and 5.8°C). Incubation studies were started with surface seawater samples (20 -50 m depth) at three selected stations

along the cruise track Fig. 3.6.2). Depth profiles of those stations were sampled as described in WP1 including sampling for bromoform concentration, DOM and phytoplankton composition.

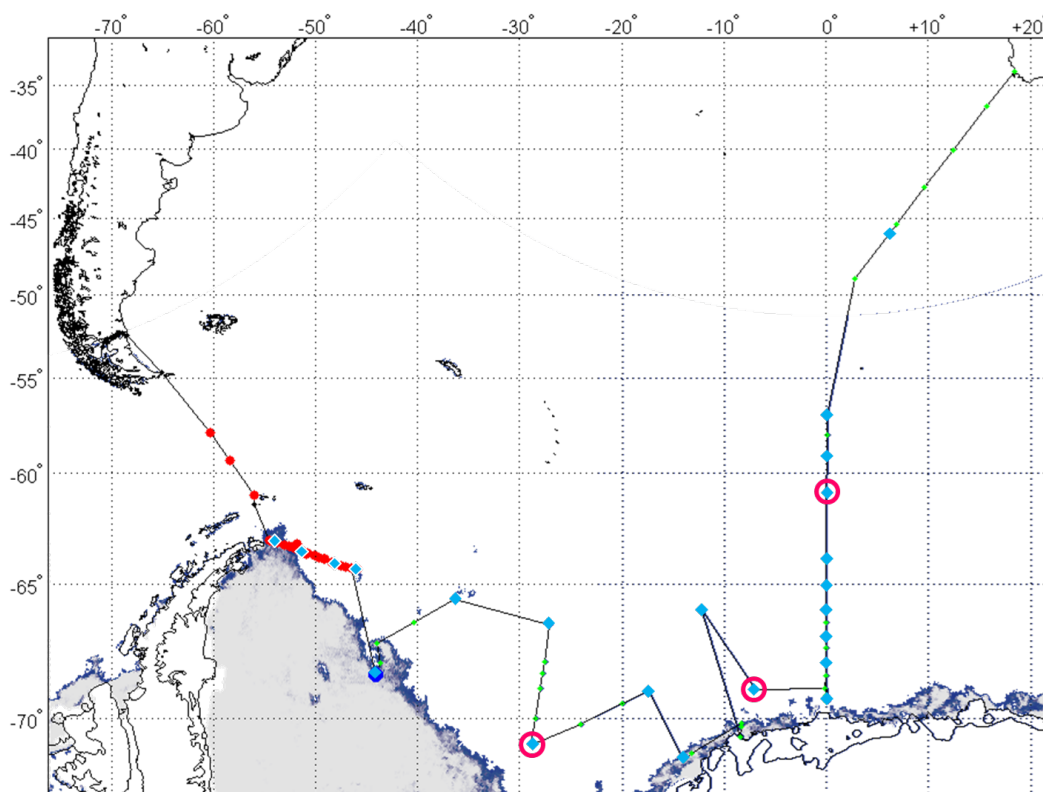


Fig. 3.6.2: Expedition track, sampled CTD stations (blue squares) and positions of selected stations where bromoform incubation studies were started (pink circles)

In order to account for heterotrophic bromoform degradation in the incubations, ^{13}C -labeled bromoform was added to all treatments as an internal standard. Incubations run at a light:dark cycle of 20:4h. To test whether it is the reactive bromine or the organic compounds, which limits bromoform production, the yield of bromoform following bromoperoxidase or alginate additions were tested (treatment “BrPO” and “Alg”, respectively) and compared to a not manipulated seawater treatment (“SW”) (Fig. 3.6.3). To differentiate between biological and chemical processes, abiotic controls using ultrapure water amended with alginate and bromoperoxidase were included (treatment “MQ”). Replicate bottles were sampled every second day for microbial cell abundances, as well as bromoform and dissolved organic carbon (DOC) concentrations. Microbial net activity (estimated by oxygen consumption and production), bromoperoxidase activity were determined and samples for DOM composition (combined carbohydrates and amino acids) were taken on day 0, 4, 6 and 10 of the incubation period.

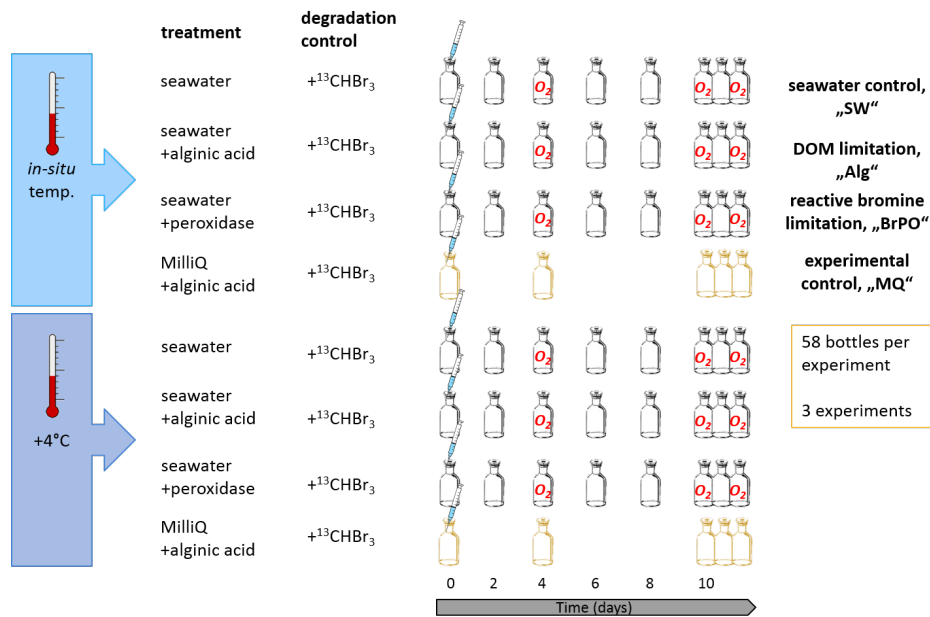


Fig. 3.6.3: Experimental setup of the bromoform incubation studies

Results of *WP 1* will be used to calculate fluxes of carbohydrate- and protein-rich gel particles and the impact of bacterial remineralisation on gel particle recycling. Furthermore, attained depth profiles of extracellular enzyme activities and halocarbon concentrations will be compared to several physical and biogeochemical parameters including oxygen, sea surface temperature, salinity, and DOM concentrations. This will help to identify possible sources and processes related to halocarbon production and their oceanic emissions. Biogeochemical and microbiological profiles will be related to rates of halocarbon cycling attained in *WP3*. Results of *WP2* will increase the knowledge on temperature effects on heterotrophic bacterial organic matter degradation. Estimated activation energies for hydrolytic extracellular enzymes are useful to improve model projections on effects of warming in the Southern Ocean.

Preliminary and expected results

First results indicate, that bacteria adjust their enzymatic activity according to the availability of substrate, since the highest enzymatic activity of the leucine aminopeptidase were found in the deep chlorophyll a maximum (DCM) depth (Fig. 3.6.4).

The increase in temperature resulted in a higher bacterial enzymatic activity (*WP 2*) as results from Station *PS103_4* imply (Fig. 3.6.5). In a future ocean scenario, this may increase the fraction of organic matter, which is degraded at the surface, and lower the efficiency of particle export and carbon sequestration fluxes to the ocean depth.

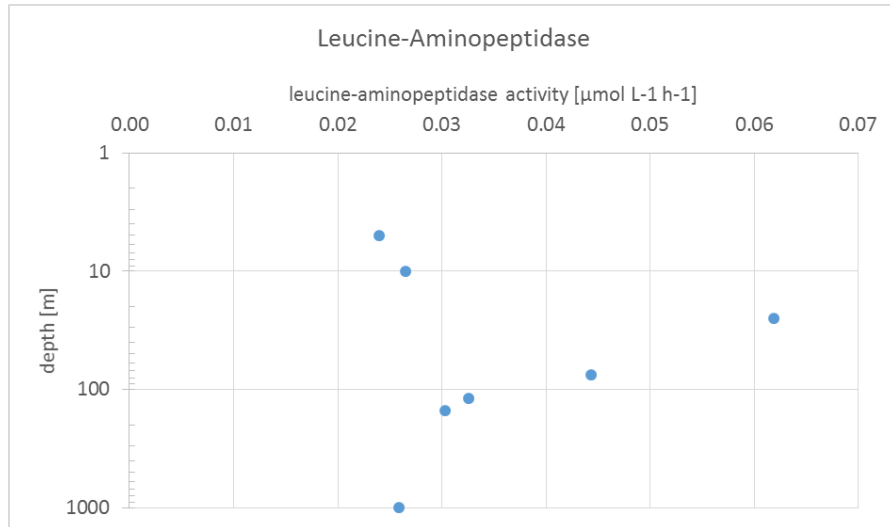


Fig. 3.6.4: Depth profile of leucine aminopeptidase activity at in-situ temperature (1.8°C) from station PS103_5

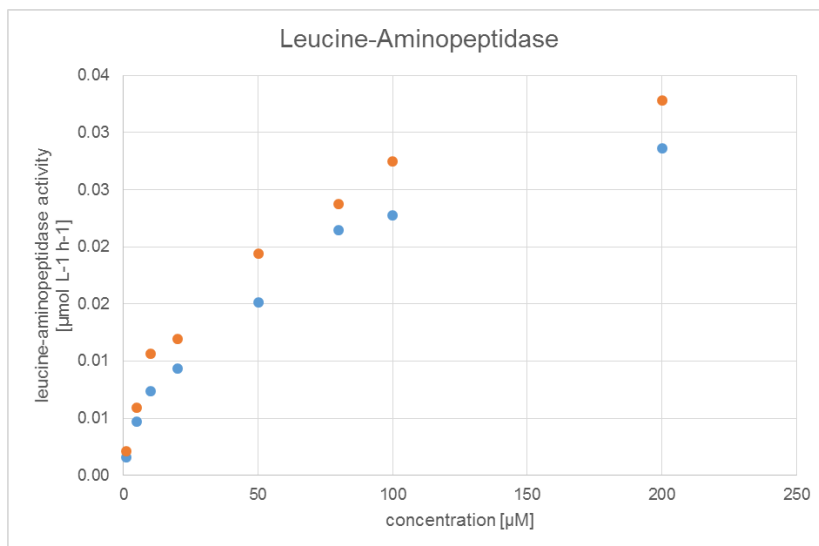


Fig. 3.6.5: Kinetics of leucine aminopeptidase activity at in-situ (1.8°C, blue) and elevated temperature (5.8°C, orange) at station PS103_4

No bromoperoxidase activity could be detected at any of the tested stations. Oxygen measurements in the incubation bottles indicate high primary production in the “SW” and “BrPO” treatments compared to the “Alg” and “MQ” treatments.

Samples for bacterial cell abundances, carbohydrate- and protein-rich gel particles, nutrients, DOC and bromoform concentrations, as well as phytoplankton and DOM composition of both, CTD sampling and experimental studies, were preserved and stored at +4°C and -20°C, respectively, and will be analyzed in the home laboratory at GEOMAR in Kiel.

Data management

Sample analysis will be finalized within one year after the cruise. Data analysis and publication in international journals is planned within two years after the cruise. Data will be made available to the public via PANGAEA after publishing.

References

- Allredge AL, Passow U, Logan BE (1993) The abundance and significance of a class of large transparent organic particles in the ocean. *Deep-Sea Research I* 40:1131–1140.
- Bhaskar P V, Grossart H P, Bhosle N B & Simon M (2005). Production of macroaggregates from dissolved exopolymeric substances (EPS) of bacterial and diatom origin. *FEMS Microbiology Ecology*, 53(2), 255-264.
- Delille D (1992) Marine bacterioplankton at the Weddell Sea ice edge, distribution of psychrophilic and psychrotrophic populations. *Polar Biology* 12, 205-210.
- Fierer N, Crain JM, McLauchlan K, and Chimel JP (2005) Litter quality and the temperature sensitivity of decomposition. *Ecology* 86, 320-326.
- Helmke E, and Weyland H (1995) Bacteria in sea ice and underlying water of the eastern Weddell Sea in midwinter. *Marine Ecology Progress Series* 117, 269-287.
- Hughes C, Chuck AL, Rossetti H, Mann PJ, Turner SM, Clarke A, Chance R, Liss P (2009) Seasonal cycle of seawater bromoform and dibromomethane concentrations in a coastal bay on the western Antarctic Peninsula. *Glob. Biogeochem. Cycles*. <http://dx.doi.org/10.1029/2008GB003268>.
- Hughes C, Johnson M, Utting R, Turner S, Malin GI, Clarke A, Liss P (2013) Microbial control of bromocarbon concentrations in coastal waters of the western Antarctic Peninsula, *Marine Chemistry* 151, 35–46.
- Hughes C and Sun S (2016) Light and brominating activity in two species of marine diatom, *Marine Chemistry* 181:1–9.
- Kritzberg ES, Duarte CM, and Wassmann P (2010) Changes in Arctic marine bacterial carbon metabolism in response to increasing temperature. *Polar Biology* 33, 1673-1682.
- Liss P S Trace gas emissions from the marine biosphere, *Philosophical Transactions of the Royal Society A: Mathematical, Physical and Engineering Sciences* 365, 1697–1704 (2007).
- Liss P S, Marandino, C A et al. in *Ocean-Atmosphere Interactions of Gases and Particles*, edited by P S Liss & M. T. Johnson (Springer, Berlin, Heidelberg, 2014), pp. 1–54.
- Liu L, Thornton D, Bianchi, TS, Arnold W A, Shields, M. R., Chen, J, Yvon-Lewis, S A (2015) Dissolved Organic Matter Composition Drives the Marine Production of Brominated Very Short-Lived Substances, *Environ. Sci. Technol.*, 49:3366–3374.
- Montzka SA and Reimann, S in *Scientific Assessment of Ozone Depletion: 2010, Global Ozone Research and Monitoring Project, Report No. 52*, edited by World Meteorological Organization (Geneva, Switzerland, 2011), pp. 1–108.
- Orr JC, Maier-Reimer E, Mikolajewicz U, Monfray, P, Sarmiento, JL et al. (2001) Estimates of anthropogenic carbon uptake from four three-dimensional global ocean models. *Global Biogeochemical Cycles* 15, 43–60.
- Passow U (2002a) Production of transparent exopolymer particles (TEP) by phyto- and bacterioplankton. *Marine Ecology Progress Series* 236:1–12.

- Passow U (2002b) Transparent exopolymer particles (TEP) in aquatic environments. *Progress In Oceanography* 55:287–333.
- Piontek J, Sperling M, Nötig E-M, Engel A (2015) Multiple environmental changes induce interactive effects on bacterial degradation activity in the Arctic Ocean. *Limnology and Oceanography* 60(4):1392–1410.
- Pomeroy LR and Deibel, D (1986) Temperature regulation of bacterial activity during the spring bloom in Newfoundland coastal waters. *Science* 233, 359-361.
- Robinson C (2008) Heterotrophic bacterial respiration. In *Microbial Ecology of the Oceans* (ed. D.L. Kirchman), pp. 299-334. Wiley-Blackwell, New York.
- Salawitch R J (2005) Sensitivity of ozone to bromine in the lower stratosphere, *Geophys. Res. Lett.* 32.
- Steinweg JM, Jagadamma S, Frerichs J, and Mayes MA (2013) Activation energy of extracellular enzymes in soils from different biomes. *Plos One* 8, e59943.
- Stemmler I, Hense I, Quack B (2014) Marine sources of bromoform in the global open ocean – global patterns and emissions, *Biogeosciences Discuss.*, 11, 15693–15732.
- Takahashi, T, Sutherland SC, Sweeney C, Poisson A, Metzl N, Tilbrook B, Bates N, Wanninkhof R, Feely RA, Sabine C, Olafsson J, and Nojirih Y (2002) Global sea-air CO₂ flux based on climatological surface ocean pCO₂, and seasonal biological and temperature effects. *Deep-Sea Research II* 49, 1601-1622.
- Usbeck R, van der Loeff MR, Hoppema M, and Schlitzer R (2002) Shallow remineralization in the Weddell Gyre. *Geochemistry Geophysics Geosystems* 3, 1008.

3.7 ISOTAM: Stable N - isotopes of ammonium and ammonia in and over the Atlantic Ocean

Heinrich Kreilein¹, Marion Kreilein¹, Edgar
Tunsch¹
Gode Gravenhorst¹ (not on board)

¹Uni Göttingen

Grant-No. AWI_PS103_06

Objectives

The ice shield of Antarctica is a huge archive for past global biogeochemical properties and earth system processes. Deposition rates of excess-sulphate, of non-continental nitrate and of ammonium in Antarctica do not seem to differ markedly in glacial and interglacial periods (e.g. Kaufmann et al. 2010, The sources of the ionic constituents in polar firn and ice cores are, therefore, still a matter of debate. The atmosphere is an open system with global connections in space and time. The gateway from the lower latitudes of the Atlantic to Antarctica is, therefore, one special road of interest for understanding traits in Antarctic ice constituents and their relation to earth system processes.

Antarctic ice constituents could have their primary sources in the Southern Ocean (Andreae and Crutzen 1997) and on continents (e.g. Duce et al. 2008). Sulphate, nitrate, ammonium and sodium are major targets of ice core analyses and their interpretations. The $\delta^{34}\text{S}$ isotope ratio as tracer for sulphur in Antarctic and Greenland ice cores has been evaluated. (e.g. Delmas 1995). However N-isotopes of ammonium in ice cores are not measured yet. Especially the source of their ammonium constituent is rather uncertain.

Ammonia gas (NH_3) is the main alkaline gaseous compound in the atmosphere. It is the source of ammonium (NH_4^+) in atmospheric particles, droplets and ice cores. Ammonia is emitted into the atmosphere on a global scale mainly by volatilisation from liquid cattle waste. (e.g. Lenhard and Gravenhorst 1980, Dentener and Crutzen, 1994). In the marine atmosphere NH_3 could have its source in the ocean surface water (Bell 2006, Paulot et al. 2015). The concentrations of gaseous NH_3 and particulate NH_4^+ seem to drop by about one order of magnitude from the open ocean to the sea ice covered ocean (Ibrom et al. 1991). NH_3 can flow between the atmosphere and the ocean in both directions (e.g. Schaefer et al. 1998, Paulot et al. 2015). The ocean was divided to be a sink in high and, therefore, cold latitudes and a source in low and, therefore, warm latitudes (Johnson et al 2008). Maritime airborne ammonium is mainly found in the nucleation and accumulation mode (e.g. Gravenhorst 1978, Gravenhorst et al. 1979, Schaefer et al 1993). Airborne NH_4^+ and non-sea-salt sulfate in remote areas frequently show molar ratios between 1 and 2 (e.g. Gravenhorst 1978, Paulot et al. 2015). A reaction of acidic sulphate and alkaline ammonia seems to be realistic (Gravenhorst 1978, Beilke and Gravenhorst 1978, Johnson et al. 2008). NH_4^+ is produced within the ocean via N_2 fixation, ammonification of organic material, denitrification of nitrite and excretion by organisms and leaves the water via assimilation uptake, nitrification within the ocean, reaction of NH_4^+ with NO_2^- (anammox) and by emission of NH_3 into the atmosphere. The free NH_4^+ - N pool in the global ocean is only a small fraction (less than one permil) of the NO_3^- N pool (e.g. Gruber and Galloway 2008). NH_4^+ sea water concentrations along a latitudinal transect across the Atlantic was around 10 to 250 $\mu\text{mol} / \text{m}^3$ (Woodward 2006, Paulot et al. 2015).

$\delta^{15}\text{N}$ ratios of ammonia and ammonium in the atmosphere

Stable isotopes can indicate sources and transfer routes of atmospheric trace substances. Ratios of ^{15}N - NH_4^+ and ^{15}N - NH_3 isotope values in atmospheric samples are very rare. The particulate ammonium in the atmosphere has a high $\delta^{15}\text{N}$ value similar to the $\delta^{15}\text{N}$ value of the

NH₃-source material. The rain $\delta^{15}\text{N-NH}_4^+$ value seems to fall between $\delta^{15}\text{N}$ values for gaseous airborne NH₃ and for particulate airborne NH₄⁺. All NH₃ and NH₄⁺ and their isotopes in updrafts at cloud base can be assumed to be incorporated into cloud droplets and subsequent into rain drops (Gravenhorst 1983).

$\delta^{15}\text{N}$ values of ammonia and ammonium in sea water

The N-cycle in the ocean is connected to the atmosphere (e.g. Duce 1986, Schaefer et al 1999, Voss et al. 2013). N cycling has been characterized with $\delta^{15}\text{N}$ values in different transformation processes (e.g. Sigman et al. 2009).

We want to measure actual concentrations of sea water NH₄⁺ and NH₃ x H₂O and their ¹⁵N -isotope ratios (Holmes et al. 1998, Woodward 2006, Watson et al. 2005) in comparison with atmospheric particulate NH₄⁺ and gaseous NH₃. Cruise PS103 traverses open water and sea ice covered regions. Oceanic flux of NH₃ from the ocean into the atmosphere or vice versa should therefore be strongly reduced. This should be reflected in atmospheric concentrations of NH₃, NH₄⁺ and their isotope ratios.

Our aim is, therefore, to determine on the Northern and the Southern Atlantic from northern mid- latitudes to Antarctica the background pattern of the ratios of stable isotopes ¹⁵N / ¹⁴N of NH₄⁺ and of NH₃ in the air and in the surface water to characterize possible sources of atmospheric NH₄⁺ and their regional distribution. Our questions are:

- What ¹⁵N / ¹⁴N-isotope ratios are found in ammonium of size separated airborne particles and in gaseous ammonia over the Atlantic?
- What differences in NH₄⁺ - and NH₃ - concentrations and in N - isotope ratios do exist between air over the North Atlantic, the South Atlantic and air over the ice- covered Atlantic?
- Can we differentiate NH₃ -source and - sink regions on the Atlantic?
- What finger prints do ammonia and ammonium, dissolved in the surface water of the Atlantic, leave in the atmosphere?

Work at sea

Concentrations of gaseous NH₃ and particulate NH₄⁺ in the lower atmosphere as well as physically dissolved NH₃ x H₂O and NH₄⁺ in the surface sea water had been determined on the latitudinal transects of *Polarstern* from Bremerhaven to the Weddell Sea and further to Punta Arenas.

NH₃ - and NH₄⁺ sampling in the atmosphere

For NH₃ and NH₄⁺ concentrations as well as $\delta^{15}\text{N-NH}_3$ and $\delta^{15}\text{N-NH}_4^+$ isotope measurements the NH₄⁺ and NH₃-gas molecules had been accumulated on filter pack systems (90 mm diameter). The filter pack system consists of one Teflon-membrane filter in front to accumulate particles and three acidified membrane filters behind to absorb gas phase ammonia. Four individual standalone systems (filter pack, gas pump, gas meter, wind direction controller) had been installed on the deck above the bridge (Fig. 3.7.1). For the case of wind blowing from the tail a similar filter pack system had been installed on the stern. Depending on NH₄⁺ mass found on each NH₄⁺ - particle filter and on each NH₃ ammonia filter the solutions of filters will have been used for NH₄-N - and NH₃-N isotope analyses on land according to Watson et al. (2005), Holmes et al. (1998).

Two identical high - volume samplers (ca. 70 m³ / h) collected size-fractionated airborne particles with a 5 stage impactor (Fig. 3.7.2.) (Marple and Willeke 1976). The 5 stages of the impactor (ca. < 10 μm to > 0.1 μm radius) were covered by a Teflon foil and backed up with a Teflon membrane filter (filter Ø = 22 cm, particle r < 0.1 μm radius). The impactors were installed on the deck above the bridge. About 5,000 m³ sample sizes (3 - 5 days of sampling) are necessary to collect enough NH₄⁺- N, and SO₄⁼ - S for isotope analyses for the different particle size ranges.



Fig. 3.7.1: Four filter pack systems collecting samples of NH₃ and NH₄⁺

Fig. 3.7.2: High-volume-impactor (top), the pumps for the filter pack systems and gas meters



On board analyses of dissolved NHy (the sum of NH₄⁺ + NH₃ x H₂O)

These analyses of NHy in the ocean surface water are a critical point, since the concentrations of NHy are up to now often below detection limit and biased with artefacts. At the moment it is still a challenging task to measure on board lowest concentrations of NHy in sea water. We have determined concentrations of NHy in sea water with a Systea μMac100 Analyser connected with the Ferry Box. The detection limit of the μMac1000 is about 0.3 μMol/l.

Preliminary and expected results

NH₃ - and NH₄⁺ sampling in the atmosphere

Because of the weather conditions (too high air humidity, snow, too low horizontal wind velocity and wind directions from about ± 80 degrees against the ship's course) and the need to reach the minimum of sample volume we only could accumulate atmospheric air samples of gaseous ammonia and particulate ammonium at 7 times. Tab. 3.7.1 und Fig. 3.7.3 show positions and sampling times at *Polarstern* cruise track between Cape Town and Punta Arenas.

Tab. 3.7.1: Positions and sampling times between Cap town and Punta Arenas

Sample set	Date	Start		End		
		Pos-Longitude	Pos-Latitude	Date	Pos-Longitude	Pos-Latitude
1	17.12.2016	15.804163	-36.585832	20.12.2016	6.730673	-45.547090
2	20.12.2016	6.286686	-45.952483	24.12.2016	0.076727	-59.048859
3	26.12.2016	-0.017331	-64.012652	31.12.2016	0.021613	-69.012866
4	31.12.2016	-0.014557	-68.995946	09.01.2017	-8.137360	-70.532097
5	09.01.2017	-8.196640	-70.386556	15.01.2017	-27.148472	-66.603668
6	15.01.2017	-27.233635	-66.608224	23.01.2017	-45.870156	-64.373844
7	23.01.2017	-47.079132	-64.257914	27.01.2017	-51.830051	-63.270991

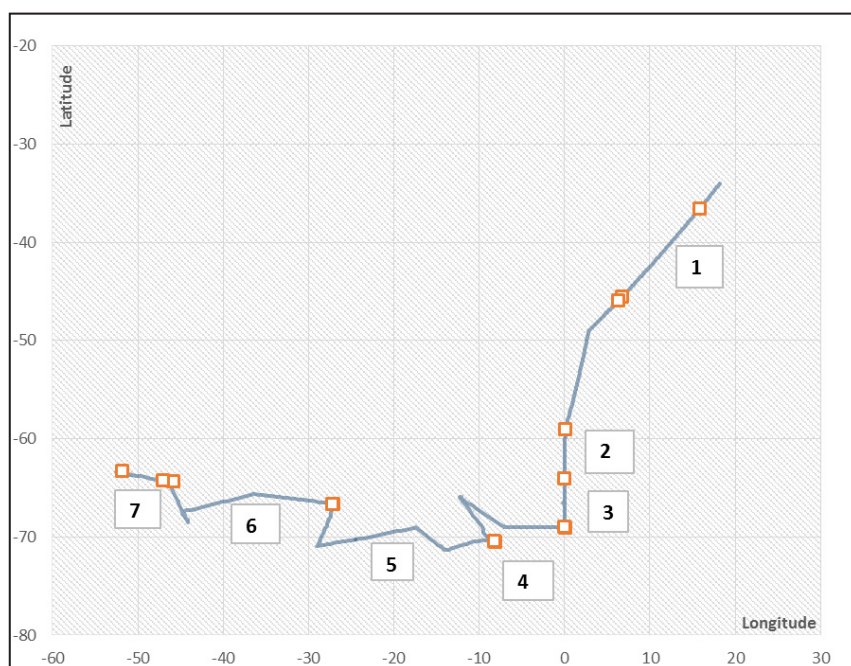


Fig. 3.7.3: Expedition track and position of sampling data

On board analyses of dissolved NH_y

During the entire cruise, the measurements of NH_y in the ocean surface water had been below the detection limit until Grahamland. From 47.492618° W, 64.215394° S to 54.733783° W, 62.158917° S we have measured values up to 1.1 µmol/l of N-NH_y in the upper surface layers.

Storing samples

All filter samples have been stored in PE-bottles at temperature slightly above freezing point (4 °C) to prevent lysis of microbiological cells.

Analyses

All the samples will be analysed at Uni Göttingen in order to obtain the NH₃- and the NH₄⁺-concentrations as well as their N- isotope ratios.

In order to estimate regions of air mass sources, apart from backtracking air trajectories, we will analyse some filter samples for the determination of aerosol bulk composition. We will also quantify the input of nutrients and trace metals into the ocean by aerosol deposition.

The back trajectories of the air masses reaching Polarstern are important indicators for possible sources and reactions of air borne trace substances. They have large influence on the history of components and their appearance at the sampling site. The daily trajectories have been taken from DWD and NOAA analyses.

Data management

Samples of airborne particles and gases will be analysed chemically in home laboratories. Data will first be evaluated in bachelor and master theses. Concentrations and stable N-isotopes of these constituents will be discussed in a Polar Research report. Tabulated results will be submitted to PANGAEA. Results will be submitted to scientific journals for atmospheric and marine sciences.

References

- Andreae RA and Crutzen P J (1997) Atmospheric aerosols: biogeochemical sources and role in atmospheric chemistry. *Science*, 276, 5315, 1052-1058.
- Beilke S and Gravenhorst G (1978) Heterogeneous SO₂ oxidation in the droplet phase. *Atm. Env.*, 12, 231 - 239.
- Bell Th (2006) Dimethylsulfide and ammonia in remote marine regions – an Atlantic Meridional Transect Study. Diss. Univ. East Anglia.
- Dentener and Crutzen PJ (1994) A three-dimensional model of the global ammonia cycle. *J. Atm. Chem.*, 19(4), 331-369.
- Delmas R (1995) Ice Core Studies of Global Biochemical Cycles. *Nato Adv. Res. Workshop 1993*, Annecy, France, R. Delmas (ed), Springer.
- Duce RA (1986) The impact of atmospheric nitrogen, phosphorus and iron species on marine biological productivity. In: *The role of air sea exchange in geochemical cycling*, (ed. P Buat-Menard) Reidel, Dordrecht, 497-529.
- Duce RA et al. (2008) Impacts of atmospheric anthropogenic nitrogen on the open ocean. *Science* 320, 893-897.

3.7 ISOTAM: Stable N - isotopes of ammonium and ammonia in and over the Atlantic Ocean

- Georgii HW and Gravenhorst G (1975) The ocean as source or sink of reactive trace gases. *Pure and Appl. Geophys.* 115, 503-511.
- Gravenhorst G (1978) Maritime sulfate over the North Atlantic. *Atm. Env.*, 12, 707-713.
- Gravenhorst G et al. (1979) Inorganic nitrogen in marine aerosols Gesellschaft fuer Aerosolforschung; Mainz; *Aerosols in Science, Medicine and Technology*, 7th conference, pp 182-187.
- Gravenhorst G (1983) Der Einfluss von Wolken und Niederschlag auf die vertikale Verteilung von Spurenstoffen in einem eindimensionalen reaktionskinetischen Modell. *Berichte des Instituts für Meteorologie und Geophysik der Univ. Frankfurt*, Nr. 42.
- Gruber N and Galloway JN (2008) An earth system perspective of the global nitrogen cycle. *Nature*, 451(7176), 293 - 296.
- Holmes RM et al. (1999) A simple and precise method for measuring ammonium in marine and freshwater ecosystems. *Can. J. Fish. Aquatic Sci.*, 56(10) 1801-1808.
- Ibrom A, Qi L, Cai Y, Bredemeier M and Gravenhorst G (1991) Reaktive Stickstoffkomponenten über dem Nordatlantik. Abschlussbericht, DFG Az. Gr 738/6-1.
- Johnson MT. et al. (2008) Field observations of the ocean-atmosphere exchange of ammonia: Fundamental importance of temperature as revealed by a comparison of high and low latitudes. *Global Biogeochemical Cycles*, 22, 1.
- Kaufmann P et al. (2010) Ammonium and non-sea salt sulfate in the EPICA ice cores as indicator of biological activity in the Southern Ocean. *Quaternary Science Reviews*, 29, 1-2, 313-323.
- Legrand M et al. (1988) Vostok (Antarctica) ice core: Atmospheric chemistry changes over the last climatic cycle (160,000 years). *Atm. Env.* 22, 317-331.
- Lenhard U and Gravenhorst G (1980) Evaluation of ammonia fluxes into the free atmosphere over western Germany. *Tellus*, 32, 48-55.
- Marple VA and Willeke K (1976) Inertial impactors; theory, designation, use. In : *Fine particles: Aerosol generation, measurements and use*, BYH Liu (ed) N.Y. Academic, 411- 446.
- Paulot et al. (2015). Global oceanic emission of ammonia: Constraints from seawater and atmospheric measurements, *Global Biogeochem. Cycles*, 29, 1165-1178.
- Schaefer P et al. (1998) Variation of the $\delta^{15}\text{N}$ values and hydrolyzable amino acids in settling particles in the ocean. *Isot. Env. Health Studies*, 34, 191-199.
- Schaefer P, Kreilein H, Mueller M and Gravenhorst G (1993) Cycling of inorganic nitrogen compounds between atmosphere and ocean in tropical areas off South East Asia. *SCOPE/UNEP*, Heft 76, 19-36.
- Sigman DM et al. (2009) 'Nitrogen isotopes in the Ocean'. In: JH Steele, KK Turekian, and SA Thorpe (eds), *Encyclopedia of Ocean Sciences*. Ac. Press, London, 4138-4153.
- Voss M et al. (2013) The marine nitrogen cycle: recent discoveries, uncertainties and the potential relevance of climate change. *Phil. Trans. Roy. Soc. B*, 368, 1621.
- Watson RJ et al. (2005) Flow-injection analysis with fluorescence detection for the determination of trace levels of ammonium in seawater. *J. Environ. Monit.* 2005 Jan; 7(1), 37-42, E - .
- Woodward M (2006) Ammonia concentrations and processes in oligotrophic ocean waters ; www.nine-esf.org/files/obergurgl/presentations/woodward.pdf .

3.8 PHYTOOPTICS

Rafael Gonçalves-Araujo¹, Julia Oelker²
Astrid Bracher¹, Sonja Wiegmann¹ (not on board)

¹AWI
²Uni Bremen

Grant-No. AWI_PS103_07

Objectives

Marine phytoplankton is the basis of the marine food web and also a main component of biogeochemical fluxes, thus, an important source of dissolved and particulate organic substances. At this cruise we focused to broaden our sampling frequency of information on phytoplankton, particulate and chromophoric dissolved organic matter (CDOM) abundance and composition by taking continuous optical measurements which directly give information on inherent and apparent optical properties (IOPs, and AOPs, respectively). These can later be inverted to extract information on the above listed parameters. The specific objectives of our working group on the PS103 cruise was to

- Collect a high spatial and temporal resolved data set on phytoplankton (total and composition) and its degradation products at the surface using continuous optical observations during the cruise calibrated with data on pigment concentration and particulate, phytoplankton and CDOM measured throughout the cruise from discrete water samples.
- Develop and validate (global and regional) ocean color algorithms, especially the data products of the new sensor OLCI (Ocean and Land Colour Imager) on Sentinel-3.
- Identify bio-physical-chemical coupling in the Atlantic sector of the Southern Ocean by combining the highly resolved biooptical data with physical data obtained during this cruise with remote sensing data and coupled ice-ocean-ecosystem modelling in order to detect shifts in phytoplankton community biomass and composition and the factors driving the variability and changes in phytoplankton community and CDOM

Work at sea

Equipment and measurements on board

- Hyperspectral *in-situ*-spectrophotometer (AC-S; Wetlabs): This instrument operated in flow-trough mode acquired continuous measurements of inherent optical properties (IOPs) in the surface water. The instrument was mounted to a seawater supply taking water from about 11 m depth out off the ship's moonpool and measured alternating between filtered and non-filtered water regularly total and non-particulate light absorption and attenuation spectra for both parameters in the wavelength range between 400 and 740nm (see examples in Fig. 3.8.1).

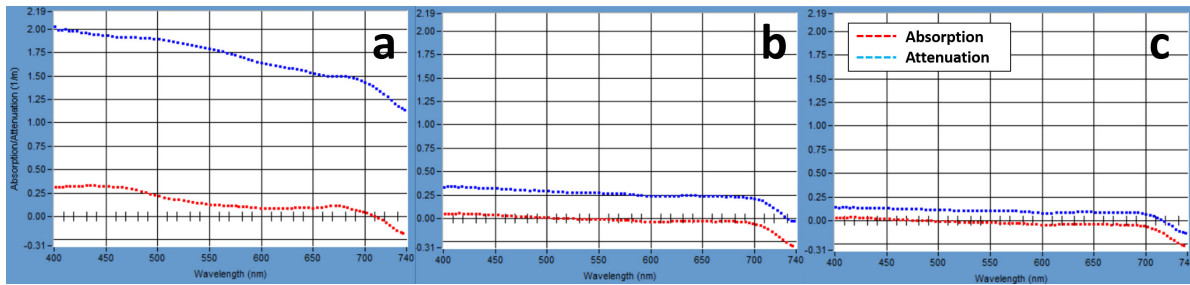


Fig. 3.8.1: Examples of absorption (red) and attenuation (blue) spectra acquired with the AC-S instrument. (a) Non-filtered water sample during passage through high chlorophyll-a concentration area. (b) Non-filtered water sample during passage through low chlorophyll-a concentration area. (c) Filtered water (only pure seawater and dissolved matter - CDOM).

- Liquid waveguide capillary cell system (LWCC, WPI): this instrument measured light absorption (with a 2-m path length) by CDOM, generating spectra from 300 to 750 nm (Fig. 3.8.2). For measurements employing the LWCC instrument, water samples were filtered through 0.2 μ m filters and analyzed after warming up to room temperature. Furthermore, due to technical problems at the beginning of the expedition, a large number of the samples was stored in 4°C and then later analysed onboard, while a few samples (150 out of 436) will be analyzed at the AWI.

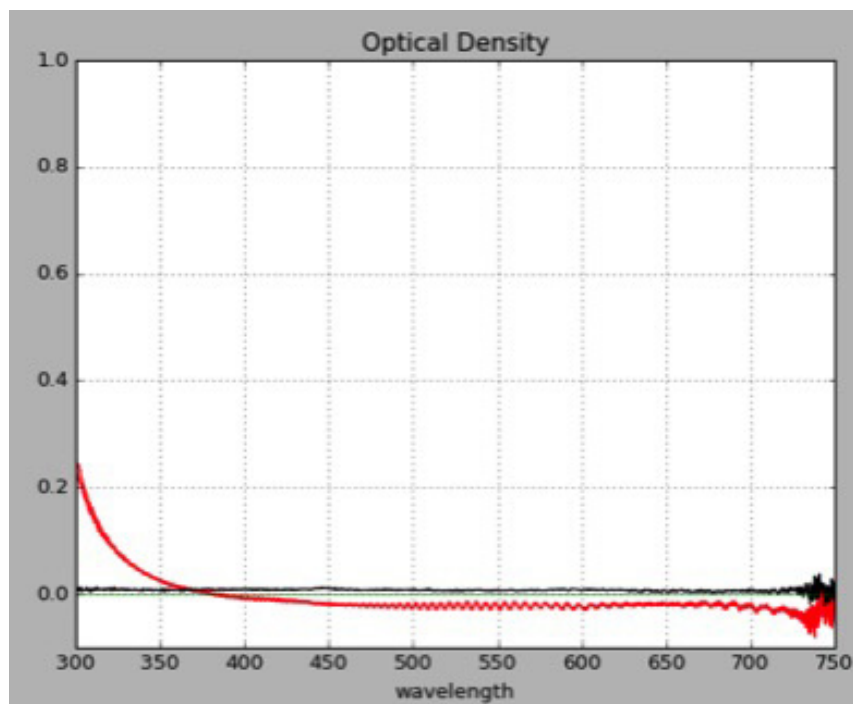


Fig. 3.8.2: Example of a typical CDOM absorbance spectrum (red) obtained with the LWCC instrument. Black line represents the baseline (blank measurement).

- Quantitative Filter Technique (QFT-ICAM): this instrument acquires light absorption spectra (350-870 nm) by particulate matter and after bleaching of filters by detritus only. After subtraction of the detritus from the particulate absorption, phytoplankton absorption is derived for each sample (Fig. 3.8.3). The analyses were performed on particles retained in glass-fiber GF/F filters and measured in a portable QFT integrating cavity setup (Röttgers et al. 2016).

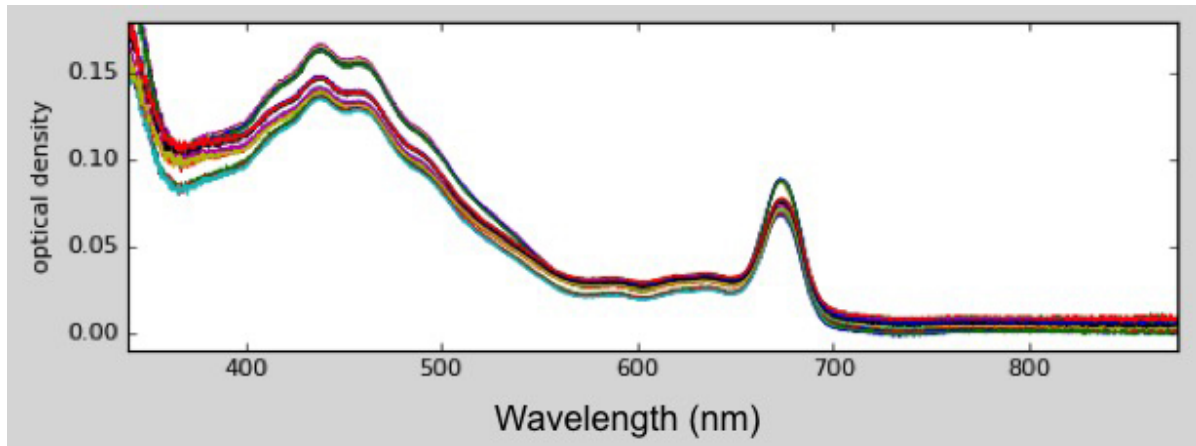


Fig. 3.8.3: Examples of typical phytoplankton absorption spectra obtained during the PS103 expedition with the QFT-ICAM technique. The colors indicate different sample measurement

- High Performance Liquid Chromatography (HPLC): samples for further characterization of phytoplankton pigments were filtered onto GF/F filters (0.7 μm) immediately after sampling and the filters were thermally shocked in liquid nitrogen. Samples were stored at -80°C until shipment at the end of the expedition and sent to the AWI by airfreight on dry ice to be analyzed at the AWI following the procedures described in Taylor et al. (2011).
- Radiometric measurements (RAMSES radiometer): a RAMSES radiometer was mounted in the upper deck of the ship to constantly measure irradiance at the ocean surface level. The equipment obtains one measurement every minute with a spectral range varying from 317-956 nm.

Sampling strategy

During the PS103 cruise, two sampling strategies were adopted: continuous sampling from the flow system and discrete water sampling.

The continuous measurements of inherent optical properties (IOPs) were performed with the AC-S spectrophotometer. The AC-S, operating in flow-through mode (starting after the ship crossed the 12 nm zone from the South African coast (17/12/2017 04:00 UTC) and stopping on the 29 of January 2017 (15:00 UTC), was mounted to a seawater supply taking surface ocean water. A flow-control with a time-programmed filter was mounted to the AC-s to allow alternating measurements of the total and the purewater and CDOM IOPs of the seawater. Flow-control and debubbler-system ensure water flow through the instrument with no air bubbles. The AC-s operated on the seawater supply at the Nasslabor-1, with seawater pumped at Kastenkiel via Spargel with the membrane pump- in order to deliver living phytoplankton cells continuously

throughout the cruise, also within the ice. Along with that, water samples (for analysis with LWCC, QFT-ICAM and HPLC) were taken every 3 hours for calibration purposes and to generate a high spatially resolved sampling along the ship's track.

Besides the discrete water samples taken from the ship's flow system, water samples were also taken along 24 oceanographic stations occupied during the cruise (Tab. 3.8.1). The sampling depths were determined based on the profiles of chlorophyll-a fluorescence acquired with a fluorometer attached to the CTD-Rosette system. Five to six samples (in the layer comprised between 0-150m) were taken at each station for analysis with LWCC, QFT-ICAM and HPLC.

At the end of the cruise, a total of 294 water samples were taken from the flow-through system, whereas 142 samples were taken within the oceanographic stations.

Tab. 3.8.1: Group during the PS103 expedition and the samples for analysis of phytoplankton pigments (with HPLC instrument), colored dissolved organic matter (CDOM, with the LWCC instrument) and particulate matter absorption (Pabs, with the QFT-ICAM instrument).

Station	Date	Sampled Depth (m)	HPLC	CDOM	PAbs
PS103/001	20/12/16	2, 30, 35, 76, 95, 100	•	•	•
PS103/002	21/12/16	4, 10, 50, 115, 120, 150	•	•	•
PS103/003	22/12/16	5, 20, 52, 95, 120, 150	•	•	•
PS103/004	23/12/16	3, 10, 24, 61, 120, 150	•	•	•
PS103/005	24/12/16	2, 10, 25, 76, 126, 150	•	•	•
PS103/006	25/12/16	2, 15, 35, 110, 120, 150	•	•	•
PS103/008	26/12/16	5, 26, 35, 60, 120, 150	•	•	•
PS103/009	27/12/16	3.5, 30, 45, 65, 120, 150	•	•	•
PS103/011	28/12/16	4, 15, 40, 75, 120, 150	•	•	•
PS103/014	29/12/16	3.5, 20, 33, 48, 120, 150	•	•	•
PS103/015	29/12/16	5, 20, 41, 80, 100, 150	•	•	•
PS103/022	01/01/17	3, 20, 45, 70, 120, 150	•	•	•
PS103/023	02/01/17	4, 20, 40, 80, 120, 150	•	•	•
PS103/027	09/01/17	2, 10, 30, 60, 120, 150	•	•	•
PS103/029	10/01/17	1.6, 9.7, 30, 45, 120, 150	•	•	•
PS103/031	11/01/17	3, 10, 25, 55, 120, 150	•	•	•
PS103/034	13/01/17	4, 35, 65, 90, 120, 150	•	•	•
PS103/039	18/01/17	3, 20, 80, 120, 150	•	•	•
PS103/040	19/01/17	3, 20, 50, 90, 120, 150	•	•	•
PS103/043	21/01/17	1.9, 30, 55.4, 75.1, 120, 150	•	•	•
PS103/045	23/01/17	2.5, 20, 35, 80, 120, 150	•	•	•
PS103/048	24/01/17	2.5, 10, 45, 120, 150	•	•	•
PS103/059	26/01/17	3, 20, 39, 70, 120, 150	•	•	•
PS103/067	28/01/17	2, 10, 24.5, 55, 120, 150	•	•	•

Data management

Data from the analyses performed onboard directly after sampling (from the AC-S, RAMSES, LWCC and QFT-ICAM equipment) is stored and will be processed at the AWI after the expedition. HPLC samples and data will be processed at the AWI. The discrete sample absorption and pigment data and absorption, scattering and surface light data will be made available after validation through the PANGAEA database. Results will be published in international journals.

References

- Taylor BB, Torrecilla E, Bernhardt A, Taylor MH, Peeken I, Röttgers R, Piera J, Bracher A (2011) Bio-optical provinces in the eastern Atlantic Ocean and their biogeographical relevance. *Biogeosciences*, 8, 3609-3629.
- Röttgers R, D Doxaran, and C Dupouy (2016) Quantitative filter technique measurements of spectral light absorption by aquatic particles using a portable integrating cavity absorption meter (QFT-ICAM), *Opt. Express*. Vol. 24, No. 2 | DOI:10.1364/OE.24.0000A1 | OPTICS EXPRESS A1.

APPENDIX

A.1 Teilnehmende Institute / Participating Institutions

A.2 Fahrtteilnehmer / Participants

A.3 Schiffsbesatzung / Ship's Crew

A.4 Stationsliste / Station List

A.1 FAHRTTEILNEHMER/PARTICIPATING INSTITUTIONS

	Address
AWI	Alfred-Wegener-Institut Helmholtz-Zentrum für Polar- und Meeresforschung Am Handelshafen 12 27570 Bremerhaven / Germany
BLE	Bundesanstalt für Landwirtschaft und Ernährung Deichmanns Aue 29 53179 Bonn / Germany
CAU	Christian-Albrechts-Universität zu Kiel Christian-Albrechts-Platz 4 24118 Kiel / Germany
DWD	Deutscher Wetterdienst Seeschiffahrtsberatung Bernhard-Nocht Strasse 76 20359 Hamburg / Germany
GEOMAR	GEOMAR Helmholtz Zentrum für Ozeanforschung Kiel, Düsternbrooker Weg 20 24105 Kiel / Germany
Heliservice	HeliService International GmbH, Deutschland Am Luneort 15 27572 Bremerhaven / Germany
HS B'hvn	Hochschule Bremerhaven An der Karlstadt 8 27568 Bremerhaven / Germany
Laeisz	Reederei F. Laeisz (Bremerhaven) GmbH Brückenstrasse 25 27568 Bremerhaven / Germany
TU Dresden	TU Dresden Institut für Planetare Geodäsie 01062 Dresden / Germany
Uni Bremen	Universität Bremen Postfach 33 04 40 28334 Bremen / Germany
Uni Göttingen	Universität Göttingen Busgenweg 2 37033 Göttingen / Germany

A.2 FAHRTTEILNEHMER / CRUISE PARTICIPANTS

Name/ Last name	Vorname/ First Name	Institut/ Institute	Beruf/ Profession
Allerholt	Jakob	HS Brhv. (AWI)	Stud. Mar. Tech.
Anschütz	Anna	CAU/GEOMAR	Stud. Biol. Oceanography
Beszteri	Bánk Márton	AWI	Biologist
Boebel	Olaf	AWI	Chief Scientist, Oceanographer
Buttler	Feninia	AWI	Technician, Biology
Endres	Sonja	GEOMAR	Biologist
Ehrhardt	Tom	freelance	Journalist
Falla	Maria	AWI	Engineer
Fong	Allison	AWI	Biologist
Gonçalves-Araujo	Rafael	AWI	Oceanographer
Graupner	Rainer	AWI	Technician, Oceanography
Hamm	Frieder	BLE	Biologist
Hampe	Hendrik	HS Brhv. (AWI)	Stud. Mar. Tech
Havermans	Charlotte	Uni Bremen	Biologist
Ivanciu	Ioana	CAU/GEOMAR (AWI)	Stud. Phys. Oceanography
Jager	Harold	HeliTransair	Pilot
Kreilein	Heinrich	Uni Göttingen	Physicist
Kreilein	Marion	Uni Göttingen	Computer scientist
Krusenbaum	Moritz	CAU/GEOMAR	Stud. Phys. Oceanography
Latarius	Katrin	AWI	Scientist, Oceanography
Liebe	Thomas	Laeisz	Engineer
le Paih	Nicolas	AWI	Scientist, Oceanography
Mattmüller	Ramona	Uni Bremen (AWI)	Stud. Bio.
Miller	Max	DWD	Meteorologist
Monsees	Matthias	AWI	Technician, Oceanography
Oelker	Julia	Uni Bremen	Physicist
Richter	Roland	HeliTransair	Technician
Rohardt	Gerd	AWI	Oceanographer
Rothenburg	Mark	HeliTransair	Technician
Rücker van Caspel	Mathias	AWI	Oceanographer
Schöbinger	Simon	Uni Bremen	Stud. Bio.
Schröter	Franz	Uni Bremen	Stud. Bio.

Name/ Last name	Vorname/ First Name	Institut/ Institute	Beruf/ Profession
Sonnabend	Hartmut	DWD	Technician
Spiesecke	Stefanie	AWI	Engineer
Stoye	Stefanie	freelance	Journalist
Tippenhauer	Sandra	AWI	Oceanographer
Thurmann	Michael	Laeisz	Engineer
Tunsch	Edgar	Uni Göttingen	Technician, Physics
Vaupel	Lars	HeliTransair	Pilot
Zwicker	Sarah	AWI	Stud. Bio.

A.3 SCHIFFSBESATZUNG / SHIP'S CREW

No.	Name	Rank
01.	Wunderlich, Thomas	Master
02.	Lauber, Felix	1. Officer
03.	Westphal, Henning	Ch.Eng.
04.	Spielke, Steffen	2. Officer
05.	Kentges, Felix	2. Officer
06.	Peine, Lutz	2. Officer
07.	Osbahr, Stefan	Doctor
08.	Hofmann, Jörg	Communication Officer
09.	Schnürch, Helmut	2.Eng.
10.	Buch, Erik-Torsten	2.Eng.
11.	Rusch, Torben	2.Eng.
12.	Brehme, Andreas	Elec.Tech
13.	Ganter, Armin	Electron.
14.	Markert, Winfried	Electron.
15.	Winter, Andreas	Electron.
16.	Feiertag, Thomas	Electron.
17.	Schröter, Rene	Boatsw.
18.	Neisner, Winfried	Carpenter
19.	Clasen, Nils	A.B.
20.	Schröder, Norbert	A.B.
21.	Burzan, Gerd-Ekkehard	A.B.
22.	Hartwig-Labahn, Andreas	A.B.
23.	Fölster, Michael	A.B.
24.	Müller, Steffen	A.B.
25.	Brickmann, Peter	A.B.
26.	Sedlak, Andreas	A.B.
27.	Schröder, Horst	A.B.
28.	Beth, Detlef	Storekeep
29.	Plehn, Markus	Mot-man
30.	Klein, Gert	Mot-man
31.	Krösche, Eckard	Mot-man
32.	Dinse, Horst	Mot-man
33	Watzel, Bernhard	Mot-man

No.	Name	Rank
34.	Meißner, Jörg	Cook
35.	Tupy, Mario	Cooksmat
36.	Möller, Wolfgang	Cooksmat
37.	Wartenberg, Irina	1.Stwdess
38.	Schwitzky-Schwarz, Carmen	Stwdss/KS
39.	Hischke, Peggy	2.Stwdess
40.	Grigull, Elke	2.Stwdess
41.	Krause, Tomasz	2.Steward
42.	Hu, Guo	Yong
43	Chen, Quan	Lun
44.	Ruan, Hui	Guang

A.4 STATIONSLISTE / STATION LIST PS103

Station	Date	Time	Latitude	Longitude	Depth (m)	Gear	Action	Comments
PS103_0_Underway-1	2016-12-15	06:51	-33,90972	18,43578	NA	WST	profile start	
PS103_0_Underway-1	2017-02-02	13:56	-52,92974	-70,80297	7	WST	profile end	
PS103_0_Underway-2	2016-12-16	17:00	-33,85823	18,33968	NA	ADCP_150	profile start	
PS103_0_Underway-2	2017-01-30	18:13	-58,15828	-60,28765	3828	ADCP_150	profile end	
PS103_0_Underway-3	2016-12-16	18:21	-34,04985	18,1719	126	TSG_KEEL	profile start	
PS103_0_Underway-3	2017-01-30	18:12	-58,15884	-60,28657	3824	TSG_KEEL	profile end	
PS103_0_Underway-4	2016-12-18	12:00	-39,90941	12,58073	4724	FBOX	profile start	
PS103_0_Underway-4	2017-01-03	16:00	-69,56877	-9,47823	2448	FBOX	profile end	
PS103_0_Underway-4	2017-01-11	09:58	-69,06148	-17,38235	4773	FBOX	station end	
PS103_0_Underway-4	2017-01-30	19:58	-57,96125	-60,66008	3448	FBOX	profile end	
PS103_0_Underway-5	2016-12-18	12:00	-39,90941	12,58073	4724	PCO2_GO	profile start	
PS103_0_Underway-5	2016-12-24	17:00	-59,06242	0,08174	4669	PCO2_GO	profile end	
PS103_0_Underway-5	2017-01-01	13:17	-69,01037	-6,99936	2940	PCO2_GO	profile start	
PS103_0_Underway-5	2017-01-02	00:00	-67,85149	-9,06501	4778	PCO2_GO	profile end	
PS103_0_Underway-5	2017-01-11	09:58	-69,06156	-17,38248	4773	PCO2_GO	profile start	
PS103_0_Underway-5	2017-01-30	18:12	-58,15983	-60,28466	3818	PCO2_GO	profile end	
PS103_0_Underway-6	2016-12-18	12:00	-39,90941	12,58073	4724	PCO2_SUB	profile start	
PS103_0_Underway-6	2017-01-03	16:00	-69,56877	-9,47823	2448	PCO2_SUB	profile end	
PS103_0_Underway-6	2017-01-11	09:58	-69,06152	-17,38241	4771	PCO2_SUB	profile start	
PS103_0_Underway-6	2017-01-30	18:12	-58,15931	-60,28567	3821	PCO2_SUB	profile end	
PS103_0_Underway-7	2016-12-17	10:50	-36,42394	15,95764	4621	UAS	profile start	
PS103_0_Underway-7	2017-01-30	18:37	-58,11345	-60,37235	4541	UAS	profile end	
PS103_1-1	2016-12-20	13:07	-45,95591	6,28746	2620	CTDOZE	station start	
PS103_1-1	2016-12-20	13:22	-45,95488	6,28727	NA	CTDOZE	at depth	
PS103_1-1	2016-12-20	13:32	-45,95393	6,28697	2620	CTDOZE	station end	

Station	Date	Time	Latitude	Longitude	Depth (m)	Gear	Action	Comments
PS103_1-2	2016-12-20	13:10	-45,95581	6,2875	2621	HN	station start	
PS103_1-2	2016-12-20	13:17	-45,9553	6,28735	NA	HN	station end	
PS103_1-3	2016-12-20	13:48	-45,95379	6,28682	2622	MN_S5	station start	
PS103_1-3	2016-12-20	14:01	-45,9524	6,28664	2627	MN_S5	at depth	
PS103_1-3	2016-12-20	14:18	-45,95159	6,2867	2633	MN_S5	station end	
PS103_1-4	2016-12-20	14:33	-45,95094	6,28705	2635	BONGO	station start	
PS103_1-4	2016-12-20	14:36	-45,95107	6,28722	2633	BONGO	at depth	
PS103_1-4	2016-12-20	14:50	-45,95284	6,28674	2625	BONGO	station end	
PS103_1-5	2016-12-20	14:57	-45,95281	6,28653	2625	BONGO	station start	
PS103_1-5	2016-12-20	15:16	-45,95644	6,28297	2621	BONGO	at depth	
PS103_1-5	2016-12-20	15:45	-45,96223	6,27537	2640	BONGO	station end	
PS103_2-1	2016-12-21	16:06	-49,00606	2,84266	4065	PIES	station end	
PS103_2-2	2016-12-21	14:36	-49,01545	2,8411	NA	MN_S5	station start	
PS103_2-2	2016-12-21	14:53	-49,0151	2,8466	4076	MN_S5	at depth	
PS103_2-2	2016-12-21	15:14	-49,01444	2,85158	4090	MN_S5	station end	
PS103_2-3	2016-12-21	14:37	-49,0155	2,84136	4065	HN	station start	
PS103_2-3	2016-12-21	14:45	-49,01545	2,84391	4070	HN	station end	
PS103_2-4	2016-12-21	16:42	-49,01375	2,83648	4056	CTDOZE	station start	
PS103_2-4	2016-12-21	18:17	-49,01385	2,83712	4058	CTDOZE	at depth	
PS103_2-4	2016-12-21	19:52	-49,01291	2,83771	4059	CTDOZE	station end	
PS103_2-5	2016-12-21	20:00	-49,01327	2,83768	4059	BONGO	station start	
PS103_2-5	2016-12-21	20:09	-49,01325	2,83797	4060	BONGO	at depth	
PS103_2-5	2016-12-21	20:26	-49,0142	2,83654	4056	BONGO	station end	
PS103_2-6	2016-12-21	20:33	-49,01388	2,8361	4056	BONGO	station start	
PS103_2-6	2016-12-21	20:42	-49,0142	2,83604	4055	BONGO	at depth	
PS103_2-6	2016-12-21	21:00	-49,01579	2,8345	4053	BONGO	station end	
PS103_3-1	2016-12-22	13:15	-51,9943	2,10195	2844	CTDOZE	station start	
PS103_3-1	2016-12-22	13:29	-51,99347	2,10024	2833	CTDOZE	at depth	
PS103_3-1	2016-12-22	13:42	-51,99263	2,09928	2827	CTDOZE	station end	
PS103_3-2	2016-12-22	13:20	-51,99408	2,10074	2836	HN	station start	
PS103_3-2	2016-12-22	13:23	-51,99387	2,10075	2834	HN	station end	
PS103_3-3	2016-12-22	13:58	-51,99398	2,09733	2813	MN_S5	station start	
PS103_3-3	2016-12-22	14:23	-51,99296	2,09751	2815	MN_S5	at depth	
PS103_3-3	2016-12-22	14:41	-51,99226	2,0981	2814	MN_S5	station end	
PS103_3-4	2016-12-22	14:46	-51,99259	2,09622	2810	BONGO	station start	
PS103_3-4	2016-12-22	15:06	-51,99013	2,09735	2822	BONGO	at depth	
PS103_3-4	2016-12-22	15:26	-51,98312	2,09611	2857	BONGO	station end	
PS103_3-5	2016-12-22	15:29	-51,98218	2,09795	2871	BONGO	station start	
PS103_3-5	2016-12-22	15:48	-51,97673	2,09704	NA	BONGO	at depth	
PS103_3-5	2016-12-22	15:59	-51,97317	2,09711	2912	BONGO	station end	
PS103_3-6	2016-12-22	16:10	-51,97242	2,09883	2912	BONGO	station start	
PS103_3-6	2016-12-22	16:13	-51,97234	2,0988	2913	BONGO	at depth	
PS103_3-6	2016-12-22	16:16	-51,97227	2,09876	2912	BONGO	station end	

A.4 Stationsliste / Station List PS103

Station	Date	Time	Latitude	Longitude	Depth (m)	Gear	Action	Comments
PS103_4-1	2016-12-23	13:05	-55,87674	1,05541	4085	CTDOZE	station start	
PS103_4-1	2016-12-23	13:18	-55,87745	1,05563	4088	CTDOZE	at depth	
PS103_4-1	2016-12-23	13:31	-55,87776	1,05602	4089	CTDOZE	station end	
PS103_4-2	2016-12-23	13:06	-55,87684	1,05558	4037	HN	station start	
PS103_4-2	2016-12-23	13:14	-55,87728	1,05585	4041	HN	station end	
PS103_4-3	2016-12-23	13:45	-55,87968	1,06404	4182	BONGO	station start	
PS103_4-3	2016-12-23	13:49	-55,87932	1,06276	4179	BONGO	at depth	
PS103_4-3	2016-12-23	14:05	-55,876	1,05138	4031	BONGO	station end	
PS103_4-4	2016-12-23	14:31	-55,8736	1,04724	4092	BONGO	station start	
PS103_4-4	2016-12-23	14:47	-55,86946	1,03618	3968	BONGO	at depth	
PS103_4-4	2016-12-23	15:02	-55,86645	1,02573	3974	BONGO	station end	
PS103_5-1	2016-12-24	08:11	-59,04551	0,09179	4644	MOOR	station start	
PS103_5-1	2016-12-24	09:30	-59,04961	0,07907	4652	MOOR	station end	
PS103_5-2	2016-12-24	09:49	-59,04973	0,07971	4653	CTDOZE	station start	
PS103_5-2	2016-12-24	11:24	-59,04926	0,07784	4652	CTDOZE	at depth	
PS103_5-2	2016-12-24	12:49	-59,04668	0,07793	4649	CTDOZE	station end	
PS103_5-3	2016-12-24	09:53	-59,04962	0,07986	4652	HN	station start	
PS103_5-3	2016-12-24	09:55	-59,04967	0,07989	4655	HN	station end	
PS103_5-4	2016-12-24	09:55	-59,04969	0,07988	4653	HN	station start	
PS103_5-4	2016-12-24	09:58	-59,04987	0,07985	4653	HN	station end	
PS103_5-5	2016-12-24	13:23	-59,06871	0,17954	4623	MOOR	station start	
PS103_5-5	2016-12-24	15:00	-59,04937	0,10532	4641	MOOR	station end	
PS103_5-6	2016-12-24	16:30	-59,05962	0,10532	4655	BONGO	station start	
PS103_5-6	2016-12-24	16:32	-59,0598	0,10333	4657	BONGO	at depth	
PS103_5-6	2016-12-24	16:46	-59,06085	0,09254	4665	BONGO	station end	
PS103_5-7	2016-12-24	16:51	-59,06142	0,08917	4666	BONGO	station start	
PS103_5-7	2016-12-24	16:56	-59,06221	0,08494	4668	BONGO	at depth	
PS103_5-7	2016-12-24	17:12	-59,06189	0,07328	4668	BONGO	station end	
PS103_6-1	2016-12-25	08:00	-61,00027	-0,00151	5385	CTDOZE	station start	
PS103_6-1	2016-12-25	10:01	-61,00029	-0,00032	5392	CTDOZE	at depth	
PS103_6-1	2016-12-25	11:59	-60,99955	0,0007	5434	CTDOZE	station end	
PS103_6-2	2016-12-25	08:10	-61,00058	-0,00177	5161	HN	station start	
PS103_6-2	2016-12-25	08:13	-61,00061	-0,00178	5385	HN	station end	
PS103_6-3	2016-12-25	08:13	-61,0006	-0,00176	5385	HN	station start	
PS103_6-3	2016-12-25	08:16	-61,00051	-0,00161	5396	HN	station end	
PS103_6-4	2016-12-25	12:17	-60,99836	0,00721	5393	BONGO	station start	
PS103_6-4	2016-12-25	12:27	-60,99451	0,0098	5395	BONGO	at depth	
PS103_6-4	2016-12-25	12:42	-60,9874	0,01286	5414	BONGO	station end	
PS103_6-5	2016-12-25	12:48	-60,98492	0,01338	5414	BONGO	station start	
PS103_6-5	2016-12-25	12:58	-60,98102	0,01438	5395	BONGO	at depth	
PS103_6-5	2016-12-25	13:15	-60,97365	0,01718	5393	BONGO	station end	
PS103_6-6	2016-12-25	13:35	-60,97157	0,02144	5388	CTDOZE	station start	
PS103_6-6	2016-12-25	13:42	-60,97157	0,02172	5395	CTDOZE	at depth	

Station	Date	Time	Latitude	Longitude	Depth (m)	Gear	Action	Comments
PS103_6-6	2016-12-25	13:47	-60,97174	0,02152	5388	CTDOZE	station end	
PS103_7-1	2016-12-26	08:08	-63,91904	-0,00658	5208	MOOR	station start	
PS103_7-1	2016-12-26	09:22	-63,91725	-0,00027	5209	MOOR	station end	
PS103_7-2	2016-12-26	10:03	-64,00829	-0,01093	5197	MOOR	station start	
PS103_7-2	2016-12-26	14:10	-64,01432	-0,03575	5196	MOOR	station end	
PS103_7-3	2016-12-26	15:20	-64,02729	-0,14122	5194	MOOR	station start	
PS103_7-3	2016-12-26	17:35	-64,0054	-0,00555	5198	MOOR	station end	
PS103_7-4	2016-12-26	18:47	-63,99304	0,06422	5197	CTDOZE	station start	
PS103_7-4	2016-12-26	20:45	-63,99617	0,0647	5197	CTDOZE	at depth	
PS103_7-4	2016-12-26	22:27	-63,99893	0,06405	5196	CTDOZE	station end	
PS103_7-5	2016-12-26	18:58	-63,99378	0,06189	5197	HN	station start	
PS103_7-6	2016-12-26	19:02	-63,99389	0,06248	5197	HN	station start	
PS103_8-1	2016-12-27	04:08	-65,00303	0,0253	3717	BONGO	station start	
PS103_8-1	2016-12-27	04:10	-65,00289	0,02691	3705	BONGO	at depth	
PS103_8-1	2016-12-27	04:23	-65,00325	0,03928	3705	BONGO	station end	
PS103_8-2	2016-12-27	04:28	-65,00354	0,04304	3700	BONGO	station start	
PS103_8-2	2016-12-27	04:33	-65,00374	0,04857	3697	BONGO	at depth	
PS103_8-2	2016-12-27	04:46	-65,00402	0,06101	3688	BONGO	station end	
PS103_8-3	2016-12-27	05:12	-65,00086	0,02477	3670	CTDOZE	station start	
PS103_8-3	2016-12-27	06:31	-65,00183	0,03181	3710	CTDOZE	at depth	
PS103_8-3	2016-12-27	07:54	-65,00228	0,03056	3711	CTDOZE	station end	
PS103_9-1	2016-12-27	13:37	-66,00029	-0,00051	3413	CTDOZE	station start	
PS103_9-1	2016-12-27	15:10	-66,00208	0,00461	3425	CTDOZE	at depth	
PS103_9-1	2016-12-27	16:26	-66,00475	0,00435	3420	CTDOZE	station end	
PS103_9-2	2016-12-27	14:17	-66,00122	0,00405	3421	HN	station start	
PS103_9-2	2016-12-27	14:20	-66,00145	0,0023	3420	HN	station end	
PS103_10-1	2016-12-27	22:28	-67,0003	-0,00155	4709	CTDOZE	station start	
PS103_10-1	2016-12-28	00:07	-67,00041	0,00348	4709	CTDOZE	at depth	
PS103_10-1	2016-12-28	01:47	-67,00232	0,0051	4709	CTDOZE	station end	
PS103_10-2	2016-12-28	02:10	-67,00143	0,01423	4707	BONGO	station start	
PS103_10-2	2016-12-28	02:16	-67,00117	0,02197	4708	BONGO	at depth	
PS103_10-2	2016-12-28	02:32	-67,00088	0,03916	4707	BONGO	station end	
PS103_10-3	2016-12-28	02:36	-67,00086	0,04393	4708	BONGO	station start	
PS103_10-3	2016-12-28	02:47	-67,00068	0,05672	4706	BONGO	at depth	
PS103_10-3	2016-12-28	03:05	-67,00012	0,07902	4706	BONGO	station end	
PS103_11-1	2016-12-28	05:58	-66,53823	-0,00071	4599	CTDOZE	station start	
PS103_11-1	2016-12-28	07:32	-66,5369	0,00952	4593	CTDOZE	at depth	
PS103_11-1	2016-12-28	09:01	-66,53799	0,01037	4594	CTDOZE	station end	
PS103_11-2	2016-12-28	07:36	-66,53692	0,0096	4594	HN	station start	
PS103_11-2	2016-12-28	07:38	-66,53694	0,00967	4593	HN	station end	
PS103_11-3	2016-12-28	09:27	-66,50862	-0,01726	4533	MOOR	station start	
PS103_11-3	2016-12-28	11:25	-66,50328	-0,01024	4550	MOOR	station end	
PS103_11-4	2016-12-28	12:33	-66,53474	-0,20213	4637	MOOR	station start	

A.4 Stationsliste / Station List PS103

Station	Date	Time	Latitude	Longitude	Depth (m)	Gear	Action	Comments
PS103_11-4	2016-12-28	15:23	-66,51605	-0,07115	4606	MOOR	station end	
PS103_12-1	2016-12-28	18:38	-67,02919	0,00138	4725	HN	station start	
PS103_12-1	2016-12-28	18:42	-67,02954	-0,00001	4712	HN	station end	
PS103_12-2	2016-12-28	18:48	-67,03019	0,00022	4712	BONGO	station start	
PS103_12-2	2016-12-28	19:00	-67,03218	0,00733	4712	BONGO	station end	
PS103_12-3	2016-12-28	19:02	-67,0327	0,0089	4653	BONGO	station start	
PS103_12-3	2016-12-28	19:13	-67,03453	0,01658	4711	BONGO	station end	
PS103_13-1	2016-12-28	22:01	-67,50018	0,00059	4633	CTDOZE	station start	
PS103_13-1	2016-12-28	23:43	-67,49998	-0,00073	4634	CTDOZE	at depth	
PS103_13-1	2016-12-29	01:08	-67,50205	-0,00801	4633	CTDOZE	station end	
PS103_14-1	2016-12-29	03:59	-68,00101	-0,004	4513	CTDOZE	station start	
PS103_14-1	2016-12-29	05:37	-68,00876	0,00045	4511	CTDOZE	at depth	
PS103_14-1	2016-12-29	07:18	-68,01203	0,0106	4510	CTDOZE	station end	
PS103_14-2	2016-12-29	06:24	-68,01009	0,00602	4509	HN	station start	
PS103_14-2	2016-12-29	06:27	-68,01034	0,00457	4510	HN	station end	
PS103_15-1	2016-12-29	15:00	-69,20118	-0,00043	2867	CTDOZE	station start	
PS103_15-1	2016-12-29	16:14	-69,20457	-0,02851	2818	CTDOZE	at depth	
PS103_15-1	2016-12-29	17:19	-69,20759	-0,03739	2819	CTDOZE	station end	
PS103_15-2	2016-12-29	15:32	-69,2039	-0,0173	2840	HN	station start	
PS103_15-2	2016-12-29	15:36	-69,20436	-0,01984	2814	HN	station end	
PS103_16-1	2016-12-29	18:41	-69,39907	-0,0121	2018	CTDOZE	station start	
PS103_16-1	2016-12-29	19:32	-69,4034	-0,04327	1974	CTDOZE	at depth	
PS103_16-1	2016-12-29	20:13	-69,40647	-0,05118	1949	CTDOZE	station end	
PS103_16-2	2016-12-29	18:52	-69,40023	-0,0176	2009	HN	station start	
PS103_16-2	2016-12-29	18:55	-69,40048	-0,01976	2006	HN	station end	
PS103_16-3	2016-12-29	18:56	-69,4005	-0,02	2006	HN	station start	
PS103_16-3	2016-12-29	18:58	-69,40063	-0,02115	2005	HN	station end	
PS103_17-1	2016-12-29	20:49	-69,40415	-0,05174	1962	CTDOZE	station start	
PS103_17-1	2016-12-29	21:11	-69,4044	-0,05409	1961	CTDOZE	at depth	
PS103_17-1	2016-12-29	21:37	-69,40458	-0,05333	1960	CTDOZE	station end	
PS103_17-2	2016-12-29	20:52	-69,40421	-0,05154	1961	HN	station start	
PS103_17-2	2016-12-29	20:54	-69,4042	-0,05134	1961	HN	station end	
PS103_17-3	2016-12-29	20:56	-69,40418	-0,05135	1963	HN	station start	
PS103_17-3	2016-12-29	20:57	-69,40421	-0,05161	1962	HN	station end	
PS103_18-1	2016-12-30	04:03	-68,4996	0,04201	4266	CTDOZE	station start	
PS103_18-1	2016-12-30	05:30	-68,49917	0,03245	4267	CTDOZE	at depth	
PS103_18-1	2016-12-30	06:58	-68,49539	0,04508	4268	CTDOZE	station end	
PS103_19-1	2016-12-30	09:45	-68,9475	-0,09033	3520	CTDOZE	station start	
PS103_19-1	2016-12-30	11:03	-68,9455	-0,09648	3519	CTDOZE	at depth	
PS103_19-1	2016-12-30	12:15	-68,94509	-0,09928	3517	CTDOZE	station end	
PS103_19-2	2016-12-30	10:34	-68,94658	-0,09443	3514	HN	station start	
PS103_19-2	2016-12-30	10:37	-68,94667	-0,09545	3516	HN	station end	
PS103_19-3	2016-12-30	10:37	-68,94666	-0,09559	3512	HN	station start	

Station	Date	Time	Latitude	Longitude	Depth (m)	Gear	Action	Comments
PS103_19-3	2016-12-30	10:40	-68,94668	-0,09623	3510	HN	station end	
PS103_19-4	2016-12-30	13:53	-68,98113	-0,09674	3403	MOOR	station start	
PS103_19-4	2016-12-30	15:03	-68,97922	-0,09884	3408	MOOR	station end	
PS103_20-1	2016-12-30	17:52	-69,4285	0,06949	1970	SOSO	station start	
PS103_20-1	2016-12-30	18:18	-69,43095	0,05844	1963	SOSO	at depth	
PS103_20-1	2016-12-30	18:57	-69,43214	0,04329	1953	SOSO	station end	
PS103_21-1	2016-12-31	08:01	-69,00275	-0,01074	3392	MOOR	station start	
PS103_21-1	2016-12-31	16:31	-69,00302	0,00596	3402	MOOR	station end	
PS103_22-1	2017-01-01	08:50	-69,00561	-6,99086	2951	MOOR	station start	
PS103_22-1	2017-01-01	10:53	-69,01036	-7,02236	2955	MOOR	station end	
PS103_22-2	2017-01-01	11:23	-69,01175	-7,0221	2951	CTDOZE	station start	
PS103_22-2	2017-01-01	12:29	-69,01198	-7,01869	2948	CTDOZE	at depth	
PS103_22-2	2017-01-01	13:38	-69,00955	-6,99426	2938	CTDOZE	station end	
PS103_22-3	2017-01-01	12:09	-69,01211	-7,02261	2950	HN	station end	
PS103_22-4	2017-01-01	14:16	-68,99246	-7,1009	2988	MOOR	station start	
PS103_22-4	2017-01-01	15:35	-69,00374	-6,99732	2957	MOOR	station end	
PS103_22-5	2017-01-01	16:22	-69,01024	-6,97759	2927	CTDOZE	station start	
PS103_22-5	2017-01-01	16:31	-69,00969	-6,9783	2929	CTDOZE	at depth	
PS103_22-5	2017-01-01	16:38	-69,00947	-6,97744	2929	CTDOZE	station end	
PS103_22-6	2017-01-01	16:51	-69,01076	-6,9704	2918	BONGO	station start	
PS103_22-6	2017-01-01	16:53	-69,01101	-6,96876	2915	BONGO	at depth	
PS103_22-6	2017-01-01	17:06	-69,0132	-6,95659	2899	BONGO	station end	
PS103_22-7	2017-01-01	17:10	-69,01387	-6,95278	2894	BONGO	station start	
PS103_22-7	2017-01-01	17:17	-69,01495	-6,94605	2886	BONGO	at depth	
PS103_22-7	2017-01-01	17:30	-69,01695	-6,9324	2865	BONGO	station end	
PS103_23-1	2017-01-02	10:18	-65,9673	-12,24337	4710	MOOR	station start	
PS103_23-1	2017-01-02	13:25	-65,96477	-12,23613	5048	MOOR	station end	
PS103_23-2	2017-01-02	14:17	-65,93756	-12,12454	5047	MOOR	station start	
PS103_23-2	2017-01-02	16:24	-65,97099	-12,23713	5047	MOOR	station end	
PS103_23-3	2017-01-02	17:12	-65,97429	-12,24739	5045	BONGO	at depth	
PS103_23-3	2017-01-02	17:24	-65,97932	-12,25223	5045	BONGO	station end	
PS103_23-4	2017-01-02	17:28	-65,981	-12,25387	5045	BONGO	station start	
PS103_23-4	2017-01-02	17:46	-65,98837	-12,26132	5042	BONGO	at depth	
PS103_23-4	2017-01-02	18:02	-65,99422	-12,26726	5043	BONGO	station end	
PS103_23-5	2017-01-02	18:21	-65,99586	-12,27083	5043	CTDOZE	station start	
PS103_23-5	2017-01-02	20:03	-66,00186	-12,28581	5043	CTDOZE	at depth	
PS103_23-5	2017-01-02	21:57	-66,00314	-12,28672	5043	CTDOZE	station end	
PS103_23-6	2017-01-02	19:06	-65,99804	-12,27641	5043	HN	station start	
PS103_23-6	2017-01-02	19:08	-65,99812	-12,27659	5043	HN	station end	
PS103_24-1	2017-01-07	11:20	-70,53248	-8,14185	210	ROV	station start	
PS103_24-1	2017-01-07	12:42	-70,53248	-8,1419	210	ROV	station end	
PS103_25-1	2017-01-08	14:03	-70,53241	-8,14145	211	ROV	station start	
PS103_25-1	2017-01-08	14:05	-70,53241	-8,14144	211	ROV	station end	

A.4 Stationsliste / Station List PS103

Station	Date	Time	Latitude	Longitude	Depth (m)	Gear	Action	Comments
PS103_26-1	2017-01-09	13:59	-70,38685	-8,19665	678	HN	station start	
PS103_27-1	2017-01-09	14:22	-70,37127	-8,22075	829	BONGO	station start	
PS103_27-1	2017-01-09	14:24	-70,37045	-8,22418	821	BONGO	at depth	
PS103_27-1	2017-01-09	14:33	-70,36724	-8,2347	760	BONGO	station end	
PS103_27-2	2017-01-09	15:05	-70,36595	-8,25688	672	CTDOZE	station start	
PS103_27-2	2017-01-09	15:25	-70,36535	-8,26842	660	CTDOZE	at depth	
PS103_27-2	2017-01-09	15:41	-70,36579	-8,28215	711	CTDOZE	station end	
PS103_27-3	2017-01-09	15:25	-70,36535	-8,2688	660	HN	station start	
PS103_28-1	2017-01-10	10:43	-71,30103	-13,87108	805	ICE	station start	
PS103_28-1	2017-01-10	10:50	-71,30136	-13,87507	814	ICE	station end	
PS103_29-1	2017-01-10	13:09	-71,36293	-13,98003	396	ICE	station end	
PS103_29-2	2017-01-10	13:26	-71,36401	-13,9833	394	ROV	station start	
PS103_29-2	2017-01-10	13:58	-71,36501	-13,98379	391	ROV	station end	
PS103_29-3	2017-01-10	16:51	-71,36511	-13,97652	387	CTDOZE	station start	
PS103_29-3	2017-01-10	17:07	-71,36453	-13,97746	389	CTDOZE	at depth	
PS103_29-3	2017-01-10	17:27	-71,36391	-13,97901	394	CTDOZE	station end	
PS103_29-4	2017-01-10	16:57	-71,36486	-13,97696	386	HN	station start	
PS103_29-4	2017-01-10	16:59	-71,3648	-13,9773	386	HN	station end	
PS103_29-5	2017-01-10	17:00	-71,3648	-13,9773	386	HN	station start	
PS103_29-5	2017-01-10	17:03	-71,36464	-13,97717	387	HN	station end	
PS103_30-1	2017-01-10	18:31	-71,28363	-14,09981	1622	BONGO	station start	
PS103_30-1	2017-01-10	18:33	-71,28299	-14,09859	1623	BONGO	at depth	
PS103_30-1	2017-01-10	18:46	-71,27917	-14,08935	1648	BONGO	station end	
PS103_30-2	2017-01-10	18:49	-71,27847	-14,08764	1654	BONGO	station start	
PS103_30-2	2017-01-10	18:58	-71,27583	-14,08127	1681	BONGO	at depth	
PS103_30-2	2017-01-10	19:13	-71,2719	-14,07148	1748	BONGO	station end	
PS103_31-1	2017-01-11	08:33	-69,05883	-17,38293	4772	MOOR	station start	
PS103_31-1	2017-01-11	09:01	-69,06101	-17,37969	4772	MOOR	station start	
PS103_31-1	2017-01-11	11:32	-69,0659	-17,37586	4772	MOOR	station end	
PS103_31-2	2017-01-11	11:43	-69,06551	-17,37547	4771	CTDOZE	station start	
PS103_31-2	2017-01-11	13:13	-69,06236	-17,39206	4771	CTDOZE	at depth	
PS103_31-2	2017-01-11	15:04	-69,07079	-17,38977	4771	CTDOZE	station end	
PS103_31-3	2017-01-11	12:17	-69,06564	-17,37159	4772	HN	station start	
PS103_31-3	2017-01-11	12:25	-69,06547	-17,37226	4771	HN	station end	
PS103_31-4	2017-01-11	15:42	-69,10223	-17,29458	4768	MOOR	station start	
PS103_31-4	2017-01-11	17:40	-69,05814	-17,39079	4773	MOOR	station end	
PS103_31-5	2017-01-11	18:38	-69,04704	-17,44005	4774	BONGO	station start	
PS103_31-5	2017-01-11	18:40	-69,04629	-17,44068	4775	BONGO	at depth	
PS103_31-5	2017-01-11	18:53	-69,04161	-17,44408	4775	BONGO	station end	
PS103_31-6	2017-01-11	18:57	-69,04	-17,44513	4776	BONGO	station start	
PS103_31-6	2017-01-11	19:06	-69,03615	-17,44801	4777	BONGO	at depth	
PS103_31-6	2017-01-11	19:21	-69,03069	-17,45261	4777	BONGO	station end	
PS103_33-1	2017-01-12	09:13	-70,2011	-23,96749	4470	Test	station start	

Station	Date	Time	Latitude	Longitude	Depth (m)	Gear	Action	Comments
PS103_33-1	2017-01-12	09:59	-70,20102	-23,96924	4470	Test	at depth	
PS103_33-1	2017-01-12	11:50	-70,19936	-23,96907	4469	Test	station end	
PS103_33-2	2017-01-12	12:26	-70,20008	-23,96808	4468	SOSO	station start	
PS103_33-2	2017-01-12	12:51	-70,20104	-23,96445	4469	SOSO	at depth	
PS103_33-2	2017-01-12	13:39	-70,20237	-23,95708	4468	SOSO	station end	
PS103_33-3	2017-01-12	13:44	-70,2029	-23,95787	4468	SOSO	station start	
PS103_33-3	2017-01-12	14:04	-70,20372	-23,95732	4467	SOSO	at depth	
PS103_33-3	2017-01-12	15:02	-70,20642	-23,95264	4468	SOSO	station end	
PS103_33-4	2017-01-12	15:12	-70,20455	-23,9444	4468	SOSO	station start	
PS103_33-4	2017-01-12	15:32	-70,20536	-23,94507	4468	SOSO	at depth	
PS103_33-4	2017-01-12	16:06	-70,20632	-23,94459	4467	SOSO	station end	
PS103_33-5	2017-01-12	16:13	-70,20413	-23,93502	4467	SOSO	station start	
PS103_33-5	2017-01-12	16:34	-70,20415	-23,93556	4468	SOSO	at depth	
PS103_33-5	2017-01-12	17:28	-70,20386	-23,93782	4469	SOSO	station end	
PS103_34-1	2017-01-13	08:07	-70,89638	-28,9008	4403	MOOR	station start	
PS103_34-1	2017-01-13	10:06	-70,90078	-28,98223	4409	MOOR	station end	
PS103_34-2	2017-01-13	10:18	-70,90017	-28,98465	4408	CTDOZE	station start	
PS103_34-2	2017-01-13	11:57	-70,90021	-28,98574	4408	CTDOZE	at depth	
PS103_34-2	2017-01-13	13:34	-70,89938	-28,98067	4407	CTDOZE	station end	
PS103_34-3	2017-01-13	10:30	-70,90016	-28,98434	4408	HN	station start	
PS103_34-3	2017-01-13	10:31	-70,90013	-28,98431	4408	HN	at depth	
PS103_34-3	2017-01-13	10:32	-70,9001	-28,98431	4407	HN	station end	
PS103_34-4	2017-01-13	10:33	-70,90008	-28,98433	4408	HN	station start	
PS103_34-4	2017-01-13	10:34	-70,90007	-28,98434	4408	HN	at depth	
PS103_34-4	2017-01-13	10:35	-70,90007	-28,98431	4408	HN	station end	
PS103_34-5	2017-01-13	14:00	-70,89309	-28,8888	4401	MOOR	station start	
PS103_34-5	2017-01-13	16:35	-70,89225	-28,8912	4403	MOOR	station end	
PS103_34-6	2017-01-13	16:56	-70,88416	-28,83912	4408	CTDOZE	station start	
PS103_34-6	2017-01-13	17:04	-70,8837	-28,83573	4410	CTDOZE	at depth	
PS103_34-6	2017-01-13	17:12	-70,88389	-28,83694	4408	CTDOZE	station end	
PS103_37-1	2017-01-14	09:11	-68,45239	-27,73709	4728	SOSO	station start	
PS103_37-1	2017-01-14	09:49	-68,4511	-27,7389	4728	SOSO	at depth	
PS103_37-1	2017-01-14	10:39	-68,4502	-27,74111	4728	SOSO	station end	
PS103_37-2	2017-01-14	10:46	-68,45052	-27,74285	4727	SOSO	station start	
PS103_37-2	2017-01-14	11:15	-68,45053	-27,74495	4727	SOSO	at depth	
PS103_37-2	2017-01-14	11:56	-68,45023	-27,74728	4727	SOSO	station end	
PS103_37-3	2017-01-14	12:02	-68,45023	-27,7476	4727	SOSO	station start	
PS103_37-3	2017-01-14	12:25	-68,44904	-27,75128	4726	SOSO	at depth	
PS103_37-3	2017-01-14	13:27	-68,44866	-27,75745	4726	SOSO	station end	
PS103_37-4	2017-01-14	13:32	-68,44878	-27,75786	4726	SOSO	station start	
PS103_37-4	2017-01-14	13:55	-68,44931	-27,75972	4725	SOSO	at depth	
PS103_37-4	2017-01-14	14:36	-68,4514	-27,76117	4726	SOSO	station end	
PS103_37-5	2017-01-14	14:40	-68,45158	-27,76164	4721	SOSO	station start	

A.4 Stationsliste / Station List PS103

Station	Date	Time	Latitude	Longitude	Depth (m)	Gear	Action	Comments
PS103_37-5	2017-01-14	15:03	-68,45315	-27,7611	4725	SOSO	at depth	
PS103_37-5	2017-01-14	16:05	-68,45732	-27,75529	4725	SOSO	station end	
PS103_39-1	2017-01-15	07:01	-66,6094	-27,12661	4872	MOOR	station start	
PS103_39-1	2017-01-15	10:22	-66,6041	-27,1539	4873	MOOR	station end	
PS103_39-2	2017-01-18	13:04	-66,60811	-27,12303	4872	MOOR	station start	
PS103_39-2	2017-01-18	15:24	-66,60751	-27,1214	4872	MOOR	station end	
PS103_39-3	2017-01-18	15:58	-66,60068	-27,23339	4872	CTDOZE	station start	
PS103_39-3	2017-01-18	17:35	-66,59895	-27,21641	4871	CTDOZE	at depth	
PS103_39-3	2017-01-18	19:10	-66,59939	-27,19946	4873	CTDOZE	station end	
PS103_39-4	2017-01-18	16:08	-66,60006	-27,23203	4871	HN	station start	
PS103_39-4	2017-01-18	16:10	-66,60002	-27,23157	4871	HN	station end	
PS103_39-5	2017-01-18	16:11	-66,60001	-27,23138	4871	HN	station start	
PS103_39-5	2017-01-18	16:13	-66,59998	-27,23095	4872	HN	station end	
PS103_40-1	2017-01-19	14:40	-65,62084	-36,42977	4778	MOOR	station start	
PS103_40-1	2017-01-19	18:33	-65,63067	-36,49512	4775	MOOR	station end	
PS103_40-2	2017-01-19	19:41	-65,72867	-36,78983	4762	MOOR	station start	
PS103_40-2	2017-01-19	22:15	-65,69491	-36,68333	4767	MOOR	station end	
PS103_40-3	2017-01-19	23:37	-65,72556	-36,73315	4762	CTDOZE	station start	
PS103_40-3	2017-01-20	00:30	-65,72571	-36,73022	4762	CTDOZE	at depth	
PS103_40-3	2017-01-20	02:16	-65,72864	-36,72365	4762	CTDOZE	station end	
PS103_40-4	2017-01-20	01:57	-65,72824	-36,72508	4762	HN	station start	
PS103_40-4	2017-01-20	02:04	-65,72831	-36,72492	4762	HN	station end	
PS103_40-6	2017-01-20	02:29	-65,73196	-36,70682	4762	BONGO	station start	
PS103_40-6	2017-01-20	02:31	-65,73114	-36,70543	4763	BONGO	at depth	
PS103_40-6	2017-01-20	02:45	-65,72615	-36,69328	4762	BONGO	station end	
PS103_40-7	2017-01-20	02:49	-65,72767	-36,68486	4763	BONGO	station start	
PS103_40-7	2017-01-20	03:07	-65,72839	-36,66101	4763	BONGO	at depth	
PS103_40-7	2017-01-20	03:30	-65,72905	-36,6366	4765	BONGO	station end	
PS103_43-1	2017-01-21	08:54	-68,48096	-44,11059	4139	MOOR	at depth	
PS103_43-1	2017-01-21	09:27	-68,48014	-44,11089	4139	MOOR	station start	
PS103_43-1	2017-01-21	09:43	-68,47975	-44,11156	4140	MOOR	station end	
PS103_43-1	2017-01-21	12:48	-68,48258	-44,1076	4140	MOOR	station start	
PS103_43-1	2017-01-21	15:36	-68,48328	-44,11858	4138	MOOR	station end	
PS103_43-2	2017-01-21	14:14	-68,48347	-44,10996	4139	ROV	station start	
PS103_43-2	2017-01-21	14:33	-68,48319	-44,11016	NA	ROV	at depth	
PS103_43-2	2017-01-21	15:18	-68,48362	-44,11351	NA	ROV	station end	
PS103_43-3	2017-01-21	16:50	-68,45897	-44,13045	4140	MOOR	station start	
PS103_43-3	2017-01-21	19:09	-68,46404	-44,14524	4138	MOOR	station end	
PS103_43-4	2017-01-21	19:48	-68,42156	-44,0998	4142	CTDOZE	station start	
PS103_43-4	2017-01-21	21:15	-68,42396	-44,09792	4143	CTDOZE	at depth	
PS103_43-4	2017-01-21	22:49	-68,4252	-44,09544	4144	CTDOZE	station end	
PS103_43-5	2017-01-21	20:07	-68,42177	-44,09761	4142	HN	station start	
PS103_43-5	2017-01-21	20:08	-68,42185	-44,09778	4142	HN	station end	

Station	Date	Time	Latitude	Longitude	Depth (m)	Gear	Action	Comments
PS103_43-6	2017-01-21	20:08	-68,42186	-44,09779	4142	HN	station start	
PS103_43-6	2017-01-21	20:11	-68,42194	-44,09798	4142	HN	station end	
PS103_44-1	2017-01-22	22:59	-64,33308	-46,44072	4426	CTDOZE	station start	
PS103_44-1	2017-01-23	00:30	-64,33228	-46,4398	4425	CTDOZE	at depth	
PS103_44-1	2017-01-23	02:00	-64,33615	-46,44061	4427	CTDOZE	station end	
PS103_45-1	2017-01-23	03:21	-64,37343	-45,97957	4461	BONGO	station start	
PS103_45-1	2017-01-23	03:25	-64,37406	-45,9751	4461	BONGO	at depth	
PS103_45-1	2017-01-23	03:40	-64,37616	-45,95946	4459	BONGO	station end	
PS103_45-2	2017-01-23	03:44	-64,37603	-45,96136	4459	BONGO	station start	
PS103_45-2	2017-01-23	03:56	-64,37798	-45,94874	4456	BONGO	at depth	
PS103_45-2	2017-01-23	04:12	-64,3803	-45,93172	4451	BONGO	station end	
PS103_45-3	2017-01-23	04:37	-64,38023	-45,94018	4454	CTDOZE	station start	
PS103_45-3	2017-01-23	06:10	-64,37998	-45,92967	4453	CTDOZE	at depth	
PS103_45-3	2017-01-23	07:44	-64,37503	-45,92204	4456	CTDOZE	station end	
PS103_45-4	2017-01-23	07:13	-64,37727	-45,92476	4455	HN	station start	
PS103_45-4	2017-01-23	07:15	-64,37717	-45,92461	4455	HN	station end	
PS103_45-5	2017-01-23	08:01	-64,38183	-45,8746	4463	MOOR	at depth	
PS103_45-5	2017-01-23	08:19	-64,38165	-45,87285	4462	MOOR	station start	
PS103_45-5	2017-01-23	11:05	-64,36909	-45,87857	4460	MOOR	station end	
PS103_46-1	2017-01-23	15:02	-64,21568	-47,49235	4293	MOOR	station start	
PS103_46-1	2017-01-23	17:25	-64,21576	-47,49027	4216	MOOR	station end	
PS103_46-2	2017-01-23	17:47	-64,20859	-47,41571	4222	CTDOZE	station start	
PS103_46-2	2017-01-23	19:22	-64,21037	-47,39662	4224	CTDOZE	at depth	
PS103_46-2	2017-01-23	20:47	-64,21053	-47,39668	4228	CTDOZE	station end	
PS103_47-1	2017-01-23	22:02	-64,25672	-47,00473	4324	CTDOZE	station start	
PS103_47-1	2017-01-23	23:35	-64,25459	-47,00005	4322	CTDOZE	at depth	
PS103_47-1	2017-01-24	00:59	-64,25642	-46,99851	4324	CTDOZE	station end	
PS103_48-1	2017-01-24	04:25	-64,06674	-48,37842	3934	CTDOZE	station start	
PS103_48-1	2017-01-24	05:44	-64,06732	-48,37274	3937	CTDOZE	at depth	
PS103_48-1	2017-01-24	07:09	-64,06724	-48,3819	3932	CTDOZE	station end	
PS103_48-2	2017-01-24	08:00	-64,06697	-48,37938	3933	MOOR	station start	
PS103_48-2	2017-01-24	08:37	-64,06642	-48,38046	3933	MOOR	station end	
PS103_48-3	2017-01-24	09:27	-64,06677	-48,38379	3931	BONGO	station start	
PS103_48-3	2017-01-24	09:32	-64,06733	-48,38315	3931	BONGO	at depth	
PS103_48-3	2017-01-24	09:47	-64,07214	-48,37583	3932	BONGO	station end	
PS103_48-4	2017-01-24	09:50	-64,07217	-48,37567	3932	BONGO	station start	
PS103_48-4	2017-01-24	10:08	-64,07728	-48,36753	3933	BONGO	at depth	
PS103_48-4	2017-01-24	10:41	-64,08251	-48,3559	3935	BONGO	station end	
PS103_49-1	2017-01-24	14:06	-63,89467	-49,08572	3510	MOOR	station start	
PS103_49-1	2017-01-24	14:18	-63,89486	-49,08304	3511	MOOR	station end	
PS103_50-1	2017-01-24	14:56	-63,91652	-49,26764	3448	MOOR	station start	
PS103_50-1	2017-01-24	15:35	-63,91708	-49,26817	3449	MOOR	station end	
PS103_50-2	2017-01-24	16:20	-63,89183	-49,08424	3507	SOSO	station start	

A.4 Stationsliste / Station List PS103

Station	Date	Time	Latitude	Longitude	Depth (m)	Gear	Action	Comments
PS103_50-2	2017-01-24	16:47	-63,89292	-49,08653	3508	SOSO	at depth	
PS103_50-2	2017-01-24	17:48	-63,89492	-49,0912	3509	SOSO	station end	
PS103_50-3	2017-01-24	17:54	-63,89473	-49,09242	3508	SOSO	station start	
PS103_50-3	2017-01-24	18:13	-63,89618	-49,08972	3513	SOSO	at depth	
PS103_50-3	2017-01-24	19:05	-63,89605	-49,08353	3514	SOSO	station end	
PS103_51-1	2017-01-24	19:15	-63,89564	-49,08186	3514	CTDOZE	station start	
PS103_51-1	2017-01-24	20:30	-63,89245	-49,08012	3510	CTDOZE	at depth	
PS103_51-1	2017-01-24	21:41	-63,8892	-49,07592	3509	CTDOZE	station end	
PS103_52-1	2017-01-24	23:14	-63,84607	-49,62069	3229	CTDOZE	station start	
PS103_52-1	2017-01-25	00:53	-63,84576	-49,62112	3228	CTDOZE	at depth	
PS103_52-1	2017-01-25	02:12	-63,8466	-49,61824	3230	CTDOZE	station end	
PS103_53-1	2017-01-25	03:39	-63,77677	-50,08586	2819	CTDOZE	station start	
PS103_53-1	2017-01-25	04:47	-63,77524	-50,08832	2818	CTDOZE	at depth	
PS103_53-1	2017-01-25	05:44	-63,77883	-50,08591	2821	CTDOZE	station end	
PS103_53-2	2017-01-25	05:57	-63,78086	-50,08967	2820	BONGO	station start	
PS103_53-2	2017-01-25	05:59	-63,78126	-50,09032	2820	BONGO	at depth	
PS103_53-2	2017-01-25	06:12	-63,78545	-50,0966	2816	BONGO	station end	
PS103_53-3	2017-01-25	06:15	-63,78632	-50,09794	2816	BONGO	station start	
PS103_53-3	2017-01-25	06:24	-63,78827	-50,10219	2814	BONGO	at depth	
PS103_53-3	2017-01-25	06:42	-63,79267	-50,11328	2809	BONGO	station end	
PS103_53-4	2017-01-25	07:57	-63,7777	-50,08916	2819	MOOR	station start	
PS103_53-4	2017-01-25	08:40	-63,77836	-50,08969	2819	MOOR	station end	
PS103_54-1	2017-01-25	10:43	-63,71907	-50,8227	2553	MOOR	at depth	
PS103_54-1	2017-01-25	11:03	-63,71824	-50,82153	2553	MOOR	station start	
PS103_54-1	2017-01-25	11:27	-63,71851	-50,82071	2553	MOOR	station end	
PS103_54-2	2017-01-25	11:50	-63,72427	-50,85654	2539	MOOR	station start	
PS103_54-2	2017-01-25	14:26	-63,72733	-50,84489	2544	MOOR	station end	
PS103_54-3	2017-01-25	15:02	-63,7308	-50,84447	2544	SOSO	station start	
PS103_54-3	2017-01-25	15:25	-63,73212	-50,84361	2544	SOSO	at depth	
PS103_54-3	2017-01-25	16:13	-63,73395	-50,85151	2541	SOSO	station end	
PS103_54-4	2017-01-25	16:22	-63,73399	-50,85256	2541	SOSO	station start	
PS103_54-4	2017-01-25	16:43	-63,73472	-50,85657	2539	SOSO	at depth	
PS103_54-4	2017-01-25	17:43	-63,74056	-50,85797	2539	SOSO	station end	
PS103_54-5	2017-01-25	18:05	-63,73127	-50,8941	2520	CTDOZE	station start	
PS103_54-5	2017-01-25	18:18	-63,73029	-50,89451	2519	CTDOZE	at depth	
PS103_54-5	2017-01-25	18:34	-63,7284	-50,89438	2519	CTDOZE	station end	
PS103_55-1	2017-01-25	19:57	-63,58754	-51,30495	2225	CTDOZE	station start	
PS103_55-1	2017-01-25	20:52	-63,58769	-51,30631	2224	CTDOZE	at depth	
PS103_55-1	2017-01-25	21:40	-63,58727	-51,30373	2227	CTDOZE	station end	
PS103_56-1	2017-01-25	23:06	-63,71021	-50,90098	2518	CTDOZE	station start	
PS103_56-1	2017-01-26	00:09	-63,71083	-50,89909	2519	CTDOZE	at depth	
PS103_56-1	2017-01-26	00:59	-63,70969	-50,90031	2519	CTDOZE	station end	
PS103_56-2	2017-01-26	01:17	-63,71343	-50,9035	2516	BONGO	station start	

Station	Date	Time	Latitude	Longitude	Depth (m)	Gear	Action	Comments
PS103_56-2	2017-01-26	01:19	-63,71486	-50,90403	2515	BONGO	at depth	
PS103_56-2	2017-01-26	01:33	-63,72159	-50,90613	2514	BONGO	station end	
PS103_56-3	2017-01-26	01:37	-63,72372	-50,90691	2513	BONGO	station start	
PS103_56-3	2017-01-26	01:46	-63,72838	-50,90852	2511	BONGO	at depth	
PS103_56-3	2017-01-26	02:03	-63,73728	-50,91112	2511	BONGO	station end	
PS103_57-1	2017-01-26	07:58	-63,65579	-50,81125	2555	MOOR	station start	
PS103_57-1	2017-01-26	10:27	-63,65603	-50,81114	2555	MOOR	station end	
PS103_58-1	2017-01-26	11:05	-63,72049	-50,83062	2550	MOOR	station start	
PS103_58-1	2017-01-26	15:03	-63,72055	-50,82872	2549	MOOR	station end	
PS103_58-2	2017-01-26	12:29	-63,71967	-50,82685	2551	ROV	station start	
PS103_58-2	2017-01-26	13:05	-63,71969	-50,82734	2550	ROV	station end	
PS103_59-1	2017-01-26	17:41	-63,51325	-51,63547	1698	MOOR	station start	
PS103_59-1	2017-01-26	18:56	-63,51454	-51,63573	1700	MOOR	station end	
PS103_59-2	2017-01-26	19:22	-63,48272	-51,59208	1957	CTDOZE	station start	
PS103_59-2	2017-01-26	20:16	-63,48323	-51,59636	1956	CTDOZE	at depth	
PS103_59-2	2017-01-26	21:11	-63,48313	-51,60023	1902	CTDOZE	station end	
PS103_59-3	2017-01-26	20:08	-63,48272	-51,59558	1960	HN	station start	
PS103_59-3	2017-01-26	20:13	-63,48307	-51,59615	1949	HN	station end	
PS103_60-1	2017-01-26	23:46	-63,47182	-52,16707	886	CTDOZE	station start	
PS103_60-1	2017-01-27	00:11	-63,4709	-52,16736	884	CTDOZE	at depth	
PS103_60-1	2017-01-27	00:37	-63,47085	-52,16731	884	CTDOZE	station end	
PS103_61-1	2017-01-27	01:18	-63,40313	-52,28419	672	CTDOZE	station start	
PS103_61-1	2017-01-27	01:46	-63,4041	-52,28939	677	CTDOZE	at depth	
PS103_61-1	2017-01-27	02:03	-63,40568	-52,29225	670	CTDOZE	station end	
PS103_61-2	2017-01-27	02:19	-63,40511	-52,2985	659	BONGO	station start	
PS103_61-2	2017-01-27	02:22	-63,40437	-52,30136	658	BONGO	at depth	
PS103_61-2	2017-01-27	02:36	-63,40094	-52,31538	641	BONGO	station end	
PS103_61-3	2017-01-27	02:39	-63,40037	-52,31844	639	BONGO	station start	
PS103_61-3	2017-01-27	02:50	-63,39825	-52,32996	625	BONGO	at depth	
PS103_61-3	2017-01-27	03:07	-63,39512	-52,34717	607	BONGO	station end	
PS103_62-1	2017-01-27	03:57	-63,37837	-52,6004	500	CTDOZE	station start	
PS103_62-1	2017-01-27	04:13	-63,3781	-52,6034	498	CTDOZE	at depth	
PS103_62-1	2017-01-27	04:25	-63,37793	-52,60563	499	CTDOZE	station end	
PS103_63-1	2017-01-27	08:31	-63,48471	-52,10084	968	MOOR	station start	
PS103_63-1	2017-01-27	16:09	-63,48511	-52,1014	966	MOOR	station end	
PS103_63-2	2017-01-27	14:00	-63,48215	-52,09771	967	ROV	station start	
PS103_63-2	2017-01-27	14:20	-63,48182	-52,0979	966	ROV	station end	
PS103_64-1	2017-01-27	10:09	-63,26124	-51,82841	949	MOOR	station start	
PS103_64-1	2017-01-27	10:35	-63,2593	-51,82865	949	MOOR	station end	
PS103_65-1	2017-01-27	17:26	-63,4786	-51,87804	1188	CTDOZE	station start	
PS103_65-1	2017-01-27	18:01	-63,48034	-51,88093	1186	CTDOZE	at depth	
PS103_65-1	2017-01-27	18:30	-63,48282	-51,88031	1189	CTDOZE	station end	
PS103_66-1	2017-01-27	23:14	-63,32041	-53,05275	457	CTDOZE	station start	

A.4 Stationsliste / Station List PS103

Station	Date	Time	Latitude	Longitude	Depth (m)	Gear	Action	Comments
PS103_66-1	2017-01-27	23:29	-63,32041	-53,05333	458	CTDOZE	at depth	
PS103_66-1	2017-01-27	23:47	-63,32078	-53,05493	462	CTDOZE	station end	
PS103_67-1	2017-01-28	02:46	-63,22203	-53,70245	315	CTDOZE	station start	
PS103_67-1	2017-01-28	02:59	-63,22234	-53,70282	315	CTDOZE	at depth	
PS103_67-1	2017-01-28	03:10	-63,22344	-53,70149	318	CTDOZE	station end	
PS103_67-2	2017-01-28	02:56	-63,22215	-53,70305	316	HN	station start	
PS103_67-2	2017-01-28	03:03	-63,22269	-53,70234	315	HN	station end	
PS103_67-3	2017-01-28	03:25	-63,23135	-53,67816	347	BONGO	station start	
PS103_67-3	2017-01-28	03:26	-63,23143	-53,67855	347	BONGO	at depth	
PS103_67-3	2017-01-28	03:39	-63,23218	-53,69177	333	BONGO	station end	
PS103_67-4	2017-01-28	03:42	-63,23216	-53,69319	331	BONGO	station start	
PS103_67-4	2017-01-28	03:46	-63,23149	-53,69607	329	BONGO	at depth	
PS103_67-4	2017-01-28	03:57	-63,22855	-53,70596	308	BONGO	station end	
PS103_68-1	2017-01-28	08:58	-63,40328	-52,28602	672	MOOR	station start	
PS103_68-1	2017-01-28	09:45	-63,40324	-52,28691	672	MOOR	station end	
PS103_69-1	2017-01-28	16:26	-63,15528	-54,16429	253	CTDOZE	station start	
PS103_69-1	2017-01-28	16:37	-63,15653	-54,16899	250	CTDOZE	at depth	
PS103_69-1	2017-01-28	16:45	-63,15742	-54,16899	250	CTDOZE	station end	
PS103_70-1	2017-01-28	17:36	-63,14173	-54,32649	284	CTDOZE	station start	
PS103_70-1	2017-01-28	17:46	-63,1425	-54,32668	285	CTDOZE	at depth	
PS103_70-1	2017-01-28	17:55	-63,14262	-54,3279	284	CTDOZE	station end	
PS103_70-2	2017-01-28	18:23	-63,13775	-54,34206	298	BONGO	station start	
PS103_70-2	2017-01-28	18:25	-63,13703	-54,34177	299	BONGO	at depth	
PS103_70-2	2017-01-28	18:37	-63,13233	-54,33793	304	BONGO	station end	
PS103_70-3	2017-01-28	18:53	-63,14405	-54,33478	280	BONGO	station start	
PS103_70-3	2017-01-28	18:58	-63,14194	-54,33258	286	BONGO	at depth	
PS103_70-3	2017-01-28	19:10	-63,13893	-54,32459	294	BONGO	station end	
PS103_71-1	2017-01-29	15:10	-61,01711	-55,97637	319	MOOR	station start	
PS103_71-1	2017-01-29	15:35	-61,02103	-55,9809	331	MOOR	station end	
PS103_71-2	2017-01-29	16:03	-60,99601	-56,02779	750	CTDOZE	station start	
PS103_71-2	2017-01-29	16:33	-60,99921	-56,03489	772	CTDOZE	at depth	
PS103_71-2	2017-01-29	16:54	-61,00203	-56,03923	769	CTDOZE	station end	
PS103_71-3	2017-01-29	16:13	-60,99729	-56,02999	755	HN	station start	
PS103_71-3	2017-01-29	16:21	-60,9988	-56,03109	751	HN	station end	
PS103_71-4	2017-01-29	17:08	-61,00272	-56,04366	782	BONGO	station start	
PS103_71-4	2017-01-29	17:11	-61,00237	-56,04505	793	BONGO	at depth	
PS103_71-4	2017-01-29	17:24	-60,99939	-56,05275	843	BONGO	station end	
PS103_71-5	2017-01-29	17:27	-60,99922	-56,05345	846	BONGO	station start	
PS103_71-5	2017-01-29	17:37	-60,99621	-56,05919	884	BONGO	at depth	
PS103_71-5	2017-01-29	17:52	-60,99238	-56,06937	940	BONGO	station end	
PS103_72-1	2017-01-30	03:04	-59,77383	-57,81861	3729	CTDOZE	station start	
PS103_72-1	2017-01-30	03:20	-59,77457	-57,81973	3732	CTDOZE	at depth	
PS103_72-1	2017-01-30	03:33	-59,77567	-57,823	3737	CTDOZE	station end	

Station	Date	Time	Latitude	Longitude	Depth (m)	Gear	Action	Comments
PS103_72-2	2017-01-30	03:13	-59,77409	-57,81881	3730	HN	station start	
PS103_72-2	2017-01-30	03:20	-59,77455	-57,81969	3732	HN	station end	
PS103_72-3	2017-01-30	03:46	-59,77674	-57,82312	3738	BONGO	station start	
PS103_72-3	2017-01-30	03:48	-59,77593	-57,82373	3738	BONGO	at depth	
PS103_72-3	2017-01-30	04:01	-59,77091	-57,82952	3741	BONGO	station end	
PS103_72-4	2017-01-30	04:06	-59,76997	-57,83042	3738	BONGO	station start	
PS103_72-4	2017-01-30	04:14	-59,76648	-57,83425	3736	BONGO	at depth	
PS103_72-4	2017-01-30	04:32	-59,75887	-57,84302	3724	BONGO	station end	
PS103_73-1	2017-01-30	14:02	-58,47269	-59,64441	3768	CTDOZE	station start	
PS103_73-1	2017-01-30	14:15	-58,47318	-59,64478	3772	CTDOZE	at depth	
PS103_73-1	2017-01-30	14:25	-58,47384	-59,64578	3778	CTDOZE	station end	
PS103_73-2	2017-01-30	14:06	-58,47286	-59,64382	3771	HN	station start	
PS103_73-2	2017-01-30	14:11	-58,47308	-59,64429	3772	HN	station end	
PS103_73-3	2017-01-30	14:39	-58,47476	-59,64707	3787	BONGO	station start	
PS103_73-3	2017-01-30	14:43	-58,47481	-59,64857	3788	BONGO	at depth	
PS103_73-3	2017-01-30	14:56	-58,47479	-59,65862	3810	BONGO	station end	
PS103_73-4	2017-01-30	14:59	-58,47495	-59,65926	3812	BONGO	station start	
PS103_73-4	2017-01-30	15:10	-58,47507	-59,66675	3824	BONGO	at depth	
PS103_73-4	2017-01-30	15:25	-58,47448	-59,67703	3802	BONGO	station end	
Gear abbreviation	Gear							
ADCP_150	Vessel mounted Acoustic Doppler Current Profiler 150 kHz							
BONGO	Bongo Net							
CTDOZE	CTD AWI-OZE							
FBOX	FerryBox							
FLOAT	Float							
HN	Hand Net							
ICE	Ice Station							
MN_S5	Multinet Small 5 Nets							
MOOR	Mooring							
PCO2_GO	pCO2 GO							
PCO2_SUB	pCO2 Subctech							
PIES	Pies							
ROV	Remotely Operated Vehicle							
SOSO	Sound Source							
TSG_KEEL	Thermosalinograph Keel							
Test	Test							
UAS	Underway Air Sampling							
WST	Weatherstation							

Die **Berichte zur Polar- und Meeresforschung** (ISSN 1866-3192) werden beginnend mit dem Band 569 (2008) als Open-Access-Publikation herausgegeben. Ein Verzeichnis aller Bände einschließlich der Druckausgaben (ISSN 1618-3193, Band 377-568, von 2000 bis 2008) sowie der früheren **Berichte zur Polarforschung** (ISSN 0176-5027, Band 1-376, von 1981 bis 2000) befindet sich im electronic Publication Information Center (**ePIC**) des Alfred-Wegener-Instituts, Helmholtz-Zentrum für Polar- und Meeresforschung (AWI); see <http://epic.awi.de>. Durch Auswahl "Reports on Polar- and Marine Research" (via "browse"/"type") wird eine Liste der Publikationen, sortiert nach Bandnummer, innerhalb der absteigenden chronologischen Reihenfolge der Jahrgänge mit Verweis auf das jeweilige pdf-Symbol zum Herunterladen angezeigt.

The **Reports on Polar and Marine Research** (ISSN 1866-3192) are available as open access publications since 2008. A table of all volumes including the printed issues (ISSN 1618-3193, Vol. 377-568, from 2000 until 2008), as well as the earlier **Reports on Polar Research** (ISSN 0176-5027, Vol. 1-376, from 1981 until 2000) is provided by the electronic Publication Information Center (**ePIC**) of the Alfred Wegener Institute, Helmholtz Centre for Polar and Marine Research (AWI); see URL <http://epic.awi.de>. To generate a list of all Reports, use the URL <http://epic.awi.de> and select "browse"/"type" to browse "Reports on Polar and Marine Research". A chronological list in declining order will be presented, and pdf-icons displayed for downloading.

Zuletzt erschienene Ausgaben:

Recently published issues:

710 (2017) The Expedition PS103 of the Research Vessel POLARSTERN to the Weddell Sea in 2016/2017, edited by Olaf Boebel

709 (2017) Russian-German Cooperation: Expeditions to Siberia in 2016, edited by Pier Paul Overduin, Franziska Blender, Dmitry Y. Bolshiyarov, Mikhail N. Grigoriev, Anne Morgenstern, Hanno Meyer

708 (2017) The role of atmospheric circulation patterns on the variability of ice core constituents in coastal Dronning Maud Land, Antarctica, by Kerstin Schmidt

707 (2017) Distribution patterns and migratory behavior of Antarctic blue whales, by Karolin Thomisch

706 (2017) The Expedition PS101 of the Research Vessel POLARSTERN to the Arctic Ocean in 2016, edited by Antje Boetius and Autun Purser

705 (2017) The Expedition PS100 of the Research Vessel POLARSTERN to the Fram Strait in 2016, edited by Torsten Kanzow

704 (2016) The Expeditions PS99.1 and PS99.2 of the Research Vessel POLARSTERN to the Fram Strait in 2016, edited by Thomas Soltwedel

703 (2016) The Expedition PS94 of the Research Vessel POLARSTERN to the central Arctic Ocean in 2015, edited by Ursula Schauer

702 (2016) The Expeditions PS95.1 and PS95.2 of the Research Vessel POLARSTERN to the Atlantic Ocean in 2015, edited by Rainer Knust and Karin Lochte

701 (2016) The Expedition PS97 of the Research Vessel POLARSTERN to the Drake Passage in 2016, edited by Frank Lamy

700 (2016) The Expedition PS96 of the Research Vessel POLARSTERN to the southern Weddell Sea in 2015/2016, edited by Michael Schröder

699 (2016) Die Tagebücher Alfred Wegeners zur Danmark-Expedition 1906/08, herausgegeben von Reinhard A. Krause



ALFRED-WEGENER-INSTITUT
HELMHOLTZ-ZENTRUM FÜR POLAR-
UND MEERESFORSCHUNG

BREMERHAVEN

Am Handelshafen 12
27570 Bremerhaven
Telefon 0471 4831-0
Telefax 0471 4831-1149
www.awi.de

